



**Universidade do Minho**

Escola de Ciências

Vitor Sérgio Amorim e Silva

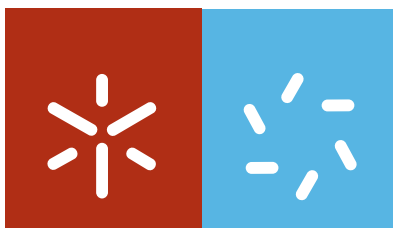
**Identification and Analysis of Regulatory  
Components of the Mevalonate Biosynthetic  
Pathway in *Arabidopsis thaliana* using  
Genetic Approaches**

Vitor Sérgio Amorim e Silva  
**Identification and Analysis of Regulatory Components of the Mevalonate  
Biosynthetic Pathway in *Arabidopsis thaliana* using Genetic Approaches**

UMinho | 2012

Maio de 2012





**Universidade do Minho**

Escola de Ciências

Vítor Sérgio Amorim e Silva

**Identification and Analysis of Regulatory  
Components of the Mevalonate Biosynthetic  
Pathway in *Arabidopsis thaliana* using  
Genetic Approaches**

Tese de Doutoramento em Ciências  
Especialidade em Biologia

Trabalho realizado sob a orientação do  
**Prof. Doutor Miguel Angel Botella**  
e do  
**Prof. Doutor Rui Manuel Tavares**  
e do  
**Prof. Doutor Herlânder Azevedo**

Maio de 2012

## **DECLARAÇÃO**

**Nome:** Vitor Sérgio Amorim e Silva

**Endereço Eletrónico:** vitorsergiosilva@gmail.com

**Telefone:** +351 914558053

**Número do Cartão de Cidadão:** 12598291

### **Título da Tese de Doutoramento:**

Identification and Analysis of Regulatory Components of the Mevalonate Biosynthetic Pathway in *Arabidopsis thaliana* using Genetic Approaches

### **Orientadores:**

Prof. Doutor Miguel Angel Botella  
(Departamento de Biología Molecular y Bioquímica, Universidad de Málaga, Espanha)

Prof. Doutor Rui Manuel Tavares  
(Departamento de Biologia, Escola de Ciências, Universidade do Minho, Portugal)

Prof. Doutor Herlânder Azevedo  
(Departamento de Biologia, Escola de Ciências, Universidade do Minho, Portugal)

**Ano de Conclusão:** 2011

**Designação do Ramo de Conhecimento do Doutoramento:** Ciências

**Especialidade:** Biologia

É AUTORIZADA A REPRODUÇÃO PARCIAL DESTA TESE APENAS PARA EFEITOS DE INVESTIGAÇÃO, MEDIANTE DECLARAÇÃO ESCRITA DO INTERESSADO, QUE A TAL SE COMPROMETE.

Universidade do Minho, Sete de Maio de 2012

Assinatura: \_\_\_\_\_

## ACKNOWLEDGMENTS

First of all, my sincere gratitude goes to my supervisors Miguel Angel Botella, Rui Tavares and Herlânder Azevedo, for giving me the opportunity to perform scientific work, the unconditional support and guidance and, finally, for the critical reading of this manuscript. I am very grateful to Rui Tavares and Herlânder Azevedo for believing in my skills as a scientist, and for the time invested on my training that permitted me to go abroad and apply for a PhD fellowship. A special thanks to Herlânder for teaching me the ground bases of the lab's work in such a committed way, for the constant coaching regarding laboratory techniques and work planning, but also for the scientific comments and discussion. A special thanks to Rui for the inspiring scientific discussions that helped me project my scientific career and for taking charge of solving all the administrative issues and troubles (not little!) that arose towards the end, with incomparable dedication, which allowed me to totally focus on the scientific work and writing. I am very grateful to Miguel Angel, for welcoming me in his lab so greatly, for believing in me and giving me the opportunity to be a member of his research group, allowing me to participate in his challenging projects, expanding my technical and scientific knowledge. Thank you for your constant guidance and interest on my orientation, to always challenge and push me to go further, for having trained my scientific thinking, not only showing me what to do next but, more important, to make the right decisions about the next step. Thank you for the constant long-distance encouragement, and most of all, for inspiring me with your passionate way of thinking and developing scientific work.

To all my colleagues in Braga I wish to thank them all for the good working atmosphere, the good-fellowship, and for all the cooperation in the lab. Hoping not to forget anyone, a special thanks goes to those who more closely followed me throughout these years of work: Alice Agasse, Cátia, Joana, Manú, Marta, Paulo, Luís, Conde, Franklin, Natacha, Mafalda and Raúl for all the support during my first steps in the lab. Juliana, Rómulo, Rute, Sara Freitas, Óscar, Daniela, Eva, João, Eduarda, Inês, Cláudia, Francisca, Daniel, Herlânder, Sara and Humberto, thank you for your companionship in and outside the lab during all these years. A special thanks to Professor Teresa and Professor Manuela for all the invaluable guidelines given and also for being such good work colleagues. I also wish to thank the entire lab teach and investigation technicians of the Biology Department for saving my life so many times. To Eduarda for borrowing me the amazing cDNA tube number eight! A special thanks to Rómulo for teaching me his expertise on constructs. A special thanks to Daniel for being such a good fellow inside and outside the lab. A very special thanks to Sara, whose friendship and companionship I could always expect, since my first beginner steps into the world of science until today, and surely it will continue to be so in the future. Thank you, Sara, for being such a great bench partner during this entire odyssey. A very special thanks to my good friend Humberto, for being always so scientific updated and available to help. You are certainly the most user-friendly "*scientific search engine*" ever created! Thank you, Humberto, for all the great ideas, for all the passionate scientific discussions and fruitful brainstorming, for being an example of how a scientist should face his work in terms of never ending motivation and high quality standards, but, most of all, thanks for your friendship.

To all my colleagues and friends in Málaga I also wish to express my deep gratitude for the warm welcome, the great working atmosphere and support, for the permanent help and good mood inside the lab and outside, and for their friendship. All of you helped me with your scientific comments and discussion to grow as a scientist! To all the members of the *Laboratorio de Bioquímica y Biotecnología Vegetal*: Vero, Fabiana, Viviana, Karen, Camilla, Paqui, Ali, Carmen, Cristina, Ana, Itziar, Edu, David, Arni, Victoriano Meco, Naoufal, Irene Araguez, Irene Nevado, Yasmine, and of course Vitoriano Valpuesta, and once again to my supervisor Miguel Angel Botella, thanks for making me feel part of the family. I also which to thanks to all the members of the genetics group in Málaga: Adela, Alberto, Rosa, Manolo, Ana, Tábata, Zaira, Miguel, Edgar, Natacha, Juanjo, Humberto and Eduardo Bejarano for all the support and friendly welcome. Can't also forget all the people that I met in Churriana lab, for the warm welcome, the great working atmosphere and support, and for the pleasant breakfasts! Also thanks to Lucas for his friendship that undoubtedly helped me a lot during those years of my Ph.D project in Málaga. A special thanks to Manolo for teaching me his expertise with Agro. A special thanks to Edu for all the scientific insight and for the support in my last experiments in Málaga with tobacco. A special thanks to David for helping me a lot during my adaptation to a new lab but and at same time to a new culture. A very special thank you to Abel Rosado Rey and Aureliano Bombarely for all the help and assistance regarding the high throughput sequencings and the bioinformatic analayis of obtained results. Very special thanks to Ali, for giving me an invaluable help with the lab experiments and for the permanent support and assistance, which allowed me to achieve my goals during these four years of my Ph.D project. Very special thanks to Vero for being such a hard worker and inspire me to follow the same path, pushing me to be more productive (*I can 't forget: "más rápido Vitooorrrr"*), and a better lab worker. Thanks, Vero, for teaching me so much during my first period in the lab, for all the scientific discussions and for being the perfect project and bench partner during all the time. To Vero and Ian, I reserve a special thank you for receiving me so well and for the constant support, also in the weekends, taking me to travel and discover new places outside the lab and the city premises!, and for your friendship that I enjoy so much.

To all my colleagues and friends in Barcelona, in particular to Pedro, Josep, Annamaria, Alex and Ombreta I wish to thank their warm welcome, their excellent work atmosphere, for all support and assistance. I am very grateful to Pedro Carvalho for the great collaboration opportunity which allowed me to work under his supervision in a different and challenging project, expanding further and diversely my technical and scientific knowledge. Thank you, Pedro, for the permanent assistance, for all the constructs provided, for the scientific discussion and all the scientific experiment suggestions and advices. I would like to thank to Alba Shaw for all the assistance with the administrative issues. I also wish to thanks to all the Pedro Carvalho's and Vivek Malhotra's group members for allowing me to be part of the scientific discussions of the group meetings and also bringing me into the social events like the volleyball tournaments. To Josep I wish to express my deep gratitude for teaching me the ground basis of the yeast lab work and for all the cooperation and technical support. A special thanks to Josep and Annamaria for all the scientific insight and the experimental support and help during all my stay in the lab and mainly during my last experiments in Barcelona.

A special thank you goes to my friends that are at the same time also work colleagues: Humberto, João, Miguel, Sara, Rómulo, Isabel, Jorge, Regina, Marisa, Alberto, Francisca, Susana, Luís, for the great moments during these last years prior and during my Ph.D. Also thanks to those of my colleagues who, one way or another, helped me during this endeavor and that I haven't mentioned for forgetfulness. A very special thanks to Mr. Barbosa, Mrs. Rosa and Carla for the "online support" and the nice meals over the writing period. "*Um obrigado muito especial ao Sr. Barbosa, à D. Rosa e à Carla pelo apoio on-line e pelas refeições agradáveis durante o período de escrita*". A very special thanks to my whole family. I am deeply grateful to my sister Marisa and my good friend Filipe for being such a good buddies, and for having always available their facilities for me over the writing period. I am deeply grateful to my parents Firmino and Rosa for being always present and for the unconditional dedication. "*Gostaria de expressar a minha gratidão aos meus pais, Firmino e Rosa, por estarem sempre presente e pela sua dedicação incondicional*".

Last but not least, the most special thanks to you Teresa, my love, for the incredible serenity that you bring to my life and consequently to my work. Thank you for motivating me to live my work as a vocation, for supporting me both in the hard and in the good moments, and encourage me to learn how to enjoy what I am doing each time. Thank you for imprinting on me the fortitude to face failure and respond positively. Thank you for critical reading my ideas prior and during the writing of this manuscript. Thank you for driving me to proactively search for a resolution not just about the tricky but also the common difficulties. Thank you for being the one that can do all this for me and for my work, and most of all, thank you because this is just a small part!

"All praise be to A LOVE SUPREME to whom all praise is due"

*John Coltrane*

O presente trabalho, incluindo a sua publicação beneficiou do seguinte apoio da Fundação para a Ciência e a Tecnologia:

**Bolsa de Doutoramento - SFRH/BD/38583/2007**

Bolsa de Investigação no âmbito do QREN - POPH - Tipologia 4.1 - Formação Avançada, comparticipado pelo Fundo Social Europeu e por fundos nacionais do MCTES.





# Identification and Analysis of Regulatory Components of the Mevalonate Biosynthetic Pathway in *Arabidopsis thaliana* using Genetic Approaches

## ABSTRACT

The capacity of plants to survive under conditions of abiotic stresses is the result of complex and coordinated responses involving hundreds of genes. These responses are affected by interactions between different environmental factors and the developmental stage of the plant and could result in shortened life cycle, reduced or aborted seed production, or accelerated senescence. Drought or continuous water deficit is arguably one of the most important factors affecting plant growth, development, survival and crop productivity. The current marginal success in increasing crop yield under unfavourable environmental conditions is partially due to the large number of cellular processes affected by abiotic stresses which in turn cause severe impact on plant growth, development and finally production. Thus, an essential aspect of abiotic stress research in plants is to determine both, how plants sense and acclimate to abiotic stress conditions, and which are the genetic determinants involved in these processes. Significant progress has been made in understanding the physiological, cellular and molecular mechanisms of plant responses to environmental stress factors, and significant achievements with relevance to agriculture have been obtained, in many cases due to the use of *Arabidopsis thaliana* as a genetic model system in abiotic stress research. *Arabidopsis* has facilitated the functional characterization of numerous genes by use of loss- or gain-of-function experimental approaches.

In a previously study, the *Arabidopsis dry2/sqe1-5* mutant was isolated by its extreme sensitivity to drought stress. *DRY2/SQE1-5* encodes a hypomorphic allele of the squalene epoxidase 1 involved in sterol biosynthesis. Further analysis of the *dry2/sqe1-5* mutant indicated that this mutant is affected in the function of NADPH oxidases, revealing a central role the regulation of this pathway in drought tolerance and regulation of Reactive Oxygen Species (ROS) production. In the present work, to identify new regulatory components of the mevalonate (MVA) pathway in *Arabidopsis*, it was performed a suppressor screening of the *dry2/sqe1-5* mutant, which is affected in the MVA pathway due to the decrease of the activity of the squalene epoxidase 1 (SQE1). Several mutants (named *sud* for *suppressors of dry2 defects*) that reversed most of the *dry2/sqe1-5* developmental phenotypes, including drought hypersensitivity were isolated and characterized, thus allowing the identification of new genetic components regulating the MVA

pathway. In this pathway, the 3-hydroxy-3-methylglutaryl coenzyme A reductase (HMGR) enzyme is located upstream of SQE1, and catalyzes a rate-limiting step of the MVA pathway from which isoprenoids and sterols are synthesized. In animals and yeasts, an essential regulatory mechanism of the MVA pathway is the ubiquitin-mediated degradation of HMGR by the Endoplasmic Reticulum-Associated Protein Degradation (ERAD) HRD pathway. Still, in plants very little is known about the regulatory mechanisms controlling HMGR activity. The analysis of four semidominant *dry2/sqe1-5* suppressors led to the identification of *SUD1*, which encodes a protein showing sequence and structural homology to the E3 ubiquitin ligases involved in ERAD pathway. However, while in yeasts and animals the HMGR regulation occurs by controlling the protein stability through the HRD pathway, the regulation of HMGR in plants by SUD1 is exerted at the activity level by the alternative ERAD Doa10 pathway. Thus, this work contributed to the identification of common elements but mechanistic differences in HMGR regulation between plants, yeast and animals

# Identificação e Análise de Componentes Reguladores da Via Biosintética do Mevalonato em *Arabidopsis thaliana* usando Abordagens Genéticas

## RESUMO

A capacidade de plantas para sobreviverem em condições de stresse abiótico é o resultado de respostas complexas e coordenadas envolvendo centenas de genes. Estas respostas são afetados pelas interações entre os diferentes fatores ambientais e o estágio de desenvolvimento da planta e podem resultar no encurtamento do ciclo de vida, produção reduzida (ou mesmo inexistente) de sementes ou ainda senescência acelerada. A seca ou (ou deficit hídrico contínuo) é sem dúvida um dos fatores mais importantes que afetam o crescimento das plantas e, conseqüentemente a sobrevivência, desenvolvimento e produtividade das culturas de interesse. O escasso sucesso obtido no aumento da produtividade de cultivares de interesse, quando sujeitas a condições ambientais desfavoráveis deve-se, em parte, ao elevado número de processos celulares afetados pelo stresse abiótico, conduzindo à diminuição da produtividade vegetal. Assim, torna-se essencial na investigação sobre stresse abiótico em plantas, determinar como as plantas percebem e se aclimatam a essas condições de stresse, e quais os determinantes genéticos envolvidos nestes processos. Progressos significativos na compreensão dos mecanismos fisiológicos, celulares e moleculares de respostas das plantas a fatores de stresses ambiental, e a aplicação deste conhecimento na agricultura têm sido obtidos e, em muitos casos, conseguidos devido ao uso de *Arabidopsis thaliana* como modelo de estudo. Com efeito, a utilização desta espécie tem permitindo a caracterização funcional de genes utilizando estratégias de ganho- ou de perda de função.

Em trabalhos anteriores, o mutante de *Arabidopsis dry2/sqe1-5* foi identificado através da sua extrema sensibilidade ao stresse hídrico. O gene *DRY2/SQE1-5* codifica um alelo hipomórfico da enzima esqualeno epoxidase 1, envolvida na biossíntese de esteróis. Estudos ulteriores, efetuados neste mutante indicam que ele está afetado ao nível da atividade de NADPH oxidases, o que sugere fortemente um papel central da regulação da via biossintética de esteróis na tolerância à seca e na produção de espécies reactivas de oxigénio. Neste trabalho, para identificar novos componentes reguladores da via do mevalonato (MVA) em *Arabidopsis*, foi realizado um rastreio de supressores do mutante *dry2/sqe1-5*, o qual está afetado ao nível da via do MVA, devido à diminuição da atividade da esqualeno epoxidase 1 (SQE1). Foram isolados e caracterizados vários

mutantes *sud* (supressores dos defeitos de *dry2*) que revertem a maioria dos fenótipos de desenvolvimento do mutante *dry2/sqe1-5*, incluindo a hipersensibilidade à secura, permitindo a identificação de novos componentes genéticos reguladores da via do MVA. Nesta via metabólica, a enzima 3-hidroxi-3-metilglutaril coenzima A redutase (HMGR) está localizada a montante da enzima SQE1, e catalisa um passo limitante desta via, através da qual são sintetizados os isoprenóides e os esteróis. Em animais e leveduras foi já assinalado que um mecanismo de regulação essencial da via do MVA consiste na degradação, mediada por ubiquitina, da enzima HMGR (via HRD), ao nível da via de degradação de proteínas associada ao retículo endoplasmático (ERAD). Contudo, em plantas, permanece reduzido o conhecimento sobre os mecanismos reguladores que controlam a atividade da enzima HMGR. No presente trabalho, a análise de quatro supressores de *dry2/sqe1-5* semidominantes conduziu à identificação de *SUD1*, que codifica uma proteína que apresenta homologia quer ao nível da sequência nucleotídica e aminoacídica quer ao nível estrutural com ubiquitina E3 ligases envolvidas na via ERAD em leveduras e em animais. Enquanto em leveduras e em animais a regulação da HMGR ocorre através do controlo da estabilidade da proteína, através da via HRD, em plantas, a regulação desta enzima por *SUD1* é exercida ao nível da sua atividade, pela via ERAD alternativa Doa10. Os resultados obtidos no presente trabalho, contribuem significativamente para a identificação de elementos comuns, mas apresentando diferenças mecanísticas na regulação da HMGR entre plantas, fungos e animais.

# TABLE OF CONTENTS

<b>ACKNOWLEDGMENTS</b>	iii
<b>TITLE AND ABSTRACT</b>	vii
<b>TÍTULO E RESUMO</b>	ix
<b>TABLE OF CONTENTS</b>	xi
<b>ABBREVIATIONS AND SYMBOLS</b>	xv

## CHAPTER 1

---

### General Introduction

<b>1.1. THE CHALLENGE OF PLANT ABIOTIC STRESS IN CROP PRODUCTION</b>	3
Drought Stress and Stomatal Regulation	4
<b>1.2. REACTIVE OXYGEN SPECIES IN PLANT DEVELOPMENT</b>	5
Production of ROS in plants	6
Cellular localization and coordination of the ROS scavenging pathways of plants	7
NADPH Oxidases Generate ROS Involved in Stomatal Regulation and Plant Development	9
Small GTPases Spatially Control ROS Production and Growth	11
<b>1.3. THE SELECTIVE DEGRADATION OF PROTEINS IN CELLULAR REGULATION AND QUALITY CONTROL</b>	12
The Ubiquitin Proteasome System	12
The Endoplasmic Reticulum-Associated Degradation in Protein Quality Control	14
Distinct ERAD Pathways for the Degradation of ER Proteins in Yeast	14
The Endoplasmic Reticulum-Associated Degradation in Cellular Regulation	16
Conserved Endoplasmic Reticulum-Associated Protein Degradation in Plants	16
<b>1.4. STEROL IN PLANTS</b>	17
Biosynthetic Pathway of Plant Sterols	18
Regulation of the Plant Sterol Biosynthetic Pathway by HMGR	20
Sterol Metabolism in Plants	21
<b>1.5. GENETIC APPROACHES TOWARDS THE STUDY OF STEROL BIOSYNTHESIS AND FUNCTION</b>	22
Squalene Epoxidase Gene Family	23
Phenotypical Analysis of Squalene Epoxidase Mutants	24
Chemical Analysis of Squalene Epoxidase Mutants	24
Arabidopsis <i>dry2/sqe1-5</i> Mutant Reveals a Central Role for Sterols in Drought Tolerance and Regulation of ROS	26
Isolation and Characterization of <i>dry2</i> Suppressors	28
<b>1.6. AIMS AND OUTLINE OF THE THESIS</b>	32

## CHAPTER 2

---

### Investigating the role of Reactive Oxygen Species in *dry2*

2.1. INTRODUCTION	37
2.2. RESULTS AND DISCUSSION	38
ROS Generators Suppress Root Branching Defects in <i>dry2</i>	38
Suppressors Recover Wild-type ROS Production	41
Imaging Intracellular Hydrogen Peroxide Production using HyPer	43
2.3. MATERIALS AND METHODS	45
Plant Material	45
Plant Manipulation and Growth Conditions	45
Root Branching Measurements	45
Detection of Reactive Oxygen Species	45
Generation of Transgenic HyPer-As Constructs/Plants	46
Arabidopsis Transformation by Floral Dipping	46
Selection of Arabidopsis Transformants	47

## CHAPTER 3

---

### Identification of *dry2* Suppressor Mutations

3.1. INTRODUCTION	51
3.2. RESULTS AND DISCUSSION	52
Four <i>dry2</i> Suppressor Mutations are Semi-dominants	52
Map-based Cloning of the <i>sud</i> Mutations	53
Four <i>dry2</i> Suppressors are Independent <i>sud1</i> Mutant alleles	58
3.3. MATERIALS AND METHODS	60
Plant Material	60
Plant Manipulation and Growth Conditions	60
Arabidopsis Cross-fertilization	60
Identification of homozygous plants for the <i>dry2</i> and <i>sud22</i> mutations	61
Map-based Cloning of SUD1	61
Bioinformatic Tools Used for Identification of <i>SUD1</i>	61

## CHAPTER 4

---

### *In Silico* Analysis of *SUD1* Expression and Whole-genome

#### Transcript Profile of wild-type, *dry2*, *dry2/sud9*, and *dry2/sud22*

4.1. INTRODUCTION	65
4.2. RESULTS AND DISCUSSION	66
<i>In Silico</i> Analysis of <i>SUD1</i> Expression	66
Effect of <i>SUD1</i> Inactivation on <i>dry2</i> Whole-genome Transcriptional Activity	68
4.3. MATERIALS AND METHODS	75
Plant Material	75
Plant Manipulation and Growth Conditions	75
Biological Sample preparation for Microarray Hybridization	75
Microarray Hybridization and Evaluation	75
Microarray Bioinformatic Data Analysis	75

## CHAPTER 5

---

### ***In Silico* Structural and Phylogenetic Analysis of SUD1**

<b>5.1. INTRODUCTION</b>	79
<b>5.2. RESULTS AND DISCUSSION</b>	79
Structural Features of SUD1	79
Topology Model for SUD1 Protein	82
Identification of Essential Amino Acid Residues for SUD1 Function	85
Phylogenetic Analysis of SUD1	87
<b>5.3. MATERIALS AND METHODS</b>	90
Bioinformatic Tools Used for <i>in Silico</i> Structural Analysis of SUD1	90
Bioinformatic Tools Used for Phylogenetic Analysis of SUD1	90

## CHAPTER 6

---

### **Functional Characterization of *Arabidopsis thaliana* SUD1, HRD1A and HRD1B**

<b>6.1. INTRODUCTION</b>	93
<b>6.2. RESULTS AND DISCUSSION</b>	94
Molecular Cloning of <i>SUD1</i> in <i>E. coli</i>	94
<i>SUD1</i> Complementation of Yeast <i>doa10Δ</i> Mutation	95
Degradation of Yeast Doa10 Substrates in <i>doa10-G498E</i> Mutant Cells	97
<i>AtHRD1</i> Complementation of Yeast <i>hrd1Δ</i> Mutation	99
Investigating the Function of the Arabidopsis ERAD E3-ligases	105
<b>6.3. MATERIALS AND METHODS</b>	105
Plant Material	105
Plant Manipulation and Growth Conditions	105
Yeast Strains and Plasmids	105
Yeast Genetic Manipulation	106
Molecular Cloning of Arabidopsis ERAD-Homolog Genes in Shuttle Vectors	106
Site-directed mutagenesis to construct <i>doa10-G498E</i> Mutant Strain	107
ERAD-Substrate Degradation Experiments	106
Site-directed Mutagenesis to Construct <i>doa10-G498E</i> Mutant Strain	108
Immunoblotting	108

## CHAPTER 7

---

### **Investigating Use of Grafting in the Study of Long-distance Isoprenoid-derived Signalling in *dry2***

<b>7.1. INTRODUCTION</b>	111
<b>7.2. RESULTS</b>	112
Grafting analysis of long-distance signalling in <i>dry2</i>	112
Rejection of Wild-type and <i>dry2/sud1-9</i> Scions by <i>dry2</i> Rootstocks	114
Wild-type Rootstocks Do Not Complement <i>dig4</i> Mutant Shoot Defects	115
<b>7.3. DISCUSSION</b>	117
The Nature of the Long-distance Signal Impaired in <i>dry2</i>	117
<b>7.4. MATERIALS AND METHODS</b>	118
Plant Material	118
Arabidopsis Grafting	119
Sequencing Analysis to Confirm Successful Grafting Unions	119

## CHAPTER 8

---

### Concluding Remarks and Future Perspectives

<b>8.1. CONCLUDING REMARKS</b>	123
A Genetic Approach to Identify Regulators of the MVA Biosynthetic Pathway	123
<b>8.2. CONCLUDING REMARKS AND FUTURE PERSPECTIVES</b>	123
Regulation of HMGR Activity by SUD1	123
Looking for the Identification of a New MVA-derived Signal Putatively Involved into Plant Long-distance Signalling	125

## CHAPTER 9

---

<b>Bibliographic References</b>	129
---------------------------------	-----

## APPENDIXES

---

### Appendix I – Standard Molecular Biology Methods

1. NUCLEIC ACID METHODS	149
1.1. DNA Methods	149
1.1.1. Oligonucleotide Design and Preparation	149
1.1.2. Plant Genomic DNA Isolation	149
1.1.3. Plasmid Isolation	150
1.1.4. DNA Fragment Purification	150
1.1.5. DNA Precipitation	150
1.1.6. DNA Digestion with Endonucleases	150
1.1.7. Amplification of DNA Fragments by Polymerase Chain Reaction (PCR)	151
1.1.8. DNA Sequencing	151
1.1.9. Gateway Cloning	151
1.1.10. Subcloning of PCR Fragments into pGEM-T Easy	151
1.1.11. Cloning of PCR Fragments into a Vector	152
1.2. RNA Methods	152
1.2.1. RNA Extraction	152
1.2.2. cDNA Synthesis	152
1.3. Quantification of Nucleic Acids	153
1.4. Nucleic Acids Electrophoretic Separation	153
2. TRANSFORMATION OF BACTERIA	153
2.1. Transformation of <i>E. coli</i> cells	153
2.1.1. <i>E. coli</i> Competent Cells Preparation	154
2.1.2. <i>E. coli</i> Transformation	154
2.2. Transformation of Agrobacterium Cells	154
2.2.1. Preparation of Electrocompetent Cells	154
2.2.2. Electroporation Method	154
<b>Appendix II – Oligonucleotides used for Map-based Cloning</b>	155
<b>Appendix III – Vectors Maps</b>	157



## ABBREVIATIONS AND SYMBOLS

$^1\text{O}_2$	singlet oxygen
ABA	abscisic acid
Acetyl-CoA	acetyl-coenzyme A
APX	ascorbate peroxidase
ARS	autonomously replicating sequences
Atm	atmosphere
Atrboh	<i>Arabidopsis thaliana</i> respiratory burst oxidase homologues
BRs	brassinosteroids
CAPs	cleaved amplified polymorphisms
CAT	catalase
CDS	coding sequence
CEN	centromere
CHX	cyclohexamide
Col-0	Colombia-0
CPY*	mutant carboxypeptidase Y
DAB	3,3-diaminobenzidine
DMAPP	dimethylallyl diphosphate
DPI	diphenylene iodonium
ER	endoplasmic reticulum
ERAD	endoplasmic reticulum associated protein degradation
FPP	farnesyl pyrophosphate
FW	fresh weight
GAL	galactose
GPX	glutathione peroxidase
HA	hemagglutinin
HMG-CoA	3-hydroxy-3-methylglutaryl-CoA
HMGR	3-hydroxy-3-methylglutaryl CoA reductase
HO·	hydroxyl radical
Hr	hour
IPI	Isopentenyl isomerase
IPP	isopentenyl diphosphate
JAs	jasmonates
Ler	Landsberg <i>erecta</i>
Min	minute
MLO	mildew-resistance locus O
MVA	mevalonate
NBT	nitroblue tetrazolium
NOXs	NADPH oxidases
$\text{O}_2^{\cdot-}$	superoxide
PCR	polymerase chain reaction
PFD	photon flux density
PrxR	Peroxioredoxin
RH	relative humidity
Sec	second
SOD	superoxide dismutase
SSLPs	simple sequence length polymorphisms
TD	TEB4-Doa10
TM	Transmembrane
Ub	ubiquitin
UPS	ubiquitin-26S proteasome system
YCp	yeast centromere plasmid
YFP	yellow fluorescent protein

## Amino acids

A	Ala	Alanine
C	Cys	Cysteine
D	Asp	Aspartate
E	Glu	Glutamate
F	Phe	Phenylalanine
G	Gly	Glycine
H	His	Histidine
I	Ile	Isoleucine
K	Lys	Lysine
L	Leu	Leucine
M	Met	Methionine
N	Asn	Asparagine
P	Pro	Proline
Q	Gln	Glutamine
R	Arg	Arginine
S	Ser	Serine
T	Thr	Threonine
V	Val	Valine
W	Trp	Tryptophane
Y	Tyr	Tyrosine
X		Unspecific amino acid

## Nucleotides

A	Adenine	
C	Cytosine	
G	Guanine	
T	Thymine	
U	Uracil	
R	A or G	Purine
Y	C or T	Pyrimidine
W	A or T	
S	C or G	
M	A or C	
K	G or T	
B	C, G or T not A	
D	A, G or T not C	
H	A, C or T not G	
V	A, C or G not T	
N	A, C, G or T	Any nucleotide
ATP	Adenosine-5'-triphosphate	
dATP	2'-deoxyadenosine-5'-triphosphate	
dCTP	2'-deoxycytidine-5'-triphosphate	
dGTP	2'-deoxyguanosine-5'-triphosphate	
dNTP	2'-deoxynucleotide-5'-triphosphate	
dTTP	2'-deoxythymidine-5'-triphosphate	
GDP	Guanosine-5'-diphosphate	
GTP	Guanosine-5'-triphosphate	

# Chapter 1

## General Introduction

### **CONTENTS**

---

- 1.1. THE CHALLENGE OF PLANT ABIOTIC STRESS IN CROP PRODUCTION
- 1.2. REACTIVE OXYGEN SPECIES IN PLANT DEVELOPMENT
- 1.3. THE SELECTIVE DEGRADATION OF PROTEINS IN CELLULAR REGULATION AND QUALITY CONTROL
- 1.4. STEROL IN PLANTS
- 1.5. GENETIC APPROACHES TOWARDS THE STUDY OF STEROL BIOSYNTHESIS AND FUNCTION
- 1.6. AIMS AND OUTLINE OF THE THESIS



## 1.1. THE CHALLENGE OF PLANT ABIOTIC STRESS IN CROP PRODUCTION

Climate changes on Earth and the course of millions of years of evolution contributed to a high genetic diversity, demonstrating living creatures capacity to adapt to the environment and its fluctuations (Zhu, 2002; Koiwa *et al.*, 2006). Environmental stresses can either be biotic, when imposed by living organisms, or abiotic, when they are the result of a deficit or an excess in the physical or chemical environment. During their life span, plants are normally exposed to a variety of different conditions/stresses that affect their growth, development and productivity. As sessile organisms, plants are particularly vulnerable to abiotic stress challenges, and have developed an amazing array of responses to face stress imposition (Buchanan *et al.*, 2000). Current climatic conditions, such as prolonged drought and heat episodes, pose a serious challenge for agricultural production worldwide, affecting plant growth and yield. This abiotic stress conditions cause extensive losses to agricultural production worldwide (Mittler, 2006; Mittler and Blumwald, 2010). Transgenic crops provide a promising avenue to reduce yield losses, improve growth, and provide a secure food supply for a growing world population (Lemaux, 2008, 2009; Mittler and Blumwald, 2010). The acclimation of plants to abiotic stress conditions is a complex and coordinated response involving hundreds of genes. These responses are also affected by interactions between different environmental factors and the developmental stage of the plant and could result in shortened life cycle, reduced or aborted seed production, or accelerated senescence (Mittler and Blumwald, 2010).

The central dogma of abiotic stress research in plants is to study how plants sense and acclimate to abiotic stress conditions, and then use this knowledge to develop crops with enhanced tolerance to abiotic stresses (Mittler and Blumwald, 2010). Significant progress has been made in understanding the physiological, cellular and molecular mechanisms of plant responses to environmental stress factors, and significant achievements with relevance to agriculture has been obtained (Vinocur and Altman, 2005; Mittler and Blumwald, 2010). In fact, the development of new methodologies has been a major driving force in this research. For instance, microarray technology have driven much of the research into transcriptional networks during abiotic stress, whole-genome sequencing and chromatin immunoprecipitation have driven research into epigenetic control of gene expression during stress, and metabolic profiling has driven research into metabolic networks and their role in stress tolerance (Mittler and Blumwald, 2010).

Gene-centered functional studies, either by forward genetics, in which the mutant population is screened for a phenotype of interest or by reverse genetics, which goes from gene selection to detection of a visible phenotype, allow to get information about the function of genes within the complex network that is the plant abiotic stress response (Alonso and Ecker, 2006; Azevedo *et al.*, 2011). Modulating the response of these genes in crops and cultivars-of-interest is a most relevant strategy for plant improvement, and fundamental knowledge obtained in *Arabidopsis thaliana* has been systematically translated to plants of higher agronomic interest. Recent examples include an easier and cheaper method to extract sugars from plant material developed in *Arabidopsis* to meet biofuel demands; identification of a master regulator of plant root hair growth as the nutrient mining machinery to enhance the plant root system; the extraction of petroleum precursors from plants to produce green plastic; an *Arabidopsis* gene that confers resistance in Brassica; insight into chromosome imbalances and predictable plant defects; and an *Arabidopsis* gene employed by the Monsanto company to improve soybean yields (MASC Report, 2011). These studies, in their gene-centric approach, are best carried out in model organisms such as *Arabidopsis thaliana*. Therefore, they will continue to be pivotal tools in the extending of knowledge that will allow us to face the challenges ahead, increasing crop yield and tolerance, and ultimately diminishing hunger worldwide (MASC Report, 2011). Although, despite this enormous research endeavor, knowledge on the capacity of plants to cope with all these stresses is still clearly insufficient, as the roles of many genes in enhancing abiotic stress tolerance are still functionless in the whole-plant concept (Ahuja *et al.*, 2010).

### **Drought Stress and Stomatal Regulation**

Drought or continuous water deficit is one of the most important factors affecting plant growth, development, survival and crop productivity (Boyer, 1982; Ahuja *et al.*, 2010). Physiological responses to drought include stomatal closure, decreased photosynthetic activity, altered cell wall elasticity, and even generation of toxic metabolites causing plant death. Concomitant molecular re-programming includes extensive changes in gene expression incurring alterations in the biochemical and proteomic machinery (Ahuja *et al.*, 2010). As the control of transpirational water movement through stomata is a major factor in drought tolerance and water balance (Hetherington and Woodward, 2003), in the present thesis, specific focus is given to briefly stomatal regulation.

The opening and closing of stomata is mainly regulated by the plant hormone abscisic acid (ABA) (Li *et al.*, 2006). Although ABA has broad functions in plant growth and development, its main function is to promote plant adaptation to distinct stress factors, mainly drought (Ahuja *et al.*, 2010). The importance of ABA in response to water stress is arguably due to its involvement in stomatal closure, as this process is critical for the regulation of plant water balance and osmotic stress tolerance (Horton, 1971; Tucker and Mansfield, 1971; Li *et al.*, 2006). The concentration of ABA increases under drought and induces stomatal closure through second messengers such as ROS (Pei *et al.*, 2000; Borsani *et al.*, 2002). The obvious result of stomatal closure is decreased transpiration rate and, consequently, the water consumed by the plant. The decline in stomatal conductance (and the parallel decline concentration values of intercellular CO<sub>2</sub>) leads to a reduction assimilation of CO<sub>2</sub> and induces other associated effects, such as the accumulation of reducing power and susceptibility to photoinhibition and/or photooxidation (Ma *et al.*, 2006). The guard cells, which generate the stomatal pore, respond to changes in water levels using the ABA as the main signal. Plants ABA-deficient mutants or insensitive to ABA tend to wilt and cannot withstand water stress conditions due to stomatal closure deregulation (Zhu, 2002). The closing of stomata is mediated by a reduction in pressure of guard cell turgor due to water outlet, which is caused by efflux of K<sup>+</sup>, the sucrose removal and conversion of malate into starch, which is osmotically inactive (Schroeder *et al.*, 2001). ABA induces hydrogen peroxide production and reorganization of the cytoskeleton, specifically actin that is a key to stomatal closure (Eun and Lee, 1997; Hwang and Lee, 2001). Hydrogen peroxide in turn activates Ca<sup>2+</sup> channels causing an increase in cytosolic Ca<sup>2+</sup>, which is the responsible for the regulation of ion channels (McAinsh, 1990; Pei *et al.*, 2000).

## 1.2. REACTIVE OXYGEN SPECIES IN PLANT DEVELOPMENT

Highly reactive reduced oxygen molecules, usually designated **Reactive Oxygen Species** (ROS), are continuously produced in plants as byproducts of aerobic metabolism (Halliwell and Gutteridge, 1999). In plants, the major ROS include hydrogen peroxide (H<sub>2</sub>O<sub>2</sub>), superoxide anion (O<sub>2</sub><sup>-</sup>), singlet oxygen (<sup>1</sup>O<sub>2</sub>) and hydroxyl radical (HO·) (Mittler *et al.*, 2004; Moller *et al.*, 2007). ROS are the products of the sequential reduction of molecular oxygen (Figure 1.1).

One-electron reduction of  $O_2$  forms the  $O_2^{\cdot-}$  and  $HO_2^{\cdot}$ . A second one-electron reduction forms  $H_2O_2$ , and a third one-electron reduction produces the  $HO^{\cdot}$ . Water is formed when  $HO^{\cdot}$  is further reduced (Halliwell and Gutteridge, 1999).

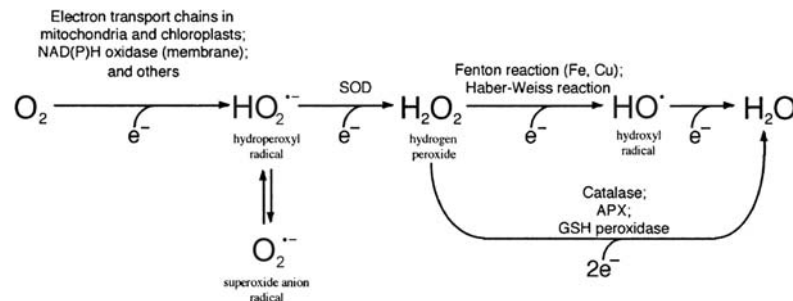


**Figure 1.1 – Major Reactive Oxygen Species in Plants**

In the sequential univalent process by which  $O_2$  undergoes reduction, several intermediates are formed. Some of the important enzymes in reactive oxygen species metabolic pathways like superoxide dismutase (SOD), catalase, ascorbate peroxidase (APX) and glutathione (GSH), are illustrated. Adapted from Mori and Schroeder (2004).

Depending on the nature of the ROS species, some are highly toxic and rapidly detoxified by various cellular enzymatic and nonenzymatic mechanisms (Apel and Hirt, 2004). Whereas plants are surfeited with mechanisms to combat increased ROS levels during abiotic stress conditions, in other circumstances plants appear to purposefully generate ROS as signalling molecules to regulate processes such as growth, development, hormone signalling, and biotic and abiotic stresses (Apel and Hirt, 2004; Laloj *et al.*, 2004; Mittler *et al.*, 2004; Moller *et al.*, 2007). In plants, controlling ROS toxicity while enabling ROS to act as signalling molecules appears to require a large genetic network. Different developmental or environmental signals feed into the ROS signalling and perturb ROS homeostasis in a cell-specific or even compartment-specific manner. The intensity, duration and localization of the different ROS signals are determined by interplay between the ROS-producing and ROS-scavenging pathways of the cell (Mittler *et al.*, 2004; Mittler *et al.*, 2011).

### Production of ROS in plants

Organelles with a highly oxidizing metabolic activity or with an intense rate of electron flow, such as chloroplasts, mitochondria and peroxisomes, are a major source of ROS production in plant cells (Mittler *et al.*, 2004; Moller *et al.*, 2007). The chloroplasts produce  $^1O_2$  at photosystem II and  $O_2^{\cdot-}$  at photosystem I (Asada, 2006) and photosystem II (Pospisil *et al.*, 2004) as byproducts (Figure 1.1). The mitochondria produce  $O_2^{\cdot-}$  at complexes I and III, also as byproducts (Figure 1.1).



An estimated 1-5% of the oxygen consumption of isolated mitochondria results in ROS production (Moller, 2001). The peroxisomes produce  $O_2^{\cdot-}$  and  $H_2O_2$  in several key metabolic reactions (del Rio *et al.*, 2006). And, finally, the NADPH oxidase in the plasma membrane produces  $O_2^{\cdot-}$ , which participates in processes such as development and tolerance to biotic and abiotic stresses (Torres and Dangl, 2005) (Figure 1.1). During endogenous ROS elevation, the superoxide anion produced by a plasma membrane NADPH oxidase can be converted to  $H_2O_2$  by superoxide dismutases (SOD) in the apoplast.  $H_2O_2$  can give rise to  $HO^{\cdot}$  through the Fenton reaction, which is catalysed mainly by free transition metal ions (such as  $Cu^{2+}$  or  $Fe^{2+}$ ) (Fry, 1998; Halliwell and Gutteridge, 1999; Foreman *et al.*, 2003) (Figure 1.1).  $HO^{\cdot}$  are the most reactive and toxic ROS and interact directly with most target biomolecules (Halliwell and Gutteridge, 1999).

### **Cellular localization and coordination of the ROS scavenging pathways of plants**

The balance between ROS production and the activities of these ROS-removing systems determines the type and concentration of ROS present and thus to what extent signalling and/or damage will occur. Plant cells possess a range of non-enzymatic as well as enzymatic mechanisms to scavenge oxygen radicals (Apel and Hirt, 2004). A sensible energetic effort is diverted to the removal of  $O_2^{\cdot-}$  and  $H_2O_2$ , which are the main oxygen radicals being produced and are the source of  $HO^{\cdot}$  (Halliwell and Gutteridge, 1999; Mittler, 2002). Detoxification of  $O_2^{\cdot-}$  and  $H_2O_2$  is possible through enzymatic catalysis. The main enzymatic mechanisms of scavenging ROS include the enzymes superoxide dismutase (SOD), catalase (CAT), ascorbate peroxidase (APX) and glutathione peroxidase (GPX) (Mittler, 2002). SODs catalyse the dismutation of  $O_2^{\cdot-}$  into  $H_2O_2$ , whereas CAT, APX and GPX are involved in  $H_2O_2$  detoxification (Bowler *et al.*, 1991; Mittler, 2002) (Figure 1.1). Unlike CAT, APX and GPX require reducible substrates such as the antioxidants ascorbate and reduced glutathione, respectively (Noctor and Foyer, 1998). Peroxiredoxin (PrxR) is also capable of  $H_2O_2$  reduction (Rouhier and Jacquot, 2002).

The various scavenging enzymes can be found in almost every subcellular compartment. In addition, usually more than one enzymatic scavenging activity per a particular ROS can be found in each of the different compartments (e.g. GPXs, PrxRs and APXs in the cytosol and chloroplast, and APXs and CATs in peroxisomes) (Mittler *et al.*, 2004) (Figure 1.2). When the relative function of the different enzymes in the different cellular compartments is considered, it is important to remember that ROS such as  $H_2O_2$  can diffuse between different compartments (Bienert *et al.*, 2006; Bienert *et al.*, 2007). Furthermore, transporters for the antioxidants ascorbic acid and

glutathione are central in determining the specific concentrations of these compounds and the redox potential in the different cellular compartments (Noctor and Foyer, 1998; Pignocchi and Foyer, 2003; Mittler *et al.*, 2004).

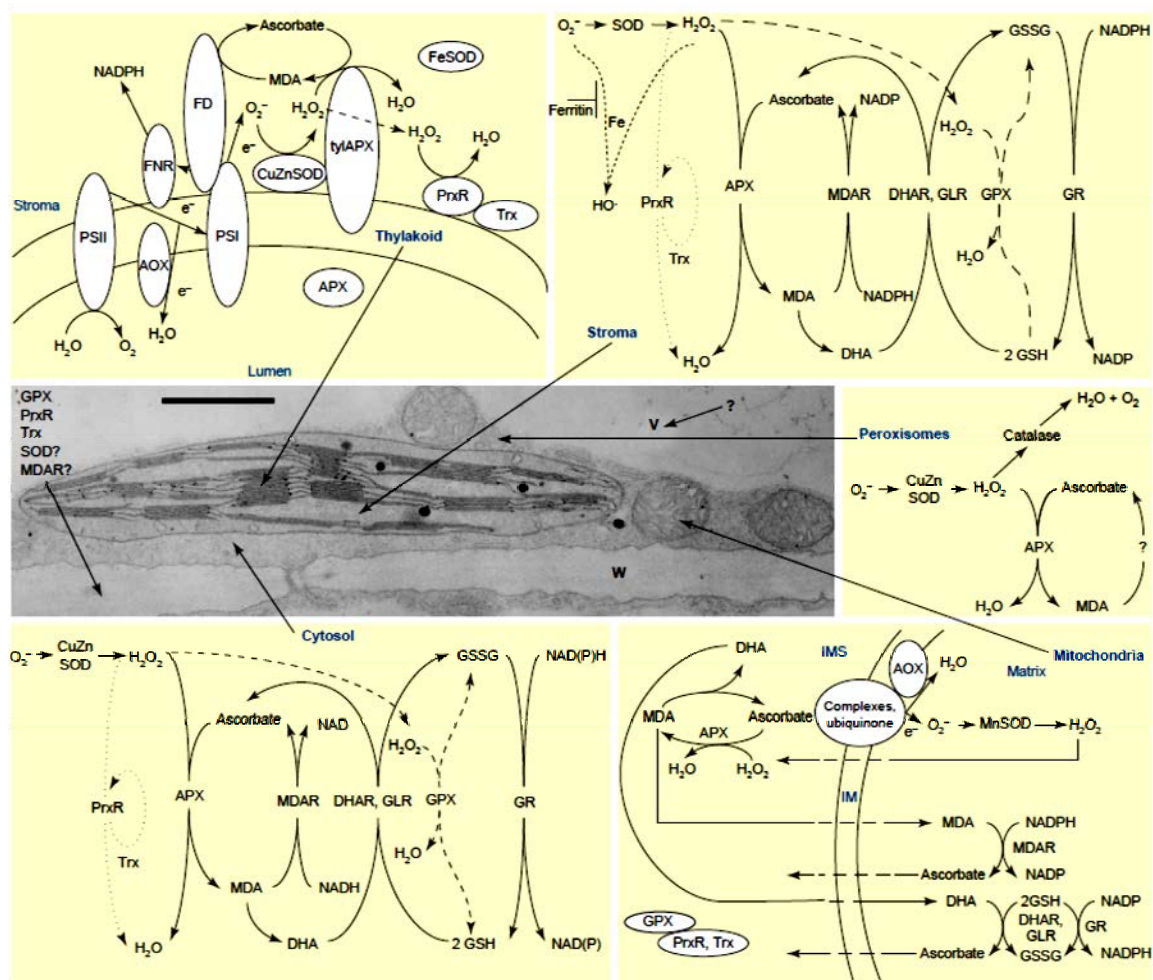


**Figure 1.2 – Subcellular ROS Generated Compartments and Major ROS Scavenging Pathways**

The enzymatic pathways responsible for ROS detoxification are in different cell compartments. In chloroplasts, the water–water cycle detoxifies  $O_2^-$  and  $H_2O_2$ , and alternative oxidase (AOX) reduces the production rate of  $O_2^-$  in thylakoids (top left). ROS that escape this cycle and/or are produced in the stroma undergo detoxification by the stromal ascorbate–glutathione cycle involving ascorbate peroxidase (APX) and Cu, Zn-SOD or Fe-SOD. Peroxiredoxin (PrxR) and glutathione peroxidase (GPX) are also involved in  $H_2O_2$  removal in the stroma (top right). ROS produced in peroxisomes during photorespiration, fatty acid oxidation or other reactions are decomposed by SOD, catalase (CAT) and APX (middle right). SOD and other components of the ascorbate–glutathione cycle are also present in mitochondria. In addition, AOX prevents oxidative damage in mitochondria (bottom right). In principle, the cytosol contains the same set of ROS-scavenging enzymes found in the stroma (bottom left). The enzymatic components responsible for ROS detoxification in the apoplast and cell wall (W), and the ROS scavenging pathways at the vacuole (V) are not described in the present figure. Membrane-bound enzymes are depicted in white, GPX pathways are indicated by dashed lines and PrxR pathways are indicated by dotted lines in the stroma and cytosol. Although the pathways in the different compartments are mostly separated from each other,  $H_2O_2$  can easily diffuse through membranes and antioxidants such as glutathione and ascorbic acid (reduced or oxidized) can be transported between the different compartments. (DHA, dehydroascorbate; DHAR, DHA reductase; FD, ferredoxin; FNR, ferredoxin NADPH reductase; GLR, glutaredoxin; GR, glutathione reductase; GSH, reduced glutathione; GSSG, oxidized glutathione; IM, inner membrane; IMS, IM space; MDA, monodehydroascorbate; MDAR, MDA reductase; PSI, photosystem I; PSII, photosystem II; Trx, thioredoxin; tyl, thylakoid). From Mittler *et al.* (2004).

## **NADPH Oxidases Generate ROS Involved in Stomatal Regulation and Plant Development**

ROS that have been shown to play a role in development and stomatal closure are produced by NADPH oxidases (NOXs) (Torres and Dangl, 2005; Gapper and Dolan, 2006; Kwak *et al.*, 2006). The plant NOX proteins are analogs to the enzymes first identified in mammals that are responsible for the respiratory burst that occurs in activated mammalian neutrophils (Segal and Abo, 1993) and were identified by their homology to the catalytic subunit gp91<sup>phox</sup> of mammalian phagocyte NOX (Torres *et al.*, 1998). In Arabidopsis (*Arabidopsis thaliana*), NADPH oxidases genes are referred to as ***Arabidopsis thaliana* respiratory burst oxidase homologues (*Atrboh*)** (Keller *et al.*, 1998; Torres *et al.*, 1998). Plant NADPH oxidases are predicted to be localized in the plasma membrane, where they transfer electrons from cytosolic NADPH or NADH to apoplastic oxygen, leading to the production of apoplastic superoxide (Sagi and Fluhr, 2006). It is important to note that, O<sub>2</sub><sup>-•</sup> produced by NADPH oxidases readily gives rise to other ROS including H<sub>2</sub>O<sub>2</sub>, by dismutation, and the HO<sup>•</sup> via the Fenton reaction (Halliwell and Gutteridge, 1999), like previously described in this chapter.

In Arabidopsis, there are 10 known members of the *rboh* gene family (Torres and Dangl, 2005). The activity of three members of this family has been shown to be involved in various aspects of stomatal regulation (Kwak *et al.*, 2003) and root growth (Foreman *et al.*, 2003). The regulation of stomatal closure involves various control points that help the plant to adapt to a variety of environments (Hetherington and Woodward, 2003). ROS are essential signals in this complex regulatory network, mediating stomatal closure induced by the plant hormone ABA (Kwak *et al.*, 2006). In stomata, ABA induces the production of H<sub>2</sub>O<sub>2</sub> in guard cells, that activate the calcium-permeable channels in the plasma membrane, which in turn increase the cytosolic concentration of Ca<sup>2+</sup> and lead to stomatal closure (McAinsh, 1990; Pei *et al.*, 2000). The NADPH oxidases proteins *AtrbohD* and *AtrbohF* were identified as the responsible for the H<sub>2</sub>O<sub>2</sub> production during ABA-induced stomatal closure (Kwak *et al.*, 2003). If H<sub>2</sub>O<sub>2</sub> production by *AtrbohD* and *AtrbohF* NADPH oxidases is blocked, ABA-induced closure of stomata is inhibited. The *atrbohD/F* double mutations impair ABA-induced stomatal closing, ABA promotion of ROS production, ABA-induced cytosolic Ca<sup>2+</sup> increases and ABA activation of plasma membrane calcium-permeable channels in guard cells while exogenous H<sub>2</sub>O<sub>2</sub> rescues both Ca<sup>2+</sup>-channel activation and stomatal closing in *atrbohD/F* double mutant (Kwak *et al.*, 2003). However, ROS derived from the *AtrbohD* and *AtrbohF* proteins are not only involved in the stomatal response to ABA, but rather in the ABA-signalling mechanism that controls plant growth responses in drought conditions.

The roots of plants lacking both *AtrbohD* and *AtrbohF* (*atrbohD/F* double mutants) are indistinguishable from the wild-type, indicating that they are not involved in growth per se under standard conditions, but the double-mutant roots are less sensitive to the inhibitory effects of ABA on root elongation (Kwak *et al.*, 2003). Another NADPH oxidase, the *AtrbohC* protein, also known as ROOT HAIR DEFECTIVE2 (*RHD2*), is known to be required for root elongation under normal growth conditions. The roots of plants homozygous for loss-of-function *rhd2* mutations have decreased levels of ROS and are 20% shorter than the wild-type, indicating that cell expansion is defective in these plants (Foreman *et al.*, 2003). Similarly, inhibitor experiments suggest that the promotion of maize root growth may be under the control of NADPH oxidases (Liszky *et al.*, 2004). Therefore, there are at least two distinct ROS-requiring mechanisms that occur during root growth in *Arabidopsis*. There is the requirement of *RHD2/AtrbohC* for elongation (Foreman *et al.*, 2003) and there is an ABA related growth inhibition process that requires *AtrbohD* and *AtrbohF* (Kwak *et al.*, 2003). In addition to its role in root elongation, the *AtrbohC* protein is required for root hairs development mediated by activation of  $Ca^{2+}$  channels (Foreman *et al.*, 2003). The *RHD2/AtrbohC* activity produces ROS that accumulate at the tip of root hairs allowing their growth. Relatively high cytoplasmic  $Ca^{2+}$  are found at the tip, leading to the formation of a so-called tip-high calcium gradient, and this gradient is absent in the *rhd2* mutant (Wymer *et al.*, 1997; Foreman *et al.*, 2003).

Whereas the above evidence supports clearly a role for NADPH oxidases in root elongation and root hairs development, there is also evidence that NADPH oxidase-derived ROS are required for plant development during the growth of other organs besides roots. During leaf expansion, a wave of ROS-dependent cell growth sweeps through the leaf (Rodriguez *et al.*, 2002). This local expansion zone is the site of the accumulation of ROS, and inhibition of ROS formation by treatment with diphenylene iodonium (DPI), a general inhibitor of flavin-containing enzymes, inhibits leaf growth. This indicates that not only are ROS involved in growth, but also that a flavin-containing oxidase such as a NADPH oxidase is required for its production (Gapper and Dolan, 2006). Furthermore, the accelerated elongation that occurs upon auxin treatment is accompanied by the formation of higher levels of ROS than in coleoptiles grown without auxin treatment (Rodriguez *et al.*, 2002; Schopfer *et al.*, 2002). This suggests that the rate of cell growth may be proportional to the amount of ROS produced in growing organs (Gapper and Dolan, 2006). Suppression of tomato *rboh* gene expression by the antisense approach not only had both reduced NADPH oxidases activity and ROS levels, but also exhibited a number of morphological defects,

including reduced apical dominance, leading to an increase in branching, reduced leaf lobbing, and curled leaflets (Sagi *et al.*, 2004). These phenotypes suggest that ROS control more developmental processes than just cell expansion, like apical dominance and leaf shape (Gapper and Dolan, 2006).

### **Small GTPases Spatially Control ROS Production and Growth**

The regulation of NADPH oxidase is an issue of an important consideration to understand NADPH oxidase derived ROS controls plant growth and development. In addition to the NOX catalytic subunit, gp91<sup>phox</sup>, mammalian phagocyte NOX consists of a complex of different regulatory subunits, among which the small GTPase of the Rho class, Rac2, is a key regulator of the NOX activity (Diekmann *et al.*, 1994; Diebold and Bokoch, 2001). In the absence of other homologs of the mammalian NOX subunits (Sagi and Fluhr, 2001), the small GTPase of the Rho class (called ROPs in plants) becomes a prime candidate for being a regulator of plant NADPH oxidase. There are 11 genes encoding ROP GTPases in Arabidopsis with different expression profiles as reviewed by (Vernoud *et al.*, 2003). In *A. thaliana*, ROP2, ROP4 and ROP6 have been shown to be involved in correct cellular expansion in the root elongation zone, the establishment of the tip-high Ca<sup>2+</sup> gradient and root-hair growth (Molendijk *et al.*, 2001; Jones *et al.*, 2002), and experimental studies with rice Rboh proteins revealed that binding of a Rho-GTPase to the N-terminal a rice NADPH oxidase is important for activating NADPH oxidase activity (Wong *et al.*, 2007). Furthermore, genetic evidences obtained through the characterization of Rho GTPase GDP dissociation inhibitor (RhoGDI), suggest that ROPs are involved in spatial regulation of ROS production, which leads to spatial control of growth (Carol *et al.*, 2005; Carol and Dolan, 2006). The RhoGDI proteins are thought to negatively regulate the GTPase 'switch' by maintaining the GTPase in a GDP-bound 'inactive' state (Yang, 2002). In Arabidopsis, loss of function of one member of the RhoGDI family, called SUPERCENTIPEDE1 (SCN1)/AtRhoGDI1, results in both spatially deregulated ROS accumulation and root hair outgrowth. Additionally, the ectopic sites of ROS accumulation in the *scn1/atrhogdi1* mutant require the activity of RHD2/AtrbohC, indicating that spatial regulation of RHD2/AtrbohC involves SCN1/AtRhoGDI1 (Carol *et al.*, 2005). Like RHD2/AtrbohC, ROPs (ROP2, ROP4 and ROP6) also localize to the growing region of the hair tip (Molendijk *et al.*, 2001; Jones *et al.*, 2002; Takeda *et al.*, 2008). SCN1/RhoGDI1 is likely to act by regulating a ROP. It can interact with ROP4 and ROP6 in yeast two-hybrid and in vitro assays (Bischoff *et al.*, 2000). Knowing that, it has been proposed that, if SCN1/AtRhoGDI1 were active in the spatial control of growth, then it

might be expected that its regulatory targets, the ROP GTPases, should also be involved (Gapper and Dolan, 2006).

### **1.3. THE SELECTIVE DEGRADATION OF PROTEINS IN CELLULAR REGULATION AND QUALITY CONTROL**

Several aspects of plant physiology, growth, and development are controlled by the selective removal of short-lived regulatory proteins. Moreover, as sessile organisms, plants must adapt their growth and development to protect themselves from detrimental conditions by triggering a variety of signaling pathways, including the activation of the ubiquitin-mediated protein degradation pathway. The removal of these proteins by various quality control pathways within the ubiquitin-26S proteasome system (UPS) is critical for cell survival. Genome-wide studies have revealed that the UPS in particular is a large and complex mechanism for protein removal, occupying nearly 6% of the *Arabidopsis thaliana* proteome, with potentially thousands of additional proteins serving as targets (Vierstra, 2003; Smalle and Vierstra, 2004). Moreover, genetic studies enabled by genome-based programs such as the *Arabidopsis* 2010 project, revealed that the UPS impacts nearly every aspect of plant growth and development including the cell-cycle, embryogenesis, senescence, defense, environmental responses, and hormone signaling (Vierstra, 2009). The ubiquitin-proteasome pathway is of such importance for cellular regulation that in 2004 the Nobel Prize in Chemistry was awarded to Aaron Ciechanover, Avram Hershko and Irwin Rose for their pioneering biochemical studies utilizing a reticulocyte lysate expression system to discover and characterize ubiquitin and the enzyme activities required to conjugate it to substrates (Wilkinson, 2005).

#### **The Ubiquitin Proteasome System**

The selective degradation of many short-lived proteins in eukaryotic cells is carried out by the ubiquitin proteasome system. In the ubiquitin proteasome system a small protein, ubiquitin (Ub), is covalently attached to target proteins and either regulates their function or marks them for destruction by the multisubunit 26S proteasome (Figure 1.3) (Hershko and Ciechanover, 1998; Mukhopadhyay and Riezman, 2007; Deshaies and Joazeiro, 2009). The consequence of this post-

translational modification depends on the extent of polyubiquitination and the position of the ubiquitin linkage in the polyubiquitin chain (Chau *et al.*, 1989; Thrower *et al.*, 2000; Haglund *et al.*, 2003; Hicke *et al.*, 2005).

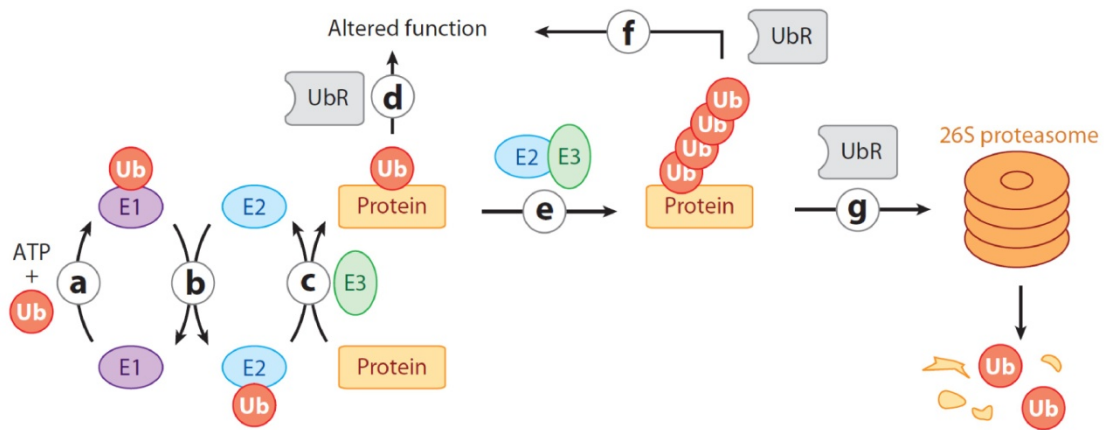


**Figure 1.3 – Schematic Representation of the Ubiquitin Proteasome System**

(a) Ubiquitin (Ub) and ubiquitin-like proteins are activated for transfer by E1 (ubiquitin-activating enzyme). (b) Activated ubiquitin is transferred in thioester linkage from the active-site cysteine of E1 to the active-site cysteine of an E2 ubiquitin-conjugating enzyme. (c) The E2-Ub thioester next interacts with an E3 ubiquitin ligase, which effects transfer of Ub from E2-Ub to a lysine residue of a substrate. Monoubiquitinated substrate can either dissociate from E3 (d) or can acquire additional Ub modifications in the form of multiple single attachments (not shown) or a ubiquitin chain (e). The chain can be knit together via different lysine residues of ubiquitin. Whereas monoubiquitin and some types of chains (e.g., those assembled via Lys63 of ubiquitin) serve mainly to alter the function of the modified protein (f) (by changing its structure, binding partners, cellular localization, etc.), polyubiquitin chains assembled via the Lys48 residue of ubiquitin typically direct the appended substrate to the proteasome for degradation (g). The biological outcome of ubiquitination, be it degradation or signaling, is normally dictated by ubiquitin receptors (UbR) that bind and interpret the ubiquitin signal. Figure retrieved from (Deshaies and Joazeiro, 2009)

Usually, proteins that are targeted for degradation by the 26S proteasome are covalently modified by the attachment of a polyubiquitin chain (Figure 1.3). This is achieved in a multistep reaction, sequentially involving an E1 enzyme (ubiquitin activating enzyme), an E2 enzyme (ubiquitin-conjugating enzyme [UBC]), and an E3 enzyme (ubiquitin ligase) (Hershko and Ciechanover, 1998). Substrate specificity is mainly determined by E2 but mainly by E3 enzymes. Therefore, in the *Arabidopsis thaliana* genome, there are 37 E2s and over 1400 E3s (Vierstra, 2009). The E3 ubiquitin ligases comprise a diverse family of proteins or protein complexes that can be distinguished based on the type of interaction domain (RING domain, U-box domain, or HECT domain) used to bind E2 enzymes and whether they act as single subunits or multisubunit complexes (Moon *et al.*, 2004; Santner and Estelle, 2010). In the *Arabidopsis* UPS, the most abundant E2 interaction domain is found in the approximately 465 RING (Really Interesting New Gene) proteins that are characterized by a approximately 70 amino acid motif known as a RING

finger (Deshaies and Joazeiro, 2009; Santner and Estelle, 2010). The RING finger is a zinc-binding motif that binds to the E2 Ub-conjugating enzyme during the ubiquitin conjugation cascade (Deshaies and Joazeiro, 2009). Moreover, the RING E3s ligases are enzymes that bind ubiquitin-conjugating (E2) enzyme and substrate catalyzing direct transfer of ubiquitin from E2 to substrate (Deshaies and Joazeiro, 2009).

### **The Endoplasmic Reticulum-Associated Degradation in Protein Quality Control**

Some nascent proteins that fold within the endoplasmic reticulum (ER) never reach their native state. It was estimated that ~30% of newly synthesized proteins in mammalian cells are inappropriately folded (Schubert *et al.*, 2000). The accumulation of unfolded proteins in the ER can be induced by impairment of protein folding derived from mutation, perturbation of protein-protein interactions, or different biotic and abiotic stress stimuli (Vembar and Brodsky, 2008). Misfolded proteins accumulating in the lumen or membrane of the endoplasmic reticulum (ER) cause the unfolded protein response (UPR), a collection of signaling pathways that adapt cells to ER stress (Travers *et al.*, 2000). These misfolded proteins are removed from the folding machinery, dislocated from the ER into the cytosol, and degraded in a series of pathways collectively referred to as **Endoplasmic Reticulum-Associated Degradation (ERAD)** (Vembar and Brodsky, 2008; Smith *et al.*, 2011). ERAD is a specific ubiquitin/proteasome system associated with the ER. Similar to the general ubiquitination/degradation systems, it requires ubiquitin-activating enzyme (E1), ubiquitin-conjugating enzyme (E2), ubiquitin ligase (E3), and 26S proteasome, as well as other associated proteins (Hampton and Garza, 2009).

### **Distinct ERAD Pathways for the Degradation of ER Proteins in Yeast**

Proteins transiting the ER can be soluble or membrane bound with significant portions in the lumen, membrane, and cytosol. To accommodate the topological diversity, distinct pathways work side by side to monitor misfolding. Substrates are targeted to an appropriate ERAD pathway depending on the site of the misfolded lesion (Ismail and Ng, 2006). Most of our knowledge on ERAD came from genetic/biochemical studies in yeast and mammalian systems (Hampton and Garza, 2009). Due to the availability of mutant strains and well-characterized ERAD substrates, recently studies performed in yeast allowed an extensive comprehension of the ERAD system. Yeast has at least three different ERAD pathways, known as ERAD-L, ERAD-M, and ERAD-C, to remove misfolded proteins with folding defects exposed in the ER lumen (L), ER membrane (M),



and cytosol (C), respectively (Vashist and Ng, 2004; Carvalho *et al.*, 2006). The central component of the three ERAD pathways is an ER membrane-localized ubiquitin ligase (E3) Doa10<sup>a</sup> and Hrd1, both containing multiple transmembrane segments and a cytosolic-facing E3-catalytic RING domain, that ubiquitinates misfolded proteins (Kostova *et al.*, 2007). The Doa10 and Hrd1 E3 ligases form two distinct membrane protein complexes that define the distinct ERAD pathways: the Doa10 complex used by the ERAD-C pathway and Hrd1p complex used by the ERAD-L/-M pathway (Ismail and Ng, 2006). The Doa10 complex, aside from Doa10 E3 ligase, contains an E2 complex (Ubc7 and its membrane-anchoring factor Cue1) and the Cdc48 complex (the AAA-ATPase Cdc48, its cofactors Ufd1 and Npl4, and its membrane anchorage protein Ubx2 (Carvalho *et al.*, 2006) (Figure 1.4). The Hrd1 complex shares some common components with the Doa10 complex, namely the Ubc7/Cue1 dimer and the Cdc48 complex, partners of Doa10 (Carvalho *et al.*, 2006). In addition, other components, like: Hrd3 protein, an ERAD factor with a large ER luminal domain that form a 1:1 complex with Hrd1 protein (Gardner *et al.*, 2000); Der1 protein; Yos9 protein; and Usa1 protein are unique to the Hrd1 complex (Figure 1.4) (Carvalho *et al.*, 2006). Analysis of pathway-specific substrates showed that the same Hrd1 core complex is employed in both ERAD-M and ERAD-L, although only a subset of the components is functionally required for ERAD-M (Carvalho *et al.*, 2006).

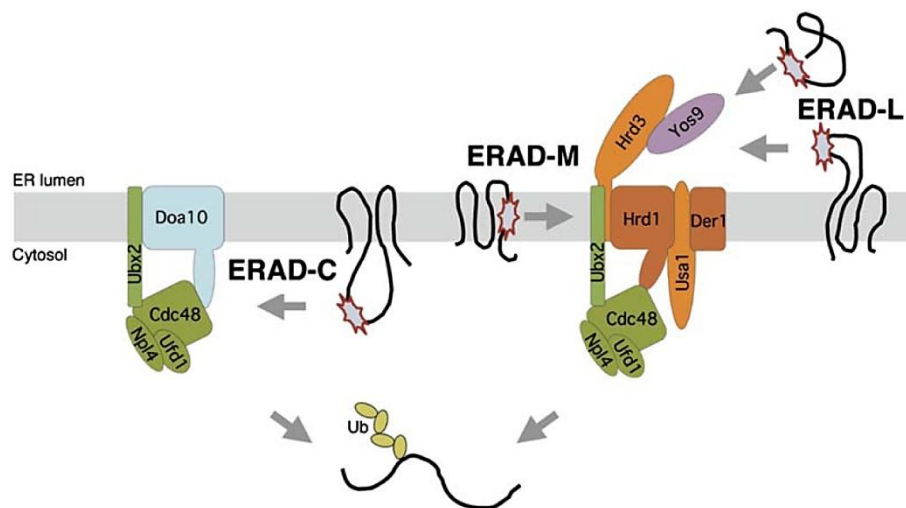


**Figure 1.4 – Distinct Ubiquitin-Ligase Complexes Defining Different ERAD Pathways in Yeast**

The scheme shows the ubiquitin-ligase complexes involved in the ERAD-L, -M, and -C pathways. Components in orange and green belong to the Hrd1 protein core and Cdc48 protein ATPase complexes, respectively. Stars show the location of the misfolded domain of a substrate. Ub is ubiquitin. Figure retrieved from Carvalho *et al.* (2006).

<sup>a</sup> *Saccharomyces cerevisiae* proteins are referred to by the relevant gene symbol, non-italic, initial letter uppercase.

## **The Endoplasmic Reticulum-Associated Degradation in Cellular Regulation**

So far, in the present thesis, ERAD system was described in the context of protein degradation as quality control. The ERAD process is responsible for the destruction of proteins transiting the ER, that can be soluble or membrane bound with significant portions in the lumen, membrane, and cytosol. This degradation process functions in protein quality control, where damaged or unfolded proteins are selectively targeted for degradation, while correctly folded ones are spared. However, ERAD is not restricted to aberrant proteins and is also employed for selective degradation of correctly folded proteins underlying cellular regulation (Hampton, 2002; Hampton and Garza, 2009). In yeast and mammalian cells, the ERAD system is employed for the regulated degradation of normal proteins such as the **HMG**-coenzyme (CoA) **R**eductase (HMGR) (Hampton and Garza, 2009). HMGR is a rate-limiting enzyme of the mevalonate pathway, by which sterols and a variety of essential isoprenoids are synthesized (for details, see above). In yeast and mammalian cells, feedback regulation of the sterol pathway centers on regulated degradation of HMGR (Hampton and Garza, 2009). When flux through the sterol pathway is high, degradation rate is high and therefore the levels of HMGR are reduced. When flux is low, degradation rate is low and enzyme levels increase in order to activate the pathway. Depending on cell type and signal strength, HMGR half life can vary between >10 h, and <20 min (Hampton, 2002). Yeast has two HMGR isozymes, Hmg1 and Hmg2. Nevertheless, only the Hmg2 isozyme undergoes regulated degradation, in a manner strikingly similar to the mammalian enzyme: high flux through the sterol pathway promotes more degradation, while diminished production of sterol pathway products causes high stability (Hampton and Garza, 2009). In yeast, numerous genetic analyses were conducted to find the HRD genes responsible for **Hmg-CoA R**eductase **D**egradation, and only the Hrd1/Hrd3 ERAD complex has been associated with regulated degradation of HMGR (Hampton et al., 1996). Moreover, in yeast, the ER-associated Hrd1p ligase is absolutely required for regulated degradation of Hmg2p. In the absence of Hrd1, Hmg2 is completely stable no matter what the level of sterol pathway activity (Hampton *et al.*, 1996).

## **Conserved Endoplasmic Reticulum-Associated Protein Degradation in Plants**

Compared with the level of knowledge regarding ER stress signalling in yeast and mammalian cells, understanding of these processes in plants is limited. As most components of ERAD are evolutionarily conserved, the basic conclusions derived from studies performed using yeast and mammals are likely to be applicable to all eukaryotes. In yeast, one cellular function of

the Cdc48 protein is a direct contribution to the retrotranslocation of ERAD substrates at an intermediate step preceding proteasomal protein degradation in mammalian cells and yeast (Jarosch *et al.*, 2002). An earlier study suggested the involvement of Arabidopsis Cdc48 homolog, in the degradation of mutated barley **mildew-resistance locus O** (MLO) protein when expressed in Arabidopsis (Muller *et al.*, 2005). In yeast, Der1 is a small protein that spans the ER membrane four times and was one of the first ERAD factors identified and it comes in direct contact with substrates (Knop *et al.*, 1996). Other study reported the complementation of an ERAD defect of a yeast *der1Δ* mutant by two maize homologs of the yeast/mammalian Derlins (Kirst *et al.*, 2005). Two genome wide gene-expression analyses reported up-regulation of Arabidopsis genes encoding potential homologs of the known yeast/mammalian ERAD components in response to ER stresses (Martinez and Chrispeels, 2003; Kamauchi *et al.*, 2005). More recently, the identification and characterization of some crucial components of the Hrd1 complex, as the ubiquitin E3 ligase and E2 conjugase, that operates in ERAD system, have been reported in Arabidopsis (Liu *et al.*, 2011; Su *et al.*, 2011; Cui *et al.*, 2012). However, the Doa10 complex is still uncharacterized in plants.

#### **1.4. STEROLS IN PLANTS**

Sterols are isoprenoid-derived lipids that play essential roles in plant growth and development (Benveniste, 2004; Phillips *et al.*, 2006). Plant sterols have been extensively studied with a major focus on biosynthetic and biochemical aspects (Schaller, 2003). Sterols are important not only as structural components of eukaryotic cell membranes with an important role in membrane fluidity and permeability (Hartmann, 1998), but also because they are the biosynthetic precursors of steroid hormones in animals, insects and plants (Clouse, 2002; Schaller, 2004). The role of animal steroids in the regulation of embryonic and postembryonic development along with adult homeostasis is well known (Beato *et al.*, 1995). However, cholesterol itself can also serve as a signaling molecule, without conversion to steroid hormones (Farese and Herz, 1998; Edwards and Ericsson, 1999; Bensinger *et al.*, 2008). Whereas in animals, cholesterol is the only structural sterol, plant membranes consist of a variable mixture of several phytosterols, being sitosterol the most abundant (Schaller, 2004).

Brassinosteroids (BRs) are the only sterol derived steroid hormones in plants. The diverse functions of BRs in growth and development have been deeply investigated (Vert *et al.*, 2005; Gendron and Wang, 2007) but little is known about the putative regulatory roles of other phytosterols. Several lines of evidence support the hypothesis that, beside their structural roles, plant sterols also have signaling roles independent of BRs (Clouse, 2002). First, sterol deficient mutants show defects in embryogenesis while BRs-deficient mutants do not. In addition sterol mutants cannot be rescued by BRs treatment (Clouse, 2002). Second, typical sterols such sitosterol and stigmasterol thought to have exclusively a structural role induce the specific expression of genes involved in cell expansion and division (He *et al.*, 2003). Third, lipid/sterol-binding StAR-related lipid transfer (START) protein domains have been identified in plants (Schrick *et al.*, 2004). In fact, START domains are more common in plants than in animals and are primarily found within homeodomain (HD) transcription factors, suggesting a mechanism by which lipid/sterol ligands can directly modulate transcription in plants (Clouse, 2002). Fourth, an intermediate sterol such obtusifoliol can be transported to distal parts of the plant away from the sprayed leaves (O'Brien *et al.*, 2005).

### **Biosynthetic Pathway of Plant Sterols**

Acetyl-Coenzyme A (Acetyl-CoA) serves as a precursor molecule for sterol biosynthesis and is converted into mevalonate (MVA) via several steps (Figure 1.5). The rate-limiting step from 3-hydroxy-3-methylglutaryl-CoA (HMG-CoA) to MVA is catalyzed by HMG-CoA Reductase (HMGR). This enzyme catalyzes the first committed step of the MVA pathway for isoprenoid biosynthesis (Stermer *et al.*, 1994). In plants, the MVA pathway provides precursors for a wide variety of isoprenoid products that are required for sterols biosynthesis, but also for several other functions including: membrane biogenesis, sesquiterpenoid phytoalexins and steroid glycoalkaloids for defense, brassinosteroids and cytokinins for control of growth and development, farnesyl and geranyl groups for protein prenylation, dolichols for protein glycosylation, and ubiquinone for respiration (Stermer *et al.*, 1994; Chappell, 1995).

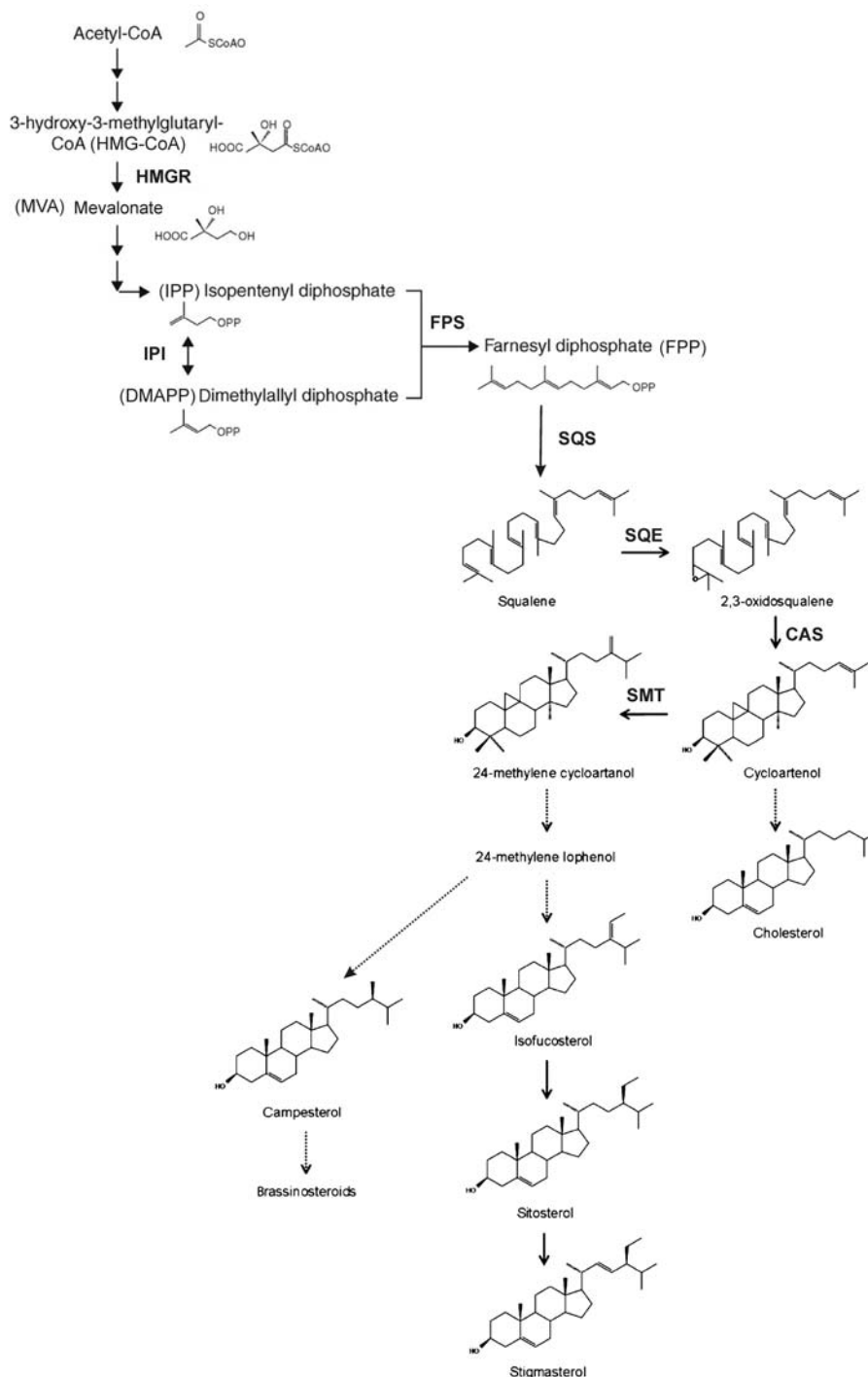


**Figure 1.5 – Simplified Scheme of the Sterol Biosynthesis in Arabidopsis**

Mevalonate (MVA) synthesis from 3-hydroxy-3-methylglutaryl coenzyme A (HMG-CoA) is catalyzed by HMG-CoA Reductase (HMGR). A later step involves isopentenyl isomerase (IPI) that catalyzes the isomerization between isopentenyl diphosphate (IPP) and dimethylallyl diphosphate (DMAPP) in the MVA pathway. These serve as substrates for the production of farnesyl diphosphate (FPP) catalyzed by farnesyl phosphate transferase (FPS). The synthesis of squalene is catalyzed by squalene synthase (SQS) and its epoxidation catalyzed by squalene epoxidase (SQE), producing 2,3-oxidosqualene that is mainly cyclized to cycloartenol which requires cycloartenol synthase (CAS). Cycloartenol is further metabolized to produce steroids, including membrane sterols and brassinosteroids. In sterol biosynthesis schematic representation, only selected steps of sterol biosynthesis are indicated. Downstream squalene, only those intermediates whose levels are discussed below, on the present thesis, are shown. Dashed arrows indicate multiple reactions. The figure is an adaptation of the schemes presented in Boutte and Grebe (2009) and Pose *et al.* (2009).

Sterols are synthesized from isopentenyl diphosphate (IPP) produced through the mevalonate pathway located in the cytosol/endoplasmic reticulum (Figure 1.5). Isopentenyl isomerase (IPI) catalyses the isomerisation between isopentenyl diphosphate (IPP) and dimethylallyl diphosphate (DMAPP) in the MVA pathway. One molecule of DMAPP and two molecules of IPP condense to form farnesyl pyrophosphate (FPP). The tail-to-tail coupling of two molecules of FPP yields squalene, the first committed precursor to the sterol pathway, by action of squalene synthase (SQS), and its epoxidation is catalyzed by squalene epoxidase (SQE), converting squalene to 2,3-oxidosqualene, which is the first oxygenation step in the sterol biosynthetic pathway (Benveniste, 2004; Boutte and Grebe, 2009). From 2,3-oxidosqualene, plant cells use a sterol biosynthetic pathway that is different to that of other eukaryotes (Figure 1.5) (Schaller, 2003; Benveniste, 2004; Schaller, 2004). Following conversion of 2,3-oxidosqualene to cycloartenol, the first cyclic intermediate of plant sterol biosynthesis, the pathway is essentially linear until reaching 24-methylene lophenol. After formation of this compound, there is a bifurcation leading to either 24-methyl sterols, which include campesterol and its derivatives, the brassinosteroids, or 24-ethyl sterols, which include the structural sterols sitosterol and stigmasterol (Clouse, 2002) (Figure 1.5).

### **Regulation of the Plant Sterol Biosynthetic Pathway by HMGR**

Several evidences support that HMGR is the main rate-limiting step in isoprenoid biosynthesis and has a key role in the regulation of the metabolic flux through plant sterol biosynthetic pathway (Figure 1.5). The genome of *Arabidopsis thaliana* contains two differentially expressed HMGR genes, *AtHMG1* and *AtHMG2* that encode three HMGR isoforms: HMGR1S (short isoform), HMGR1L (long isoform) and HMGR2 (Enjuto *et al.*, 1994; Lumbreras *et al.*, 1995). HMGR1S and HMGR1L proteins derive from the HMG1 gene and are identical in sequence, but the 1L isoform has an N-terminal extension of 50 amino acid residues. The analysis of a null HMG1 mutant (*hmg1-1*) evidenced the essential role of this gene in plant development (Suzuki *et al.*, 2004). The *hmg1-1* plants show dwarfism, early senescence, and male sterility. By contrast, disruption of HMG2 does not affect the phenotype neither the fertility of the plant under normal growth conditions, but chemical phenotypes of the *hmg1* and *hmg2* mutants demonstrated that HMG2 as well as HMGR1 is responsible for the biosynthesis of triterpenes in spite of the lack of visible phenotypes in *hmg2* (Ohyama *et al.*, 2007). Moreover, complete blockage of the MVA pathway in *hmg1 hmg2* double mutant results in male gametophyte lethality (Suzuki *et al.*, 2009). More evidences supporting a limiting role of plant HMGR in the biosynthesis of MVA-derived

products has been obtained by the overexpression of the Arabidopsis HMGR isoforms in transgenic Arabidopsis plants that led to an increase accumulation of leaf plant sterols (Manzano *et al.*, 2004). However, regulation of downstream enzymes in the plant sterols biosynthetic pathway still limit the production of end-of-chain plant sterols, and excess of intermediates, accumulate in lipid droplets in the cytosol of HMGR overexpressing plant cells (Schaller *et al.*, 1995).

In yeast and mammals HMGR activity is tightly regulated at different levels, from transcriptional to post-translational (Goldstein and Brown, 1990; Hampton *et al.*, 1996). Moreover, yeast and mammals HMGR is feedback regulated at post-translational level by a mechanism that involves ERAD system and has described previously in the present thesis (DeBose-Boyd, 2008; Hampton and Garza, 2009). In plants, the knowledge of regulatory mechanisms controlling HMGR activity is still limited, but some key aspects of HMGR regulation have been uncovered. All known plant HMGR variants have a diverged N-terminal region and a conserved catalytic domain located in the cytosol, and a membrane domain whereas only a short stretch of amino acids connecting the two transmembrane segments is in the lumen (Campos and Boronat, 1995). It is known that the membrane domain of plant HMGR exerts negative regulation on the catalytic domain, thus limiting plant sterols biosynthesis (Harker *et al.*, 2003).

Recently, the regulation of plant HMGR was reviewed leading to conclude that HMGR has a key regulatory role in the MVA pathway, critical not only for normal plant development, but also for the adaptation to demanding environmental conditions. Consistent with this notion, plant HMGR is modulated by endogenous signals and external stimuli, such as phytohormones, calcium, calmodulin, light, blockage of isoprenoid biosynthesis, chemical challenge, wounding, elicitor treatment, and pathogen attack (Stermer *et al.*, 1994; Rodríguez-Concepción *et al.*, 2011). It has been proposed that the major changes in HMGR activity would be determined at the transcriptional level, whereas the post-translational control would allow a finer and faster adjustment (Chappell, 1995). Whereas transcriptional modulation of HMGR has been demonstrated in many plant systems, evidence of post-translational regulation is still scarce (Rodríguez-Concepción *et al.*, 2011).

### **Sterol Metabolism in Plants**

Two sets of experiments studies performed with a tobacco mutant line (*sterol*, *sterol overproduce*) overproducing sterols have shown that the free sterol content of this mutant remained close to this of wild-type plants and that the excess of sterols was converted into steryl

esters (mostly steryl palmitate, oleate, linoleate and linolenate) that accumulated as lipid droplets (Gondet *et al.*, 1994; Schaller *et al.*, 1994; Benveniste, 2002). These results, emphasized the importance of sterol metabolism in order to maintain a level of free sterols in membranes compatible with their vital functions (Benveniste, 2002; Schaller, 2004). At least three pathways are universally involved in sterol metabolism in plants and especially in Arabidopsis: sterol acylation, sterol glycosylation and oxydative conversion of sterols into brassinosteroids (Benveniste, 2002; Schaller, 2004). Other pathways involved in sterol metabolism (e.g. formation of ecdysteroids, steroidal alkaloids, cardiotoxic steroidal glucosides) have also been reported, but associated to the secondary metabolism in specific plant families and therefore would not be relevant of the general plant metabolism (Benveniste, 2002).

## **1.5. GENETIC APPROACHES TOWARDS THE STUDY OF STEROL BIOSYNTHESIS AND FUNCTION**

Genetic approaches based on mutants isolation and characterization have been essential in the elucidation of mechanisms underlying plant growth and development, as well as those used by plants to cope with environmental stresses. Sterols are isoprenoid-derived lipids that play essential roles in plant growth and development (Benveniste, 2004; Phillips *et al.*, 2006). Critical for elucidation of the biological functions of sterols and their role in plant growth and development has been the identification of Arabidopsis mutants with altered sterol profiles due to disruption of specific enzymatic steps of the of the sterol pathway (Clouse, 2002; Schaller, 2004; Boutte and Grebe, 2009).

Recently, the isolation of novel mutations affecting the early part of the sterol biosynthesis pathway allowed the identification and characterization of physiological processes regulated by sterols, that otherwise would be concealed. The Identification of the hypomorphic *dry2/sqe1-5* allele revealed a central role for sterols in drought tolerance and regulation of Reactive Oxygen Species, ROS (Pose *et al.*, 2009). ROS are emerging as essential regulators of plant development. The location at which ROS production takes place is also an important factor controlling plant growth and development (Laloi *et al.*, 2004; Gapper and Dolan, 2006; Kwak *et al.*, 2006; Swanson and Gilroy, 2010). Furthermore, the identification of a large number of independent mutants that



reverted the extreme drought sensitivity and other developmental defects of sterol biosynthesis pathway mutant *dry2/sqe1-5*, opened new possibilities for study the role sterol and isoprenoid pathway in plant development and ROS production (Pose, 2008). Recent progress on the isolation and characterization of novel *Arabidopsis* mutants affected in the regulation of sterol and isoprenoid biosynthetic pathways are on the bases of the experimental work presented in this thesis and will be further summarized.

### **Squalene Epoxidase Gene Family**

Squalene epoxidase (SQE) enzymes convert squalene into 2,3-oxidosqualene, in an oxidation process important in sterol biosynthesis. Yeast and mammals only contain one gene encoding for SQE (Landl *et al.*, 1996; Nagai *et al.*, 1997). In contrast, multiple genes putatively encoding SQEs have been described in several plants (Schafer *et al.*, 1999; Suzuki *et al.*, 2002; Rasbery *et al.*, 2007), suggesting that this step of sterol biosynthesis may be subject to additional regulation in plants. In *Arabidopsis thaliana*, six putative *SQE* genes were identified based on sequence homology (Rasbery *et al.*, 2007). However, only *SQE1*, *SQE2* and *SQE3* cDNAs were able to complement the yeast *erg1*, a mutant that lacks the *SQE*, functionally demonstrating enzymatic SQE activity for the proteins encoded by the three genes (Rasbery *et al.*, 2007). The other *Arabidopsis* genes that show homology to *SQEs* (*SQE4*, *SQE5* and *SQE6*) are expected to have different catalytic activity, which is evidenced by its location in a different phylogeny clade with the others and the inability to complement the yeast *erg1* mutant (Rasbery *et al.*, 2007; Laranjeira, 2011). Therefore, the function of *SQE2* and *SQE3* could potentially overlap with that of *SQE1*. Expression analysis based on microarray databases, suggests that *SQE1* is the SQE that is most highly expressed in roots, *SQE2* is expressed at low levels in most tissues and *SQE3* is highly expressed in leaves and expressed at low levels in roots. GUS histochemical analysis revealed that *SQE1* is expressed in the shoot and in the elongation zone of the root whereas *SQE3* is expressed in the entire seedling, with predominance in the cotyledon (namely the stomata, the vasculature and meristematic tissues) (Pose *et al.*, 2009; Laranjeira, 2011), thus, suggesting that some tissue specificity exists within SQEs.

## Phenotypical Analysis of Squalene Epoxidase Mutants

Phenotypic analyses of the *SQE1* loss-of-function *sqe1-3* mutant allele showed defects in development, including reduced and highly branched roots, hypocotyl elongation and production of unviable seeds leading to sterility in this mutant. These defects were not rescued by brassinolide, suggesting that their phenotypes are not associated with BR deficiency (Rasbery *et al.*, 2007). Recently, the **drought hypersensitive/squalene epoxidase 1-5** (*dry2/sqe1-5*) mutant, was identified by its extreme hypersensitivity to drought stress, having altered stomatal responses and root defects because of a point mutation in the *SQUALENE EPOXIDASE 1* (*SQE1*) gene (Pose *et al.*, 2009). Generally, the *dry2/sqe1-5* phenotypes are similar but less severe than those exhibited by the *sqe1-3* mutant. In contrast to *SQE1* loss-of-function *sqe1-3* mutant that are sterile, *dry2/sqe1-5* mutant produce viable seeds suggesting that *DRY2/SQE1-5* is a hypomorphic allele of *DRY2/SQE1* (Rasbery *et al.*, 2007; Pose *et al.*, 2009). Because *dry2/sqe1-5* mutant produce viable seed, this mutant has been used as a tool in order to gain insight into the regulation of the sterol and isoprenoid pathway and their role in plants development (Pose, 2008; Pose *et al.*, 2009).

Analysis of the loss-of-function mutants *sqe2-1* and *sqe3-1* indicates the absence of visible differences in development relative to wild-type in standard growth conditions. However, *sqe3-1* mutants exhibited increased lethality in the presence of the inhibitor of squalene epoxidase activity terbinafine during germination. Importantly, the *dry2/sqe1-5 sqe3-1* double mutant was unviable, worsening the already acute pleiotropic phenotype of *dry2/sqe1-5* and highlighting a role for *SQE3* in sterol biosynthesis (Laranjeira, 2011).

## Chemical Analysis of Squalene Epoxidase Mutants

Gas chromatography (GC)-MS analysis was used in the determination of the content of squalene and free sterols in leaves and roots of 15-day-old wild-type and *dry2/sqe1-5*. Consistent with the expression data, this analysis indicated that *dry2/sqe1-5* seedlings has altered squalene and free sterol composition in roots but wild-type sterol composition in shoots, demonstrating an essential role for *SQE1* in root sterol biosynthesis (Pose *et al.*, 2009). In roots of *dry2/sqe1-5* there is a substantial reduction in the two major bulk sterols, sitosterol and stigmasterol, concomitant with a significant accumulation of the 4,4-dimethylsterols, cycloartenol and 24-methylene cycloartanol (Pose *et al.*, 2009). Similarly, an increased level of cycloartenol and 24-methylene cycloartanol has been reported in tobacco BY-2 cells treated with terbinafine, likely due to

secondary regulatory mechanisms (Wentzinger *et al.*, 2002). The effect of the *dry2/sqe1* mutation on the sterol profile in shoots and roots is fully consistent with its effect on squalene levels, the substrate of SQE enzymes, in these organs. Slightly increased levels of squalene are detected in shoots whereas a dramatic accumulation of the SQE substrate is observed in roots (Figure 1.6A). Moreover, the activity of the enzyme HMGR, the major rate-limiting enzyme in the MVA pathway, remains unaltered in shoots but is enhanced approximately 3-fold in roots (Figure 1.6B) (Pose *et al.*, 2009). Based on these findings it was proposed that in roots, HMGR is up-regulated in an attempt to compensate for the reduced levels of major sterols, which in turn may lead to the dramatic accumulation of squalene observed in this organ (Pose *et al.*, 2009). Because, campesterol levels are similar between wild-type and *dry2/sqe1-5* it was proposed that a defective brassinosteroid biosynthesis is not causing the phenotype (Pose *et al.*, 2009). This was supported by the inability of epibrassinolide to complement the defective growth of *dry2/sqe1-5* (Pose *et al.*, 2009) or the complete loss of function *sqe1-3* allele (Rasbery *et al.*, 2007).

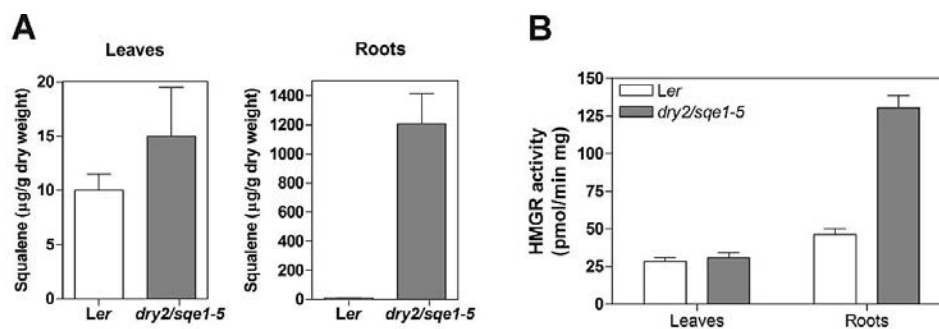


**Figure 1.6 – The *dry2/sqe1-5* Mutant Shows Increased Accumulation of Squalene and Higher HMGR Activity than Wild-type in Roots but Not in Shoots**

(A) Squalene content in leaves and roots of 15-day-old wild-type Ler and *dry2/sqe1-5* seedlings. Data represent mean values  $\pm$  SD ( $n = 3$ ). (B) HMGR activity in leaves and roots of 15-day-old *dry2/sqe1-5* seedlings. Data represent mean values  $\pm$  SD ( $n = 3$ ). Adapted from Pose *et al.* (2009).

Because *sqe3-1* mutants exhibit a hypersensitivity to terbinafine, a role of *SQE3* gene in sterol biosynthesis was proposed (Laranjeira, 2011). In 14-day-old wild-type and *sqe3-1* Arabidopsis seedlings *sqe3-1* roots accumulates  $\sim 2$ -fold more squalene than wild-type, consistent with a reduction of SQE activity, while the free sterols analysed in this tissue remains mainly unaltered. In addition to the squalene accumulation in the *sqe3-1* root tissue, there is a  $\sim 3$ -fold increased accumulation of squalene in shoot tissues of *sqe3-1* mutants relatively to the wild-type, while the sterols analysed in this tissue are just slightly altered (Laranjeira, 2011). Despite SQE1 being foretold as the main enzyme in the conversion of squalene, these results show that some

tissue specificity exists within SQEs. In terms of biochemical analysis of the mutants, SQE1 role is more important in roots, while SQE3 (probably together with SQE1) seems to have a major role in shoots (Laranjeira, 2011).

### **Arabidopsis *dry2/sqe1-5* Mutant Reveals a Central Role for Sterols in Drought Tolerance and Regulation of ROS**

The EMS recessive mutant *dry2/sqe1-5* was identified by its drought hypersensitivity (Figure 1.7A) (Pose *et al.*, 2009). In low relative humidity (RH) conditions (35% RH) *dry2* plants are smaller than wild type and also have a pale green phenotype because of a reduced chlorophyll content (Figures 1.7B,C,E). *dry2* seedlings also shows increased proline levels (Figure 1.7F), an osmolyte that accumulates under conditions of water deficit. However, in ~95% RH, *dry2* mutant shows a phenotype and both chlorophyll and proline content similar to *Ler* (Figures 1.7D,E,F) (Pose *et al.*, 2009). The extreme sensitivity of *dry2/sqe1-5* mutant to dehydration suggests that shoot developmental defects could be caused by a defective water balance. *dry2/sqe1* is impaired in stomatal function, showing a defective response to the decrease of the HR (Figure 1.7G) (Pose *et al.*, 2009).

Root architecture is very affected in *dry2/sqe1-5*. The length of its primary root and root hairs are shorter than that of wild type (Figure 1.8A) and developed branched root hairs (Figure 1.8B) and more than one hair per trichoblast (Figure 1.8C), implicating *SQE1* in both root hair initiation and polar growth (Pose *et al.*, 2009). Because superoxide ( $O_2^{\cdot-}$ ) accumulation in root hairs is defective in *dry2/sqe1-5* (Figure 1.8D), the altered morphology of root hairs in *dry2/sqe1-5* mutants is proposed to be caused by de-localization of RHD2 NADPH oxidase (Figure 1.8E) (Pose *et al.*, 2009).

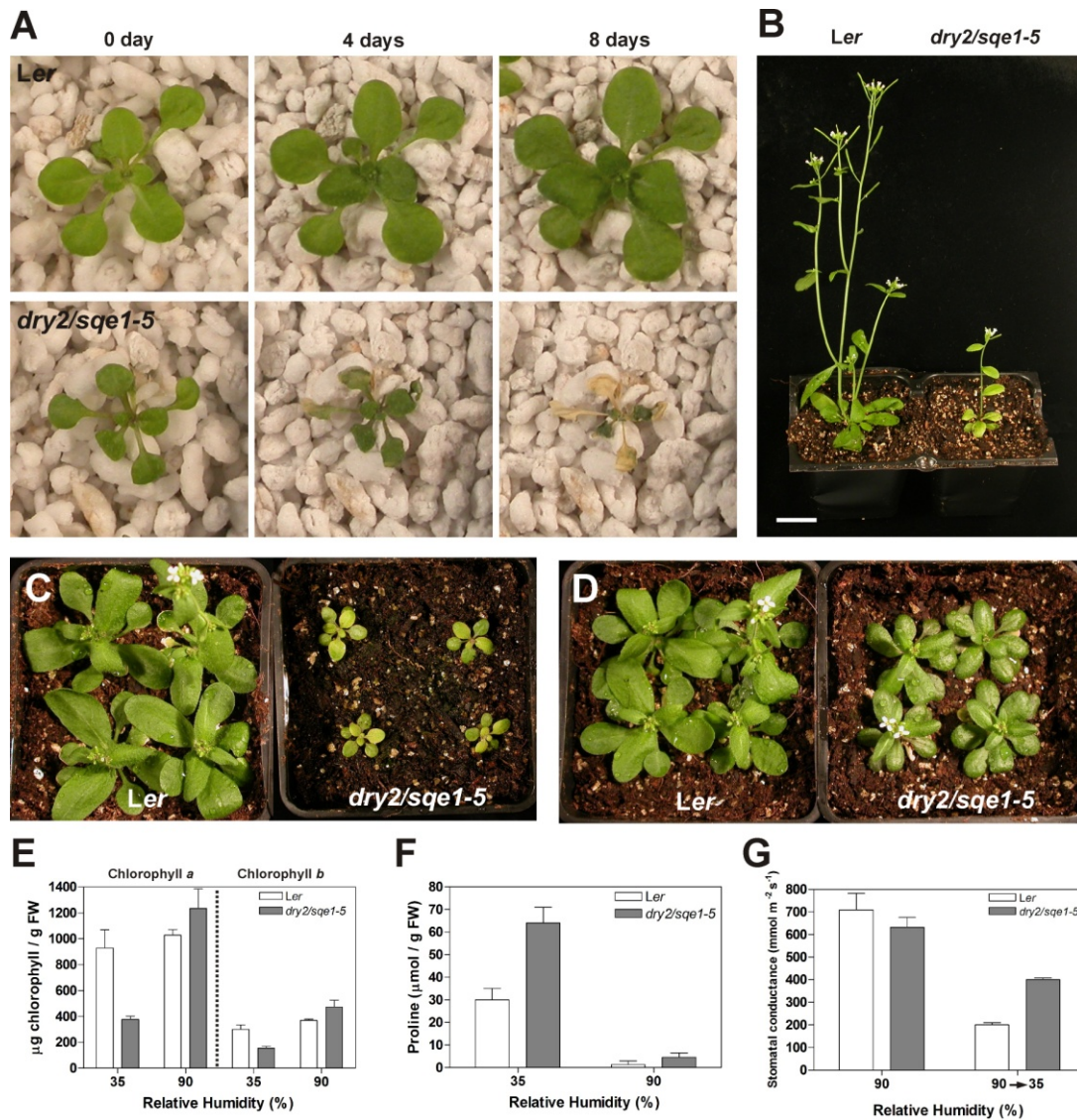


**Figure 1.7 – The *dry2/sqe1-5* Mutant is Hypersensitive to Dehydration and Has Developmental Defects and Impaired Stomatal Responses**

(A) Drought tolerance assay. Twelve-day-old wild-type *Ler* and *dry2/sqe1-5* seedlings grown on MS medium were transferred to perlite and grown for an additional 7 days with abundant nutrient solution. Thereafter, watering was withheld, and photographs were taken at the times indicated. (B) Thirty four-day-old plants of *Ler* and the *dry2/sqe1-5* mutant grown at 35% relative humidity (RH). *dry2/sqe1-5* plants show reduced size and pale green leaves compared to wild-type plants. Scale bar = 2 cm. (C,D) *dry2/sqe1-5* leaves show reduced size at 35% RH (C), but this phenotype is partially suppressed when grown at 90% RH (D). (E,F) The chlorophyll a and b content (E) and proline content (F) of *Ler* and *dry2/sqe1-5* plants grown under the same conditions as in (C) and (D). Data represent mean values  $\pm$  SD ( $n = 3$ ). (G) The *dry2/sqe1-5* mutant shows impaired stomatal response to changes in the RH. Data represent mean values  $\pm$  SD ( $n = 3$ ). Adapted from Pose *et al.* (2009).

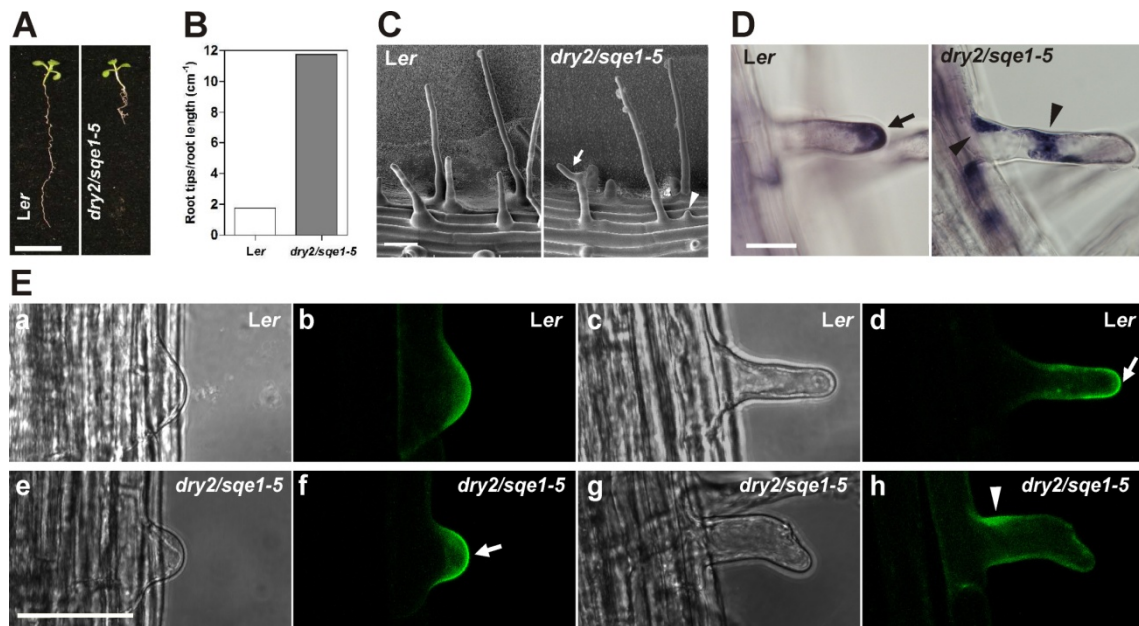


**Figure 1.8 – Defective Root Phenotypes of *dry2/sqe1-5* Mutant Seedling**

**(A)** Root phenotypes of wild-type *Ler* and *dry2/sqe1-5* mutant seedling. Scale bar = 1 cm. **(B)** Root branching of *Ler* and the *dry2/sqe1-5* mutant determined by counting the number of root tips per length of primary root. **(C)** Scanning electron micrograph showing root hair phenotypes of wild-type (*Ler*) and *dry2/sqe1-5*. In *dry2/sqe1-5* mutant, approximately 40% of the root hairs were branched (arrow) and showed more than a single site of growth per cell (arrowhead). Scale bar = 500  $\mu$ m. **(D)** Superoxide ( $O_2^{\cdot-}$ ) localization by staining roots with NBT.  $O_2^{\cdot-}$  is localized at the tips of wild-type *Ler* and root hairs (arrow). In *dry2/sqe1-5* mutants,  $O_2^{\cdot-}$  production is localized either at the base or the middle of root hairs (arrowheads), and eventually more than one focus are stained in the same cell (arrowheads). Scale bar = 50  $\mu$ m. **(E)** Bright-field (a, c) and confocal images (b, d) of *Ler* root hairs showing GFP-RHD2 located at the tip of emerging (a, b) and growing (c, d, arrow) root hairs. Bright-field (e, g) and confocal images (f, h) of *dry2/sqe1-5* root hairs showing GFP-RHD2 located at the tip of an emerging root hair (e, f, arrow) but with ectopic accumulation later in development (g, h, arrowhead). Scale bar = 50  $\mu$ m. Adapted from Pose *et al.* (2009).

### Isolation and Characterization of *dry2* Suppressors

The screening for second-site mutations that suppress the phenotype of a given mutant is a common strategy used to identify genetic components related with the given mutation, that help to understand the mechanisms where the affected genes are involved. In *Arabidopsis*, several suppressor screening has been performed, leading to the identification of gene implicated for instance: in plant defense and programmed cell death (Xiao *et al.*, 2004; Zhang *et al.*, 2008); in signalling of  $^1O_2$ -dependent nuclear gene expression changes (Wagner *et al.*, 2004; Lee *et al.*, 2007); or in conserved endoplasmic reticulum-associated degradation system to eliminate mutated receptor-like kinases (Su *et al.*, 2011).

To further investigate if *dry2/sqe1-5* phenotypes could be caused by defective sterol signaling, rather than structural defects, a suppressor screening was performed by Posé and co-workers (Pose, 2008). The authors set out to identify second-site mutations induced by EMS that abrogated the drought hypersensitivity phenotype observed in *dry2/sqe1-5* as this phenotype

is easily scored. This screening led to the identification of a large number of independent mutants that revert the extreme drought sensitivity of *dry2/sqe1-5* and other developmental defects. In this screening, a total of 27 independent M2 lines, originating from 131 different pools of 50 M<sub>1</sub> plants that showed a significant reversion of *dry2/sqe1-5* drought hypersensitivity, were identified. The suppressors affected were named *sud* for **s**uppressor of *dry2/sqe1-5* **d**efects and subsequently named *dry2/sud1* to *dry2/sud27* (Pose, 2008). After analyzing the suppression of *dry2* phenotypic defects in the next generation, 4 suppressors (*dry2/sud9*, *dry2/sud22*, *dry2/sud26*, *dry2/sud27*) were selected for further characterization, because in addition to the drought hypersensitivity also suppressed the root growth defects of *dry2/sqe1-5* (Doblas, Amorim-Silva *et al.* Submitted). Sequencing of the *DRY2/SQE1-5* gene in the 4 suppressors confirmed that they contained the *dry2/sqe1-5* mutation and the recovery of the phenotypes was not caused by seed contamination of wild-type plants (Pose, 2008).

A more detailed phenotypic characterization of *dry2/sud9* and *dry2/sud22* roots relative to wild-type and *dry2/sqe1-5* mutant (hereafter named *dry2*) was performed. The root length of *dry2/sud9* and *dry2/sud22* was double than that of *dry2*, reaching ~70% that of the primary root length of wild-type plants (Figure 1.9A,B) and also showed decreased number of lateral roots compared to *dry2* (Figure 1.9C) (Pose, 2008). *dry2* also showed striking defects in root hairs. While almost an 80% of root hairs from wild-type plants were over 300  $\mu\text{m}$  in length, most root hairs of *dry2* were shorter than 200  $\mu\text{m}$  (Pose *et al.*, 2009). As shown in Figure 1.9D and 1.9E, second site mutations in *dry2/sud9* and *dry2/sud22* substantially restore the root hair defects (Pose, 2008). Root hair growth requires the localized production of ROS by RHD2/AtrbohC NADPH oxidase (Foreman *et al.*, 2003; Carol *et al.*, 2005; Takeda *et al.*, 2008) and *dry2* show defective ROS production caused by a misslocalization of AtrbohC (Pose *et al.*, 2009). As shown in Figure 1.9F, *dry2/sud9* and *dry2/sud22* showed wild-type H<sub>2</sub>O<sub>2</sub> production at the bulge of the root tip, which is consistent with the restoration of the growth defects (Doblas, Amorim-Silva *et al.* Submitted).

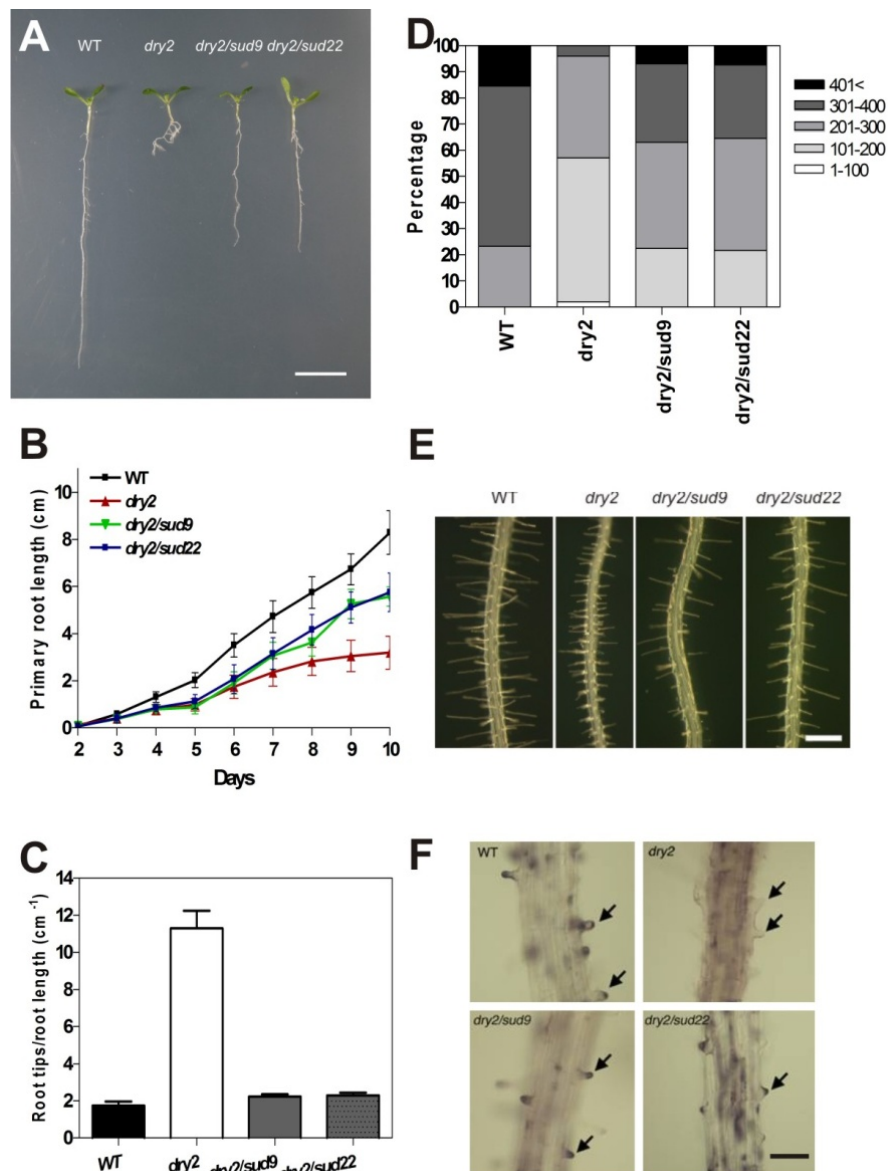


**Figure 1.9 – Suppressors Rescue the Root Growth Defects of *dry2* Mutant**

(A) Root phenotypes of wild-type (WT) *Ler*, *dry2* and *dry2/sud9* mutant seedling. Scale bar = 1 cm. (B) Primary root growth over 10 days for *Ler*, *dry2*, *dry2/sud9* and *dry2/sud22*. (C) Root branching of wild type *Ler*, *dry2*, *dry2/sud9*, and *dry2/sud22* estimated by counting the number of root tips per primary root length. (D) Percentage root hair length of *Ler*, *dry2*, *dry2/sud9*, and *dry2/sud22*. (E) Roots of wild-type *Ler*, *dry2*, *dry2/sud9*, and *dry2/sud22*. Scale bar = 500  $\mu\text{m}$ . (F) ROS staining in roots using DAB.  $\text{H}_2\text{O}_2$  is localized at the tips of *Ler*, *dry2/sud9* and *dry2/sud22* root hairs and not in *dry2* (arrows) Scale bar = 200  $\mu\text{m}$ . Figure A-E adapted from (Pose, 2008) and figure F adapted from Doblas, Amorim-Silva *et al.* (Submitted).

Although at seedling stage *dry2/sud9* and *dry2/sud22* show a slight delay in development, shoot growth recover and reach similar size in adult to wild-type plants (Figure 1.10A) (Doblas, Amorim-Silva *et al.* Submitted), however the extreme drought sensitivity that exhibit *dry2* is suppressed in *dry2/sud9* and *dry2/sud22* (Pose, 2008). *dry2* show insensitivity to ABA-induced stomatal closure. Treatment with exogenously applied 20  $\mu\text{M}$  ABA only reduced  $\sim 20\%$  of stomatal



conductance compared with the ~80% reduction that occurs in wild-type plants (Figure 1.10B) (Pose *et al.*, 2009). *dry2/sud9* showed similar stomatal responses as wild-type plants (Figure 1.10B) indicating a suppression of this phenotype (Pose, 2008). Proline content in *dry2/sud9* is also similar to wild-type plants indicating a restoration of water relations (Figure 1.10C) (Pose, 2008).

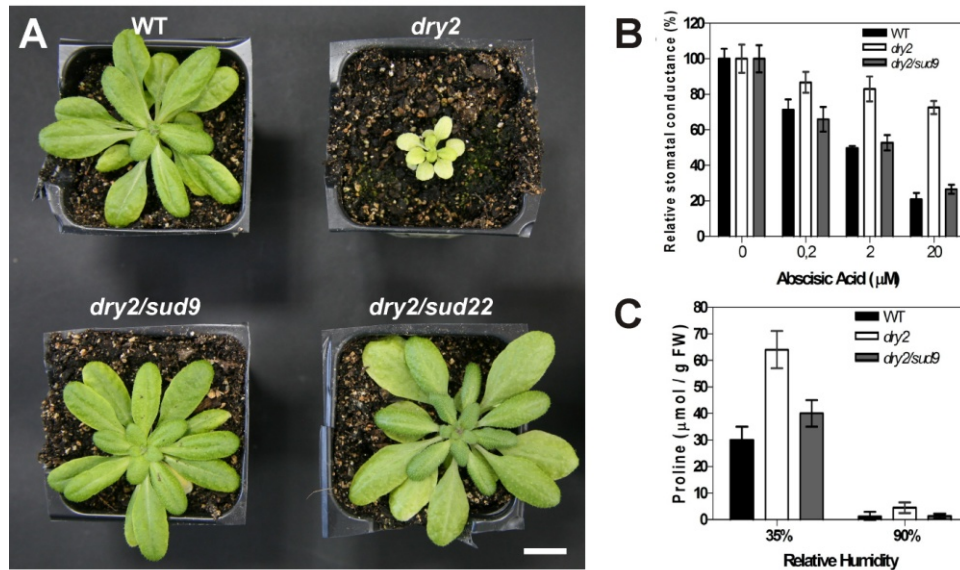


**Figure 1.10 – Suppressors Show Wild-type Shoot Growth**

**(A)** Shoot phenotype of 28 days-old plant of wild-type (WT) *Ler*, *dry2*, *dry2/sud9* and *dry2/sud22*. **(B)** Stomatal conductance of wild-type *Ler*, *dry2* and *dry2/sud9* four hours after spraying the indicated Abscisic Acid (ABA) concentrations. The *dry2* mutant shows reduced stomatal responses to exogenous ABA compared to *Ler* and to *dry2/sud9*. Data represent mean values  $\pm$  SD ( $n = 3$ ). **(C)** Proline content was determined in *Ler*, *dry2* and *dry2/sud9* plants grown at 35% and 90% Relative Humidity. Data represent mean values  $\pm$  SD ( $n = 3$ ). Figure 1.10A was adapted from Doblaz, Amorim-Silva *et al.* (Submitted). Figure 1.10B and C was adapted from Pose *et al.* (2009).

Suppression of *dry2* defects is not likely to be caused by a restoration of sterol composition. However the roots of *dry2* shows important differences in sterol content relative to wild-type, sterol composition of *dry2/sud9* was similar to *dry2* and both significantly different from wild-type (Table 1.1) (Pose, 2008). Therefore, the reversion of *dry2/sud9* root defects cannot be simply explained by a recovery of major sterols to wild-type levels.

**Table 1.1 – Mass Spectral Analysis of Sterols from *Ler*, *dry2* and *dry2/sud9***

Sterol	Root			Shoot		
	WT ( <i>Ler</i> )	<i>dry2</i>	<i>dry2/sud9</i>	WT ( <i>Ler</i> )	<i>dry2</i>	<i>dry2/sud9</i>
Cycloartenol	32 <sup>a</sup> (0,76) <sup>b</sup>	125 (4,48)	105 (4,12)	25 (0,91)	31 (1,14)	21 (0,76)
24-Methylenecycloartenol	46 (1,09)	89 (3,19)	109 (4,27)	46 (1,67)	47 (1,72)	41 (1,47)
Isofucosterol	67 (1,59)	50 (1,79)	76 (2,98)	60 (2,18)	65 (2,38)	81 (2,91)
Sitosterol	2723 (64,68)	1576 (56,49)	1526 (59,82)	2133 (77,34)	2086 (76,52)	2153 (77,45)
Stigmasterol	894 (21,23)	358 (12,83)	336 (13,17)	57 (2,07)	52 (1,91)	62 (2,23)
Campesterol	410 (9,74)	574 (20,57)	370 (14,50)	395 (14,32)	401 (14,71)	373 (13,42)
Cholesterol	38 (0,90)	18 (0,65)	29 (1,14)	42 (1,52)	44 (1,61)	49 (1,76)

(a) Values are given in  $\mu\text{g/g}$  dry weight

(b) Percentage of the total sterol content is shown in parentheses.

Table was retrieved from (Pose, 2008).

Additional analysis of *dry2* suppressor mutants and the identification of the genes affected, could determine whether or not sterols other than BRs have a signalling role in plant development. Consequently, this mutants will be a valuable tool, not only to study the sterol biosynthesis pathway, but also for better understanding the role of *DRY2/SQE1-5* gene mediating ROS production and sterol metabolism in drought stress response.

## 1.6. AIMS AND OUTLINES OF THE THESIS

The current marginal success in increasing crop yield under unfavourable environmental conditions is partially due to the large number of cellular processes affected by abiotic stresses which in turn cause severe impact on plant growth, development and finally production. An essential aspect of abiotic stress research in plants is to determine both, how plants sense and acclimate to abiotic stress conditions, and which are the genetic determinants involved in these processes. The final aim is then to use this knowledge to develop crops with enhanced tolerance to abiotic stresses. Significant progress has been made in understanding the physiological, cellular and molecular mechanisms of plant responses to environmental stress factors, and significant achievements with relevance to agriculture have been obtained. Key in the recent progress in understanding fundamental processes of cellular function is primarily due to the use of *Arabidopsis* as a genetic model system in abiotic stress research. *Arabidopsis* has facilitated the functional

characterization of numerous genes by use of loss- or gain-of-function experimental approaches. In a previous study, the extreme drought hypersensitive *dry2/sqe1-5* mutant was isolated and used to perform a suppressor screening. Several mutants (named *sud* for *suppressors of dry2 defects*) that reversed most of the *dry2/sqe1-5* developmental phenotypes, including its drought hypersensitivity were isolated. Thus, within this Ph.D thesis, the main aim was to identify the molecular nature of the *dry2* suppressors and determine mechanistically how they restore wild-type phenotypes. This was initiated by the positional cloning of the gene affected by the suppressor mutations that led to the identification of *SUD1*. Later, a detailed physiological, biochemical and molecular characterization of *dry2/sud1-9* and *dry2/sud1-22* suppressors was performed. Following the phenotypic characterization of these genes, research was ultimately focused on the identification of gene function, thus allowing the identification of new genetic components regulating the MVA pathway. The present thesis is organised in an outline that reflects specific aims:

**Chapter 1** provides a general introduction to the effects that abiotic stresses cause in crop production, underlying research strategies that try to meet the worldwide demand of increased crop yield. In addition, a review is presented on related research issues related with the present thesis, like the role of reactive oxygen species in plant development, the selective degradation of proteins and their function in cellular regulation and quality control, sterol production and function in plants, and finally genetic approaches towards the study of sterol biosynthesis. Chapters 2 to 7 are devoted for specific aims subordinated to the global aim of the thesis, each chapter including a brief introduction, results and discussion, and materials and methods used to perform the experiments and analysis presented in the given chapter. In **Chapter 2** is investigated the role of reactive oxygen species in *dry2* and *dry2* suppressors. In **Chapter 3** is presented the map-based cloning of four semidominant *dry2* suppressors that led to the identification of *SUD1*. In **Chapter 4** is described the *in silico* analysis of *SUD1* expression and the microarray-based whole-genome transcript profiling of wild-type, *dry2*, *dry2/sud9*, and *dry2/sud22*. **Chapter 5** is devoted to the *in silico* structural and phylogenetic analysis of *SUD1*, which encodes a protein showing sequence and structural homology to the E3 ubiquitin ligases involved in ERAD-C pathway. **Chapter 6** describes the series of experiments that were conducted as an effort to functionally characterize the likely Arabidopsis *DOA10* ortholog gene *SUD1* using yeast. Because *SUD1* is a putative member of the ERAD pathway, the two Arabidopsis redundant genes *AtHRD1A* and *AtHRD1B*, which are the most likely orthologs of the yeast ERAD component

Hrd1, were also included in this chapter. **Chapter 7** describes the use of micro-grafting in the study of long-distance isoprenoid-derived signalling in *dry2*. **Chapter 8** includes the final remarks and future prospects concerning the presented research lines. **Chapter 9** details the bibliographic references cited throughout this manuscript.

The specific Materials and Methods are included in the correspondent thesis chapter. Standard molecular biology methods are presented in more detail in Appendix I. Detailed information regarding the genetic markers in Arabidopsis chromosomes used for map-based cloning of *SUD1* are presented in Appendix II and maps of commercial vectors used for cloning procedures are depicted in Appendix II.

# Chapter 2

## Investigating the role of Reactive Oxygen Species in *dry2*

### CONTENTS

---

#### 2.1. INTRODUCTION

#### 2.2. RESULTS AND DISCUSSION

ROS Generators Suppress Root Branching Defects in *dry2*

Suppressors Recover Wild-type ROS Production

Imaging Intracellular Hydrogen Peroxide Production using HyPer

#### 2.3. MATERIALS AND METHODS



## 2.1. INTRODUCTION

The *Arabidopsis dry2* mutant in the *Ler* ecotype was originally identified by its extreme sensitivity to drought stress (Pose *et al.*, 2009). The increased sensitivity to dehydration observed in *dry2* mutant was associated with an impaired stomatal response. In addition to its drought hypersensitivity, the *dry2* mutant also had several development defects, like a reduced root and hypocotyl elongation, a diminished size, decreased chlorophyll content and defective stomata responses, which in turn causes a water deficit leading to increased proline (Pro) accumulation.

It was proposed that pleiotropic developmental defects and the impaired stomatal responses observed in *dry2* mutant are caused by a defective functioning of NADPH oxidases and the concomitant altered production of Reactive Oxygen Species (ROS) (Pose *et al.*, 2009). Root architecture is very affected in *dry2*. As previously described in the present thesis, the length of its primary root and root hairs are shorter than that of wild type plants. In addition, *dry2* mutants developed branched root systems where the primary root cannot be easily distinguished (Pose *et al.*, 2009). Thus, *SQE1* was implicated in both root hair initiation and polar growth (Pose *et al.*, 2009). ROS produced by NADPH oxidases (NOXs) are known to play an important role in root development (Torres and Dangl, 2005; Gapper and Dolan, 2006; Swanson and Gilroy, 2010; Marino *et al.*, 2012). Root hair growth requires the localized production of ROS by RHD2 (AtrbohC NADPH oxidase) (Foreman *et al.*, 2003; Carol *et al.*, 2005; Takeda *et al.*, 2008) and *dry2* shows defective ROS production caused by a misslocalization of AtrbohC (Pose *et al.*, 2009). Because superoxide ( $O_2^{\cdot-}$ ) accumulation in root hairs is defective in *dry2*, the altered morphology of root hairs in *dry2* mutants was proposed to be caused by de-localization of RHD2 NADPH oxidase (Pose *et al.*, 2009). Moreover, *dry2* suppressors (*dry2/sud9* and *dry2/sud22*) showed wild-type ROS production at the bulge of the root tip, which is consistent with the restoration of the growth defects (Doblas, Amorim-Silva *et al.* Submitted).

In the present chapter, the suppression of the *dry2* developmental defects by the exogenous application of ROS generators and the recovery of ROS production in *dry2* mutant by second-site mutations will be investigated. Also, the development of new techniques for *in vivo* detection of ROS will be discussed.

## 2.2. RESULTS AND DISCUSSION

### ROS Generators Suppress Root Branching Defects in *dry2*

In order to determine whether *dry2* root defects correlated with ROS production or were caused by a defective ROS production, the suppression of *dry2* root defects by ROS generators was investigated. In addition to a reduction in the length of the primary root, *dry2* seedlings were shown to develop a branched root system, with approximately six times more lateral roots than wild-type plants (Pose *et al.*, 2009). Since root branching can be accurately quantified by estimating the number of root tips per length unit of primary root, the suppression of the *dry2* root branching phenotype by the exogenous application of oxidative-stress causing agents was investigated.

Polarized root hair growth requires the localized production of ROS by RHD2/AtrbohC NADPH oxidase at the growing root tip and root hairs tips (Foreman *et al.*, 2003; Carol *et al.*, 2005; Takeda *et al.*, 2008). The plasma membrane NADPH oxidase is responsible for the one-electron reduction of oxygen at the surface of cells, yielding superoxide anion ( $O_2^{\cdot-}$ ). The  $O_2^{\cdot-}$  may be further converted into  $H_2O_2$  spontaneously or by superoxide dismutase in the apoplast (Halliwell and Gutteridge, 1999).  $H_2O_2$  can give rise to  $HO\cdot$  through the Fenton reaction, which is catalysed mainly by free transition metal ions (such as  $Cu^{2+}$  or  $Fe^{2+}$ ) (Fry, 1998; Halliwell and Gutteridge, 1999; Foreman *et al.*, 2003).  $HO\cdot$  has a loosening effect on cell walls and is therefore very important for cell elongation (Liszka *et al.*, 2004).

The spatial regulation of ROS production is defective in *dry2* (Pose *et al.*, 2009). Therefore, we investigated the role of  $O_2^{\cdot-}$  and  $H_2O_2$  in root development and architecture, was investigated, by using the ROS generator methyl viologen, commercially known as Paraquat (Pq). Pq is a redox-active molecule that is taken up by the cell, undergoing univalent reduction and subsequently transferring one electron to oxygen, forming the  $O_2^{\cdot-}$ . The process regenerates oxidized Pq, that may engage in successive rounds of redox cycling (Halliwell and Gutteridge, 1999). Even if photoreduction in chloroplasts represents the most efficient pathway, Pq can be reduced by several enzymes and electron transfer systems. Plants treated in the absence of light with Pq shown an activation of the antioxidant stress response suggesting that, although to a less extend, Pq is active in non photosynthesizing tissues (Tsang *et al.*, 1991). The basis of this oxidative stress induction that is unrelated to photosynthesis, it is possible that the reduction of Pq occurs by microsomal or mitochondrial electron transfer reactions. In animal cells, Pq metabolism occurs by redox cycling, a common mechanism with quinones and related species, in which the Pq is reduced by a



flavoenzyme such as cytochrome P450 reductase to a radical that then reacts with oxygen to generate superoxide (O'Brien, 1991; Winterbourn, 2008). Based on this information, Pq is oxidative stress-causing agent, suitable to be used for the generation of ROS, namely  $O_2^{\cdot-}$  and subsequently  $H_2O_2$  and  $HO^{\cdot}$  in roots of *in vitro*-grown *Arabidopsis*. Results show that supplying the growing medium with 0.001 or 0.01  $\mu M$  of Pq did not reduced root defects of *dry2* (Figure 2.1A,B). However the highest concentration produced toxicity as it significantly induced root branching in wild-type *Ler* plants (Figure 2.1B,D), suggesting that Pq cannot be used for estimating root branching phenotypes.

Rose bengal (RB), which is a typical photosensitizer known to generate mainly singlet oxygen ( $^1O_2$ ) when excited by light in the visible range (Tomita *et al.*, 1969; Lee and Rodgers, 1987; Lambert *et al.*, 1996), was also used to evaluate if ROS generators could suppress the reduced length and root branching phenotypes of the *dry2* mutant. As shown in Figure 2.1 C and D, root branching of wild-type plants were not affected at the concentrations of RB used in this experiment. However, a progressive suppression of *dry2* root branching together with a concomitant increase of the root length occurred in plants grown in half-strength MS medium supplemented with increasing concentrations of RB (Figure 2.1C,D). The suppression of root defects by the external application of RB suggests that singlet oxygen-dependent signaling events complement, at least partially, the *dry2* root branching phenotype.

The analysis of the root branching using ROS generators confirmed the causal relationship between ROS production and *dry2* phenotype. Although Pq did not recover *dry2* root branching defects and has induced a root branching phenotype in wild-type seedlings, RB suppress the root branching defects of *dry2*. There can be several explanations for this. Every ROS species has different properties in terms of reactivity, cellular site of production, half-life, diffusion within the cell, etc. (Moller *et al.*, 2007). In fact different ROS produce different signalling responses and different gene expression patterns (Apel and Hirt, 2004; Laloi *et al.*, 2004; Gadjev *et al.*, 2006; Laloi *et al.*, 2007; Mittler *et al.*, 2011). Depending on the type of ROS ( $H_2O_2$ ,  $HO^{\cdot}$ , or  $^1O_2$ ) or its production site, a different physiological, biochemical, and molecular response can be activated. The  $HO^{\cdot}$  radical has a loosening effect on cell walls and is therefore very important for cell elongation (Liszky *et al.*, 2004). However, it is also possible that  $HO^{\cdot}$  needs to be produced in the right place and at the right concentration to be effective. Increasing ROS levels in root of the root hairs defective mutant *rhd2* (loss of function mutant for the AtrbohC NADPH oxidase) by treatment with  $HO^{\cdot}$  led to depolarized root hair and growth-hairs expanded on all surfaces, leading to the

formation of spherical outgrowths (Foreman *et al.*, 2003). The formation of non-polarized hairs upon homogeneous treatment with  $\text{HO}\cdot$  suggests that the polarized production of ROS is required for the formation of a polarized hair outgrowth (Foreman *et al.*, 2003). In fact, *dry2* show a defective localization of AtRbohC (Pose *et al.*, 2009) as well as AtRobhD (Jinxing Lin, personal communication), thus suggesting that superoxide production is defective in *dry2*.

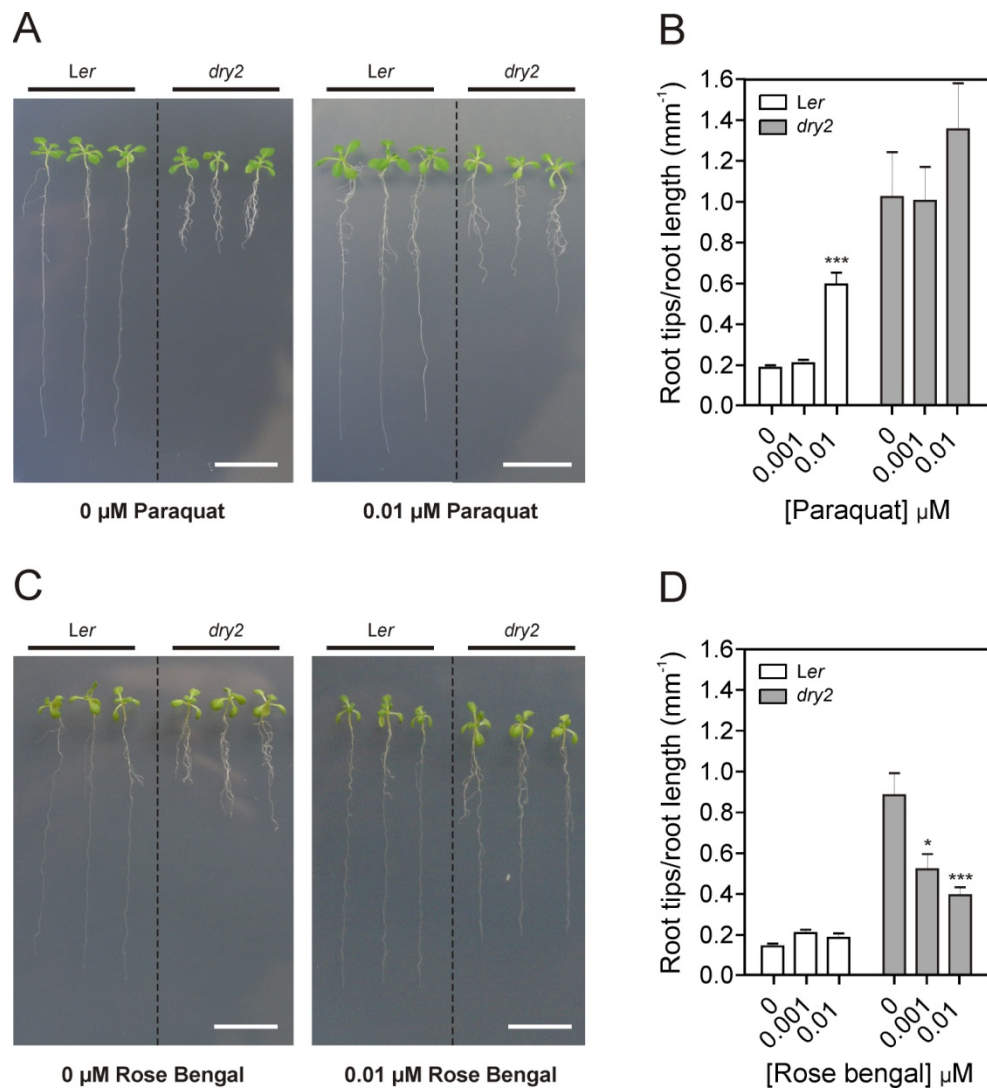


**Figure 2.1 – Suppression of *dry2* Root Defects by ROS Generators**

A progressive suppression of *dry2* root branching occurred at plants grown in half-strength MS growing medium supplied with increasing concentrations of Rose Bengal (RB). **(A)** Root phenotype of wild-type (*Ler*) and *dry2* seedlings growing in control medium and with increasing concentrations of Rose Bengal. Seedlings were grown for 7 days in MS medium and then transferred to half-strength MS medium (control) or supplemented with RB to the final concentrations indicated and photographed 8 days later. Scale bar: 1 cm. **(B)** Quantification of root branching for seedlings treated as described for (A). Root branching was determined by estimating the number of root tips per length of primary root. Data represent mean values  $\pm$  SEM ( $n=15$ ). **(C)** As in (A) but with Paraquat instead RB as the ROS generator. **(D)** As in (B) but with Paraquat instead RB as the ROS generator. Asterisks represent statistically significant differences between root branching values for seedlings growing with increasing concentrations of Paraquat (B) or RB (D) compared with seedlings growing in control medium from the same genotype (One-way analysis of variance “ANOVA”, Bonferroni’s Multiple Comparison Test; \*,  $P<0.05$ ; \*\*,  $P<0.01$ ; \*\*\*,  $P<0.001$ ).

In animals,  $^1\text{O}_2$  production leads to the activation of distinct signalling pathways (Robson and Vanlerberghe, 2002; Klotz *et al.*, 2003), some of which are selectively activated by  $^1\text{O}_2$  but not by superoxide (Godar, 1999) or  $\text{H}_2\text{O}_2$  (Zhuang *et al.*, 2000). In plants, experimental strategies have been described that allow the analysis of  $^1\text{O}_2$  biological activity. In the conditional fluorescent (*flu*) mutant of *Arabidopsis*,  $^1\text{O}_2$  is selectively produced within the plastid compartment whenever the mutant plants are returned to the light after a short period in the dark (op den Camp *et al.*, 2003). In the *flu* mutant, after the release of  $^1\text{O}_2$ , drastic changes in nuclear gene expression occur that affect approximately 5% of the total genome of *Arabidopsis thaliana*. Several of these genes respond selectively to the release of  $^1\text{O}_2$  and are not affected during a treatment by Pq. Therefore, it is possible that *dry2* shows defective singlet oxygen production and hence a  $^1\text{O}_2$ -dependent signalling events.

### Suppressors Recover Wild-type ROS Production

In the present study it was investigated the defective ROS production in *dry2* mutant in the *Ler* ecotype, *dry2* suppressors *dry2/sud9* and *dry2/sud22* carrying second-site mutations in the *dry2* background and an introgression line with *dry2* mutation in a *Col* ecotype (*dry2<sup>Col</sup>*). Although at an early development stage *dry2/sud9* and *dry2/sud22* show a slight delay in development (Figure 2.2A), adult *dry2/sud9* and *dry2/sud22* shoots reach similar adult size than wild-type plants. The introgression line *dry2<sup>Col</sup>* shows similar developmental defects than the *dry2* mutant in roots and shoots (Figure 2.2) and will be detailed in next chapter of the present thesis.

A previous study shows that *dry2* is defective in  $\text{H}_2\text{O}_2$  production in leaves, based on based on 3,3-diaminobenzidine (DAB) staining (Pose *et al.*, 2009), most likely through the defective activity of NADPH oxidases highly expressed in leaves such as RbohD, since  $\text{O}_2^{\cdot-}$  produced by a NADPH oxidases is further converted into  $\text{H}_2\text{O}_2$  spontaneously or by the action of superoxide dismutases (Halliwell and Gutteridge, 1999). However, since  $\text{O}_2^{\cdot-}$  is the direct product of NADPH oxidases, *in situ* superoxide production was analyzed using the nitroblue tetrazolium (NBT) staining method (Jabs *et al.*, 1996). In the presence of  $\text{O}_2^{\cdot-}$ , NBT is reduced and produce a blue formazan deposit (Fryer *et al.*, 2002). Three-week old leaves of *dry2<sup>Col</sup>*, similar to *dry2* leaves, did not accumulate  $\text{O}_2^{\cdot-}$  at normal grown conditions. However, *dry2* plants are still able to produce superoxide in response to physical damage. When entire three week-old plants were harvested and stained with NBT for *in situ*  $\text{O}_2^{\cdot-}$  detection, no NBT specific coloration was observed. However, for *dry2* leaves that were cut prior to NBT staining,  $\text{O}_2^{\cdot-}$  is produced in the local of physical damage

(Figure 2.2B). Plants has the ability to recognise wounding damage (Vickers *et al.*, 2009) and NADPH oxidases are involved in wounding responses in tomato (Sagi *et al.*, 2004). Also, AtRbohD is required for rapid wound-induced systemic ROS generation mediating the systemic acclimation to several abiotic stresses (Miller *et al.*, 2009).

*In situ* analysis of leaf  $O_2^{\cdot-}$  by NBT staining confirm that *dry2* is defective in the production of NADPH oxidases-derived ROS. Therefore, it is likely that in addition to root and root hairs polarised growth, anisotropic growth of leaves also require ROS production regulated by *DRY2/SQE1-5*. It is expected that plants with compromised ability to produce ROS are also impaired in their responsiveness to leaf damage by wounding. Interestingly, results show that *dry2* produce  $O_2^{\cdot-}$  in response to physical damage. This suggests that this  $O_2^{\cdot-}$  is produced by a different source other than NADPH oxidase or that the regulation of NADPH oxidases in response to this damage-induced ROS is different, possible thought a mechanism involving jasmonates (JAs). Plant JAs include jasmonic acid, methylJA, their isomers, biosynthetic precursors, and several derivatives including jasmonoyl-amino acid (Liechti and Farmer, 2002) that are known to regulate plant responses to a variety of abiotic and biotic stress factors, such as wounding (Wasternack, 2007). JAs are known to induce ROS production when applied exogenously (Zhang and Xing, 2008), and when produced *de novo* in response to leaf wounding (Orozco-Cardenas and Ryan, 1999; Soares *et al.*, 2009). Thus, ROS production and containment may be essential components for wound responses (Soares *et al.*, 2009), and jasmonates (JAs) likely play a role in regulating the ROS production in wounded plant tissues.

To determine whether the recovery of *dry2* developmental phenotypes was caused by a defective ROS production, the accumulation of superoxide was analyzed in two different *dry2* phenotypes suppressors (*dry2/sud9* and *dry2/sud22*). These two *dry2* suppressors containing second-site mutations recovered most of the development defects of *dry2*. As shown in Figure 2.2B, the superoxide levels estimated by NBT staining in leaves of *dry2 sud1-9* and *dry2 sud1-22*, are similar to the wild-type, showing that suppression of *dry2* phenotype by second-site mutations occur with a concomitant recovery in  $O_2^{\cdot-}$  production. Additional evidence that defective ROS production is a direct consequence of *dry2/sqe1-5* mutation is provided by the lack of superoxide production in *dry2<sup>Col</sup>* during leaf development (Figure 2.2B).

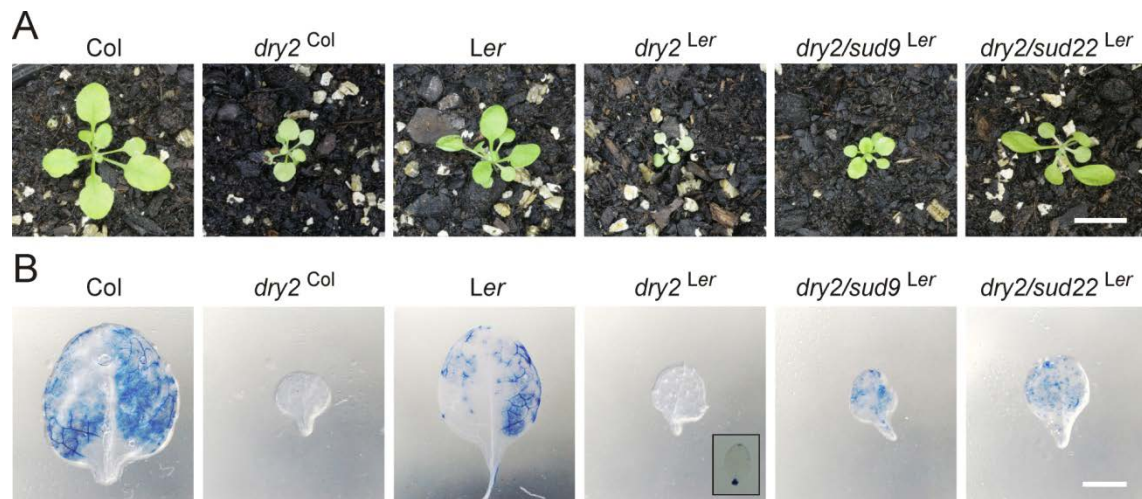


**Figure 2.2 – *In Situ* Detection of Superoxide ( $O_2^{\cdot-}$ )**

**(A)** Shoot morphology of three week-old *Arabidopsis* plants used for NBT staining in (B). Scale bar: 1 cm. **(B)** NBT staining for *in situ* superoxide ion presence. Samples shown are representative of three independent experiments (three plants per experiment). The entire three week-old plants represented in (A) were harvested and stained immediately during 1 hour. Additionally for *dry2*, four leaves per experiment were cut prior to NBT staining (representative leaf is boxed inside *dry2* figure). Scale bar: 2 cm.

### Imaging Intracellular Hydrogen Peroxide Production using HyPer

The analysis of root branching using ROS generators confirmed the causal relationship between ROS production and *dry2* phenotypic defects. Additionally, the shoot recovery of the suppressors also correlates with the reestablishment of  $O_2^{\cdot-}$  production to wild-type levels. Taking together, this results support that defective production of NADPH oxidases-derived ROS in *dry2*, most likely through the defective activity of NADPH RbohC in root and NADPH RbohD in shoots, is responsible for the *dry2* developmental defects. Thus, to further investigate the role of  $H_2O_2$  in living plant cells, more comprehensive analyses of  $H_2O_2$  metabolism is needed. Several approaches have been used to estimate  $H_2O_2$  production *in vitro* (Palmer and Dittmer, 2010). The *in situ* detection of  $O_2^{\cdot-}$  and  $H_2O_2$  by NBT and DAB respectively are just qualitative approaches to estimate the accumulation of ROS. These *in situ* staining techniques cannot be easily used to estimate ROS production *in vivo*, since the staining depend on how efficiently the chemicals penetrate into the tissues and additional problem related with diffusion of the stain within tissues should be considered. In order to get a deeper understanding of ROS homeostasis in plants, an adequate method is required for the detection and quantification of these molecules in tissues and particularly inside living cells. Recently, a newly developed molecular fluorescent indicator of intracellular  $H_2O_2$  levels, named HyPer, is available (Belousov *et al.*, 2006). HyPer is a genetically encoded ratiometric sensor that is highly selective for  $H_2O_2$  over other ROS. HyPer consists of the

bacterial H<sub>2</sub>O<sub>2</sub>-sensitive transcription factor OxyR fused to a circularly permuted yellow fluorescent protein (YFP). Cysteine oxidation of the OxyR part induces a conformational change that increases emission excited at 500nm (YFP<sub>500</sub>) and decreases emission excited at 420nm (YFP<sub>420</sub>). This change is rapidly reversible within the reducing cytoplasmic environment, allowing dynamic monitoring of intracellular H<sub>2</sub>O<sub>2</sub> concentration. HyPer has been proved to be an effective tool in the observation of H<sub>2</sub>O<sub>2</sub> concentration changes in HeLa cells and zebrafish (Belousov *et al.*, 2006; Niethammer *et al.*, 2009). Recently, it was demonstrated that the HyPer protein can be targeted to different subcellular compartments of plant cells, such as the cytoplasm and peroxisomes and specifically sense H<sub>2</sub>O<sub>2</sub> (Costa *et al.*, 2010).

To investigate H<sub>2</sub>O<sub>2</sub> spatiotemporal distribution in leaving plant cells, the *dry2* and its suppressors discussed in the present study are presented as a good plant model, because of *dry2* lack of H<sub>2</sub>O<sub>2</sub> accumulation during development that is rescued by the suppressor mutations. Thus, stable transgenic Arabidopsis lines constitutively expressing HyPer within the cytoplasm, were generated first Col and *Ler* background to subsequently generate by genetic crosses, *dry2* and suppressors line expressing the HyPer protein. The Gateway® HyPer-As entry clone is an *Evrogen* commercially available vector, containing a *HyPer* gene variant with codon usage optimized for high expression in Arabidopsis and *Saccharomyces*. The *HyPer* gene variant *HyPer-As* was cloned into a pMDC32 vector containing a dual CaMV35S promoter to drive the constitutive ectopic gene expression in transgenic plant cells. Stable transgenic Arabidopsis lines were transformed with the construct to generate a constitutively expressing *HyPer* within the cytoplasm. Arabidopsis independent transgenic lines were generated in Col and *Ler* background and homozygous lines (10 Hm Col-0 and 4 Hm *Ler* lines) were isolated after three generations. These lines will be employed for imaging experiments and a selected line stably expressing the HyPer-As sensor will be employed for crossing experiments with *dry2* and suppressor mutants. Given the NBT staining phenotype of *dry2*, the *dry2 HYPER-AS* double mutant will allow a more comprehensive and sensitive approach to elucidate the mechanism of ROS distribution affected in the *dry2* mutant, that is restored into the *dry2* suppressors.

## 2.3. MATERIALS AND METHODS

### Plant Material

The *Arabidopsis thaliana* ecotypes Landsberg *erecta* (*Le*) and Columbia-0 (*Col-0*) were used as wild-type controls in the present study. Mutants used in this study have been previously described: *dry2* (Pose *et al.*, 2009); *dry2/sud9* and *dry2/sud22* (Pose, 2008). The *dry2*<sup>*Col-0*</sup> introgression line was obtained by crossing *dry2* into the *Col-0* ecotype for seven generations. For more details concerning the development of the *dry2*<sup>*Col-0*</sup> introgression line see *Material and Methods – Arabidopsis Cross-fertilization* section in Chapter 3.

### Plant Manipulation and Growth Conditions

*Arabidopsis* standard handling procedures and conditions were employed to promote seed germination and growth. Before growing, seeds were cold treated for three days at 4°C. Seeds surface sterilization was performed in a horizontal laminar flow chamber (*BBH4 BRAUN Horizontal*). Seeds were sequentially immersed in 70% (v/v) ethanol for 5 min and 20% (v/v) commercial bleach for 10 min before washing five times with sterile ultra-pure water. Seeds were resuspended in sterile 0.25% (w/v) agarose. After being surface sterilized, seeds were sowed onto MS agar plates and grown vertically in a culture chamber at 23°C, under cool white light (photon flux density (PFD) of 60–100  $\mu\text{mol photon m}^{-2} \text{s}^{-1}$ ) with a long-day photoperiod (16-h light/8-h dark cycle). When required, seedlings were transferred to soil after seven days of *in vitro* growth and watered every two days. Plants were grown in a mixture of organic substrate and vermiculite (4:1 v/v) under controlled conditions: 21–22°C, 16-h light/8-h dark cycle with a PFD of  $\sim 150 \mu\text{mol photon m}^{-2} \text{s}^{-1}$ . Seeds were collected at the end of the life cycle (approximately eight weeks), using an appropriate sieve with metallic mesh.

### Root Branching Measurements

For root branching measurements, 7-day-old seedlings grown on phytagel-solidified MS medium were transferred to half-strength phytagel-solidified MS medium deprived of supplementation (control) or supplemented with Rose Bengal (Sigma) or Paraquat (methyl viologen; Sigma) to the final concentrations of 0.001 and 0.01  $\mu\text{M}$ . Root branching was determined by estimating the number of root tips per length of primary root. Results were statistically analyzed using One-way analysis of variance “ANOVA”, with Bonferroni's Multiple Comparison Test.

### Detection of Reactive Oxygen Species

Plant infiltration with Nitroblue Tetrazolium (NBT) (Sigma) allowed the *in situ* detection of superoxide ion in leaves. The whole plant was treated with NBT staining method as described by Jabs *et al.* (1996), with the following modifications. Five-week old entire plants, or cut leaves, were harvested and vacuum-infiltrated (three cycles of 5 min) with 0.5  $\text{mg mL}^{-1}$  NBT in 10 mM sodium phosphate buffer,

pH 7.8. Samples were incubated for 1 h in the dark at room temperature and then cleared in 96% ethanol at 70°C until complete removal of chlorophyll. The leaves were imaged under dark-field illumination with a Leica *MZ FLII* stereomicroscope coupled to a *Nikon Coolpix 4500* digital camera.

### Generation of Transgenic *HyPer-As* Constructs/Plants

The *HyPer* gene variant *HyPer-As* was ordered from the *Evrogen* commercially available Gateway *HyPer-As* entry clone. For more details concerning this commercial vector, see appendix III (Figure AIII.1). This plasmid was transformed into *E. coli* DH5 $\alpha$  and analyzed by restriction following miniprep, to confirm that it was the correct vector. The *HyPer-As* entry clone was recombined through an LR clonase recombination step, and according to Invitrogen's indications, with the Gateway compatible destination vector pMDC32 (Curtis and Grossniklaus, 2003). For more details concerning this commercial vector, see appendix III (Figure AIII.2). The insertions were confirmed by restriction and sequencing, using the primers displayed in Table 2.1. The plasmid was mobilized into the *Agrobacterium tumefaciens* GV3101::pMP90 strain (Koncz and Schell, 1986), and subsequently used to transform the wild-type Col-0 or *Ler Arabidopsis thaliana* ecotypes by the floral dipping method.

**Table 2.1 – Primers used to Sequence the *HyPer-AS* Insertion Cloned into the pMDC32 Vector**

Primer Name	Sequence (5'→3')	Primer size (bp)
pMDC 30 32 Fw seq1	ttaactagttagagcgccg	22
pMDC 30 32 Fw seq2	ctctagaggatccccgggta	20
pMDC 30 32 Rv seq3	gagatctcctagggcccat	20

### *Arabidopsis* Transformation by Floral Dipping

Stable transgenic *Arabidopsis* lines constitutively expressing *HyPer* were generated by floral dipping. *Arabidopsis* floral dip transformation was performed according to a modification of the procedure described by Clough and Bent (Clough and Bent, 1998). *Arabidopsis* plants were grown in four large pots, at a density of 4 plants per pot, under normal conditions, until the early bolting stage. *Agrobacterium* single colonies were obtained by growing cells in appropriate selection medium, at 28°C, and used to inoculate a 7 mL culture of LB liquid media supplemented with Rifampicin to a final concentration of 50 mg mL<sup>-1</sup>, which was grown ON at 28°C and 200 rpm. An aliquot of 500  $\mu$ L from this culture was used to inoculate 200 mL of LB\* liquid medium (supplemented with Kanamycin to a final concentration of 50 mg mL<sup>-1</sup> and acetosyringone to a final concentration of 19.6 mg mL<sup>-1</sup>), and incubated ON at 28°C and 200 rpm. Cells were collected by centrifugation for 12 min at RT and 5000 rpm, and the pellet was resuspended in a 500 mL glass vial containing 250 mL of 5% (w/v) sucrose. Prior to the transformation, 125  $\mu$ L of Silwet L-77 were added to the *Agrobacterium* suspension. The aerial part of plants (from which already developed siliques were previously removed) was dipped in the solution for 30 seconds. Plants were laid down in a tray, covered with plastic and placed in the dark for two days. The plastic was then removed, and plants were grown normally for the rest of their life cycle.



**Selection of Arabidopsis Transformants**

After transformed plants completed the life cycle, T1 seeds were collected and grown in 0.8% (w/v) agar-solidified MS medium containing hygromycin ( $40 \mu\text{g mL}^{-1}$ ) and ticarcillin ( $250 \mu\text{g mL}^{-1}$ ) for transformant selection. Positive control (resistant) seeds were also sowed onto the plate. Positive T1 transformants (similar to control plants) were transferred to soil after 10 days to complete their life cycle. A total of 20-40 T2 seeds per T1 plant were germinated in identical selective medium. Plants presenting a 3:1 (positive:negative) ratio, indicative of only one T-DNA insert, were selected and grown on soil. Seeds were again collected (T3) and germinated in the same conditions to verify if the T2 line was homozygous (1:0 ratio) or heterozygous (3:1 ratio) for the T-DNA insertion. Homozygous plants were selected for further analysis.



# Chapter 3

## Identification of *dry2* Suppressor Mutations

The experimental work presented in the present chapter was performed in collaboration with Verónica G. Doblas from Instituto de Hortofruticultura Subtropical y Mediterránea, Universidad de Málaga, Consejo Superior de Investigaciones Científicas, IHSM-UMA-CSIC, Málaga, Spain; that equal contributed to the data obtained.

### **CONTENTS**

---

#### 3.1. INTRODUCTION

#### 3.2. RESULTS AND DISCUSSION

Four *dry2* Suppressor Mutations are Semi-dominants

Map-based Cloning of the *sud* Mutations

Four *dry2* Suppressors are Independent *sud1* Mutant alleles

#### 3.3. MATERIALS AND METHODS



### 3.1. INTRODUCTION

Reverse genetic approaches tend to rely on prior knowledge that the gene that is being mutated is involved in a particular process (Azevedo *et al.*, 2011). Meanwhile, in functional studies based on a forward genetics approaches, a mutant population is screened for a phenotype-of-interest leading to the identification of important gene(s) involved in the process. Map-based cloning, also called positional cloning, is the process of identifying the genetic basis of a mutant phenotype by looking for linkage to markers whose physical location in the genome is known. In the Map-based cloning process, no prior assumptions are needed in order to identify genes responsible for a given phenotype. Map-based cloning in Arabidopsis can be divided in two steps: i) to obtain a raw mapping position, and ii) to perform a fine-scale mapping that narrows down the region containing the gene-of-interest to a few candidates (Jander *et al.*, 2002). As a first step in the mapping process, the mutant is crossed with a polymorphic ecotype. F2 seeds are collected from self-pollination of the F1 plants, and usually, a population of around 40-50 plants are grown for a first mapping. As plants are growing, the phenotype of the F2 plants is determined, and plants are genotyped with molecular markers, spaced roughly apart on the five chromosomes. Next, it is necessary to analyse a larger F2 population for fine-resolution mapping. The ultimate goal of fine mapping is to narrow down the region containing the gene of interest to approximately 100 kb or less. Depending on the interval there are several possibilities to analyze the final unmapped region, but recently the use of high throughput sequencings is become the favorite approach due to its speed and reliability.

In a previous work, a drought stress hypersensitive mutant *dry2/sqe1-5* affected in the sterol biosynthetic *Squalene Epoxidase 1 (SQE1)* gene was identified (Pose *et al.*, 2009). Since the regulatory mechanisms controlling the sterol biosynthetic pathway in plants are largely unknown, the hypomorphic *dry2/sqe1-5* mutant allele, which is fertile in contrast to the null *sqe1-3* allele, was used to perform a suppressor screening in order to identify second-site mutations induced by EMS that abrogated the extreme drought hypersensitive phenotype of the *dry2* mutant previously described (Chapter 1). Using this strategy, several mutants (named *sud* for *suppressors of dry2 defects*) that reverted most of the *dry2* developmental phenotypes were isolated. The identification of the mutations causing suppression of *dry2* phenotypes, will allow identifying previously uncharacterized regulatory elements able to restore the developmental defects observed in the *dry2* mutant.

The present chapter will describe the positional cloning of four independent *dry2* suppressor mutations (*sud9*, *sud22*, *sud26* and *sud27*), using a combination of map-based cloning and high-throughput Illumina next-generation sequencing strategy.

## 3.2. RESULTS AND DISCUSSION

### Four *dry2* Suppressor Mutations are Semi-dominants

A critical aspect of map-based cloning is the ability to accurately detect the allelic state of the mutation being mapped (homozygous mutant, homozygous wild-type, or heterozygous) in these recombinant plants by looking at the phenotype in a representative sample of progeny in the F<sub>2</sub> generation. However, to detect the allelic state of the mutation being mapped in the recombinant plant, it is first necessary to determine if the mutation is dominant or recessive. Thus, the *dry2/sud9*, *dry2/sud22*, *dry2/sud26* and *dry2/sud27* mutants were back-crossed with *dry2*. Presence of an intermediate phenotype in the F<sub>1</sub> generation for all the tested crosses indicates that all *sud* mutations are semi-dominant. The intermediate phenotype of an F<sub>1</sub> cross between *dry2/sud22* and *dry2*, compared with wild-type, *dry2* and *dry2/sud22* are depicted in Figure 3.1. Similar results were obtained for *dry2/sud9*, *dry2/sud26* and *dry2/sud27* (data not shown). Since all four *dry2* suppressor mutations appear to be semi-dominant, it was not possible to establish at first, based on an allelism test, whether these mutants were alleles of the same gene or were affected in different genes (Koornneef *et al.*, 2006).

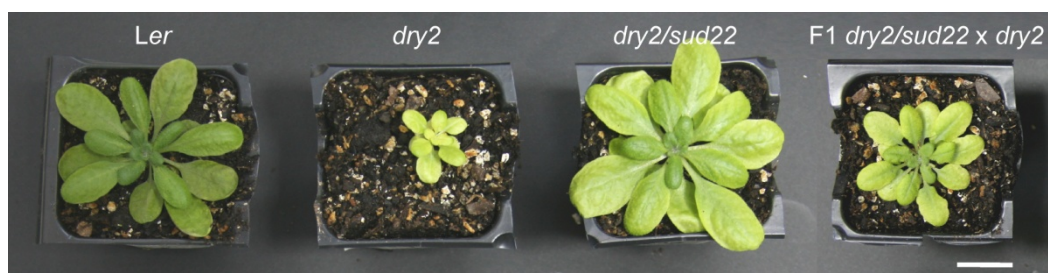


**Figure 3.1 – Intermediate Phenotype in the F<sub>1</sub> Generation of *dry2/sud22* Mutant Back-crossed with *dry2***

Shoot phenotype of 28-day-old plants of wild-type *Ler*, *dry2*, *dry2/sud22* and F<sub>1</sub> *dry2/sud22* x *dry2* reveals that the *sud22* mutation is semidominant. Scale bar: 2 cm.

### Map-based Cloning of the *sud* Mutations

In order to perform a first-pass mapping to determine the raw mapping position of the *sud22* mutation, *dry2/sud22* (on *Ler* ecotype) was crossed with a Col-0 plant. Seeds (F2) were collected from self-pollination of the F1 plants, and plants with *dry2* and *dry2/sud22* phenotypes were identified. Assuming that the *dry2* and *sud22* mutations will segregate independently, in the F2 mapping population it is expected that only 1 in every 16 plants will carry both *dry2* and *sud22* mutations in homozygosity. Thus, informative individuals were identified following two distinct steps. First, plants with wild-type phenotypes were identified (Figure 3.2A). Even though the wild-type phenotypes could be due to the presence of the suppressor in the *dry2* background, most plants would present wild-type phenotypes because they did not contain homozygous *dry2*. Next, plants with wild-type phenotype but carrying the homozygous *dry2* mutation were identified by diagnostic PCR (Figure 3.2B).

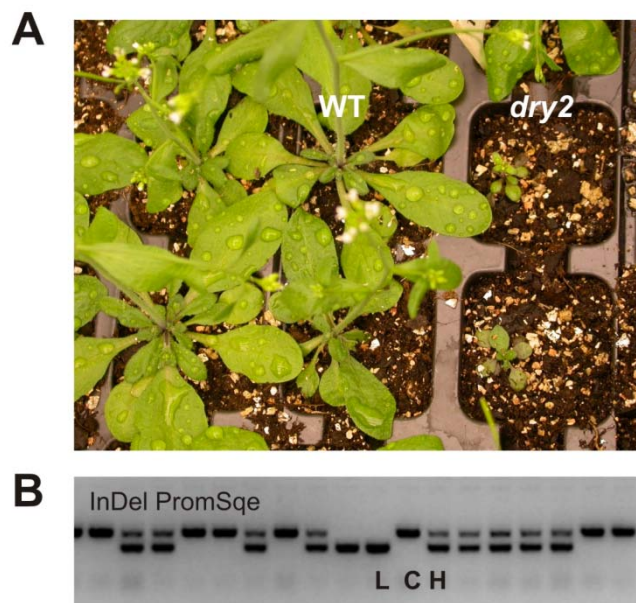


**Figure 3.2 – Isolation of homozygous plants for *dry2* and *sud22* mutations presenting wild-type phenotype**

**(A)** Shoot wild-type (WT) and *dry2* phenotype of the F2-segregating mapping population obtained from a cross between *dry2/sud22* and wild-type (Col-0) plants. **(B)** Genotyping of plants represented in (A) by PCR amplification of the InDel PromSqe InDel Col-0/*Ler* polymorphism. PCR amplification of the region containing the polymorphism allows detection of those plants that are genetically *Ler* (L) in homozygosity at the chromosomal region of the *SQE1/DRY2-5* gene, from those that are Col-0 (C), or heterozygous (H).

A total of 1412 plants were analysed to obtain a *sud22* mapping population. From these plants, only 66 plants were homozygous for *dry2* based on PCR analysis and *sud22* because they presented wild-type phenotypes. These 66 plants of the mapping population were then used to determine a rough map position of *sud22* by analysing genetic markers in the five chromosomes of *Arabidopsis* (Figure 3.3 and Appendix II). All information regarding the molecular markers used in the map-based cloning was obtained from TAIR (<http://www.arabidopsis.org/>). A genetic marker not linked to the mutation has a frequency of 25% Col homozygous, 50% heterozygous Col/*Ler* and 25% *Ler* homozygous (1 Col: 2 Col/*Ler*: 1 *Ler*) while a genetic marker linked to *sud22* will present higher a frequency of *Ler*. Table 3.1 shows the analysis of molecular markers in the mapping population. As expected, the majority of the markers were not linked to the mutation (1Col: 2Col/*Ler*: 1*Ler*). In addition, the expected linkage to *Ler* genotype was observed to *dry2*. Importantly, the genetic markers F13C5, F11C18, F26P21 and F8D20 of chromosome 4 were enriched in *Ler*, indicating an obvious linkage. By analysing the recombinant plants for the genetic markers F26P21 and F8D20 it is possible to locate the *sud22* mutation within the 1,01 Mb region delimited by these two genetic markers (Figure 3.3).

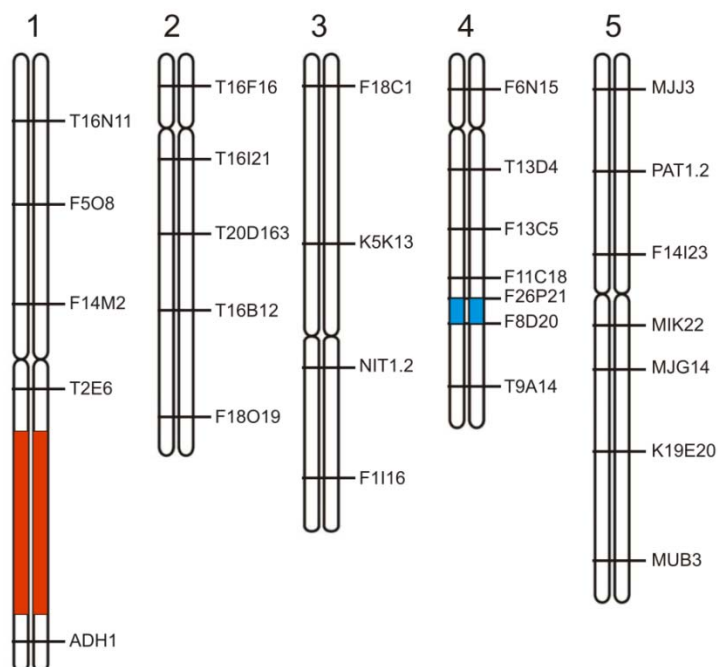


**Figure 3.3 –Diagram of the genetic markers positions used to determine the rough location of the *sud22* mutation**

The region linked to the *dry2* mutation is represented in red and the region between F13C5 and F8D20 markers that encompasses the *sud22* mutation, is represented in blue.



**Table 3.1 – Genotype of F2 *dry2/sud22* x Col-0 Mapping Population using genetic markers for the rough positioning of the *sud22* mutation**

(a) Represents the number of plants genotyped as Homozygous Col-0 or Heterozygous Col-0/*Ler* using a genetic marker dominant for the Col-0 genotype. (b) Represents the number of plants genotyped as Homozygous *Ler* or Heterozygous Col-0/*Ler* using a genetic marker dominant for *Ler* genotype. The genetic markers most closely linked to the *sud22* mutation are shown in gray.

Molecular Marker	No. Analysed Plants	No. Homozygous Col-0	No. Col-0 <sup>a</sup>	No. Heterozygous Col-0/ <i>Ler</i>	No. <i>Ler</i> <sup>b</sup>	No. Homozygous <i>Ler</i>
<b>Chromosome 1</b>						
T16N11	65	18			47	
F508	66	10		35		21
F14M2	66	0		33		33
T2E6	66	0		6		60
ADH1	66	6		21		39
<b>Chromosome 2</b>						
T16F16	59	13			46	
T16I21	57	27		24		6
T20D163	65	19		40		6
T16B12	57	18		21		18
F18O19	65	14		39		12
<b>Chromosome 3</b>						
F18C1	66	19		24		23
K5K13	66		55			11
NIT1.2	66	12		45		9
F1I16	53	10		24		19
<b>Chromosome 4</b>						
F6N15	60	14		31		15
T13D4	64		42			22
F13C5	61	1		33		27
F11C18	66		30			36
F26P21	60	0		20		40
F8D20	66	3		24		39
T9A14	64	3		30		31
<b>Chromosome 5</b>						
MJJ3	63	33		21		9
PAT1.2	66	25		35		6
F14I23	66	15		27		24
MIK22	66	9		33		24
MJG14	65	23		38		5
K19E20	66	18		33		30
MUB3	65		59			6

Once the *sud22* mutation was located within the 1,01 Mb region delimited by two genetic markers on the bottom part of the larger arm of chromosome 4, it was necessary to perform a fine-scale mapping to narrow down the region containing the gene of interest to approximated 100 kb or less. To do this, it should have been necessary to generate a larger F2 population in order to increase the recombination events within this interval. This approach, although valid for raw mapping, was too laborious to pursue. In order to perform a fine-scale

mapping of *sud22* mutation, a line that contained the introgressed *dry2* mutation in Col-0 background was generated in parallel to the raw mapping. To achieve this, the *dry2*<sup>Ler</sup> mutant allele was introgressed into wild-type Col-0 over seven generations to create *dry2*<sup>Col-0</sup>. The *dry2*<sup>Col-0</sup> line was analyzed using genetic markers to confirm that most of the genome was Col-0 with the exception of the region flanking *DRY2* (Table 3.2). The *dry2*<sup>Col-0</sup> line was phenotypically identical to the original *dry2* in shoot and root growth (Figure 3.4) and also accumulated undetectable levels of ROS (Chapter 2, Figure 2.2). This line was used to generate a mapping population for *dry2/sud22* and determine a fine position for the mutation.

**Table 3.2 – *dry2*<sup>Col-0</sup> Genotype for the Genetic Markers in the 5 Arabidopsis Chromosomes**  
The genetic markers linked to *SQE1/DRY2* are highlighted

	Marker	Genotype
<b>Chromosome 1</b>		
	T16N11	Col-0
	F508	Col-0
	F14M2	Col-0/Ler
	T2E6	Ler
	ADH1	Ler
<b>Chromosome 2</b>		
	T16F16	Col-0
	T20D163	Col-0
	F18019	Col-0
<b>Chromosome 3</b>		
	F18C1	Col-0
	K5K13	Col-0
	NIT1.2	Col-0
<b>Chromosome 4</b>		
	F6N15	Col-0
	T13D4	Col-0
	F13C5	Col-0
	F11C18	Col-0
	F26P21	Col-0
	F8D20	Col-0
	T9A14	Col-0
<b>Chromosome 5</b>		
	PAT1.2	Col-0
	MJG14	Col-0
	MUB3	Col-0

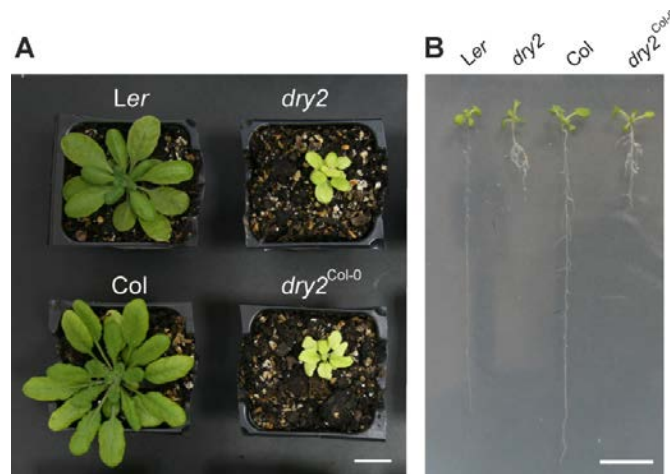


**Figure 3.4 – Phenotype of *dry2*<sup>Col-0</sup> Line Generated for Map-based cloning of the *sud22* Mutation**

The introgression line *dry2*<sup>Col-0</sup> is phenotypically identical to the *dry2* mutant at the shoot (A) and root (B). Phenotype of the introgression line *dry2*<sup>Col-0</sup> and *dry2* mutant are presented side by side with the respective wild-types (WT) Col-0 and *Ler*. Scale bar: 2 cm (A) and 1 cm (B).

Once the *sud22* mutation was known to localise between F26P21 and F8D20, a fine-scale mapping was designed using new SSLPs (Simple Sequence Length Polymorphisms) or CAPs (Cleaved Amplified Polymorphisms) genetic markers, located in the BACs F17M5, T16L1, T17I5, F28A23, F10M10 and T4L20 (Appendix II). A total of 1402 plants (2804 chromosomes) of the *dry2/sud22* × *dry2*<sup>Col-0</sup> F<sub>2</sub> population with any phenotype were analyzed with these new markers. The number of recombinants per each marker is detailed in Figure 3.5. No recombinant was found for F28A23 marker. After analysis of 335 more total plants (670 chromosomes), still no new recombinants were found, and it was decided to stop the mapping process. Thus, *sud22* was finally mapped to a 117 Kb region on chromosome 4 between the SSLP markers T17I5 and F10M10, encompassing 36 candidate genes.

To test whether mutations *sud9*, *sud26* and *sud27* occurred in the the same gene that was affect by the *sud22* mutation, a first-pass map-based cloning approach was used to confirm if those mutations co-segregated with the marker more closely linked to the *sud22* mutation. For this purpose, an F<sub>2</sub> mapping population using the three suppressor mutants and a line that contained the *dry2* mutation in Col-0 background (*dry2*<sup>Col-0</sup> introgression line) was obtained. As shown in Table 3.3, all three *sud* mutations co-segregated with markers located in the same region of chromosome 4, strongly suggesting that all mutations occurred in the same gene. For *sud9*, a chromosome 2 genetic marker was analyzed as control.

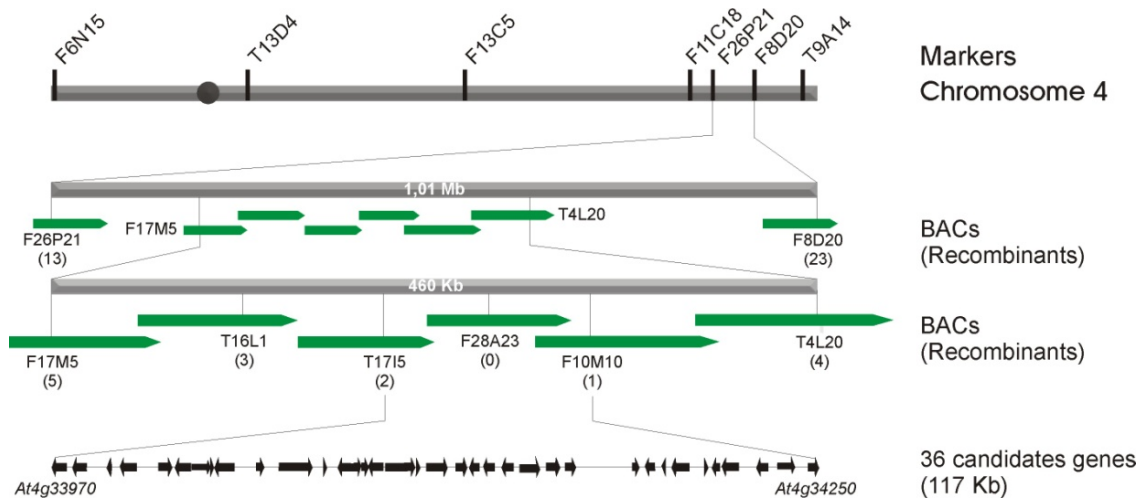


**Figure 3.5 – Fine-scale mapping of the *sud22* mutation**

The SSLP (Simple Sequence Length Polymorphism) and CAPs (Cleaved Amplified Polymorphisms) markers for the fine-scale mapping and the BACs from which these markers were derived are shown. *sud22* was mapped to a 117 kb region on chromosome 4, between the SSLP markers T17I5 and F10M10. The grey bars represent regions on chromosome 4, systematically enlarged. The green bars represent the BACs where molecular markers have been designed. The number of recombinants of each marker is represented by brackets. The black arrows represent the 36 candidate genes.

**Table 3.3 – Genotype of Positional Cloning F2 Mapping Population for *sud9*, *sud26* and *sud27***

The genetic markers closely linked to the mutation *sud9*, *sud26* and *sud27* are highlighted.

Chromosome	Molecular Marker	No. Analysed Plants	No. Homozygous Col-0	No. Heterozygous Col-0/Ler	No. Homozygous Ler
<b>F2 <i>dry2/sud9</i> x <i>dry2</i><sup>Col-0</sup></b>					
2	F18019	28	9	14	5
4	F26P21	102	0	6	96
4	F8D20	102	0	5	97
<b>F2 <i>dry2/sud26</i> x <i>dry2</i><sup>Col-0</sup></b>					
4	F17I5-2	10	0	0	10
4	F8D20	10	0	0	10
<b>F2 <i>dry2/sud27</i> x <i>dry2</i><sup>Col-0</sup></b>					
4	F17I5-2	6	0	0	6
4	F8D20	6	0	0	6

### Four *dry2* Suppressors are Independent *sud1* Mutant alleles

Using map-based cloning, the *sud22* mutation was located in a 117 kb region that contains 36 annotated genes, according to the latest Arabidopsis genome annotation available in the TAIR database (<http://www.arabidopsis.org/>). In order to identify *sud22*, the whole genome of *dry2/sud22* was sequenced using Solexa (Illumina Genome Analysis System technique) at the University of California Riverside. The resulting 117 kb candidate sequences were compared with

the public sequence in order to identify single nucleotide polymorphisms (SNPs) (<http://1001genomes.org/>). A total of six non-synonymous mutations within the coding regions of the 36 candidate genes were found. The analysis of Arabidopsis ecotype natural variations based on the Perlegen (Clark *et al.*, 2007) and Ossowski (Ossowski *et al.*, 2008) data, revealed that four out of six non-synonymous mutations found in the *dry2/sud22* sequences corresponded to natural ecotype variations and therefore do not affect conserved amino acids and were excluded as candidates. The number of candidate genes was thus narrowed down to only two (*At4g34100* and *At4g34135*). The genomic DNA fragment of *At4g34100* and *At4g34135* was independently amplified from two individual *dry2/sud22* plants, sequenced by traditional Sanger sequencing and compared with the *dry2* mutant. A mutation affecting the *At4g34135* gene was found to be a false positive of the Illumina sequencing while the mutation in *At4g34100* was confirmed. Therefore, by using a combination of first-pass mapping, fine-scale map-based cloning and high-throughput sequencing, it was finally determined that the second-site mutation responsible for the suppression phenotypes of *dry2/sud22* was a G→A substitution in the *At4g34100* gene (hereafter named *SUD1*). This mutation caused a G360E substitution in the predicted *SUD1* amino acid sequence (Table 3.4).

**Table 3.4 –Nucleotide Changes and Predicted Amino Acid Substitution of five *sud1* alleles**

The position of mutated nucleotide in coding sequence of the *sud1* alleles and the corresponding amino acid substitution in the corresponding protein are indicated.

Allele	Mutation	Amino Acid Substitution
<i>sud1-9</i>	G → A (652)	Gly 218 → Arg
<i>sud1-26</i>	G → A (731)	Arg 244 → Lys
<i>sud1-22</i>	G → A (1079)	Gly 360 → Glu
<i>sud1-27</i>	G → A (1626)	Trp 542 → stop codon

Targeted sequencing of the three additional suppressors identified additional mutations in the *SUD1* gene, *dry2/sud9* (G218R substitution), *dry2/sud26* (R244K substitution), and *dry2/sud27* (premature stop codon at position 542) (Table 3.4). These results indicated that mutations in the *SUD1* locus caused the suppression of the *dry2* defects. The fact that the four suppressors contained the second-site mutations in the same *SUD1* gene, and correspond to different alleles, lead us to the rename the *dry2/sud9*, *dry2/sud22*, *dry2/sud26* and *dry2/sud27* to *dry2/sud1-9*, *dry2/sud1-22*, *dry2/sud1-26* and *dry2/sud1-27* (Figure 3.6).



**Figure 3.6 – Schematic Diagram of the *At4g34100* Gene Structure**

The amino acid substitutions of four *sud1* alleles are indicated. Exons are represented as orange boxes and the introns represented by a gray line. The 5' UTR and 3' UTRs are represented by the terminal gray box and a gray arrow, respectively.

### 3.3. MATERIALS AND METHODS

#### Plant Material

The *Arabidopsis thaliana* ecotypes Landsberg *erecta* (*Le*) and Columbia-0 (Col-0) were used as wild-type controls in the present study. Mutants used in this study have been described previously: *dry2* (Pose *et al.*, 2009), *dry2/sud9*, *dry2/sud22*, *dry2/sud26* and *dry2/sud27* (Pose, 2008). Suppressor F1 and F2 combinations generated in this work were obtained by classical genetic crosses. For more details see Arabidopsis Cross-fertilization section in the present chapter. The F1 population from crosses between suppressors and *dry2* were used for genetic analysis to determine the dominance/recessiveness of the suppressor gene alleles. The F2 population from the cross between *dry2/sud22* and Col-0 was used to perform a first-pass mapping and determine the raw mapping position of the *sud22* mutation. The F2 population from the cross between *dry2/sud22* and a line that contained the *dry2* mutation in Col-0 background (*dry2*<sup>Col-0</sup> introgression line) was used to generate a mapping population for *dry2/sud22* and determine a fine position for the *sud22* mutation. The *dry2*<sup>Col-0</sup> introgression line was obtained by crossing *dry2* into the Col-0 ecotype for at least seven generations. The F2 populations from crosses between suppressors *dry2/sud9*, *dry2/sud26* and *dry2/sud27* and *dry2*<sup>Col-0</sup> were used to perform a first-pass mapping and determine the raw mapping position of *sud9*, *sud26* and *sud27* mutations.

#### Plant Manipulation and Growth Conditions

*Arabidopsis* standard handling procedures and conditions were employed to promote seed germination and growth, as previously described in Materials and Methods section of Chapter 2.

#### Arabidopsis Cross-fertilization

Plants were subjected to artificial fertilisation by classical genetic crosses as now described. Crosses were made with the assistance of a *Leica Zoom 2000* bench stereomicroscope and special crossing tweezers. Siliques, flowers, and opened buds were removed from female donors. The closed buds were opened and all organs were removed with the exception of the carpel. In the male donor, a flower was removed with a closing tweezer, and the pollen from the anthers was placed at the surface of the carpel stigma of the female donor to promote fertilisation. After crossing, the stem of the plant was

signalled and formation of a viable silique was observed within two days. Fully developed seeds were later recovered.

### Identification of homozygous plants for the *dry2* and *sud22* mutations

Homozygous plants for the *dry2* and *sud22* mutations were identified using two distinct steps. First, plants presenting wild-type phenotypes were identified. The wild-type phenotypes could be due to the presence of the suppressor in the *dry2* background, but most plants would still present wild-type phenotypes because they either did not contain *dry2* or *dry2* was in heterozygous condition. Next, plants with wild-type phenotype but carrying the homozygous *dry2* mutation were identified by PCR amplification of the SSLP *InDel PromSqe Col-0/Ler* polymorphism. PCR amplification of the region containing the *InDel PromSqe Col-0/Ler* polymorphism located at the *DRY2/SQE1* promoter region, using the primers displayed in Table 3.5, allowed to distinguish those plants that were genetically *Ler* homozygous at the chromosomal region of *SQE1/DRY2-5* gene, from those that were Col-0 or heterozygous. Since the *dry2* mutation was in *Ler* background in the parental plant used for the cross between *dry2/sud22* and wild-type (Col-0) plants, in the F2 segregating population those plants that were genetically *Ler* homozygous at the chromosomal region of the *SQE1/DRY2-5* gene, are most likely homozygous for the *dry2* mutation.

**Table 3.5 – Primers used to Specifically Amplify the SSLP *InDel PromSqe Col-0/Ler* Polymorphism**

Name	Sequence (5'→3')	Annealing temperature (°C)	Polimorfism type	Col-0 Amplification product size (bp)	<i>Ler</i> Amplification product size (bp)
<i>InDel PromSqe Fw</i>	TGCTCGCTCGTACTTTTGAG	55	SSLP	628	365
<i>InDel PromSqe Rv</i>	GAATCAAATAACGCGAGGTGA				

### Map-based Cloning of *SUD1*

The standard molecular biology methods, used in the present work, are presented in more detail in Appendix I. All information regarding the genetic markers used in the map-based cloning of *SUD1* was obtained from TAIR (<http://www.arabidopsis.org/>). The detailed information regarding the genetic markers is presented in more detail in Appendix II.

### Bioinformatic Tools Used for Identification of *SUD1*

The second-site mutation responsible for the suppression phenotypes of *dry2* (*SUD1*) was identified using a combination of map-based cloning and high throughput sequencing. Using map-based cloning, the *sud1-22* mutation was mapped to a 117 kb region that contained 36 annotated genes according to the TAIR database (<http://www.arabidopsis.org/>). The whole genome of *dry2/sud22* was sequenced using Solexa (Illumina Genome Analysis System technique) at the University of California Riverside, by Dr. Abel Rosado Rey. The resulting 117 kb candidate sequences were analysed with the aid of bioinformatic tools, at the Boyce Thompson Institute for Plant Research, by Dr. Aureliano Bombarely, as following described. The sequences obtained by high throughput sequencing were pre-processed using the FastX-Toolkit ([http://hannonlab.cshl.edu/fastx\\_toolkit/](http://hannonlab.cshl.edu/fastx_toolkit/)) program and aligned with the *Arabidopsis*

*thaliana* reference genome annotated in TAIR9 (<http://www.arabidopsis.org/>), using BWA (<http://bio-bwa.sourceforge.net/>) (Li and Durbin, 2009). The alignments were processed and the variations were calculated using SAMtools (<http://samtools.sourceforge.net/>) (Li *et al.*, 2009). The variations corresponding to the *Ler* ecotype were eliminated using an informatics script to compare the coordinates of the variations from *dry2/sud22* sequencing with the variations from *Ler* sequencing data from Prof. Joe Ecker at the 1001 genomes project ([http://1001genomes.org/data\\_providers.html](http://1001genomes.org/data_providers.html)). The resulting *dry2/sud22* variations, corresponding to single nucleotide polymorphisms (SNPs), were classified according to their position as exon-SNP, cds-SNP, intron-SNP and intergenic-SNP.



# Chapter 4

## ***In Silico* Analysis of *SUD1* Expression and Whole-genome Transcript Profile of Wild-type, *dry2*, *dry2/sud9*, and *dry2/sud22***

### **CONTENTS**

---

4.1. INTRODUCTION

4.2. RESULTS AND DISCUSSION

*In Silico* Analysis of *SUD1* Expression

Effect of *SUD1* Inactivation on *dry2* Whole-genome Transcriptional Activity

4.3. MATERIALS AND METHODS



## 4.1. INTRODUCTION

Genomic technologies have led to a paradigm shift in biological experimentation, because they allow the simultaneous yet efficient profiling of most (if not all) components of one class of molecules, like for instance transcripts. High-throughput transcript profiling offers the largest coverage and a wide dynamic range of gene expression information. Although RNAseq is becoming increasingly common, microarrays are still the most popular technique used in transcript profiling. Of all the different technology providers, Affymetrix microarrays are the most commonly used in plant biology research, and the ones that show the highest reproducibility (Redman *et al.*, 2004). Because of their robust sample processing and analysis pipeline, microarrays are also a preferable choice for projects that involve large numbers of samples in model organisms with well-annotated genomes (Baginsky *et al.*, 2010).

With the increase in high-throughput data becoming a reality, advanced software has been developed to extract essential information from large-scale gene expression data sets. Bioinformatic tools such as Genevestigator (Hruz *et al.*, 2008) and the “Bio-Array Resource for Plant Biology” BAR (<http://bar.utoronto.ca/welcome.htm>) organize large gene expression datasets and analyze them for relational networks within a single experiment or across many experiments (Baginsky *et al.*, 2010; Pitzschke and Hirt, 2010). Some of the functionalities of the bioinformatic tools include searching through a wide variety of experiments (*e.g.* developmental stages, tissue specificity or endo- and exogenous stimuli), to study the expression pattern of a given gene-of-interest. They also allow the estimation of transcript variations in different genetic backgrounds including mutants.

The current Chapter presents and discusses the *in silico* expression analysis of *SUDI* based on publicly available microarray-based transcript data. Also, the impact of the *sud1-9* and *sud1-22* second-site mutations on *dry2* background was investigated using microarray experiments that were carried out in the context of the present thesis.

## 4.2. RESULTS AND DISCUSSION

### *In Silico* Analysis of *SUD1* Expression

The *in silico* expression pattern of *SUD1* was analysed to gain new insights on the functional role of this gene, through the use of the web-based resource Genevestigator (<https://www.genevestigator.com/gv/plant.jsp>) (Hruz *et al.*, 2008). As shown in Figure 4.1, *SUD1* is highly expressed across different developmental stages of Arabidopsis. Moreover, *SUD1* is highly expressed in almost every Arabidopsis analysed tissues (Figure 4.2).

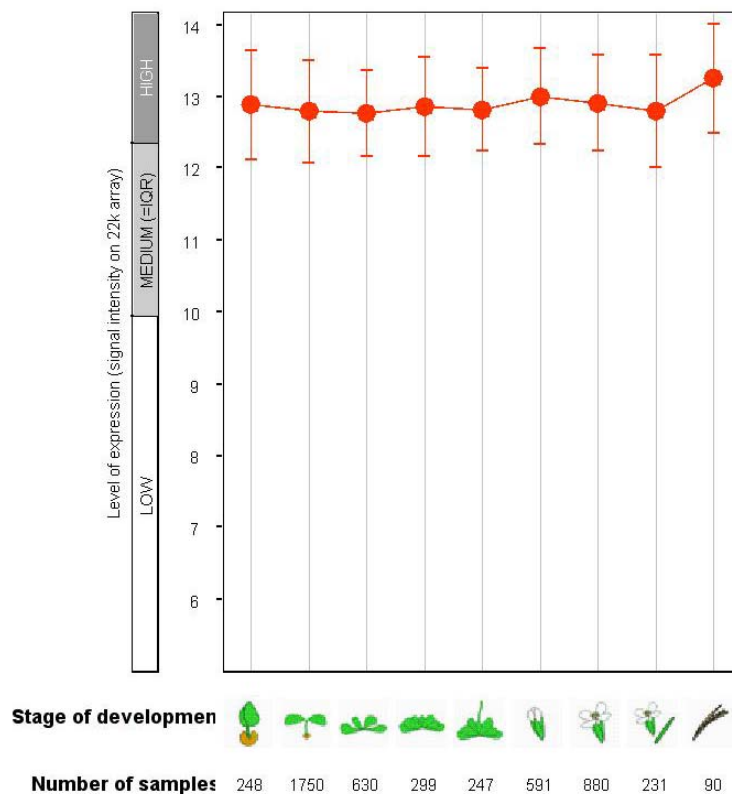


**Figure 4.1 – *SUD1* Expression across Different Stages of Arabidopsis Developmental**

Scatterplot of the Arabidopsis *SUD1* expression pattern (Affymetrix Arabidopsis Genome Array ATH1; probe set: 253267\_at), obtained using the *Development tool* in the *Condition search* toolset from *Genevestigator 4 - Plant Biology* (<https://www.genevestigator.com/gv/plant.jsp>) (Hruz *et al.*, 2008). Levels of expression are scaled to the expression potential (maximum expression a probe set reaches across all experiments). Results are displayed in log<sub>2</sub>-scale. Indicated values in each developmental stage are an average over all samples that were annotated as such. Standard error of the mean is represented on the graph. Total number of samples included into a given developmental stage is indicated at the bottom of the graphs. Development is defined strictly as a time-related dimension with different lapses between precisely defined states of development, from germination to the adult plant.

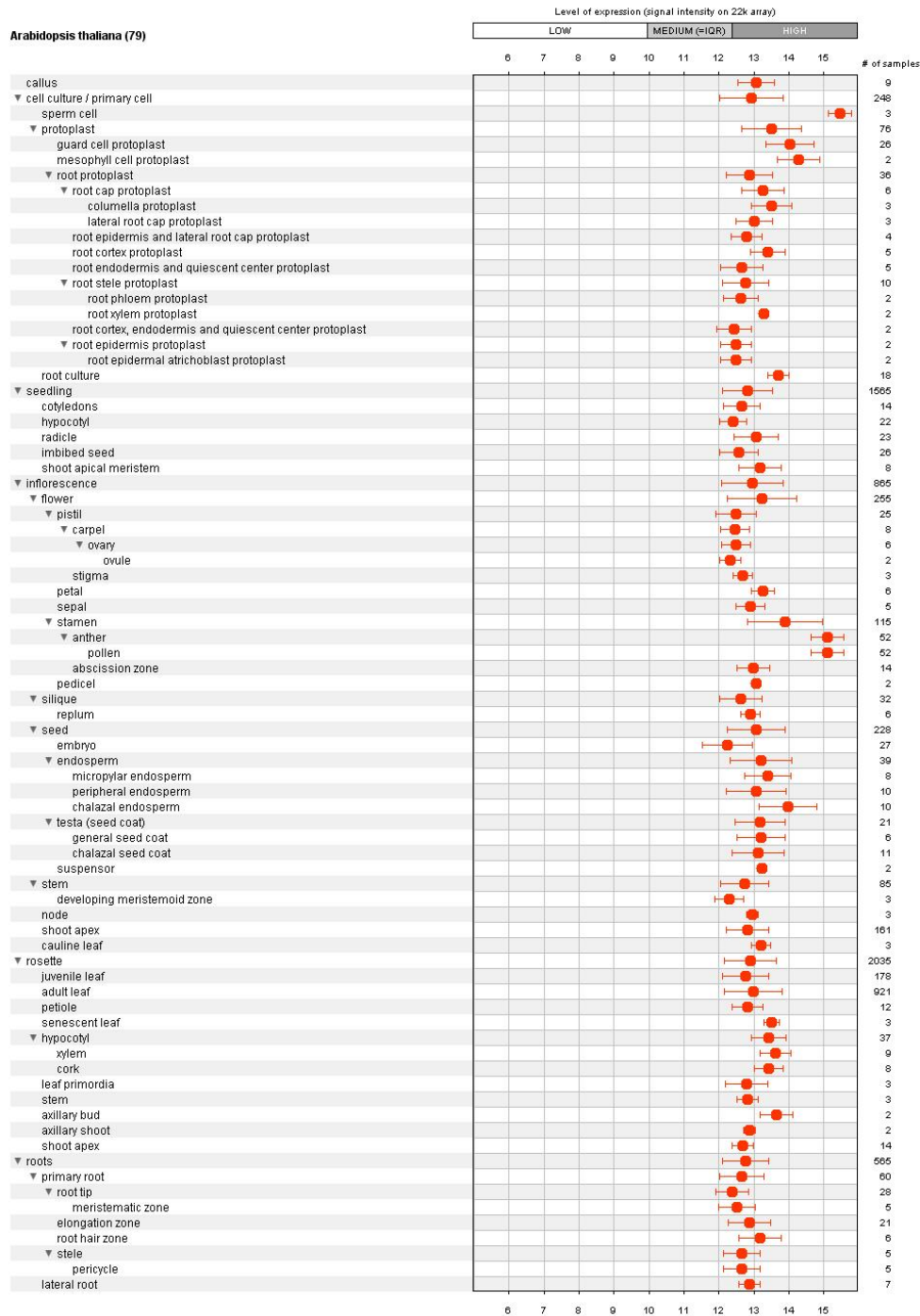


**Figure 4.2 – *SUDI* Expression in Different Arabidopsis Anatomical Categories**

Scatterplot of the Arabidopsis *SUDI* expression pattern (Affymetrix Arabidopsis Genome Array ATH1; probe set: 253267\_at), obtained using the *Development tool* in the *Condition search* toolset from *Genevestigator 4 - Plant Biology* (<https://www.genevestigator.com/gv/plant.jsp>) (Hruz *et al.*, 2008). The Arabidopsis anatomical categories presented include tissues and cell cultures. Levels of expression are scaled to the expression potential (maximum expression a probe set reaches across all experiments). Results are displayed in log<sub>2</sub>-scale. The level of expression within a tissue type is the average expression across all samples that were annotated with that particular tissue type. Standard error of the mean is represented on the graph. Since the anatomical parts are shown as a tree, parent nodes represent the average expression of all samples within this branch. The number of samples that were included to calculate this average is indicated on the right of the graph. Total number of samples included into a given developmental stage is indicated at the bottom of the graphs. The results are displayed as a tree of anatomical parts next to a scatterplot.

Subsequently, analysis was performed on *SUD1* transcriptional activity in different environmental conditions and in response to a wide range of exogenous stimuli on several *Arabidopsis* wild-type genotypes, as well as in different mutant backgrounds. *SUD1* expression was analysed in response to biotic and abiotic stresses, hormone or chemical treatments, light quality, intensity and photoperiod. The results indicate that *SUD1* is not differently expressed (p-value <0.05 and at least 2-fold change) in response to any of the investigated stimuli (data not shown). Moreover, the analysis of *SUD1* expression in different mutant backgrounds revealed that its expression is not de-regulated (p-value <0.05 and at least 2-fold change) in any mutant backgrounds in the Genevestigator 4 database (data not shown). Overall, the analysis of *SUD1* transcript profiling, based on public available microarray data, indicates that *SUD1* is transcribed at a relatively constitutive level and its expression is unaffected by the tested experimental conditions, suggesting that *SUD1* has a housekeeping function in plants.

### **Effect of *SUD1* Inactivation on *dry2* Whole-genome Transcriptional Activity**

Global changes of gene expression in the *dry2* mutant relative to wild-type shoots were previously investigated in RNA samples obtained from 20-day-old *Ler* and *dry2* leaves, using microarray analysis (Pose *et al.*, 2009). According to these authors, 3937 out of the 25327 sampled genes presented statistically significant differential expression in *dry2* compared to the wild-type. In addition, Pose *et al.*, (2009) also found that genes related to abiotic stress responses, genes involved in ROS production and detoxification, and genes involved in sterol biosynthesis were de-regulated in the *dry2* mutant, consistent with the biochemical and molecular phenotypes of the *dry2* mutant. However, since 20-day-old *dry2* plants already present pleiotropic developmental phenotypes, it is difficult to conclude if the de-regulated genes are the cause of the phenotypes or if they are de-regulated because of the *dry2* developmental defects.

Whole-genome analysis of *sud1* mutants in the *dry2* background could help understand how suppression of the *dry2* defect by the second-site mutation affecting *SUD1* affects the *dry2* transcription profile. Therefore, in the present study, the impact of the *sud1-9* and *sud1-22* second-site mutations on *dry2* background was investigated using microarray analysis. For this study, the gene expression in shoots of seedlings was analysed in younger plants, when the *dry2* developmental defects were not evident. We reasoned that this approach would narrow down the total number of de-regulated genes providing mechanistic insights. Thus, total RNA was extracted

from shoot tissue of 13-day-old *Ler*, *dry2*, *dry2/sud1-9* and *dry2/sud1-22* *in vitro*-grown seedlings (Figure 4.3). RNA was first transcribed into cDNA and then into biotinylated complementary RNA, that was hybridized onto Affymetrix ATH1 gene chips.

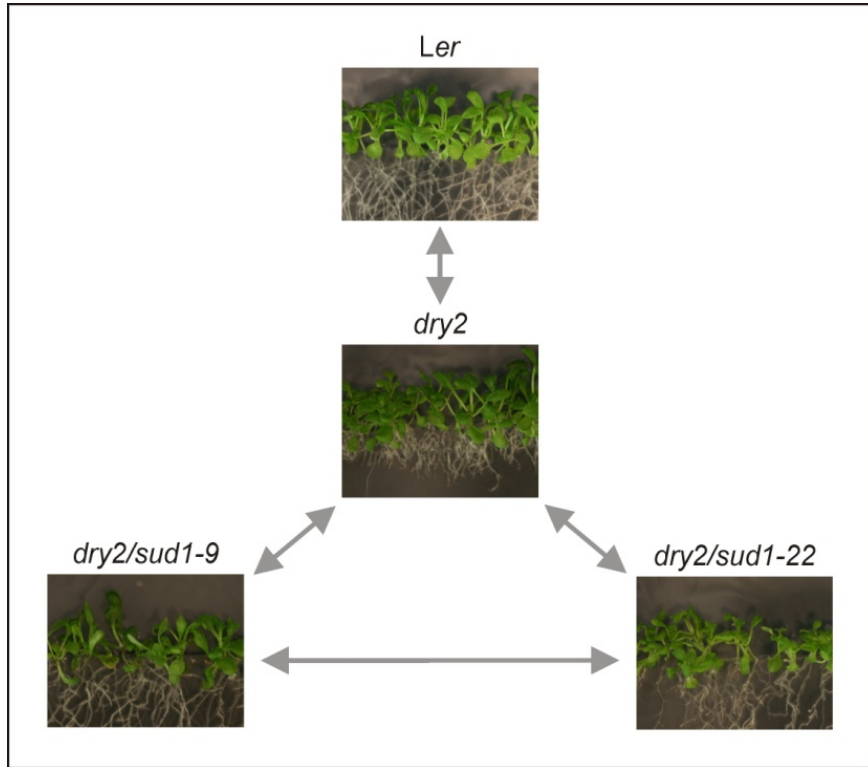


**Figure 4.3 – Schematic Representation of the Microarray Analysis Experimental Design**

Experimental design of the microarray analysis allows comparison of the expression profiles of the analyzed plant lines, as represented by gray arrows. Three biological replicates per genotype were used for microarray analysis. Each biological replica was prepared using 2 independent extractions from shoot tissues of 13-day-old *Ler*, *dry2*, *dry2/sud1-9* or *dry2/sud1-22* *in vitro*-growing seedlings. Total RNA from 3 biological replicates was transcribed into cDNA and then biotinylated complementary RNA was hybridized onto Affymetrix ATH1 gene chips to perform gene whole-genome expression analysis.

The Arabidopsis ATH1 Genome Array contains more than 22,500 probe sets representing approximately 24,000 gene sequences on a single array. The impact of *dry2* and *sud1* mutations on *dry2* background on global gene expression profile was investigated. The average, from three replicate experiments, of the logarithmic intensity values of the more than 22,500 probe sets present on the ATH1 microarray were plotted as dots shown in scatter plots of *dry2* vs *Ler*, *dry2* vs *dry2/sud1-9*, *dry2* vs *dry2/sud1-22* and *dry2/sud1-9* vs *dry2/sud1-22*, as shown in Figure 4.4.

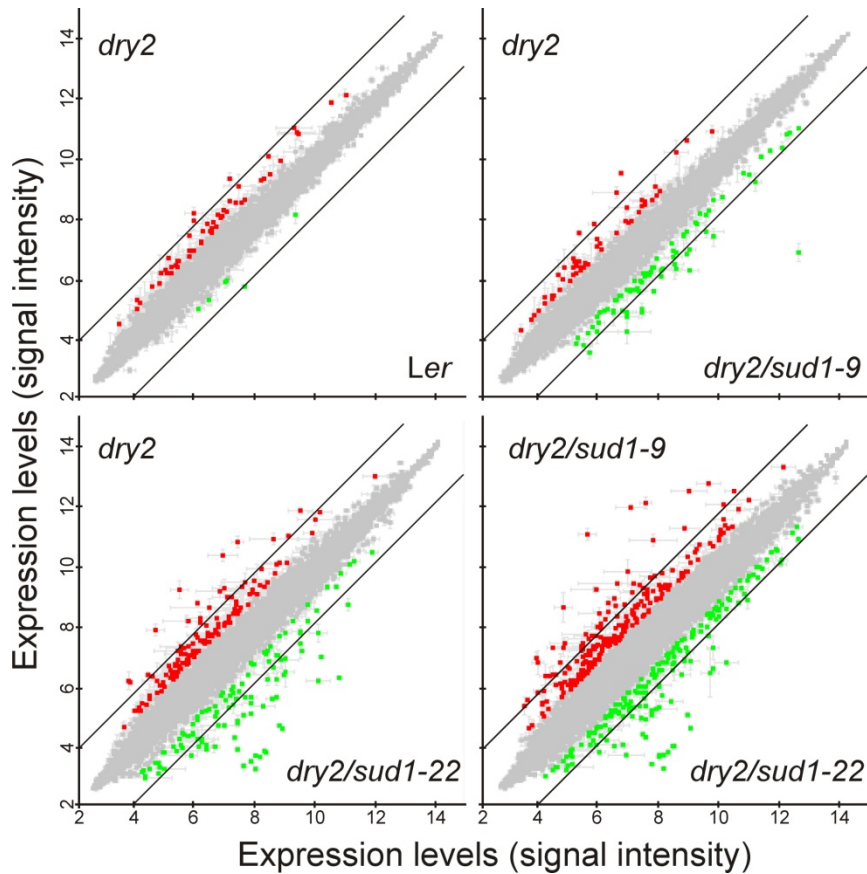


**Figure 4.4 – The Impact of *dry2* and *sud1* Mutations on *dry2* Background on Global Gene Expression**

Scatter plot graph comparing the relative expression profiles of *dry2* vs *Ler*, *dry2* vs *dry2/sud1-9*, *dry2* vs *dry2/sud1-22* and *dry2/sud1-9* vs *dry2/sud1-22*. Global changes in transcript levels were determined using Affymetrix ATH1 gene chips. The individual dots shown on the scatter plots were derived as the average of the logarithmic expression values from three replicate experiments. The average, from three biological replicates, of the log-expression values for each probe set were plotted as dots in scatter plots graphs making use of Fiesta Viewer (<http://bioinfo.gp.cnb.csic.es/tools/FIESTA>) (Oliveros, 2007). For each comparison, red and green dots represent probe sets that match gene sequences at least 2-fold up- or down-regulated, respectively, in the genotype indicated on the top of each scatter plot. Diagonal lines indicate 4-fold differences in either direction in gene expression levels.

Comparison of global gene expression profiles based on differences in normalized probe set intensities among mutant lines, allowed us to graphically visualize the *sud1* mutation's effect on global gene expression (Figure 4.4). Due to constant changes in the annotation of Arabidopsis genome, many probe-sets in the ATH1 platform code for more than one Arabidopsis gene, and many genes are identified by multiple probe sets. In the present study, the oligonucleotide sequences of the probe sets were mapped to the Arabidopsis transcripts dataset from the Arabidopsis genome TAIR9 version (<http://www.arabidopsis.org/>), and only genes that match with unambiguous probe sets were taken into consideration for the analysis of de-regulated genes. Genes with at least 2-fold de-regulation in transcript levels in comparison to the control, and with a p-value <0.05, were considered to be significantly up- or down regulated.



Analysis of statistically significantly de-regulated genes in shoots of 13-day-old *dry2* revealed a total of 50 genes up-regulated and 6 genes down-regulated when compared to wild-type *Ler*. Function classification of the *dry2* vs *Ler* de-regulated genes by gene ontology confirmed that biological processes like abiotic stress responses, ROS production and detoxification, as well as secondary metabolism are the most represented categories (data not shown), consistent with the previously published microarray expression data for the *dry2* mutant (Pose *et al.*, 2009). However, as expected, a much smaller number of de-regulated genes were observed in shoots of *dry2* 13-day-old seedling that did not yet present severe developmental defects when compared to 20-day-old *dry2* plants.

In order to investigate the profile of the transcriptional response specifically activated by the mutations affecting *SUD1* in the *dry2* background, the global gene expression profile of *dry2/sud1-9* and *dry2/sud1-22* was compared to *dry2* (Figure 4.5). Results revealed that *dry2/sud1-9* and *dry2/sud1-22* mutants present 73 and 90 up-regulated genes, respectively, when compared to the *dry2* background. The comparison also revealed 47 and 130 down-regulated genes in *dry2/sud1-9* and *dry2/sud1-22*, respectively. It is likely however, that de-regulation of several genes in the *dry2/sud1-9* and *dry2/sud1-22* mutant lines could be caused by independent mutations present in these lines. This happens because the suppressors were not backcrossed with *dry2* and may present a significant number of point mutations due to EMS mutagenesis.

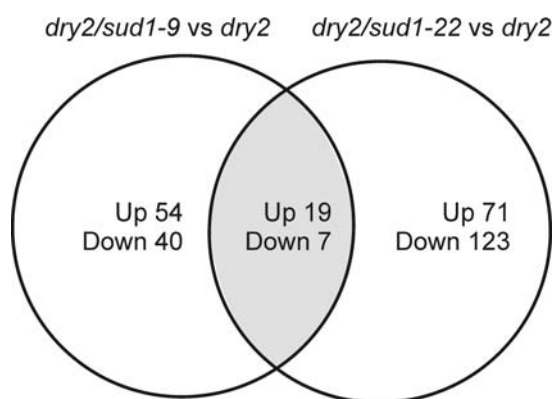


**Figure 4.5 – Venn diagram representation of de-regulated genes for *dry2/sud1-9* and *dry2/sud1-22* vs *dry2***

The relationships between two groups of genes up- or down-regulated at least 2-fold in *dry2/sud1-9* vs *dry2* and *dry2/sud1-22* vs *dry2* were analyzed by using a Venn diagram. Genes that were anti-expressed in *dry2/sud1-9* and *dry2/sud1-22* were excluded from de analysis. The subset of 19 genes up-regulated and 7 genes down-regulated simultaneously in *dry2/sud1-9* and *dry2/sud1-22* are listed in Table 4.1 and 4.2 respectively. Venn analysis was carried out using Venn Diagram Generator ([www.pangloss.com/seidel/Protocols/venn.cgi](http://www.pangloss.com/seidel/Protocols/venn.cgi)). Microarray experiment was performed as detailed in Figure 4.3.

Because *sud1-9* and *sud1-22* mutations have been mapped in the same gene, only those genes that showed differential expression in both suppressors were further analysed. A subset of 19 genes are up-regulated simultaneously in *dry2/sud1-9* and *dry2/sud1-22* (Table 4.1), and a subset of 7 genes are down-regulated simultaneously in *dry2/sud1-9* and *dry2/sud1-22* (Table 4.2), when compared to *dry2* (Figure 4.5). None of the genes that are up- or down-regulated simultaneously in *dry2/sud1-9* vs *dry2* and *dry2/sud1-22* vs *dry2* was found to be de-regulated in *dry2* vs wild-type. These results suggest that *SUD1* does not act by suppressing of *dry2*-dependent gene de-regulation.

**Table 4.1 – Arabidopsis Genes induced in both *dry2/sud1-9* and *dry2/sud1-22* when compared to *dry2***

Genes were distributed according to their molecular function as annotated in TAIR. AGI, Arabidopsis Genome Initiative.

Probe set ID	Fold Change <i>dry2/sud1-9</i> vs <i>dry2</i>	Fold Change <i>dry2/sud1-22</i> vs <i>dry2</i>	AGI Gene ID	Gene Annotation
<b>Catalytic activity</b>				
263228_at	+2.60	+2.00	At1g30700	FAD-binding Berberine family protein
263231_at	+2.55	+4.36	At1g05680	UGT74E2, Uridine diphosphate glycosyltransferase 74E2
256459_at	+2.40	+8.11	At1g36180	ACC2, acetyl-CoA carboxylase 2
253046_at	+2.38	+4.01	At4g37370	CYP81D8, cytochrome P450, family 81, subfamily D, polypeptide 8
258452_at	+2.36	+4.97	At3g22370	AOX1A, alternative oxidase 1A
264868_at	+2.20	+3.44	At1g24090	RNase H family protein
264042_at	+2.14	+5.06	At2g03760	AtSOT1, sulphotransferase 12
<b>DNA binding transcription factor activity</b>				
251677_at	+5.80	+3.40	At3g56980	BHLH039, basic helix-loop-helix (bHLH) DNA-binding superfamily protein
245692_at	+2.91	+3.78	At5g04150	BHLH101, basic helix-loop-helix (bHLH) DNA-binding superfamily protein
261192_at	+2.34	+5.81	At1g32870	NAC13, NAC domain protein 13
<b>Other binding</b>				
259802_at	+2.38	+2.81	At1g72260	THI2.1, thionin 2.1; toxin receptor binding
<b>Transporter activity</b>				
263402_at	+2.96	+7.44	At2g04050	MATE efflux family protein
263403_at	+2.75	+2.71	At2g04040	ATDXT1, MATE efflux family protein
<b>Unknown</b>				
250515_at	+3.78	+2.99	At5g09570	Cox19-like CHCH family protein
263515_at	+3.67	+8.81	At2g21640	Encodes a protein of unknown function that is a marker for oxidative stress response
248434_at	+3.62	+5.56	At5g51440	HSP20-like chaperones superfamily protein
261684_at	+2.96	+2.31	At1g47400	unknown protein
248260_at	+2.19	+4.96	At5g53240	Protein of unknown function (DUF295)
260522_x_at	+6.05	+22.32	At2g41730	unknown protein

**Table 4.2 – Arabidopsis Genes Repressed in both *dry2/sud1-9* and *dry2/sud1-22* when compared to *dry2***

Genes were distributed according to their molecular function as annotated in TAIR. AGI, Arabidopsis Genome Initiative.

Probe set ID	Fold Change <i>dry2/sud1-9</i> vs <i>dry2</i>	Fold Change <i>dry2/sud1-22</i> vs <i>dry2</i>	AGI Gene ID	Gene Annotation
<b>Catalytic activity</b>				
247477_at	-2.18	-2.06	At5g62340	Plant invertase/pectin methylesterase inhibitor superfamily protein
246149_at	-2.04	-2.07	At5g19890	Peroxidase superfamily protein
259813_at	-2.52	-2.06	At1g49860	ATGSTF14, glutathione S-transferase (class phi) 14
<b>Unknown</b>				
267457_at	-3.05	-2.36	At2g33790	AGP30, Arabinogalactan protein 30
258419_at	-2.39	-4.89	At3g16670	Pollen Ole e 1 allergen and extensin family protein
252882_at	-2.03	-2.28	At4g39675	unknown protein
255516_at	-2.00	-2.05	At4g02270	RHS13, root hair specific 13

Arabidopsis genes up- or down-regulated simultaneously in *dry2/sud1-9* vs *dry2* and *dry2/sud1-22* vs *dry2* were further investigated using a strategy based on correlative transcriptome analysis for comparison of expression profiles. Transcriptome data using Genevestigator V3 (Hruz *et al.*, 2008) was searched in order to identify mutants whose transcriptome profiles significantly overlap with the genes listed on Tables 4.1 and 4.2. The results of coexpression analysis using the huge data set were analysed independently for genes listed in Table 4.1 and genes listed in Table 4.2. It is expected that if indeed these two lists of genes have a biological significance, genes listed in Table 4.1 and genes listed in Table 4.2 must be de-regulated by similar conditions in an opposite way. Results show that many genes up-regulated simultaneously in *dry2/sud1-9* vs *dry2* and *dry2/sud1-22* vs *dry2* are induced in *csn* mutants (*csn3-1*, *csn4-1* and *csn5*) (Figure 4.6A). Many genes down-regulated simultaneously in *dry2/sud1-9* vs *dry2* and *dry2/sud1-22* vs *dry2* were repressed *csn* mutant lines (*csn3-1*, *csn4-1* and *csn5*) in an independent correlation analysis (Figure 4.6B), validating both analysis. The *csn3-1* and *csn4-1* mutations affect the genes that encodes subunit 3 (AT5G14250) and 4 (AT5G42970), respectively, of the COP9 signalosome complex, while *csn5a-2* and *csn5b* mutations respectively affect the two distinct and functionally redundant genes AT1G22920 and AT1G71230 that encode two isoforms of the CSN5 subunit of the COP9. The COP9 signalosome (CSN) is a conserved protein complex that functions in the ubiquitin–proteasome pathway. CSN is a multi-subunit protease with eight subunits that regulates the activity of cullin–RING ligase families of ubiquitin E3 complexes (Serino and Deng, 2003). Loss of a single CSN subunit can

destabilize the entire complex resulting in a broad range of phenotypes including lethality in strong *csn* alleles (Serino and Deng, 2003). Because it is highly unlikely that independent correlation analyses of up- and down-regulated co-expressed genes identified the same *csn* mutant lines by chance, this result indicate that we are in the presence of a relevant biological association.

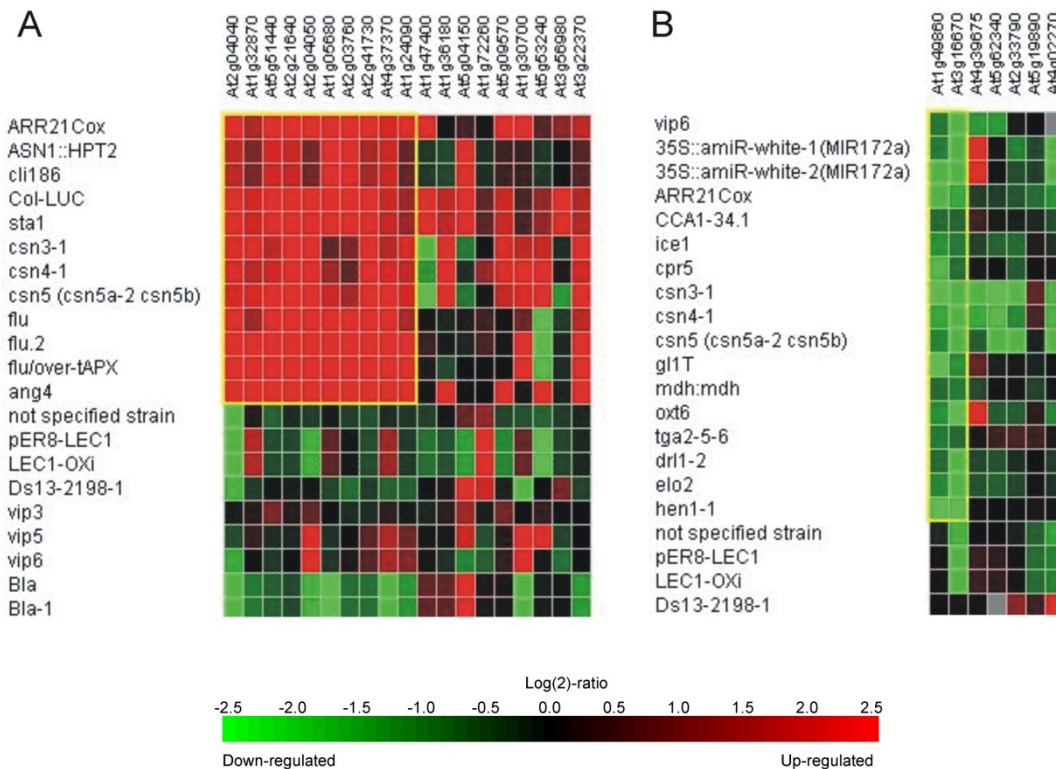


**Figure 4.6 – Genevestigator V3 Clustering Analysis of Arabidopsis Genes Up- or Down-regulated Simultaneously in *dry2/sud1-9* vs *dry2* and *dry2/sud1-22* vs *dry2***

Genes (columns) were clustered based on their expression in different mutant backgrounds (rows), using the Biclustering method (BiMax algorithm). The yellow box marks the cluster of genes, all of which are up-regulated (**A**) or down-regulated (**B**) under the indicated subset of conditions. The colour scale presented at the bottom represents the log<sub>2</sub> ratio of fold change.

Although the correlative transcriptome analysis for comparison of expression profiles does not establish proof of the nature of the relationship between genes, it allows us to formulate the hypothesis that *SUD1* is involved into an ubiquitin-proteasome pathway, which can subsequently be validated experimentally. In summary, global gene expression analysis was a valuable validation tool as starting point to study *SUD1* function by formulation of novel hypotheses about the cellular process involving *SUD1*.

## 4.3. MATERIALS AND METHODS

### Plant Material

The *Arabidopsis thaliana* ecotypes Landsberg *erecta* (*Ler*) was used as wild-type control in the present study. Mutants used in this study that have been previously described: *dry2* (Pose *et al.*, 2009), *dry2/sud9* and *dry2/sud22* (Pose, 2008).

### Plant Manipulation and Growth Conditions

*Arabidopsis* standard handling procedures and conditions were employed to promote seed germination and growth, as previously described in the Materials and Methods section of Chapter 2.

### Biological Sample preparation for Microarray Hybridization

The preparation of biological samples for microarray hybridization was performed in collaboration with Verónica G. Doblás from Instituto de Hortofruticultura Subtropical y Mediterránea, Universidad de Málaga, Málaga, Spain. The entire experiment was performed six times, providing three independent biological replicates. For each of the six experiments, all four lines, wild-type, *dry2*, *dry2/sud1-9* and *dry2/sud1-22* were grown for 13 days *in vitro* before the shoots of at least 30 plants per line were harvested. Total RNA was prepared separately for the six individual experiments. The RNA extraction was performed using the TRIZOL method. The RNA was further purified using an RNeasy Plant Mini Kit (Qiagen, <http://www.qiagen.com>). Total RNA samples from two experiments were pooled to create biological replicates. Each biological replicate consisted of equal amounts of total RNA from shoot tissues of each of the four plant lines. Total RNA (5 µg) of each biological replicate was prepared and RNA integrity was assessed by nucleic acids electrophoretic separation with a high sensitive EukaryoteTotal RNA Nano Assay, using an Agilent 2100 Bioanalyser (Agilent Technologies).

### Microarray Hybridization and Evaluation

Affymetrix *Arabidopsis* ATH1 GeneChips were used (Affymetrix, Santa Clara, CA). RNA was first transcribed into cDNA, and then into biotin-labeled cRNA, that was hybridized onto Affymetrix ATH1 gene chips. Experimental procedures concerning hybridization and raw data processing, were performed by the Genomic Unit at Centro Nacional de Biotecnología, CSIC, Campus de Cantoblanco UAM C/ Darwin 3 28049 Madrid.

### Microarray Bioinformatic Data Analysis

Meta-Profile Analysis of *SUD1* gene expression patterns in different *Arabidopsis* tissues and analysis of *SUD1* expression in different mutant backgrounds were carried out using Geneinvestigator (<https://www.geneinvestigator.com/gv/plant.jsp>) (Hruz *et al.*, 2008).

Differential expression gene sorting (fold-change between logarithmic expression values of two given samples) was performed using *Microsoft Office Excel (Microsoft)*. A cutoff value of 2-fold and a p-value <0.05 were adopted to identify genes that were differentially expressed. The logarithmic intensity levels for each ATH1 GeneChips probe were plotted using Fiesta Viewer (<http://bioinfo.pn.cnb.csic.es/tools/FIESTA>) (Oliveros, 2007). Venn analysis was carried out using Venn Diagram Generator ([www.pangloss.com/seidel/Protocols/venn.cgi](http://www.pangloss.com/seidel/Protocols/venn.cgi)). GO categorization was carried out at TAIR ([www.arabidopsis.org](http://www.arabidopsis.org)). Clustering Analysis of gene expression patterns for comparison of expression profiles was carried out using Genevestigator (<https://www.genevestigator.com/gv/plant.jsp>) (Hruz *et al.*, 2008).

# Chapter 5

## *In Silico* Structural and Phylogenetic Analysis of SUD1

### **CONTENTS**

---

5.1. INTRODUCTION

5.2. RESULTS AND DISCUSSION

Structural Features of SUD1

Topology Model for SUD1 Protein

Identification of Essential Amino Acid Residues for SUD1 Function

Phylogenetic Analysis of SUD1

5.3. MATERIALS AND METHODS





## 5.1. INTRODUCTION

With the sequencing of the first genome of a higher plant (*Arabidopsis thaliana*) (Arabidopsis Genome Initiative, 2000), plant research began determining the biological function of thousands of annotated genes, and as a consequence, various new resources for functional discovery have since become available (Feng and Mundy, 2006; Azevedo *et al.*, 2011). In addition, high-throughput and omics-based approaches in *Arabidopsis* have been thoroughly developed (MASC Report, 2011), and in this post-genomic era, a huge amount of *in silico* genomic and proteomic data has become available. Data mining of this information, easily acquired from publicly available databases, is now an essential step when studying a given gene-of-interest.

With the increase in high-throughput data becoming available, intelligent software has been developed to extract essential information from large-scale data sets. Some bioinformatics programs can aid in many ways to elucidate the function of a gene of interest, for instance by *in silico* prediction of structural features to a given gene, protein sequence alignments and phylogenetic analysis. A combined analysis resulting from several genomic-based resources will be presented next for *SUD1*.

## 5.2. RESULTS AND DISCUSSION

### Structural Features of SUD1

The *Arabidopsis SUD1* gene is predicted to encode a protein of 123 KDa. Apart from the role assigned to *SUD1* in the present work, no function has been assigned to this gene. *In silico* analysis was employed to further characterize *SUD1* to obtain protein functional information. The InterProScan database (<http://www.ebi.ac.uk/Tools/pfa/iprscan/>) (Hunter *et al.*, 2009) was used to search for conserved domains. A predicted Zinc finger, RING-CH-type motif (SMART Domains database; Accession Number: SM00744) close to the N-terminus of *SUD1* was identified between residues 67 and 115. In order to gain insight into the *SUD1* activity, a *blastp* search in the NCBI database was performed to identify putative *SUD1* orthologs, using the predicted proteome of *Saccharomyces cerevisiae* (taxid4932), *Homo sapiens* (taxid9606), *Mus musculus* (taxid10090), *Drosophila melanogaster* (taxid7227) and *Caenorhabditis elegans* (taxid6239). *SUD1*-like proteins

seem to be well conserved, since homologous proteins encoded in the genome of all these phylogenetically distant species were identified. The SUD1 orthologue in yeast and human was Doa10<sup>a</sup> and TEB4<sup>b</sup>, respectively. These proteins have been extensively studied and a great amount of information about their function and mode-of-action is currently available (Carvalho *et al.*, 2006; Kreft *et al.*, 2006; Kreft and Hochstrasser, 2011).

The Doa10 protein is a component of the **E**ndoplasmic **R**eticulum **A**ssociated Protein **D**egradation (ERAD) complex, involved in the quality control that degrades misfolded ER proteins (Swanson *et al.*, 2001). The human TEB4 protein was identified as the most likely ortholog of yeast Doa10 (Hassink *et al.*, 2005). Doa10 and TEB4 are multispinning membrane proteins with cytosolic RING finger domains that present E3 ubiquitin ligase activity (Swanson *et al.*, 2001; Hassink *et al.*, 2005). A structural features analysis for this two proteins was already published, revealing that the most homologous regions in Doa10 and TEB4 proteins are the N-terminal RING-CH domain (36% identity) and an internal block of approximately 130 residues (30% identity) that was designated as the TEB4-Doa10 (TD) domain (Swanson *et al.*, 2001).

In the present thesis, an amino acid alignment of SUD1 with related proteins from *Saccharomyces cerevisiae* (taxid4932), *Homo sapiens* (taxid9606), *Mus musculus* (taxid10090), *Drosophila melanogaster* (taxid7227) and *Caenorhabditis elegans* (taxid6239) was performed using PRALINE (<http://www.ibi.vu.nl/programs/pralinewww/>) (Simossis and Heringa, 2005), in order to order to gains insight into the SUD1 structural features (Figure 5.1). The PRALINE software performs multiple alignment containing options that optimize the information for each of the inputted sequences. Using these options, homology-extended alignment (Simossis *et al.*, 2005), predicted secondary structure and transmembrane structural information were included in the analysis. Once again, the alignment of SUD1 with related proteins from human, mouse, *Drosophila* and *C. elegans* indicates that these proteins are well conserved among these species. Analysis of amino acid identity and similarity of the full-length sequences of SUD1 homologs (Table 5.1 and 5.2) shows that the TEB4 from *H. Sapiens* and its metazoan orthologs (*M. musculus*, *D. melanogaster* and *C. elegans*) appear to be the most related proteins within the present alignment. Based on amino acid identity and similarity, TEB4 it is the most related SUD1 protein. Results also place SUD1 closer to metazoan species than the yeast Doa10. The most conserved regions of SUD1 with Doa10 and TEB4 are the N-terminal RING-CH domains (42.9% and

<sup>a</sup> *Saccharomyces cerevisiae* proteins are referred to by the relevant gene symbol, non-italic, initial letter uppercase.

<sup>b</sup> As in *Arabidopsis thaliana* proteins, *Homo sapiens* proteins are referred to by the relevant gene symbol, non-italic, uppercase letters.

57.1% identity respectively) (Figure 5.1A) and the internal region of approximately 130 amino acid, spanning SUD1 residues 524-654 (29.6% and 44.3% identity) (Figure 5.1B) that correspond to the conserved TEB4-Doa10 TD domain previously described (Swanson *et al.*, 2001).

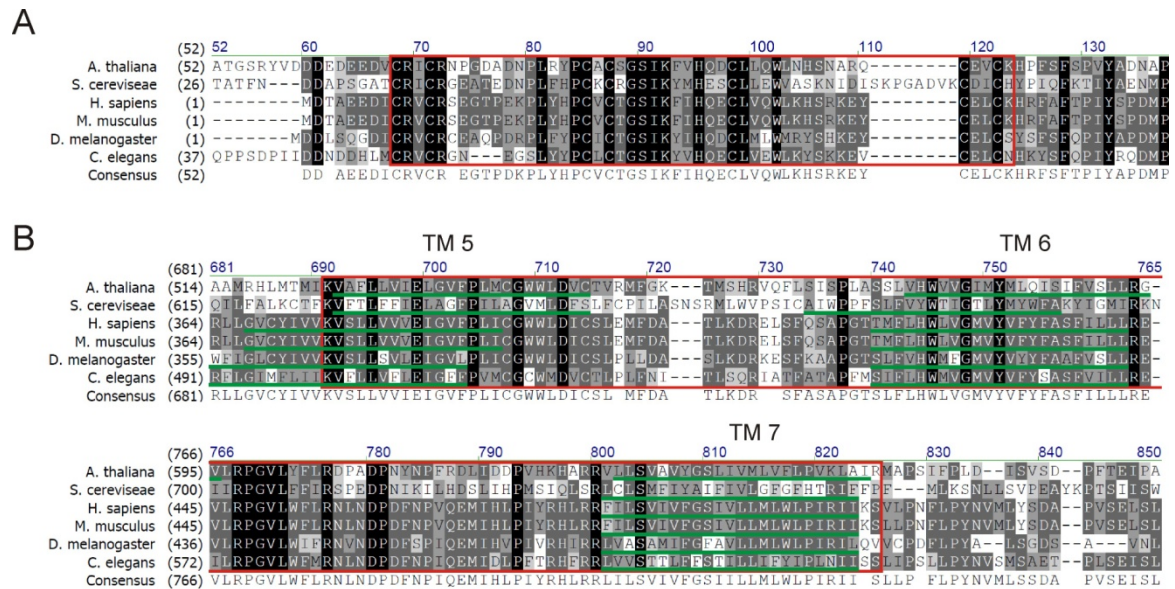


**Figure 5.1 – Protein Sequence Alignment of Arabidopsis SUD1 with Homologous Proteins from Eukaryotic Organisms**

*Arabidopsis thaliana* SUD1 (At4g34100.1; TAIR8) was analysed together with *Saccharomyces cerevisiae* Doa10 (NP\_012234.1; NCBI) (Mandart *et al.*, 1994; Swanson *et al.*, 2001), *Homo sapiens* TEB4 (NP\_005876.2; NCBI) (Hassink *et al.*, 2005), *Mus musculus* MARCH6 (NP\_766194.2; NCBI), *Caenorhabditis elegans* MARCH6 (NP\_492823.2; NCBI) and *Drosophila melanogaster* CG1317 isoform B (NP\_647715.2; NCBI) predicted protein sequences retrieved from the NCBI database. The PRALINE program was used for the multiple sequence alignment (Simossis and Heringa, 2005). *Saccharomyces cerevisiae* Doa10 transmembrane segments (TM) (underlined in green) have been experimental determined (Kreft *et al.*, 2006). For all other proteins, the underlined TM domains (underlined in green) were predicted using TMHMM2.0 program integrated into the PRALINE bioinformatics tool (Krogh *et al.*, 2001; Pirovano *et al.*, 2008). Figure shows partial segments of the sequence alignment. **(A)** The conserved Zinc finger RING-CH domains spanning SUD1 residues 68-115 are boxed in red. **(B)** The conserved TEB4-Doa10 (TD) domain spanning SUD1 residues 524-654 is boxed in red. The TM (5-7) domains of each represented protein are represented.

**Table 5.1 – Percentage of Amino Acid Identity for the Full-length SUD1 Homolog Sequences**

	<i>S. cerevisiae</i>	<i>H. sapiens</i>	<i>M. musculus</i>	<i>D. melanogaster</i>	<i>C. elegans</i>
<i>A. thaliana</i>	16	30	29	27	24
<i>S. cerevisiae</i>		17	17	17	16
<i>H. sapiens</i>			98	50	42
<i>M. musculus</i>				50	42
<i>D. melanogaster</i>					37
<i>C. elegans</i>					

**Table 5.2 – Percentage of Amino Acid Similarity for the Full-length SUD1 Homolog Sequences**

	<i>S. cerevisiae</i>	<i>H. sapiens</i>	<i>M. musculus</i>	<i>D. melanogaster</i>	<i>C. elegans</i>
<i>A. thaliana</i>	35	53	52	47	47
<i>S. cerevisiae</i>		37	37	35	36
<i>H. sapiens</i>			98	67	62
<i>M. musculus</i>				67	62
<i>D. melanogaster</i>					58
<i>C. elegans</i>					

The hydrophobicity profile is also shared among the different SUD1 homologs, being indicative of a similar membrane topology. The Doa10 protein from yeast contains 14 transmembrane (TM) domains, a topology that has been experimentally validated (Kreft *et al.*, 2006). For the remaining SUD1 homologues, the putative TM topology was predicted using the TMHMM2.0 program (Sonnhammer *et al.*, 1998; Krogh *et al.*, 2001) and included in the multiple alignment/PRALINE analysis (Pirovano *et al.*, 2008). TMHMM2.0 program ([www.cbs.dtu.dk/services/TMHMM/](http://www.cbs.dtu.dk/services/TMHMM/)) is arguably one of the most reliable protein topology prediction algorithms (Moller *et al.*, 2001; Melen *et al.*, 2003). Similar to Doa10, 14 TM domains are predicted for SUD1 and the other homologs, with the exception of the 12 TM domains of the *C. elegans* SUD1 homolog (data not shown).

### Topology Model for the SUD1 Protein

Analysis of the SUD1 structural features leads to the hypothesis that this protein is the Arabidopsis functional ortholog of the well know endoplasmic reticulum (ER) ubiquitin E3 ligases Doa10 from yeast and TEB4 from humans (Swanson *et al.*, 2001; Hassink *et al.*, 2005). An equally important aspect of membrane-localised proteins, besides the correct identification of the position of TM domains, is the prediction of the topology, i.e., the definition of the intracellular orientation of each region. Based on TMHMM2.0 predicted orientation, the SUD1 protein contains both termini facing the luminal side (Figure 5.2). However, the hydrophilic SUD1 N-terminus, which includes the E3 ligase RING-CH domain, is predicted to interact with E2 ubiquitin-conjugating enzyme(s) in the cytosol. A similar conflict arose with the *in silico* topological analysis of Doa10 and TEB4, until the location of Doa10 C and N termini in the cytosol was demonstrated through experimental validation (Kreft *et al.*, 2006) (Figure 5.3).

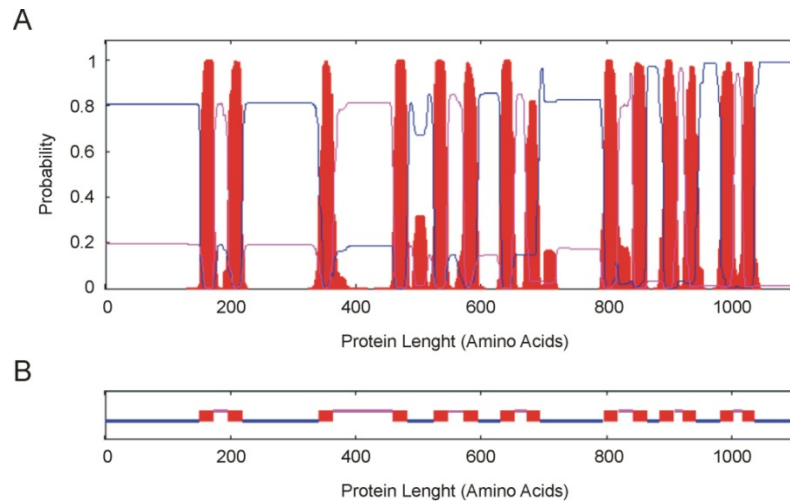


**Figure 5.2 – Prediction of Membrane Topology of SUD1 Protein by TMHMM2.0**

**(A)** Representation of the TM domains of SUD1 based on the hydrophobicity plot predicted by TMHMM2.0. The hydrophobic segments are represented in red. Blue lines represent the probability for predicted luminal loops and pink lines represent the probability for predicted cytosolic loops. **(B)** Schematic representation of the TMHMM2.0 predicted TM domains, luminal loops and cytosolic loops. The 14 TM domains are depicted as red boxes; blue lines connecting the bottom edge of these boxes represent the luminal loops and pink lines connecting the top edge represent the cytosolic loops.

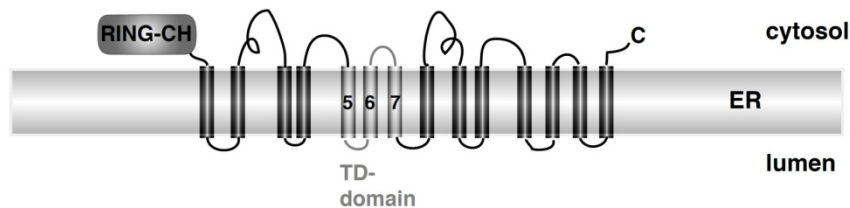


**Figure 5.3 – Topology Model for *S. cerevisiae* Doa10 Protein**

The *Saccharomyces cerevisiae* Doa10 topology model containing 14 TM domains and both termini facing the cytosol was experimentally validated (Kreft *et al.*, 2006). The RING-CH at the N terminus is highlighted in dark gray. The TEB4-Doa10 (TD) domain encompassing three TM domains (5-7) is represented in gray. Figure retrieved from Kreft and Hochstrasser (2011).

In present work, a combination of the TM domain prediction algorithm using TMHMM2.0 (Figure 5.2), sequence alignment of eukaryotic orthologs (Figure 5.1) and experimental topological information gathered for Doa10 (Figure 5.3), was used to design a topological model for SUD1. Using the experimental topological information gathered for Doa10 (Kreft *et al.*, 2006), and taken into account the SUD1 structural features identified based on sequence alignment of SUD1 with related eukaryotic orthologs (Figure 5.1), the SUD1 topology model predicted by TMHMM2.0 (Figure 5.2), it was further modelled in order to obtain the SUD1 topology represented in Figure 5.4. In this model, the N terminus (and hence the ligase activity of SUD1) and the C terminus both face the cytosol, a similar disposition as described in Doa10 likely TEB4.

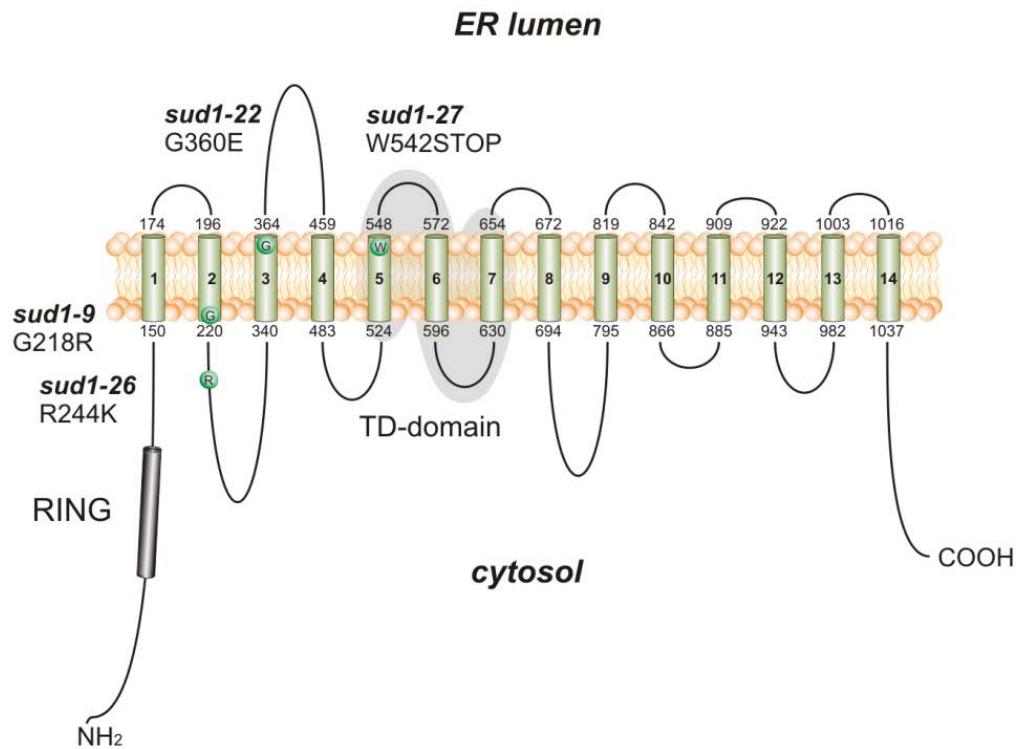


**Figure 5.4 – Topology Model for Arabidopsis SUD1 Protein and Amino Acid Mutations in the Corresponding *sud1* Alleles**

Based on TMHMM2.0 prediction of membrane topology (Figure 5.1), *A. thaliana* SUD1 (At4g34100.1 protein) exhibits 14 TM domains, represented by dark-green membrane-spanning regions. Both N and C termini are suggested to be facing the cytosol, based on the experimentally validated Doa10 topology. The amino acid substitutions in a given *sud1* allele are highlighted in light-green. Positions of these amino acid substitutions and the protein variants are indicated. The TMHMM2.0 predicted borders of each loop are also indicated. The RING-CH domain (residues 68-115) at the N terminus is shown in black. The conserved TD domain (residues 524-654) is highlighted in gray.

The conserved TD domain of Doa10 (Swanson *et al.*, 2001) comprises TM5-TM7 domains, with the cytosolic loop between TM6 and TM7 domains (cytosolic loop of TD domain) being the most conserved Doa10 region with the exception of the RING domain (Kreft and Hochstrasser, 2011) (Figure 5.3). Based on sequence alignment (Figure 5.1B), SUD1 also contains a conserved TD domain spanning the same three TM (5-7) domains. According to the proposed topology model for SUD1, the most conserved stretch (SUD1 residues 597-561) is found within the cytosolic loop of the TD domain (Figure 5.1B and Figure 5.4). Recent findings in Doa10 reveals that TM5 domain is highly sensitive to mutations reinforcing the importance of a conserved TD domain to preserve the Doa10 function in orthologs from different organisms (Kreft and Hochstrasser, 2011). Based on the model proposed in the present work, the second luminal loop presents the main difference between SUD1 and Doa10. Doa10 protein presents a second luminal loop composed of only 3 residues while the second luminal loop of SUD1 is composed of 96 residues. This second luminal loop is important in SUD1 because it was identified that *sud1-22* mutant allele carries a mutation



The mutations identified in *sud1-9* and *sud1-26* are not in amino acids conserved with Doa10 and TEB4. However, the low phylogenetic relationship between these organisms (Figure 5.4) might hinder functional inference concerning these amino acids. Therefore, an additional alignment was performed to evaluate the conservation level of SUD1 homologous proteins within plant species. For that purpose, the plant comparative genomics database PLAZA (<http://bioinformatics.psb.ugent.be/plaza/>) (Proost *et al.*, 2009) was used to search for SUD1 homologous proteins in different plant species. Conservation in amino acid sequence, the presence of a conserved RING-CH domain and the number of predicted TM domains were used as criteria to select the most homologous proteins from each species. Analysis of the sequence alignment of Arabidopsis SUD1 with homologous SUD proteins from dicots (*Vitis vinifera*, *Populus trichocarpa*, *Medicago truncatula*, *Lotus japonicus*, *Glycine max*) and monocots (*Brachypodium distachyon*, *Oryza sativa* and *Zea mays*) indicates a striking conservation of SUD1 sequence among these species (Figure 5.5). Moreover, it can be observed that the amino acid substitutions in all *sud* mutants occurs in conserved residues among monocots and dicots (Figure 5.5). The *sud1-9* and *sud1-22* mutations result in substitutions that change glycines (G) 218 and 360, a small non-polar residue, for polar residues such as arginine (R) and glutamate (E), respectively. Interestingly, both glycine (218 and 360) residues are located at the transition between a TM domain and a hydrophilic loop. Interruption of transmembrane helices by a short non-helical segment containing proline (P), glycine (G), and/or serine (S) residues has been observed in many classes of membrane proteins, namely transporters such as amino-acid antiporters (Gao *et al.*, 2009), neurotransmitter-sodium symporters (Yamashita *et al.*, 2005), and sodium-independent transporters (Schulze *et al.*, 2010). Interruption of helical structure exposes main-chain carbonyl oxygen and nitrogen atoms for hydrogen bonding and ion coordination, aspects that are essential for proper functioning of the protein (Yamashita *et al.*, 2005). A striking feature of some Doa10 orthologues is the conserved position of some G residues at the transition between TM and hydrophilic loops. Therefore, based on this information, it is possible to speculate that glycine 218 and 360 may have a similar role in SUD1 and substitution for residues with different properties is the cause of loss of function. The mutation in *sud1-26* results in a R244K substitution. Chemically, these two amino acids are very related and it might be expected that the substitution would not cause important changes. However, the finding that proteins of phylogenetically distant plant species such as monocots and dicots all maintain an R in this position (Figure 5.5), suggests an important role of this residue in SUD1 function. It can be envisaged that the loss of function in



*sud1-26* could be caused either by R244K substitution affecting the function of the first cytosolic loop predicted for SUD1, or by causing modifications in the topology, since it is generally accepted that a major determinant of topology of a give protein is the distribution of positively charged residues (Figure 5.5).

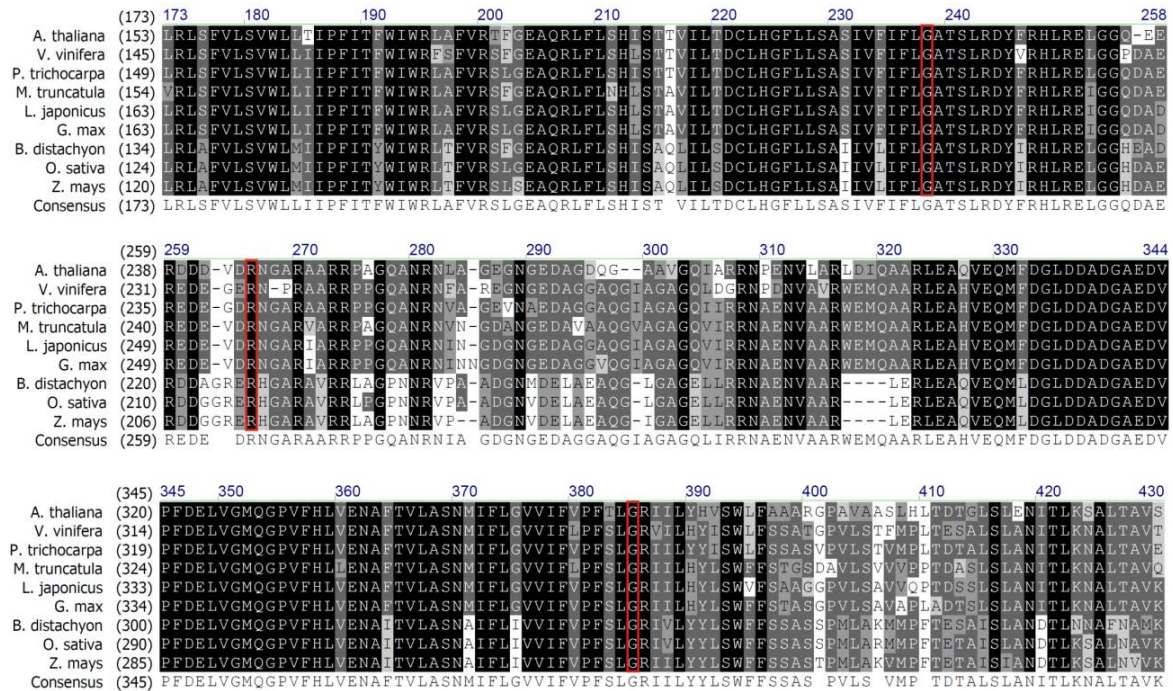


**Figure 5.6 – Protein Sequence Alignment of Arabidopsis SUD1 with Homologous Proteins from Other Plant Species Showing the Conserved Amino Acids affected by the *sud1-9*, *sud1-26* and *sud1-22* Mutations**

*Arabidopsis thaliana* SUD1 protein, encoded by *SUD1* (At4g34100.1; TAIR8) was analysed together with SUD1 homologous protein sequences from *Vitis vinifera* (VV03G06410), *Populus trichocarpa* (PT09G10040), *Medicago truncatula* (MT4G49580), *Lotus japonicas* (LJ4G008630), *Glycine max* (GM02G11570), *Brachypodium distachyon* (BD1G30330), *Oryza sativa* (OS06G43210) and *Zea mays* (ZM06G10310) retrieved from the PLAZA database (<http://bioinformatics.psb.ugent.be/plaza/>) (Proost *et al.*, 2009). The sequence alignment was performed with the software CLUSTALW2 available online on the European Bioinformatics Institute website (<http://www.ebi.ac.uk/Tools/msa/clustalw2/>). All parameters correspond to default values (Gonnet Protein Weight Matrix). The conserved Arabidopsis SUD1; G218 (*sud1-9*), R244 (*sud1-26*) and G360 (*sud1-22*) are boxed.

## Phylogenetic Analysis of SUD1

In order to define the SUD1 family in plant species, the comparative genomics resource PLAZA (Proost *et al.*, 2009) was used to search for SUD1 homologs in different plant species (BLASTP  $E\_value=1e^{-05}$ ;  $MCL\_l=2$ ). This database includes several dicot and monocot plants species, a seedless vascular plant (the lycophyte *S. moellendorffii*) and a non vascular plant (the moss *P. patens*). Phylogenetically distant species, such as yeast and human were removed in order to optimise sequence alignment. After identifying the homologous sequences, structural features were analysed and only those protein sequences that obeyed the following parameters

were selected: (1) presence of the conserved N-terminus RING-CH domain (InterPro Scan; Accession Number: IPR011016); (2) presence of an internal conserved TD domain; (3) presence of at least 10 predicted TM domains based on TMHMM2.0. Since all yeast Doa10 orthologs are characterized by the above mentioned criteria (Swanson *et al.*, 2001), sequences that fit these structural features were considered as putative SUD1/Doa10 orthologues.

Analysis was carried out using the MEGA 5 software (Tamura *et al.*, 2011), allowing a ClustalW protein sequence alignment and inference of the evolutionary history using the Maximum Likelihood method based on the JTT matrix-based model (Jones *et al.*, 1992) for tree visualization. The phylogenetic tree shows that Arabidopsis SUD1 clusters together with plant-related proteins in a clearly distinct clade (Figure 5.6 light-gray box). This clade include proteins from all species analysed, including a seedless vascular plant (a lycophyte) and a non-vascular plant (a moss) (Figure 5.6 dark-gray boxes). The ER-associated degradation (ERAD) system is an essential mechanism for the identification of misfolded, unassembled, or aberrantly modified proteins, either repairing the errors or eliminating the abnormal proteins (Vembar and Brodsky, 2008; Hirsch *et al.*, 2009; Hegde and Ploegh, 2010). Because efficient quality-control mechanisms that ensure the proper folding of proteins in the ER is central for cell survival, the presence of Doa10/TEB4 orthologs in all eukaryotic organisms is expected. Therefore, it was likely that the SUD1 clade included plant proteins involved in ERAD system and functionally related with Doa10 and TEB4. For some of the species included in the phylogenetic analysis, such as *A. lyrata*, *S. moellendorffii*, *B. distachyon*, *G. max*, *M. domestica* and *P. trichocarpa*, more than one protein was found to fit the structural features criteria of putative Doa10/TEB4 orthologs, suggesting recent duplication events. Interestingly, *A. thaliana*, *A. lyrata*, *B. distachyon* and *V. vinifera* contain several proteins that group in a separate clade despite obeying all the criteria to be considered Doa10/TEB4 orthologs. Most likely, these correspond to genes that have undergone neofunctionalization. However the lack of phylogenetically related genes in other species suggests that these are not essential for plant survival.

Following the current analysis, it was decided to gain some insight on the *At4g32670* Arabidopsis gene, using the TAIR database (<http://www.arabidopsis.org/>). However, no functional information was found apart from the description that it encodes for a membrane-localised E3 ligase based on homology search. In addition, the lack of probes for the *At4g32670* gene in the Affymetrix ATH1 GeneChip microarray, did not allow any information on its expression. After duplication, the predominant fate of duplicated genes is pseudogenization (Taylor and Raes, 2004),

however, TAIR contains 45 Expressed Sequence Tags for *At4g32670*, whose translation produced a predicted functional protein. All this led us to hypothesize that this *At4g32670* is not a pseudogene and therefore encodes a functional protein with unknown function as a result of a neofunctionalization. That said, and despite the relatively high homology with *SUD1*, the finding that mutations in *SUD1* suppress the defective phenotypes of *dry2/sqe1-5*, indicates that *At4g32670* does not act redundantly with *SUD1*.

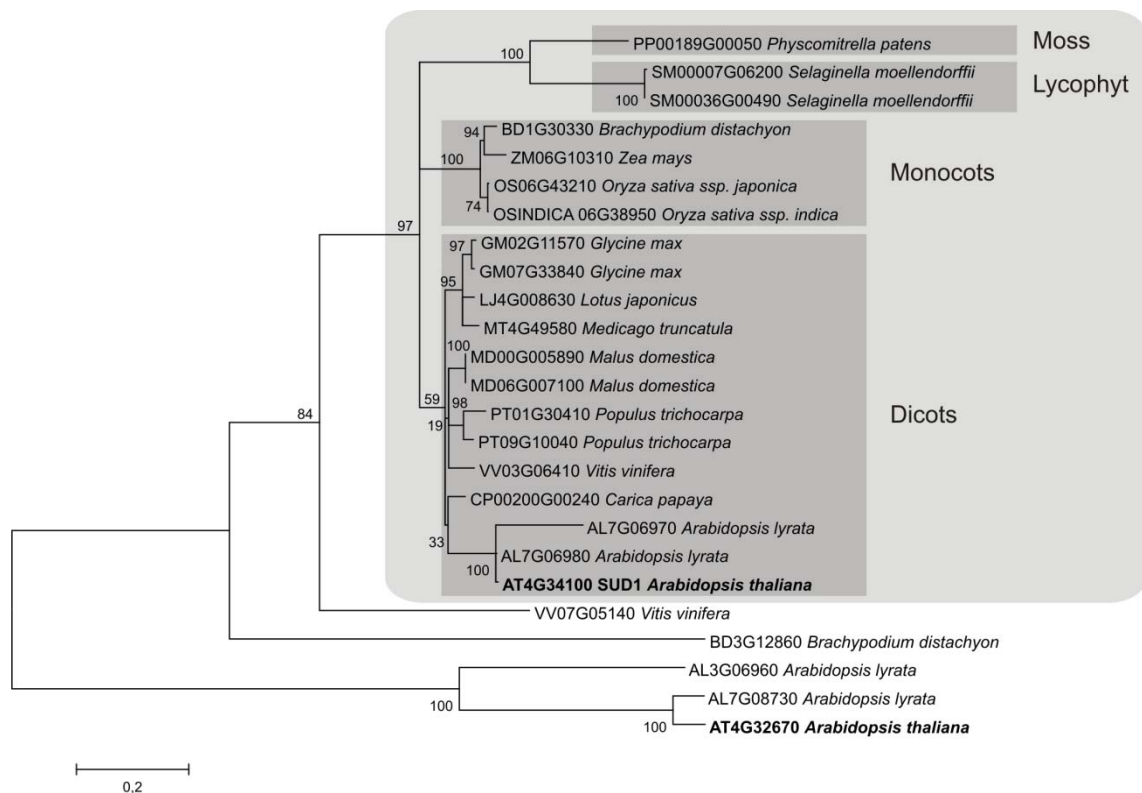


**Figure 5.7 – Phylogenetic Tree Showing the Relationship between Arabidopsis SUD1 and Homologs from Other Plants Species**

The MEGA 5 software (Tamura *et al.*, 2011) was used to perform a ClustalW (Gonnet Protein Weight Matrix (Gonnet *et al.*, 1992) protein sequence alignment of *SUD1* plant homologs, and to conduct the evolutionary analysis. The evolutionary history was inferred using the Maximum Likelihood method based on the JTT matrix-based model (Jones *et al.*, 1992), with subsequent Bootstrap analysis (500 trees). The percentage of trees in which the associated taxa clustered together is shown next to the branching sites. The tree is drawn to scale, with branch lengths measuring the number of substitutions per site (scale bar is represented). *SUD1* and its paralog from *Arabidopsis thaliana* are depicted in bold. The *SUD1* homologous protein sequences were obtained from PLAZA database (<http://bioinformatics.psb.ugent.be/plaza/>) (Proost *et al.*, 2009). Accession numbers are indicated. The proposed *SUD1* gene family is highlighted in a light-gray box. Phylogenetic groups are highlighted in dark-gray boxes.

### 5.3. MATERIALS AND METHODS

#### Bioinformatic Tools Used for *in Silico* Structural Analysis of SUD1

The InterProScan database (<http://www.ebi.ac.uk/Tools/pfa/iprscan/>) (Hunter *et al.*, 2009) was used to search for conserved domains of the SUD1 protein. The NCBI *blastp* tool (<http://blast.ncbi.nlm.nih.gov/Blast.cgi?PAGE=Proteins>) was used to identify putative SUD1 orthologs, using the predicted proteome of *Saccharomyces cerevisiae* (taxid4932), *Homo sapiens* (taxid9606), *Mus musculus* (taxid10090), *Drosophila melanogaster* (taxid7227) and *Caenorhabditis elegans* (taxid6239). The protein sequence alignment of Arabidopsis SUD1 with homologous proteins from phylogenetically unrelated eukaryotic organisms was performed using the multiple sequence alignment program PRofile ALIgNement (PRALINE) (<http://www.ibi.vu.nl/programs/pralinewww/>) (Simossis and Heringa, 2005). The PRALINE alignment was performed using the following parameters: default BLOSUM62 residue exchange matrices; the PSI-BLAST pre-profile processing strategy for homology-extended alignment (Simossis *et al.*, 2005); integration of secondary structure using PSIPRED (Jones, 1999), and transmembrane structure information (Pirovano *et al.*, 2008) using TMHMM v2.0 (Krogh *et al.*, 2001) into the alignment process. The AlignX program, part of the vectorNTI suite case, was used to visualise the alignment of the sequences previously performed using PRALINE, using the color coded according to similarities as described in Table 5.3.

The TMHMM2.0 program ([www.cbs.dtu.dk/services/TMHMM/](http://www.cbs.dtu.dk/services/TMHMM/)) was used to predict the putative TM domain topology of SUD1 based on the hydrophobicity plot (Krogh *et al.*, 2001). The plant comparative genomics resource PLAZA database (<http://bioinformatics.psb.ugent.be/plaza/>) (Proost *et al.*, 2009) was used to search for SUD1 homologous protein sequences in different plant species. The protein sequence alignment of Arabidopsis SUD1 with homologous proteins from other plant species was performed with the software CLUSTALW2, available at European Bioinformatics Institute (<http://www.ebi.ac.uk/Tools/msa/clustalw2/>). All parameters corresponded to default values (Gonnet Protein Weight Matrix (Gonnet *et al.*, 1992)).

**Table 5.3 – Color Code used to Highlight Protein Sequences According to Similarities**

Residues	Amino Acid Letter and Background Colors
Non-similar	Black letters on white background
Conservative	White letters on dark-gray background
Block of similar	Black letters on gray background
Weakly similar	Black letters on light-gray background
Identical	White letters on black background

#### Bioinformatic Tools Used for Phylogenetic Analysis of SUD1

The MEGA 5 software (Tamura *et al.*, 2011) was used to perform a ClustalW (Gonnet Protein Weight Matrix) (Gonnet *et al.*, 1992) protein sequence alignment of SUD1 plant homologs included in the phylogenetic analysis of SUD1, and to conduct the evolutionary analysis for tree visualization. The evolutionary history was inferred using the Maximum Likelihood method based on the JTT matrix-based model (Jones *et al.*, 1992), with subsequent Bootstrap analysis (500 trees).

# Chapter 6

## Functional Characterization of *Arabidopsis thaliana* *SUD1*, *HRD1A* and *HRD1B*

### CONTENTS

---

#### 6.1. INTRODUCTION

#### 6.2. RESULTS AND DISCUSSION

Molecular Cloning of *SUD1* in *E. coli*

*SUD1* Complementation of Yeast *doa10Δ* Mutation

Degradation of Yeast Doa10 Substrates in *doa10-G498E* Mutant Cells

*AtHRD1* Complementation of Yeast *hrd1Δ* Mutation

Investigating the Function of the Arabidopsis ERAD E3-ligases

#### 6.3. MATERIALS AND METHODS



## 6.1. INTRODUCTION

In the previous chapter, analysis of the structural features and phylogenetic relationships of *SUD1* indicated that this protein was the likely *Arabidopsis* ortholog of the well known endoplasmic reticulum (ER) localized ubiquitin E3 ligases Doa10<sup>a</sup> protein from yeast (Swanson *et al.*, 2001) and TEB4 protein from human (Hassink *et al.*, 2005). The Doa10 protein has been extensively studied in yeast and is a component of the ERAD complex, involved in the quality control that degrades misfolded ER proteins (Swanson *et al.*, 2001; Carvalho *et al.*, 2006; Kreft and Hochstrasser, 2011). However, ERAD is not restricted to aberrant proteins and is also employed in the feedback regulation of normal proteins such as the HMG-coenzyme (CoA) reductase (HMGR) in yeast (Hampton and Garza, 2009). There are two different ERAD complexes in yeast, the Hrd1 complex and the Doa10 complex (Hampton, 2002). Numerous genetic analyses were conducted in yeast to find the HRD genes responsible for **H**mg-CoA **R**eductase **D**egradation, and only the Hrd1 ERAD complex has been associated with regulated degradation of HMGR (Hampton *et al.*, 1996). In *Arabidopsis thaliana*, two redundant proteins were identified as the most likely orthologs of yeast Hrd1, At3g16090 and At1g65040, which were named AtHRD1A and AtHRD1B, respectively (Su *et al.*, 2011).

As was detailed, most of the knowledge on ERAD came from studies in yeast and mammalian systems (Vembar and Brodsky, 2008; Smith *et al.*, 2011). By contrast, little is known about the molecular components and biochemical mechanism of plant ERAD, despite the finding that similar ERAD processes do operate in plant cells to remove misfolded proteins (Muller *et al.*, 2005; Yamamoto *et al.*, 2010). As most components of ERAD are evolutionarily conserved, the basic conclusions derived from studies performed using yeast are likely to be applicable to all eukaryotes.

The present chapter describes the series of experiments that were conducted as an effort to functionally characterize the likely *Arabidopsis* *DOA10* ortholog gene *SUD1*, using yeast complementation. Because *SUD1* is a putative member of the ERAD pathway, the two *Arabidopsis* redundant genes *AtHRD1A* and *AtHRD1B*, which are the most likely orthologs of the yeast ERAD component Hrd1, were additionally included into the present study.

---

<sup>a</sup> While *Arabidopsis thaliana* proteins are referred to by the relevant gene symbol, non-italic, uppercase letters, *Saccharomyces cerevisiae* proteins are referred to by the relevant gene symbol, non-italic, initial letter uppercase.

In order to take advantage of all the resources and know-how available from *Saccharomyces cerevisiae*, the present work was performed on the “Organelle biogenesis and homeostasis Laboratory at Center for Genomic Regulation”, under the supervision of Dr. Pedro Carvalho in Barcelona, Spain.

## **6.2. RESULTS AND DISCUSSION**

### **Molecular Cloning of *SUD1* in *E. coli***

The coding sequence (CDS) of Arabidopsis *SUD1* was initially sub-cloned into the pGEM-T Easy vector that allows blue/white screening for recombinants and is commonly used for cloning PCR products. The *SUD1* cDNA from wild-type (Col-0) young seedlings was amplified using a proofreading DNA polymerase and the blunt-ended PCR product was adenylated and subsequently cloning into pGEM-T Easy vector was attempted. *E. coli* competent cells were transformed to allow the selective propagation of the plasmid, thus allowing for convenient amplification and subsequent DNA manipulation of *SUD1 in vitro*. Two independent *E. coli* transformations using different competent cells strains (XL1-Blue and DH5 $\alpha$ ) were performed. However, the screening for transformants containing the insert revealed no positive clones, while transformations of control inserts cloned into the pGEM-T Easy vector produced a large number of recombinant clones.

As cloning the CDS of *SUD1* into pGEM-T Easy was not successful, another approach was employed. First, the PCR product amplified with *SUD1* cDNA-specific primers (flanked by restriction sites) from wild-type (Col-0) seedlings was sequenced confirming that the amplified fragment corresponded to the *SUD1* coding region predicted by the TAIR database (*At4g34100*). Second, the amplified CDS of *SUD1* was cloned using restriction sites into the pRS316 shuttle vector. The shuttle vectors are used for gene cloning in *Saccharomyces cerevisiae*, but are also capable of replication in *E. coli*. The transformation of *E. coli* competent cells with the CDS of *SUD1* cloned into the pRS316 shuttle vector produced only two positive clones that were further confirmed by colony PCR. Similar to the pGEM-T Easy vector, transformation of the same shuttle vector containing a control insert (positive control) produced more than 40 positive clones, confirmed by colony PCR. The sequencing of the two positive clones indicated that a fragment of 686 bp (nucleotides 344-1029) was excised from the CDS of *SUD1*. This strongly suggests that the full-length *SUD1* CDS is not stably maintained in *E. coli*, thus explaining the absence in cDNA libraries



of the full-length *SUD1* cDNA. Additionally, the fact that a plasmid bearing a shorter version of the *SUD1* coding region (lacking nucleotides 344-1029), can be propagated in *E. coli* shows that the full-length *SUD1* CDS sequence is toxic for *E. coli*. It is interesting to notice that the excised 686 bp sequence is delimited on both sides by the same 7 bp sequence (GCAAGCA), at positions 341-347 and 1027-1033, which probably produces a recombination event leading to the removal of this fragment. The lack of success in cloning *SUD1* CDS in *E. coli* was not completely unexpected since the yeast Doa10 gene is also lethal for *E. coli* (Mandart *et al.*, 1994).

### ***SUD1* Complementation of Yeast *doa10Δ* Mutation**

To analyse if *SUD1* is the functional ortholog of the yeast Doa10 protein, complementation of the yeast Doa10 mutant (*doa10Δ*) with *SUD1* was attempted. However, the inability to clone *SUD1* into *E. coli* increased the difficulty of performing the yeast complementation. As an alternative strategy, the full-length *SUD1* CDS was cloned into a yeast centromere vector without a previous subcloning step in *E. coli*. For this purpose, the yeast centromere plasmid (YCp) vector pRS316 was used (Sikorski and Hieter, 1989). YCp are vectors containing an autonomously replicating sequence (ARS), and a centromere sequence (CEN) required for mitotic stabilization and segregation of the YCp during yeast division. The stability and low copy-number (1 or 2 per cell) of YCp vectors make them the ideal choice as cloning vectors for complementation studies (Romanos *et al.*, 1992).

The coding region of the Arabidopsis *SUD1* was cloned in frame with a C-terminal Hemagglutinin (HA) tag into a pRS316 derivative plasmid (bPC609), containing the PRC1 moderate promoter to drive gene expression, a triple HA tag and the PRC1 3' UTR to allow transcript stability. A bPC609 plasmid double-stranded gap was produced by cleavage at two restriction sites between the PRC1 promoter sequence and the triple HA tag sequence. The PCR fragment of *SUD1* cDNA was amplified from Col-0 seedlings by RT-PCR using *SUD1* cDNA-specific primers and reamplified using primers flanked by sequences with homology to both ends of the gapped bPC609 plasmid. Yeast *doa10Δ* was then co-transformed with the gapped bPC609 plasmid and with the PCR product containing homology to both ends of the gapped bPC609 plasmid. It was expected that the gapped plasmid would be repaired with the PCR product *via* homologous recombination in yeast. This procedure revealed particularly effective for obtaining yeast *doa10Δ SUD1* positive clones without the requirement of subcloning steps in *E. coli*. Nine independent

yeast *doa10Δ SUD1* positive clones were then analyzed by immunoblotting with two different anti-HA antibodies in order to confirm the presence of SUD1 protein in yeast. However, the anti-HA antibodies did not detect SUD1-HA protein in the immunoblots (data not shown). The yeast *doa10Δ SUD1* positive clones were nonetheless analyzed by sequencing to confirm that the cloning was correct. Since YCp vectors are present at low-copy number in yeast, the minimal amount for sequencing analysis cannot be easily obtained without previous subcloning steps in *E. coli*. Thus, bPC609 and *SUD1* specific primers were used to amplify by yeast colony PCR several overlapping fragments corresponding to the complete *promotorPRC1::SUD1::HA* construct for direct sequencing. The sequencing results confirmed that the coding region of the Arabidopsis gene *SUD1* was cloned in frame with a C-terminal triple HA tag. The sequence analysis also revealed that the cloned fragment corresponded to the *SUD1 At4g34100.2* splice variant that differs from *At4g34100.1* in only amino acid.

Considering the wide use of this expression vectors in yeast work, it was hypothesized that the SUD1 protein is unstable in yeast. Therefore, the presence of residual amount of SUD1 protein in the *doa10Δ SUD1* yeast cells, and the capacity of this putative residual amount of SUD1 protein to partially complement the yeast *doa10Δ* mutation, were further investigated. In yeast, the Doa10 E2 ubiquitin conjugase Ubc6 is constitutively turned over via the Doa10 pathway (Swanson *et al.*, 2001; Walter *et al.*, 2001), and it has been extensively used to monitor the activity of the yeast Doa10 protein (Kreft *et al.*, 2006; Ravid *et al.*, 2006; Kreft and Hochstrasser, 2011). Therefore to determine whether some residual SUD1 activity was present in *doa10Δ SUD1* yeast cells that was capable of Ubc6 degradation, wild-type, *doa10Δ* and *doa10Δ SUD1* yeast cells were transformed with an expression vector containing Ubc6 tagged with a C-terminal HA epitope. To follow the degradation of a particular substrate, cyclohexamide (CHX) is commonly used in order to inhibit *de novo* protein synthesis. A CHX pulse-chase experiment was performed so as to follow the degradation of the Ubc6-HA protein. As expected, a clear degradation of Ubc6-HA was observed in yeast wild-type cells (Figure 6.1). However, the immunoblotting showed that Ubc6-HA protein was stabilized in *doa10Δ SUD1* yeast cells like it is observed in the *doa10Δ* yeast cells (Figure 6.1). In support of these results, it has been reported a lack of genetic complementation of yeast *doa10Δ* by heterologously expressing the human TEB4 (Kreft *et al.*, 2006). Therefore, since the Arabidopsis SUD1 protein is not stable in yeast, it is not possible to functionally confirm if indeed SUD1 has a role in the ERAD system as the likely Arabidopsis Doa10 ortholog, therefore demanding further investigation in Arabidopsis.

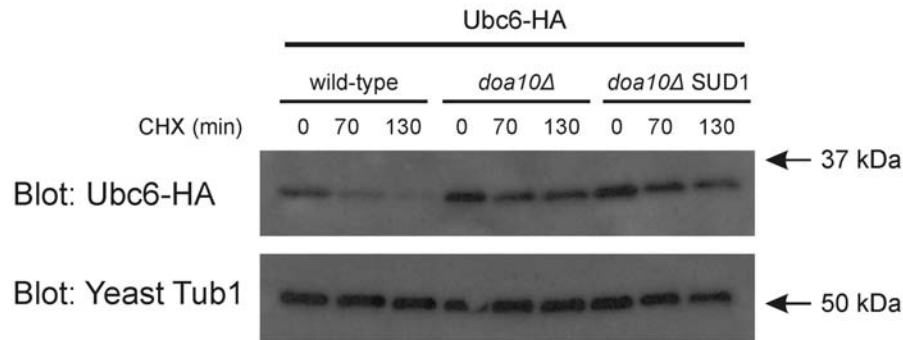


**Figure 6.1 – *SUD1* Complementation of the Yeast *doa10Δ* Mutation**

The content of the yeast Doa10 substrate Ubc6-HA was analyzed by immunoblotting in transformed wild-type, *Doa10Δ* and *Doa10Δ SUD1* yeast cells expressing the Ubc6-HA gene, following inhibition of translation with cycloheximide (CHX). Equal amounts of total protein extracts from exponentially growing cells treated with CHX were separated by SDS/PAGE and analyzed by immunoblotting, with anti-HA antibody for Ubc6-HA detection and anti-Tub1 for yeast Tub1 detection (loading control). Weights from a protein molecular weight ladder are represented.

### Degradation of Yeast Doa10 Substrates in *doa10-G498E* Mutant Cells

In the present thesis, it was described how second-site mutations in the *dry2* background of Arabidopsis plants suppress the drought hypersensitivity phenotype observed in the *dry2* mutant. The positional-cloning of this *dry2* suppressor mutations lead to the identification of *SUD1* that encodes the Arabidopsis ortholog of the yeast Doa10 protein known to be involved in the ERAD system. The present study already referred four mutant alleles that affect *SUD1* function. The *sud1-22* suppressor has a point mutation in the 3<sup>rd</sup> exon of *SUD1*, resulting in a glycine by glutamate substitution (G360E). This suppression is the only one caused by a substitution of a clearly conserved amino acid residue in yeast Doa10 (corresponding to Gly498 in Doa10), and also in others orthologs from phylogenetically unrelated eukaryotic organisms (Chapter 5, Figure 5.5). This conservation suggests an essential role of this residue for function in this class of proteins.

The yeast ubiquitin E3 ligase Doa10 has an unusually broad substrate range, being capable of recognizing aberrant proteins subjected to quality control and synthetic degron-fusion substrates, membrane proteins, and soluble proteins of the cytoplasm and nucleus (Deng and Hochstrasser, 2006; Ravid *et al.*, 2006). As previously indicated, the E2 ubiquitin conjugase Ubc6 that binds to the ER membrane via a C-terminal transmembrane anchor is a paradigm, being constitutively turned over via the Doa10 pathway (Sommer and Jentsch, 1993; Swanson *et al.*, 2001; Walter *et al.*, 2001). Another well studied membrane substrate of Doa10 is Ste6–166 (Ste6\*), a mutant form of the pheromone transporter that is missing the last 42 residues of its cytosolically disposed C-terminal domain (Loayza *et al.*, 1998; Huyer *et al.*, 2004; Vashist and Ng,

2004). Besides the well known naturally derived substrates of the yeast Doa10 pathway, synthetic degron-fusion substrates have been successfully engineered as “reporter” substrates for Doa10-mediated degradation, like the membrane synthetic protein Pca1-Sec12TM-DHFR-HA and the cytoplasmic synthetic protein MN-Mat $\alpha$ -eK-HA (Pedro Carvalho, personal communication).

To investigate if G498 is an essential amino acid residue for Doa10 function, as previously reported for the SUD1 suppressor, the degradation of Doa10 membrane and cytoplasmic “reporter” substrates in yeast *doa10-G498E* mutant cells was investigated. Since the full-length Doa10 gene is not stably maintained in *E. coli*, a pRS305 plasmid containing only part of the yeast *DOA10* coding sequence (from ORF nucleotide 814 till the last ORF codon excluding the stop codon) in frame with a C-terminal MYC epitope was used for oligonucleotide-directed mutagenesis to replace the Gly498 by Glu within the Doa10 protein.

The yeast Doa10-MYC and *doa10-G498E* mutant cells were transformed with a vector containing one of various Doa10 pathway “reporter” substrates (Pca1-Sec12TM-DHFR, Ste6\*, Ubc6 and MN-Mat $\alpha$ -eK) fused to a triple HA tag. Then, a CHX pulse-chase experiment was performed to follow the degradation of the Doa10 pathway “reporter” substrates. The degradation of Doa10 membrane or cytoplasmic “reporter” substrates in *doa10-G498E* mutant cells was analysed by immunoblotting with anti-HA antibodies (Figure 6.2). In the yeast *doa10 $\Delta$*  mutant, all the three tested degradation “reporter” substrates remained stable over time. As expected, the expression of the yeast Doa10-MYC from the chromosomal *DOA10* locus resulted in clear degradation of both membrane (Pca1-Sec12TM-DHFR, Ste6\* and Ubc6) and soluble (MN-Mat $\alpha$ -eK) “reporter” substrates, indicating complementation of the mutant phenotype. However, the expression of the *doa10-G498E* mutant allele from the chromosomal *DOA10* locus did not stabilize yeast Doa10 membrane or cytoplasmic “reporter” substrates as would be expected if the Doa10-G498E substitution was compromising the function of yeast Doa10. From these data, it is possible to conclude that the Doa10-G498E protein is still functional and able to work with the Ubc6 E2 to target Doa10 substrates for degradation, suggesting important functional differences between Doa10 and SUD1.

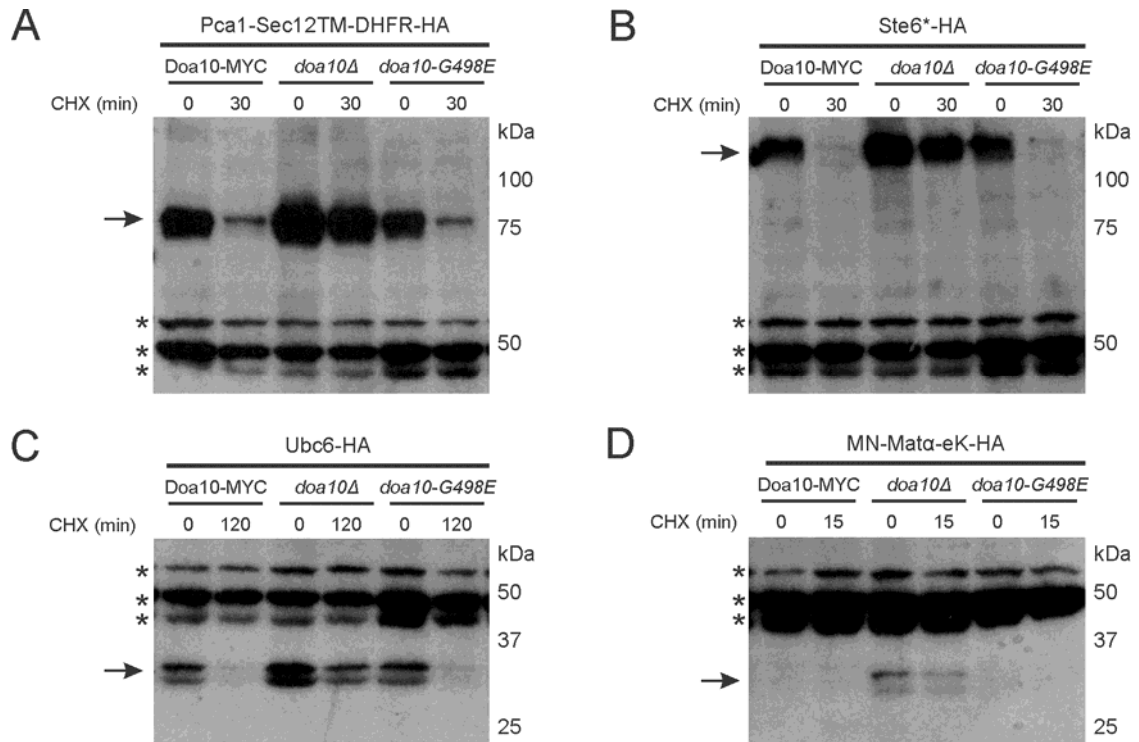


**Figure 6.2 – Degradation of Doa10 membrane or cytoplasmic “reporter” substrates in *doa10-G498E* mutant cells**

**(A)** The content of the yeast Doa10 membrane substrate Pca1-Sec12TM-DHFR-HA was analyzed by immunoblotting in transformed yeast cells expressing the indicated genes following inhibition of translation with cycloheximide (CHX). The Doa10-MYC and *doa10-G498E* alleles were expressed from the yeast chromosomal *DOA10* locus. Yeast *doa10Δ* cells were used as a negative control. Pca1-Sec12TM-DHFR-HA was expressed from a yeast centromere plasmid (YCp). Equal amounts of total protein extracts from exponentially growing cells treated with CHX were separated by SDS/PAGE and analyzed by immunoblotting with anti-HA antibody. Arrows indicate the Pca1-Sec12TM-DHFR-HA protein immunoblotting bands. Asterisks indicate three cross-reacting yeast proteins, labelled “nonspecific”, that were used as internal protein loading controls. **(B)** As in (A) but with expression of the yeast Doa10 membrane substrate Ste6\*-HA from an YCp. **(C)** As in (A) but with expression of the yeast Doa10 membrane substrate Ubc6-HA from an YCp in the presence of endogenous Ubc6. **(D)** As in (A) but with expression of the yeast Doa10 cytoplasmic substrate MN-Matα-eK-HA from an YCp.

### ***AtHRD1* Complementation of Yeast *hrd1Δ* Mutation**

Because *SUDI* is a putative member of the ERAD pathway, the two *Arabidopsis* redundant genes *AtHRD1A* and *AtHRD1B*, which are the most likely orthologs of the yeast ERAD component Hrd1, were additionally included into the present study. To test if *AtHRD1A* and *AtHRD1B* are the functional orthologs of the yeast Hrd1 protein, a yeast complementation experiment was performed. The YCp pRS316 vector was used to clone and express both the yeast *HRD1/AtHRD1* genes and the ERAD-L pathway substrate CPY\*. The coding region of the *Arabidopsis thaliana* genes *HRD1A* (*At3g16090.1*) and *HRD1B* (*At1g65040.2*) were cloned in frame with a C-terminal triple HA tag into a pRS316 vector containing the PRC1 moderate promoter (to drive the expression) and the PRC1 3' UTR (to allow transcript stability). The resulting plasmids bearing

*AtHRD1A* or *AtHRD1B*, and also the plasmid containing the yeast *HRD1* coding sequence and an empty pRS316 vector, were individually co-transformed with a mutated version of carboxypeptidase Y (CPY\*) tagged with a C-terminal FLAG epitope-expressing vector into the yeast *hrd1Δ* mutant cells. The missfolded luminal ER protein CPY\* (Finger *et al.*, 1993) is known to be a substrate of the ERAD-L pathway, dependent on Hrd1 protein for its degradation in yeast, and has been extensively used to monitor the activity of the Hrd1 protein (Ng *et al.*, 2000; Carvalho *et al.*, 2006; Carvalho *et al.*, 2010).

In order to confirm that the CPY\*-FLAG transgene is expressed; several independent yeast clones for each co-transformation were analyzed by immunoblotting with anti-FLAG specific antibodies. The CPY\*-FLAG protein can be detected by immunoblotting in all the analysed clones demonstrating that CPY\*-FLAG is being expressed (Figure 6.3). Two independent transformants for *hrd1Δ AtHRD1A* (1.1, 1.2) and *hrd1Δ AtHRD1B* (2.1, 2.2), together with the controls *hrd1Δ* yeast Hrd1 (3.1) and *hrd1Δ* empty vector (7.1), were used for the complementation assay.

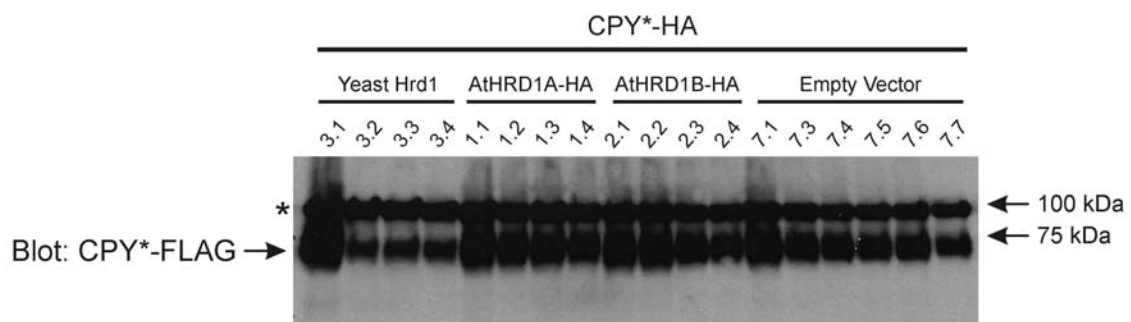


**Figure 6.3 – Yeast colony screening for CPY\*-FLAG expression**

The content of the yeast Hrd1 substrate CPY\*-FLAG was analyzed by immunoblotting in different transformed yeast *hrd1Δ* cells with clones expressing the indicated genes. Approximate amounts of yeast cells growing on plate were collected to obtain total protein extracts. Proteins were separated by SDS/PAGE and analyzed by immunoblot with anti-FLAG antibody for CPY\*-FLAG detection. Asterisk indicates a cross-reacting yeast protein, labelled “nonspecific”. The cross reacting band cannot serve as internal protein loading control since non-equal amounts of total protein extracts were used. Estimated molecular weight of the bands are indicated.

A CHX pulse-chase experiment was performed in order to follow the degradation of the ERAD-L pathway substrate CPY\*-FLAG (Figure 6.4). In the mutant yeast *hrd1Δ* transformed with the empty vector, CPY\* remained stable over time. As expected, the expression of the yeast Hrd1 resulted in a degradation of the CPY\* indicating complementation of the mutant phenotype. However the expression of the Arabidopsis *HRD1A* and *HRD1B* orthologs did not increase the degradation of the CPY\*-FLAG protein as we would expect if complementation indeed occurred. The apparently slight decrease in CPY\*-FLAG protein levels observed after 90 minutes of CHX

incubation is the result of lower levels of total loaded protein, as we can confirm by the corresponding tubuline loading control blot. Similar to what happened with *SUD1*, a possible explanation for the CPY\* stabilization in the *AtHRD1* complementation assays is that *AtHRD1A* and *AtHRD1B* are not expressed or are unstable in yeast. The protein resulting after *AtHRD1A* and *AtHRD1B* induction in yeast during the cyclohexamide pulse-chase experiment was analyzed by immunoblotting. The anti-HA detection revealed that the *AtHRD1A* cannot be detected in the immunoblot at any of the time points tested. *AtHRD1B* protein is highly abundant at 0 minutes of CHX incubation but the protein levels decrease rapidly and the protein cannot be detected within 30 minutes. Because these constructs were analyzed by sequencing, the lack of *AtHRD1* indicates that *AtHRD1* proteins are quickly degraded in yeast.

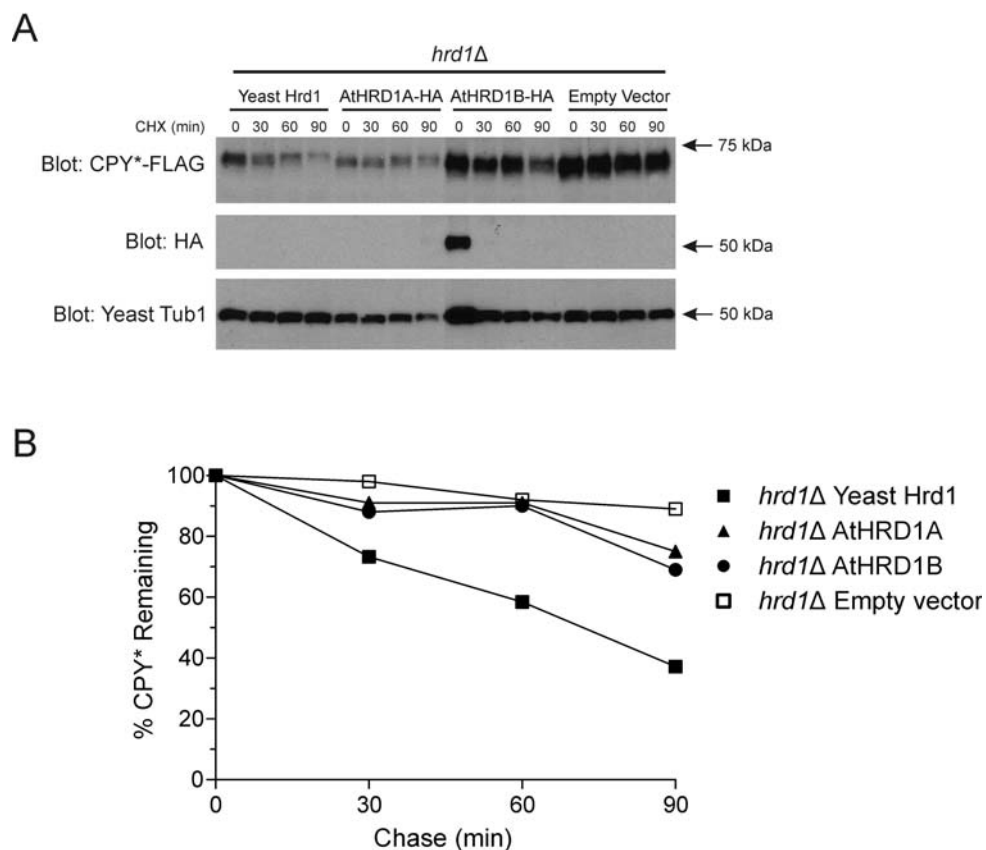


**Figure 6.4 – *AtHRD1* Complementation of the Yeast *hrd1Δ* Mutation**

**(A)** The content of the yeast Hrd1 substrate CPY\*-FLAG was analyzed by immunoblotting in transformed yeast *hrd1Δ* cells expressing the indicated genes, following inhibition of translation with cycloheximide (CHX). Equal amounts of total protein extracts from exponentially growing cells treated with CHX were separated by SDS/PAGE and analyzed by immunoblotting with anti-FLAG antibody for CPY\*-FLAG detection, anti-HA antibody for *AtHRD1A*-HA or *AtHRD1B*-HA detection, and anti-Tub1 for yeast Tub1 detection (loading control). An empty vector was used as a negative control. The *AtHRD1*-HA and yeast Tub1 proteins present a similar estimated size, and as a consequence both blots appear as overlapping in the yeast Tub1 blot. Protein molecular weight ladder is represented. **(B)** Quantification of the amount of CPY\*-FLAG by blot densitometry. Relative protein levels are expressed as the percentage of the value determined at time point zero.

It is known that in yeast, ER resident membrane proteins Hrd1 and Hrd3 form a stoichiometric complex and directly interact through the Hrd1 transmembrane domain, allowing Hrd1 stability by Hrd3-dependent control of the Hrd1 RING domain activity (Gardner *et al.*, 2000). In yeast, it is also known that the overexpression of Hrd1 protein compensates the absence of Hrd3 protein. When overexpressed, Hrd1 protein accelerates CPY\* degradation in the yeast mutant lacking Hrd3 protein (Plemper *et al.*, 1999; Gardner *et al.*, 2000; Carvalho *et al.*, 2010). Assuming that the AtHRD1A and AtHRD1B fail to properly interact with yeast Hrd3, we investigated whether the overexpression of the *AtHRD1A* and *AtHRD1B* could produce protein stabilization, which in turn would lead to CPY\*-FLAG degradation. Therefore, the coding region of the Arabidopsis genes *AtHRD1A* and *AtHRD1B* were cloned into an YCp p416GAL vector containing the strong galactose-inducible GAL1 promoter, and the CYC1 3'UTR to allow transcript stability. The resulting plasmids were individually co-transformed with the CPY\*-FLAG in *hrd1Δ* yeast cells. The previously transformed yeast cells with plasmid containing the yeast Hrd1 coding sequence and an empty pRS316 vector were used as positive and negative controls, respectively. The four different yeast strains used in this assay were grown in the presence of galactose to drive *AtHRD1A* and *AtHRD1B* overexpression. A cyclohexamide pulse-chase experiment was subsequently performed, but still no degradation of the CPY\*-FLAG was detected (Figure 6.5), suggesting that overexpressing *AtHRD1A* or *AtHRD1B* in *hrd1Δ* yeast cells is not effective to complement the mutated yeast, through the degradation of a typical yeast Hrd1 substrate. Since the Arabidopsis genes cloned in the p416GAL were not tagged with an epitope to confirm the proper protein production, two independently transformed yeast cells were used for the assays and the mean for the substrate quantification was calculated (Figure 6.5B). However, the obtained data do not allow us to conclude if the overexpression of *AtHRD1A* and *AtHRD1B* results in protein stabilization, like that observed for the yeast native Hrd1 (Carvalho *et al.*, 2010).

In yeast, the Hrd1 protein becomes unstable in the absence of Hrd3 protein, resulting in its own degradation by self-ubiquitination, a process that is mediated by the E2 ubiquitin conjugase Ubc7 (Gardner *et al.*, 2000; Bazirgan *et al.*, 2006). One likely possibility is that AtHRD1 proteins and yeast Hrd3 proteins are not properly interacting in order to ensure the AtHRD1 stabilization, which may result in self-ubiquitination and quick degradation. For this to happen, AtHRD1 needs to properly interact with the yeast E2 ubiquitin conjugase Ubc7. To test this hypothesis, the constructs containing the HA tagged AtHRD1A and B coding sequences were used to transform *hrd1Δ ubc7Δ* yeast cells. As shown in Figure 6.6, AtHRD1B increased its stability in *hrd1Δ ubc7Δ*



yeast, and protein levels can be detected even after 90 minutes of CHX incubation. However, although AtHRD1B became quite stable in the *hrd1Δ ubc7Δ* yeast background, this strain cannot be used in substrate degradation assays, since Ubc7 is the same E2 ubiquitin-conjugating enzyme involved in Hrd1-mediated CPY\* ubiquitination. In this experiment, yeast Usa1 protein was used as loading control (Figure 6.6A) and the blot confirms that equal amounts of total protein extracts were loaded for the different time point in each CHX pulse-chase experiment.

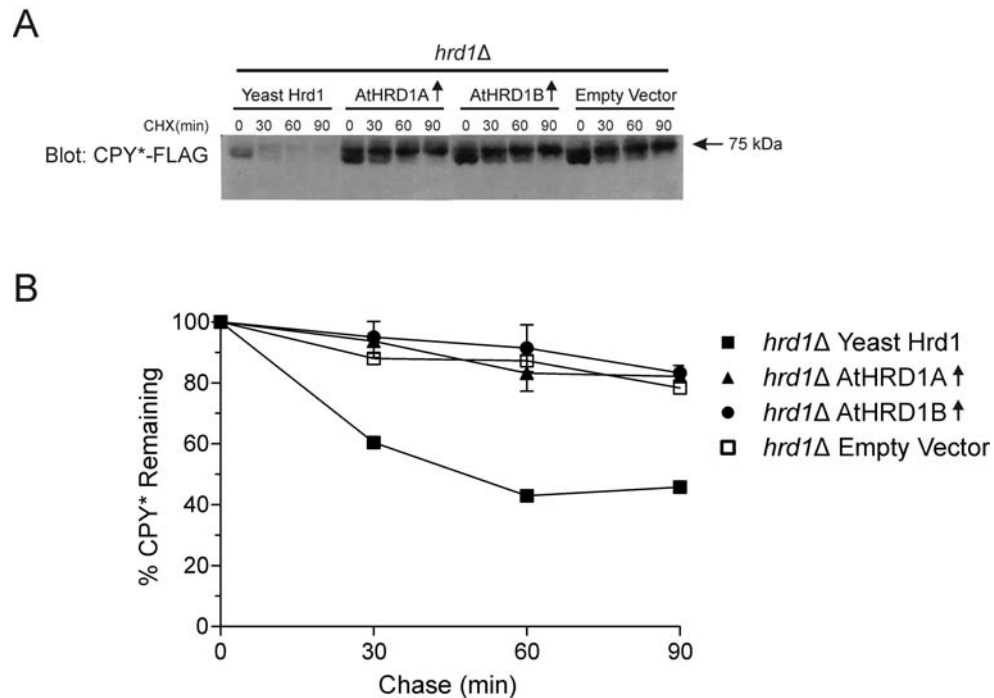


**Figure 6.5 – AtHRD1 Overexpression in *hrd1Δ* Yeast Background**

**(A)** The degradation of the yeast Hrd1 substrate CPY\*-FLAG was analyzed by immunoblotting in yeast *hrd1Δ* cells transformed with the indicated genes, following inhibition of translation with cycloheximide (CHX). Equal amounts of total protein extracts from exponentially growing cells treated with CHX were separated by SDS/PAGE and analyzed by immunoblotting with anti-FLAG antibody for CPY\*-FLAG detection. An empty vector was used as a negative control. Protein molecular weight ladder is represented.

**(B)** Quantification of the amount of CPY\*-FLAG by blot densitometry. Relative protein levels are expressed as the percentage of the value determined at time point zero.

AtHRD1A was slightly stabilized in the *hrd1Δ ubc7Δ* yeast background (Figure 6.6), but only for a short period of time, as it was no longer detected after 30 minutes. Although AtHRD1A and AtHRD1B were more stable in the *hrd1Δ ubc7Δ* yeast background, extensive degradation still occurred. It is possible that this degradation could be driven by the yeast Doa10. The absence of Ubc7 will block the self-ubiquitination of the AtHRD1A and AtHRD1B in the *hrd1Δ ubc7Δ* yeast background and it is likely that a defective folding of the heterologous AtHRD1A and AtHRD1B will activate yeast Doa10 and Ubc6 mediated degradation. When human CFTR was ectopically

expressed in yeast, its degradation depended on both Hrd1p and Doa10. This was illustrated by the strong effect of deleting both E3s, whereas deleting either of them separately gave only modest effects on the degradation of CFTR (Gnann *et al.*, 2004). Furthermore, in yeast the accumulation of ubiquitinated proteins in the ER membrane that was caused by a temperature-sensitive mutation in Npl4p mutation could be suppressed by deleting both Doa10 and Hrd1 (Hitchcock *et al.*, 2003). These data suggest that Hrd1p and Doa10p are able to complement each other in the degradation of a single substrate. However, this possible compensatory regulation between AtHRD1 and Doa10 in yeast has yet to be investigated in Arabidopsis in order to determine whether SUD1 is involved in the regulation of AtHRD1 levels.

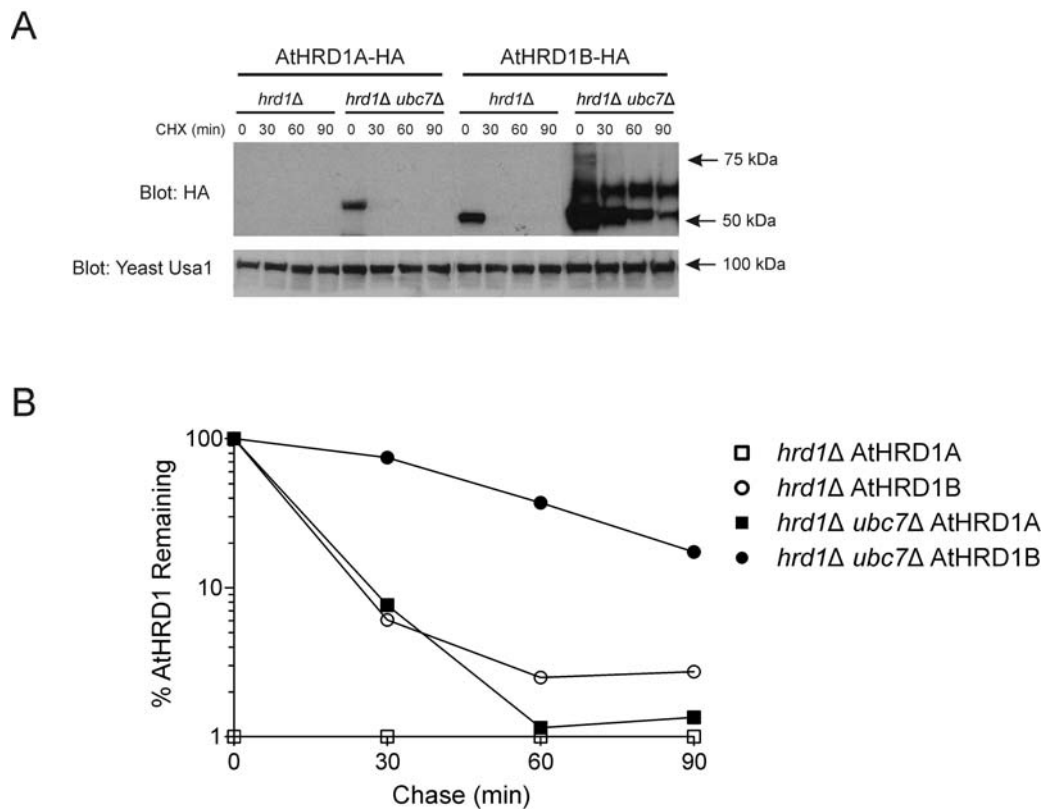


**Figure 6.6 – AtHRD1 Stabilization in *hrd1Δ ubc7Δ* Yeast Background**

**(A)** The stabilization of the AtHRD1A and AtHRD1B was analyzed by immunoblotting in yeast *hrd1Δ* and yeast *hrd1Δ ubc7Δ*, following inhibition of translation with cycloheximide (CHX). Equal amounts of total protein extracts from exponentially growing cells treated with CHX were separated by SDS/PAGE and analyzed by immunoblotting with anti-HA antibody for AtHRD1A-HA or AtHRD1B-HA detection, and anti-Usa1 for yeast Usa1 detection (loading control). An empty vector was used as a negative control. Protein molecular weight ladder is represented. **(B)** Quantification of the amount of AtHRD1A and AtHRD1B by blot densitometry. Relative protein levels are expressed as the percentage of the value determined at time point zero.

## Investigating the Function of the Arabidopsis ERAD E3-ligases

In this chapter, yeasts were used as a functional tool to investigate the function of the Arabidopsis ERAD E3-ligases. The function of AtHRD1A and AtHRD1B has been partially demonstrated, since these proteins are stabilized in the absence of Ubc7, indicating a biochemical interaction among these components. However, at the same time the absence of Ubc7 that is required for Hrd1 function makes it impossible to analyze AtHRD1 function with a *bona fide* substrate. There are studies confirming that this ERAD pathway is functional in Arabidopsis (Yamamoto *et al.*, 2010; Liu *et al.*, 2011; Su *et al.*, 2011)<sup>105</sup>. In contrast to the Hrd pathway, there is no information about the function of this pathway in Arabidopsis, with the exception of that referred in this thesis. Data obtained in this work indicates that production of stable SUD1 protein in yeast is not possible, making further experimentation unviable. However, relevant insights were provided on Doa10 and SUD1 function in a comparative manner, by showing that the G360E mutation in Arabidopsis causes loss-of-function in this protein, while Doa10 G498E has no effect in protein activity. This indicates that despite their relatively high conservation throughout evolution (Chapter 5, Figure 5.5), Doa10 and SUD1 have functionally diverged, this likely causing the impossibility of using yeast complementation for Arabidopsis E3 ERAD gene studies.

## 6.3. MATERIALS AND METHODS

### Plant Material

The *Arabidopsis thaliana* ecotype Columbia-0 (Col-0) was used for the total RNA extraction to obtain cDNA from wild-type seedlings. The standard molecular biology methods, used in the present work, are presented in more detail in Appendix I.

### Plant Manipulation and Growth Conditions

Arabidopsis standard handling procedures and conditions were employed to promote seed germination and growth, as previously described in the Materials and Methods section of Chapter 2.

### Yeast Strains and Plasmids

Yeast strains used in the present work were generously provided by Dr. Pedro Carvalho at Center for Genomic Regulation, Barcelona, Spain. The yeast *Saccharomyces cerevisiae* used in the present work

are isogenic to BY4730 (*MATa ura3DO his3D1 leu2DO met15DO*), and strains with gene deletions were performed using standard PCR-based homologous recombination.

### Yeast Genetic Manipulation

Yeast rich (YPD) and minimal (SD) plates were prepared as described in Ausubel *et al.* (1996), and standard methods were used for genetic manipulation of yeast, as described in Guthrie and Fink (1991). Yeast transformations were performed by the LiAc procedure previously described by Ito *et al.* (1983).

### Molecular Cloning of Arabidopsis ERAD-Homolog Genes in Shuttle Vectors

The Arabidopsis ERAD-homolog genes *SUD1*, *AtHRD1A* and *AtHRD1B*, were cloned into the YCp bPC609 vector. Additionally, the ERAD-homolog genes *AtHRD1A* and *AtHRD1B* were cloned into the YCp pRS416GAL vector. The bPC609 and the pRS416GAL vector were also provided by Dr. Pedro Carvalho at Center for Genomic Regulation, Barcelona, Spain. The bPC609 is an YCp, constructed on the backbone pRS316 plasmid (Sikorski and Hieter, 1989), that contains the PRC1 moderate promoter to drive gene expression, a triple HA tag and the PRC1 3' UTR to allows transcript stability. The pRS416GAL is an YCp, constructed on the backbone pRS416 plasmid (Sikorski and Hieter, 1989), that contains the GAL1 promoter to drive gene expression and the CYC1 3' UTR to allows transcript stability.

The cDNA of Arabidopsis ERAD-homolog genes, *AtHRD1A* and *AtHRD1B*, were PCR amplified using the primers detailed in Table 6.1 and the amplified fragment was cloned into the bPC609 or the pRS316 vector using the restriction sites indicated in Table 6.1, to obtain the plasmids described in Table 6.2. The *E. coli* strains XL1 Blue (Bullock *et al.*, 1987) or DH5 $\alpha$  (Griffith and Gietz, 2003) were used for in bacteria cloning purposes.

**Table 6.1 – List of Primers to Specific Amplify the cDNA Sequence of Arabidopsis ERAD-homolog genes**

The PCR annealing temperature specific used for each primer par and the amplified product size are indicated. Restriction sites in each primer are outlined in bold. Annealing temperature (A. temp).

Purpose	Primer Sequence (5'→3')	Restriction sites	A.temp (°C)	Amplification product size (bp)
<i>SUD1</i> cDNA amplification for cloning in the bPC609 vector	<b>GGTTAATTAA</b> ATGGAGATTTCCCGGCCGATTTC	PacI	60	3339
	TC <b>GCTAGC</b> AGCTTCTTGTGGATTGCACGTC	NheI		
<i>AtHRD1A</i> cDNA amplification for cloning in the bPC609 vector	<b>CTTTAATTAA</b> ATGATTCAGCTAAAGGTTTACGCGG	PacI	60	1494
	C <b>AGCTAGC</b> TGCAGTATCCGCAACGGAC	NheI		
<i>AtHRD1B</i> cDNA amplification for cloning in the bPC609 vector	<b>GATTAATTAA</b> ATGATTCGACTAAGAACATACGCAGG	PacI	60	1399
	T <b>GCTAGC</b> CTCTGCTGCATCAGCAAC	NheI		
<i>AtHRD1A</i> cDNA amplification for cloning in the pRS416GAL vector	<b>AGTCTAGA</b> ATGATTCGACTAAGAACATACGCAGG	XbaI	60	1495
	C <b>AGGATCCT</b> CACTCTGCTGCATCAGCAAC	BamHI		
<i>AtHRD1B</i> cDNA amplification for cloning in the pRS416GAL vector	<b>CTTCTAGA</b> ACAATGATTCAGCTAAAGGTTTACGC	XbaI	65	1402
	G <b>TCTCGAG</b> CTATGCAGTATCCGCAAC	XbaI		

**Table 6.2 – List of Plasmids Obtained by Cloning the cDNA Sequence of Arabidopsis ERAD-homolog genes into Yeast Centromeric Plasmids**

Plasmid	Backbone Plasmid	Composition
bPC609– <i>SUD1</i>	pRS316	<i>SUD1</i> (At4g34100.2) cDNA cloned into a pRS316 (CEN, URA, PRC1 promoter, PRC1 terminator, 3xHA tag, AmpR)
bPC609– <i>AtHRD1A</i>	pRS316	<i>AtHRD1A</i> (At3g16090.1) cDNA cloned into a pRS316 (CEN, URA, PRC1 promoter, PRC1 terminator, 3xHA tag, AmpR)
bPC609– <i>AtHRD1B</i>	pRS316	<i>AtHRD1B</i> (At1g65040.2) cDNA cloned into a pRS316 (CEN, URA, PRC1 promoter, PRC1 terminator, 3xHA tag, AmpR)
pRS416GAL– <i>AtHRD1A</i>	pRS416	<i>AtHRD1A</i> (At3g16090.1) cDNA cloned into a p416GAL (CEN, URA, GAL1 promoter, CYC1 terminator, no tag, AmpR)
pRS416GAL– <i>AtHRD1B</i>	pRS416	<i>AtHrd1B</i> (At1g65040.2) cDNA cloned into a p416GAL (CEN, URA, GAL1 promoter, CYC1 terminator, no tag, AmpR)

The full-length *DOA10* gene is not stably maintained in *E. coli*. Therefore, the full-length *SUD1* CDS was cloned into the bPC609 vector without a previous subcloning step in *E. coli*. A bPC609 plasmid double-stranded gap was produced by cleavage at the *PacI*/*NheI* restriction sites. The PCR fragment of *SUD1* cDNA was generated using *SUD1* cDNA-specific primers (Table 6.1) and reamplified using primers detailed in Table 6.3, that were flanked by sequences with homology to both ends of the gapped bPC609 plasmid. Yeast *doa10Δ* was then co-transformed with the gapped bPC609 plasmid and with the PCR product containing homology to both ends of the gapped bPC609 plasmid. The gapped plasmid was then repaired with the PCR product via homologous recombination in yeast producing the plasmid described in Table 6.2. The yeast *doa10Δ SUD1* positive clones were analyzed by sequencing to confirm that the cloning was performed correctly.

**Table 6.3 – *SUD1* cDNA-specific Primers Flanked by Sequences with Homology to Both Ends of the *PacI*/*NheI* Gapped bPC609 Plasmid**

Name	Sequence (5'→3')	Annealing temperature (°C)
<i>SUD1</i> Fw	5'-GTTTCTTTTCTACTCAACTTAAAGTATACATACGCTGCATGCTT AATTAATGGAGATTTCCTCCGCGCCGATTTC-3'	50
<i>SUD1</i> Rv	5'-GTCCGGGACGTCATAGGGATAGCCCGCATAGTCAGGAACAT CGTATGGGTAGCTAGCAGCTTCTTGTTGGATTGCACGTC-3'	

### Site-directed mutagenesis to construct *doa10-G498E* Mutant Strain

The full-length *DOA10* gene is not stably maintained in *E. coli*. Therefore, for mutagenesis of *DOA10*, yeast strains with a mutated chromosomal copy of *DOA10* were generated as following described. The *DOA10* sequence fragment, from *SacI* restriction site (located upstream the glycine 498 of the Doa10 protein sequence) to the end of the *DOA10* gene sequence, was cloned in a pRS305 vector, using the

SacI-PstI restriction sites (for detailed information about the standard molecular cloning procedures see Appendix I). Once the partial-length *DOA10* gene encompassed by SacI-PstI restriction sites was cloned in a pRS305 vector, the plasmid was site-directed mutagenized using the Quickchange Kit (*Agilent*) according to the manufacture instructions, to introduce a mutation in the coding region of *SUD1* that will result into a G498E of the protein sequence.

The pRS305 vector is a yeast integrative plasmid (YIp) vector containing the yeast selectable marker gene *LEU2*, that do not replicate autonomously (no CEN region), but integrates into the genome by homologous recombination (Sikorski and Hieter, 1989). The site of integration can be targeted by cutting the yeast segment in the YIp vector with a restriction endonuclease and transforming the yeast strain with the linearized plasmid (Romanos et al., 1992). In order to generate the *doa10-G498E* mutant strain, the pRS305 plasmid containing the *DOA10* sequence fragment (from SacI restriction site to the end of the *DOA10* gene sequence), and harboring the mutation that cause a G498E in the protein sequence, was linearized using Bsu36I restriction site, that is located upstream of the mutated nucleotide. The resulting linearized plasmid was used to transform yeast and it was integrated in the *DOA10* locus after *DOA10* ORF nucleotide 813 by homologous recombination. Since the plasmid will also integrate in the genome, only those yeast cells that have the ability to grow on SC-LEU plates, are positive clones. For confirmation of *doa10-G498E* positive clones, genomic DNA from five clones was isolated, the *DOA10* sequence that was expected to contain the mutation was PCR-amplified and sequenced.

### **ERAD-Substrate Degradation Experiments**

Plasmids coding for the ERAD substrates were generously provided by Dr. Pedro Carvalho at Center for Genomic Regulation, Barcelona, Spain. Cycloheximide pulse-chase experiments were performed as following described. Cells were adjusted to approximately 5 A<sub>1000</sub>/mL. After adding cycloheximide with a final concentration of 0.1 mg/ml, 1 mL of A<sub>1000</sub>/mL cells were removed at the indicated time points, suspended in sodium azide (NaAz) solution (final concentration of 0.04% NaAz) and kept at -4°C. Cell was resuspended in 250 µL of NaOH 0.15M, kept at -4°C for 10 minutes, and material was spin down to pellet the cells. The obtained pellet was incubated in sample buffer (8 M urea, 200 mM Tris-HCl, pH 6.8, 5% SDS, 0.1 mM EDTA, 0.03% Bromphenol Blue, 1.5% dithiothreitol and 0.1% beta-mercaptoetanol) at 65°C for 15 minutes with vigorous agitation and separated on *Criterion Tris-HCl Precast Gels* (Bio-RAD), at constant amperage of 0.12 A and maximum voltage of 250 V for 40 minutes, using the *Criterion™ Cell System* (Bio-Rad).

For experiments in which one of the ERAD components was expressed from the GAL1 promoter, cells were grown in medium containing 3% galactose, instead of sacarose, for 16 hr before performing cycloheximide pulse-chase experiments.

### **Immunoblotting**

Proteins separated by SDS-PAGE were electroblotted using *Trans-blot SD Semi-Dry Transfer Cell System* (BioRAD) onto polyvinylidene difluoride (PVDF) membranes at constant amperage of 0.2 A and maximum voltage of 18 V for 1 hours. PVDF membranes, containing electroblotted proteins, were then incubated with the appropriate primary antibody followed by the appropriate secondary antibody. All the used antibodies were generously provided by Dr. Pedro Carvalho at Center for Genomic Regulation, Barcelona, Spain. Proteins on immunoblots were visualized by using the ECL™ Western Blotting System (Amersham) according to the manufacturer's instructions, and exposing to an X-ray film for 10 sec to 20 min.

# Chapter 7

## Investigating the Use of Grafting in the Study of Long-distance Isoprenoid-derived Signalling in *dry2*

### CONTENTS

---

#### 7.1. INTRODUCTION

#### 7.2. RESULTS

Grafting analysis of long-distance signalling in *dry2*

Rejection of Wild-type and *dry2/sud1-9* Scions by *dry2* Rootstocks

Wild-type Rootstocks Do Not Complement *dig4* Mutant Shoot Defects

#### 7.3. DISCUSSION

The Nature of the Long-distance Signal Impaired in *dry2*

#### 7.4. MATERIALS AND METHODS





## 7.1. INTRODUCTION

In plants, the main mevalonate (MVA)-derived isoprenoid end products are sterols, which are integral components of the membrane and are involved in plant growth and developmental processes, the steroid hormone class of brassinosteroids, dolichol that is involved in protein glycosylation, and the prenyl groups used for protein prenylation and cytokinin biosynthesis (Benveniste, 2004; Phillips *et al.*, 2006; Schaller, 2010). A number of studies have shown the importance of a correct sterol composition in plants because of their roles in embryonic pattern formation (Jang *et al.*, 2000), cell division, elongation and polarity (Schrack *et al.*, 2000; Willemsen *et al.*, 2003; Men *et al.*, 2008), vascular patterning (Carland *et al.*, 2002), and Reactive Oxygen Species (ROS) production (Pose and Botella, 2009; Pose *et al.*, 2009). Still, little is known about the mechanisms and downstream targets by which isoprenoids in general, and sterols in particular, influence these processes (Clouse, 2002; Boutte and Grebe, 2009).

In plants, the squalene epoxidases (SQEs) catalyze the conversion of squalene, the precursor of essential MVA-derived isoprenoids such as sterols, brassinosteroids, and cyclic triterpenoids, to 2,3-oxidosqualene (Rasbery *et al.*, 2007; Pose *et al.*, 2009; Schaller, 2010). *Arabidopsis* contains six putative SQE isoforms identified based on sequence homology, being SQE1, which is annotated as drought hypersensitive 2/squalene epoxidase 1 (*DRY2/SQE1*), the main functionally characterized enzyme (Rasbery *et al.*, 2007; Pose *et al.*, 2009). In *Arabidopsis*, *DRY2/SQE1* function is required for cell elongation, root epidermal cell polarity, polar root-hair tip growth, and the stomata response to drought stress, as demonstrated by the identification of the extremely drought sensitive mutant *dry2* (Pose *et al.*, 2009). Moreover, genetic, molecular, and biochemical analyses of the hypomorphic *dry2* allele allowed the identification and characterization of physiological processes regulated by products of the MVA pathway that otherwise would be concealed. For instance, previous studies using *dry2* suggest that the root developmental phenotypes observed in *dry2* cannot be explained simply by depletion of bulk sterols but rather by alterations in the ROS signaling pathway and the increase of 3-hydroxy-3-methylglutaryl coenzyme A reductase (HMGR) activity (Pose *et al.*, 2009). Thus, a different and comprehensive approach is required to investigate the putative role of an MVA product in plant long-distance signalling.

To investigate a putative long-distance MVA signal involved in plant development, the present study concerned *Arabidopsis* micro-grafting studies. Among the different types of grafting unions, two plants can be connected between the *scion* (the shoot of one of the plants) and the

*rootstock* (the root from the other plant). With this grafting technique, native sterol biosynthesis genes expressed under normal regulatory mechanisms can be used, typically in one grafting partner, while the other partner carries a mutation. Thus, signal source and site of action (shoot or root) can be readily deduced (Turnbull *et al.*, 2002). It is important to precise that in Arabidopsis seedling grafts, the rootstock comprises not only root tissues but also a section of the hypocotyl. This hypocotyl section needs to be preserved in the rootstock in order for the graft union to be performed, and therefore should be considered as a rootstock source tissue.

## 7.2. RESULTS

### Grafting analysis of long-distance signalling in *dry2*

Based on the previous mass spectral analysis of sterols from *Ler*, *dry2* and *dry2/sud9*, we hypothesized that *dry2* is not affected in bulk sterols but in an isoprenoid-derived signalling component (Chapter 1, Table 1.1) (Pose, 2008). Previous chemical analyses also indicated that *dry2* was mainly affected in roots but not in shoots (Pose *et al.*, 2009). In order to investigate long-distance signalling and the root-to-shoot relationship, Arabidopsis seedling grafting unions were performed between: (1) *dry2* scion and *Ler* rootstock, (2) *dry2* scion and *dry2* rootstock, and (3) *Ler* scion and *Ler* rootstock (Figure 7.1A). As expected, after recovering, control grafted seedlings (*dry2* scion onto *dry2* rootstock and *Ler* scion onto *Ler* rootstock) resumed the typical development of *dry2* and *Ler* plants, respectively. Interestingly, *dry2* shoots presented an apparent wild-type phenotype when grafted onto *Ler* rootstock (Figure 7.1A).

To confirm the scion and rootstock genotypes, genomic DNA samples from shoot and root tissues of the grafted plants were sequenced. The sequencing results confirmed that *dry2* tissues carried the expected point mutation (G→A nucleotide substitution) in the 4<sup>th</sup> exon of the *At1g58440* gene (Figure 7.1Ac), which is annotated as *DRY2/SQE1*, resulting in the substitution of a conserved glycine by an arginine and therefore causing the *dry2* phenotypes.

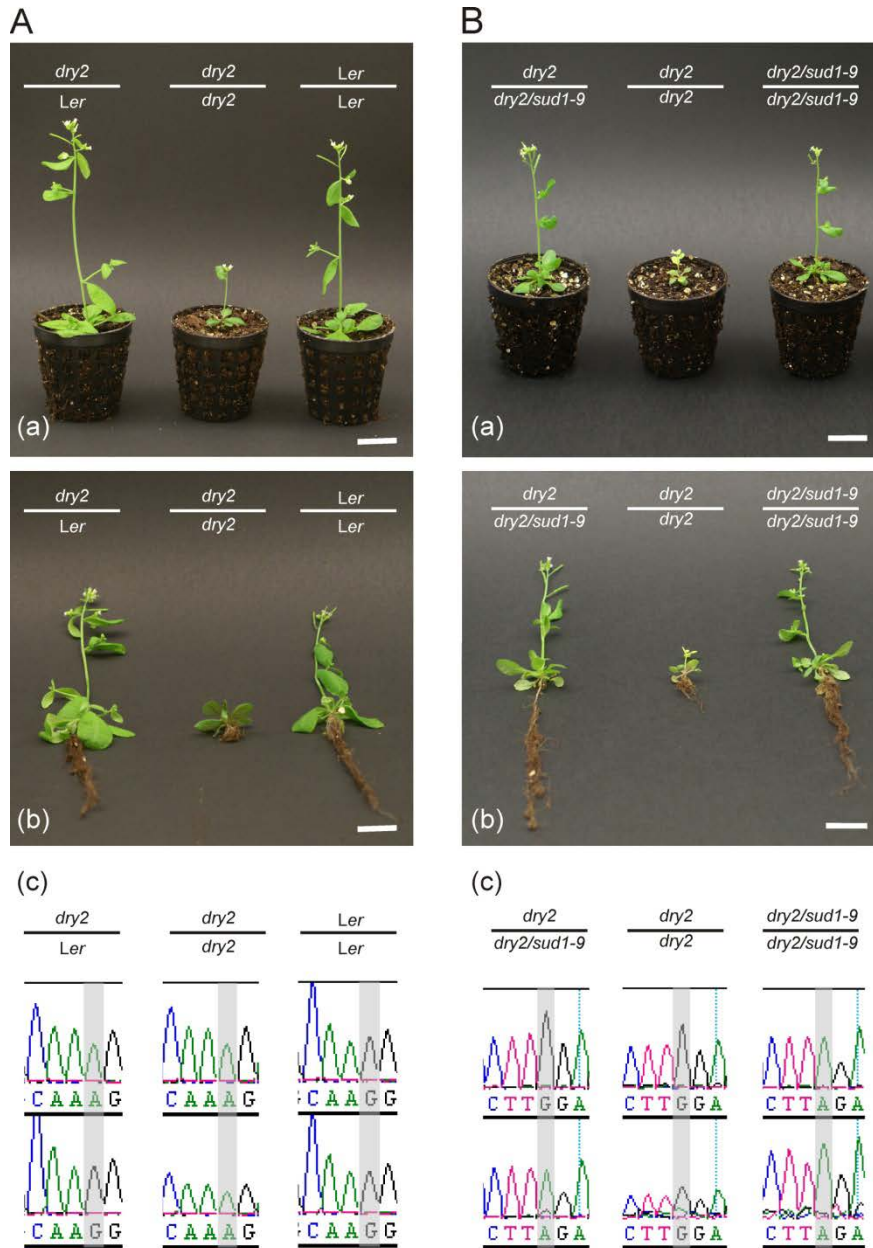


**Figure 7.1 – Suppression of *dry2* Shoot Defects by Long-distance Signalling**

**(A)** *dry2* shoot (scion) recovers the wild-type phenotype when grafted onto wild-type *Ler* rootstock. Seedlings were grown for five days in half-strength MS medium and then *dry2* scions were grafted onto wild-type *Ler* rootstocks. Grafts performed using *dry2* or *Ler* seedlings as scion and rootstock was used as control. Seedlings were transferred to soil nine days after grafting and representative plants were photographed after three weeks of growth in pot **(a)**, with soil removed to evidence the root phenotype **(b)**. Scale bar: 2 cm. The photographed plants are representative of two independent experiments with a total of 30 grafted plants per each graft combination represented. Genomic DNA samples from shoot and root tissues of the grafted plants were sequenced to confirm the genotype **(c)**. The nucleotide affected by a point mutation in *dry2* is highlighted in gray **(c)**.

**(B)** *dry2* shoot (scion) recovers the wild-type phenotype when grafted on *dry2/sud1-9* rootstock. Seedlings were grown for nine days in half-strength MS medium and then *dry2* scions were grafted onto *dry2/sud1-9* rootstocks. Grafts performed using *dry2* or *dry2/sud1-9* seedlings as scion and rootstock were used as control. Seedlings were transferred to soil nine days after grafting and representative plants were photographed 2.5 weeks after growing in pot **(a)**, with soil removed to evidence the root phenotype **(b)**. Scale bar: 2 cm. The photographed plants are representative of 20 grafted plants per each graft combination represented. Genomic DNA samples from shoot and root tissues of the grafted plants were sequenced to confirm the genotype **(c)**. The nucleotide affected by a point mutation in *sud1-9* is highlighted in gray **(c)**. It was also confirmed that scion and rootstock from all grafted plants contained the *dry2* point mutation (data not shown).

Next, it was investigated whether the suppressor mutation present in the *dry2/sud1-9* rootstock complemented the *dry2* mutant shoot. For this, Arabidopsis seedling grafting unions were performed between: (1) *dry2* scion and *dry2/sud1-9* rootstock, (2) *dry2* scion and *dry2* rootstock and (3) *dry2/sud1-9* scion and *dry2/sud1-9* rootstock (Figure 7.1B). As expected, after the recovering, control grafted seedlings (*dry2* scion onto *dry2* rootstock and *dry2/sud1-9* scion onto *dry2/sud1-9* rootstock) resumed their normal development and no phenotypic differences were observed on the grafted plants when compared with non-grafted plants. Interestingly, *dry2* shoot recovered the wild-type phenotype when grafted onto *dry2/sud1-9* rootstock (Figure 7.1B). This led to the hypothesis that the *dry2* roots but not *dry2/sud1-9* roots (or wild-type) lack a long-distance signal that impairs shoot development.

To confirm scion and rootstock genotypes, genomic DNA samples from shoot and root tissue of the grafted plants were sequenced. Results confirmed that scion and rootstock from all grafted plants contained the *dry2* point mutation in the 4<sup>th</sup> exon of the *DRY2/SQE1* gene (data not shown). Subsequently, it was also confirmed that *dry2/sud1-9* tissues carried the expected point mutation (G→A nucleotide substitution) in the 3<sup>rd</sup> exon of the *At4g34100* gene (Figure 7.1Bc), which is annotated in this study as *SUD1*, resulting in substitution of a conserved glycine by a glutamate and therefore causing the *dry2/sud1-9* phenotype.

### **Rejection of Wild-type and *dry2/sud1-9* Scions by *dry2* Rootstocks**

The effect of wild-type *Ler* scions in *dry2* rootstocks was also investigated. However, after recovering, grafted seedlings did not resume the normal development since *Ler* scions always rejected the graft union when using *dry2* as rootstocks. In many cases, *Ler* scions developed vigorous adventitious roots. A similar result was obtained when *dry2/sud1-9* scions were grafted onto *dry2* rootstocks (Figure 7.2). The genotypes of scions and rootstocks were confirmed by sequencing (data not shown). Vigorous adventitious rooting on scion indicates poor graft connections and probably a weak rootstock (Turnbull *et al.*, 2002). Since over 60 grafts were attempted, it is reasonable to conclude that a *dry2* defective root system hinders the utilization of *dry2* seedlings for rootstock of a grafting union.



**Figure 7.2 – Rejection of *dry2* Rootstock by *dry2/sud1-9* Scion**

Seedlings were grown for nine days in half-strength MS medium and then *dry2/sud1-9* scions were grafted onto *dry2* rootstocks. Grafts performed using *dry2* or *dry2/sud1-9* seedlings as scion and rootstock were used as control (not shown). Seedlings were transferred to soil nine days after grafting and representative plants were photographed eight days later. Arrows indicate location of graft union. The *dry2/sud1-9* scion developed vigorous adventitious roots from the shallow angled V shape created by the cutting performed to produce the scion. Scale bar: 0.5 cm. The photographed scion and rootstock are representative of a total of 60 grafted plants. Genomic DNA samples from shoot and root tissues of the grafted seedlings were sequenced to confirm the genotypes.

### Wild-type Rootstocks Do Not Complement *dig4* Mutant Shoot Defects

Additional information could be obtained by extending grafting experiments to other mutant lines of enzymes of the sterol pathway, thus helping to narrow down the number of candidates for the currently unrecognized long-distance signal impaired in the *dry2* mutant. However, most of these mutants are lethal due to multiple developmental defects and cannot be used for grafting experiments (Diener *et al.*, 2000; Jang *et al.*, 2000; Schrick *et al.*, 2000; Carland *et al.*, 2002; Schrick *et al.*, 2002; Souter *et al.*, 2002; Willemsen *et al.*, 2003; Kim *et al.*, 2005; Babiychuk *et al.*, 2008; Men *et al.*, 2008).

The *dig4* mutant was identified in a screening for Arabidopsis mutants that showed altered ABA responses (Liming Xiong, unpublished). The *dig4* mutant exhibited reduced responsiveness to ABA in closing stomata and had increased transpirational water loss. ABA is known to activate NADPH oxidase to produce H<sub>2</sub>O<sub>2</sub> in guard cells, triggering stomatal closure. However, *dig4* guard cells were impaired in ABA-induced H<sub>2</sub>O<sub>2</sub> production. Nonetheless, they were able to respond normally to H<sub>2</sub>O<sub>2</sub> in closing stomata, suggesting that the signaling pathway downstream of NADPH oxidase was unaffected in the mutant. These phenotypes are actually similar to those exhibited by *dry2*. *DIG4* encoded a  $\Delta$ 24-sterol-isomerase/reductase and was allelic to DW ARF1, previously shown to catalyze the biosynthesis of membrane sterols (Klahre *et al.*, 1998; Choe *et al.*, 1999). This study suggests that sterols may be important regulators of NADPH oxidase and thus may affect certain reactive oxygen species-dependent signaling in plants.

In the present study, it was investigated whether the *dig4* mutant (as previously *dry2*) was affected by a long-distance signal from roots. To investigate if the wild-type *DIG4/DWF1* gene present in the wild-type Col rootstock complements the *dig4* mutant shoot, Arabidopsis seedling grafting unions were performed between: (1) *dig4* scion and Col-0 rootstock, (2) *dig4* scion and *dig4* rootstock and (3) Col-0 scion and Col-0 rootstock (Figure 7.3). As expected, after the recovering time on plate, control grafted seedlings (*dig4* scion onto *dig4* rootstock and Col-0 scion onto Col-0 rootstock) resumed the normal development and no phenotypical differences were observed on the grafted plants when compared with non-grafted plants. Additionally, no phenotypic complementation of the *dig4* shoots when grafted onto Col-0 rootstock was observed (Figure 7.3), indicating in this case a cell-autonomous effect of *dig4* in shoot development.

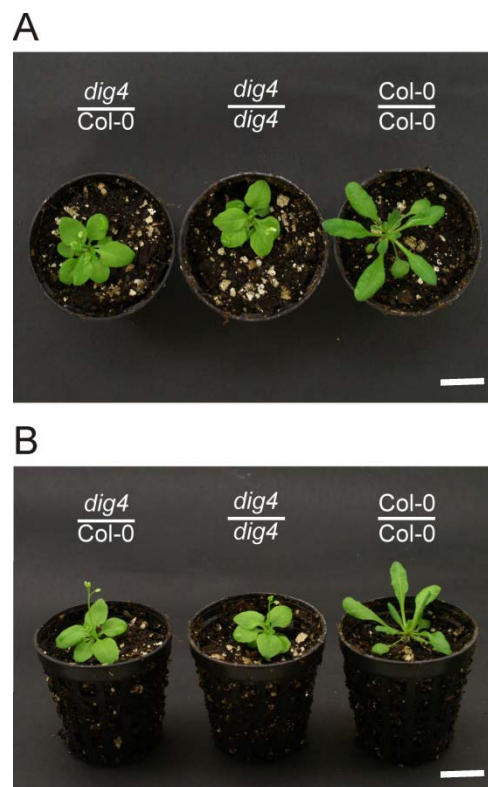


**Figure 7.3 – *dig4* Shoot Do Not Recover a Wild-type Phenotype When Grafted onto Wild-type Rootstocks**

**(A)** Shoot phenotype of *dig4* scion when grafted onto wild-type Col-0 rootstock. Seedlings were grown for eight days in half-strength MS medium and then *dig4* scions were grafted onto Col-0 rootstocks. Grafts performed using *dig4* or Col-0 seedlings as both scion and rootstock were used as control. Seedlings were transferred to soil seven days after grafting and representative plants were photographed 2.5 weeks later. Scale bar: 2 cm. The photographed plants are representative of 20 grafted plants per each graft combination. **(B)** As in (A) but with plants photographed from a different perspective to evidence shoot phenotype.

### 7.3. DISCUSSION

The most straight-forward result from the current grafting experiments was that a *dry2* scion can resume an apparent normal growth in a wild-type rootstock. This suggests that *dry2* shoots are mostly wild-type and the translocation of a signal produced in *dry2* roots is causing the developmental defects of *dry2* shoots. However, when grafted onto *dry2* rootstock, wild-type shoots form vigorous adventitious rooting on scion indicating poor graft connections. Because we have been unable to generate viable plants using wild-type as scion and *dry2* as rootstock despite many attempts, results suggest that *dry2* defective root system is weak rootstock that penalizes shoot growth and does not allow a viable plant to be produced by grafting a wild-type shoot onto a *dry2* root. The finding that a *dry2/sud1-9* rootstock behaves as a wild-type provides further support to the hypothesis that a signaling molecule accumulates in *dry2* roots that is absent in both wild-type and *dry2/sud1-9* roots. The observed phenotypes can be explained by other possibilities that are not mutually exclusive: (1) that a *dry2* defective root system architecture is unable to ensure the necessary nutrient uptake into a wild-type shoot; (2) the presence of a root mobile signal that can restore normal development of the *dry2* mutant shoot.

#### **The Nature of the Long-distance Signal Impaired in *dry2***

It is likely that the accumulation of pathway(s) intermediate(s), or derivative(s), upstream of *DRY2/SQE1* is the signal causing the *dry2* dramatic phenotypes. These signals most likely result from the reduction of *DRY2/SQE1* and the concomitant feed-back upregulation of HMGR activity. This is inferred by the findings that inhibition of HMGR with atorvastatin partially recovered *dry2* root defects and that exogenous application of MVA caused *dry2/sud1-9* and *dry2/sud1-22* (but not wild-type) to phenocopy *dry2* (Doblas, Amorim-Silva *et al.* Submitted). Additionally, as previously reported, the reduced activity of the *dry2* allele produced an important squalene accumulation and a 2- to 3-fold increase in HMGR activity, the rate-limiting enzyme of the MVA pathway, in roots but not in shoots. Interestingly, both squalene content and HMGR activity returned to near wild-type levels in *dry2/sud1-9* roots, which suggested that the observed upregulation of HMGR activity could be responsible for the *dry2* phenotypes (Doblas, Amorim-Silva *et al.* Submitted). However, it is unlikely that squalene is the signalling molecule because plants are able to deal with excess squalene, either endogenously produced or exogenously added, by storing it as remobilizable cytosolic lipid droplets without obvious phenotypic defects (Wentzinger *et al.*,

2002; Bouvier-Nave *et al.*, 2010). Interestingly, non-sterol MVA-derived compounds upstream of squalene have been related to the regulation of HMGR protein in response to changes in the levels of certain pathway products in mammals, yeast, and plants. Degradation of mammalian HMGR is accelerated by the addition of farnesol (Correll *et al.*, 1994; Meigs *et al.*, 1996), geranylgeraniol, and its precursor GGPP (Raikkonen *et al.*, 2010). GGPP is also known to regulate the degradation of HMGR2 protein in yeast (Garza *et al.*, 2009). Surprisingly, the effect of farnesol on plant HMGR activity seems to be different than in mammals. The addition of farnesol to tobacco BY-2 cells at concentrations below those causing acute toxicity had a drastic stimulatory effect on HMGR activity paralleled by activation of HMGR transcription and translation (Hemmerlin and Bach, 2000). Thus, it can be speculated that enhanced FPP-derived farnesol levels in the *dry2* background could play a role in both the observed activation of HMGR and the development of the *dry2* phenotypes, although the regulatory mechanism controlling HMGR activity in Arabidopsis and tobacco cells would operate at different levels. Although it was shown that squalene accumulates at high levels in *dry2*, and this accumulation is almost completely abolished in the suppressors, western blots analysis did not reveal differences in HMGR protein content between wild-type, *dry2*, *dry2/sud1-9* and *dry2/sud1-22* shoots and roots (Doblas, Amorim-Silva *et al.* Submitted). These results are consistent with previous observations showing that a pharmacological block of Arabidopsis squalene epoxidase activity with terbinafine leads to posttranslational up-regulation of HMGR activity (Nieto *et al.*, 2009) and, more importantly, exclude the possibility that SUD1 may have a direct effect on HMGR degradation resulting in differences in protein levels.

## 7.4. MATERIALS AND METHODS

### Plant Material

The *Arabidopsis thaliana* ecotypes Landsberg *erecta* (*Le*) and Columbia-0 (Col-0) were used as wild-type controls in the present study. Mutants used in this study that have been previously described: *dry2* (Pose *et al.*, 2009) and *dry2/sud9* (Pose, 2008). The *dig4* mutant was kindly supplied by Dr. Liming Xiong from the *Plant Stress Genomics Research Center of the King Abdullah University of Science and Technology Thuwal, Kingdom of Saudi Arabia*.



## Arabidopsis Grafting

Arabidopsis seeds were germinated in solid 0.5x MS medium containing 0.6% (w/v) phytigel (Sigma). Seedlings were grown vertically for 4 days and then transferred to a 0.22 µm sterile filter (Millipore) previously placed in contact with the medium. Seedlings were grown under long-day photoperiod and standard conditions. Three days later, seedlings were grafted in a flow chamber with the aid of a VWR stereomicroscope, a sterile razor blade (to cut), and a sterile tweezer (to move plants). The type of grafting was a wedge graft (Y shape) as described in Turnbull *et al.* (2002; 2010). Afterwards, plates were wet with sterile u.p. water, sealed with *Parafilm* and grown vertically for another seven days without moving the plates. Selected grafts were put in soil with a high content of water and covered with plastic to maintain a high humidity content. Three days later, the plastic cover was punctured to allow plants a slow but efficient adaptation to normal humidity conditions. After 3 days, the plastic was completely removed, and 3-4 days later plants started to be watered every two days. A total of 20-30 plants were grafted per each graft combination.

## Sequencing Analysis to Confirm Successful Grafting Unions

Shoot and root tissues were collected for each grafted plant and DNA extraction was performed to confirm successful grafting unions by sequencing analysis. Distinct methods were used to obtain genomic DNA from Shoot and root tissues of grafted plants. The Fast Genomic Extraction method was used to isolate genomic DNA from shoot tissue (Appendix I, section 1.1.1) and genomic DNA from root tissue was isolated using the ZR Plant/Seed DNA Kit (*Zymo Research*). Successful grafting unions were confirmed by PCR amplification and sequencing of the regions that contain the *dry2* and *sud1-9* mutations. PCR amplification and sequencing of the region containing the *dry2* mutation, using the primers displayed in Table 7.1, allowed to distinguish those plant tissues that were genetically *dry2* from those that were genetically *Ler*. PCR amplification and sequencing of the region containing the *sud1-9* mutation, using the primers displayed in Table 7.2, allowed to distinguish those plant tissues that were genetically *sud1-9* from those that were genetically *Ler*. Standard molecular biology methods, used in the present work, are presented in more detail in Appendix I.

**Table 7.1 – Primers Used to Specifically Amplify and Sequence the Region Containing the *dry2* Mutation**

Name	Sequence (5'→3')	Annealing temperature (°C)	Polymorphism	Amplification product size (bp)
At1g58440 F-Sec	ATTGTTCTCGGTTGGGTGAG	58	Substitution of glycine ( <i>Ler</i> ) by an arginine ( <i>dry2</i> )	432
At1g58440 R-Sec	ATTGTTCTCGGTTGGGTGAG			

**Table 7.2 – Primers Used to Specifically Amplify and Sequence the Region Containing the *sud1-9* Mutation**

Name	Sequence (5'→3')	Annealing temperature (°C)	Polymorphism	Amplification product size (bp)
At4g34100 – 2F	TTCTGCGGTTGAGTTTGTG	60	Substitution of glycine ( <i>Ler</i> ) by an arginine ( <i>sud1-9</i> )	1132
At4g34100 – 2R	TTCCAACAGTCAGTGGCTCA			



# Chapter 8

## Concluding Remarks and Future Perspectives

### CONTENTS

---

#### 8.1. CONCLUDING REMARKS

A Genetic Approach to Identify Regulators of the MVA Biosynthetic Pathway

#### 8.2. CONCLUDING REMARKS AND FUTURE PERSPECTIVES

Regulation of HMGR Activity by SUD1

Looking for the Identification of a New MVA-derived Signal Putatively Involved into Plant

Long-distance Signalling



## 8.1. CONCLUDING REMARKS

### A Genetic Approach to Identify Regulators of the MVA Biosynthetic Pathway

Mutations in the sterol biosynthetic *DRY2/SQE1* gene produce, in addition to extreme drought hypersensitivity, multiple developmental defects. In contrast to null alleles of *SQE1* such as *SQE1-3*, the hypomorphic *DRY2/SQE1-5* allele is fully fertile, being a useful tool to further investigations. As a way to find new components regulating lipid biosynthesis or signalling in plants a genetic screening for suppressors of *dry2* was performed (Pose, 2008). In the present study, detailed phenotypic, bioinformatic and genetic analyses of several of these suppressors was performed. Here, it is shown that all mutations affect the *At4g34100* gene that likely encodes the E3 ubiquitin ligase ortholog to the yeast Doa10 and mammalian TEB4 proteins involved in the ERAD-C pathway. By using biochemical and molecular approaches, it was revealed that the mechanism by which mutations in *SUD1* recovers the defects of *dry2* is through reverting the activity of HMGR to wild-type levels (Doblas, Amorim-Silva *et al.*, submitted).

## 8.2. CONCLUDING REMARKS AND FUTURE PERSPECTIVES

### Regulation of HMGR Activity by SUD1

Most of the information of ERAD comes from yeast and mammals (Carvalho *et al.*, 2006; Vembar and Brodsky, 2008; Carvalho *et al.*, 2010; Smith *et al.*, 2011). The HRD pathway is involved in the degradation of misfolded ER-luminal and intramembrane domains. The finding that feedback regulation of sterol synthesis in mammalian cells uses the ERAD machinery (Hampton, 2002) illustrates co-option of the basic quality control mechanism for regulatory processes and reveals potential functions in cell-to-cell signalling. In the last few years several reports are shedding light into the role of ERAD in plants. Thus, the ERAD-HRD pathway has been described to be important in the regulation of MLO and BRI proteins and has been defined as important for plant responses to environmental stress (Muller *et al.*, 2005; Liu *et al.*, 2011; Su *et al.*, 2011; Cui *et al.*, 2012).

In yeast, proteins with misfolded cytosolic domains are degraded rapidly and require the ubiquitin ligase Doa10 protein (Swanson *et al.*, 2001). Doa10 has broad substrate specificity, encompassing membrane proteins as well as soluble cytosolic and nuclear proteins and even exhibits some functional overlap with Hrd1 (Hitchcock *et al.*, 2003; Gnann *et al.*, 2004). However, Doa10 or TEB4 have not a reported role in HMGR regulation. In plants, several evidences indicated that SUD1 positively regulates HMGR activity in the presence of a likely isoprenoid or isoprenoid-derived molecule (Doblas, Amorim-Silva *et al.*, submitted). Though, SUD1 does not exert its function through controlling HMGR protein levels (Doblas, Amorim-Silva *et al.*, submitted). Because SUD1 encodes an E3 ubiquitin ligase the most likely explanation is that a negative regulator of HMGR is being degraded in a SUD1-dependent way in *dry2*. Loss of SUD1 function would impair the degradation of this negative regulator, leading to recovery of HMGR activity to wild-type levels. It has been proposed that the major changes in HMGR activity in plants would be determined at the transcriptional level, whereas the post-translational control would allow a finer and faster adjustment (Chappell, 1995). Whereas transcriptional modulation of HMGR has been demonstrated in many plant systems, evidence of regulatory mechanisms controlling HMGR activity at the post-translational level is much less known. Metabolic perturbation by enhancing or depleting the flux through the sterol pathway in Arabidopsis causes compensatory response in HMGR activity, without changes in transcript or protein levels (Nieto *et al.*, 2009). Recently, it has been shown that inactivation of the Arabidopsis WD protein PRL1 leads to reduced HMGR activity with no changes in transcript and protein levels (Flores-Pérez *et al.*, 2010). It has been suggested that this effect could be related to the ability of PRL1 to interact and to inhibit the activity of the Arabidopsis SNF1-related protein kinases (SnRK1) AKIN10 and AKIN11 (Bhalerao *et al.*, 1999), presumably targeting them for ubiquitination and proteasomal degradation (Lee *et al.*, 2008). Plant SnRK1 phosphorylates and inactivates HMGR (Dale *et al.*, 1995; Sugden *et al.*, 1999). Therefore, the loss of PRL1 function would result in increased SnRK1 activity and subsequently increased phosphorylation and decreased activity of HMGR. It has also been described that activity level of HMGR is negatively regulated by PP2A-mediated dephosphorylation (Leivar *et al.*, 2011). As a result, the negative regulators of Arabidopsis HMGR activity SnRK1 and PP2A are likely candidates mediating SUD1 regulation of HMGR activity. An alternative possibility is that SUD1 produce the direct monoubiquitination of HMGR, therefore increasing its activity, as reported for other proteins (Schnell and Hicke, 2003). Although this possibility seems unlikely, because for this to occur HMGR and SUD1 must be in the same compartment and HMGR localizes in vesicle-like structures

(Leivar *et al.*, 2005), it cannot be completely ruled out because these spherical structures are most likely derived from the ER (Leivar *et al.*, 2005) which would enable HMGR and SUD1 to directly interact. Although there is not available data for the subcellular localization of SUD1, other ERAD components, such HRD3 and UBC32, have been shown to have ER localization (Liu *et al.*, 2011; Cui *et al.*, 2012). Moreover, UBC32 has been shown to interact with the SUD1 homolog At4g32670 using luciferase complementation imaging assays (Cui *et al.*, 2012), suggesting that SUD1 will be also located in the ER.

Overall, by using a genetic, physiological, biochemical and molecular approaches it was shown that the E3 ubiquitin ligase SUD1 is a regulator of HMGR activity. Future research should help to clarify the mechanistic basis for the ERAD regulation of HMGR activity and what signals are implicated in this regulation.

### **Looking for the Identification of a New MVA-derived Signal Putatively Involved into Plant Long-distance Signalling**

An important feature of *dry2* mutation is the strong effect on ROS production. In *dry2* mutant, not only root hairs have an ectopic ROS production, but also the shoots show a significant lack of ROS, causing phenotypic defects in anisotropic growth and stomatal function (Pose, 2008). The results here presented show that ROS production are similar to wild-type in the *dry2* suppressors, indicating that the MVA-derived signal that accumulates in *dry2* is responsible for ROS regulation. The suppression of *dry2* root defects by the external application of ROS generators suggests that ROS-dependent signalling events are impaired in *dry2*. Given that, it is expected that the *dry2* *HYPER-AS* double mutant will allow a more comprehensive and sensitive approach to elucidate the mechanism of ROS distribution, that is impaired in the *dry2* mutant and restored into to the *dry2* suppressors. Additionally, the grafting results here presented show that Arabidopsis *DYR2/SQE1* gene, present in root or hypocotyls tissue, regulate a currently unrecognized signal capable of acting over long distances to regulate shoot development. Thus, implicates the *DYR2/SQE1* gene in regulation of transmissible signals involved in developmental and physiological processes. Additionally, it is demonstrated that this long-distance signal, lacking in *dry2* mutant, is restored in *dry2* mutant background by the *sud1-9* second-site mutation. Additional biochemical studies will allow confirming if *dry2* rootstock *sud1-9* scion grafted plants recover ROS production in shoots. However, further studies will be needed to uncover the nature of the long-distance signalling impaired in *dry2*.





# **Chapter 9**

## **Bibliographic References**



**BIBLIOGRAPHIC REFERENCES**

- Ahuja, I., de Vos, R.C., Bones, A.M., and Hall, R.D.** (2010). Plant molecular stress responses face climate change. *Trends Plant Sci* **15**, 664-674.
- Alonso, J.M., and Ecker, J.R.** (2006). Moving forward in reverse: genetic technologies to enable genome-wide phenomic screens in Arabidopsis. *Nat Rev Genet* **7**, 524-536.
- Apel, K., and Hirt, H.** (2004). Reactive oxygen species: metabolism, oxidative stress, and signal transduction. *Annu Rev Plant Biol* **55**, 373-399.
- Asada, K.** (2006). Production and scavenging of reactive oxygen species in chloroplasts and their functions. *Plant Physiol* **141**, 391-396.
- Ausubel, F.M., Brent, R., Kingston, R.E., Moore, D.D., Seidman, J.G., Smith, J.A., and Struhl, K.** (1996). *Current Protocols in Molecular Biology*. (New York: Grenn Publishing Associates and Wiley InterScience).
- Azevedo, H., Silva-Correia, J., Oliveira, J., Laranjeira, S., Barbeta, C., Amorim-Silva, V., Botella, M.A., Lino-Neto, T., and Tavares, R.M.** (2011). A strategy for the identification of new abiotic stress determinants in Arabidopsis using web-based data mining and reverse genetics. *OMICS* **15**, 935-947.
- Babiychuk, E., Bouvier-Nave, P., Compagnon, V., Suzuki, M., Muranaka, T., Van Montagu, M., Kushnir, S., and Schaller, H.** (2008). Allelic mutant series reveal distinct functions for Arabidopsis cycloartenol synthase 1 in cell viability and plastid biogenesis. *Proc Natl Acad Sci U S A* **105**, 3163-3168.
- Baginsky, S., Hennig, L., Zimmermann, P., and Gruissem, W.** (2010). Gene expression analysis, proteomics, and network discovery. *Plant Physiol* **152**, 402-410.
- Bazirgan, O.A., Garza, R.M., and Hampton, R.Y.** (2006). Determinants of RING-E2 fidelity for Hrd1p, a membrane-anchored ubiquitin ligase. *J Biol Chem* **281**, 38989-39001.
- Beato, M., Herrlich, P., and Schutz, G.** (1995). Steroid hormone receptors: many actors in search of a plot. *Cell* **83**, 851-857.
- Belousov, V.V., Fradkov, A.F., Lukyanov, K.A., Staroverov, D.B., Shakhbazov, K.S., Terskikh, A.V., and Lukyanov, S.** (2006). Genetically encoded fluorescent indicator for intracellular hydrogen peroxide. *Nat Methods* **3**, 281-286.
- Bensinger, S.J., Bradley, M.N., Joseph, S.B., Zelcer, N., Janssen, E.M., Hausner, M.A., Shih, R., Parks, J.S., Edwards, P.A., Jamieson, B.D., and Tontonoz, P.** (2008). LXR signaling couples sterol metabolism to proliferation in the acquired immune response. *Cell* **134**, 97-111.
- Benveniste, P.** (2002). Sterol Metabolism. *The Arabidopsis Book*, e0004.
- Benveniste, P.** (2004). Biosynthesis and accumulation of sterols. *Annu Rev Plant Biol* **55**, 429-457.
- Bhalerao, R.P., Salchert, K., Bakó, L., Ökrész, L., Szabados, L., Muranaka, T., Machida, Y., Schell, J., and Koncz, C.** (1999). Regulatory interaction of PRL1 WD protein with Arabidopsis SNF1-like protein kinases. *Proc Natl Acad Sci U S A* **96**, 5322-5327.

- Bienert, G.P., Schjoerring, J.K., and Jahn, T.P.** (2006). Membrane transport of hydrogen peroxide. *Biochim Biophys Acta* **1758**, 994-1003.
- Bienert, G.P., Moller, A.L., Kristiansen, K.A., Schulz, A., Moller, I.M., Schjoerring, J.K., and Jahn, T.P.** (2007). Specific aquaporins facilitate the diffusion of hydrogen peroxide across membranes. *J Biol Chem* **282**, 1183-1192.
- Bischoff, F., Vahlkamp, L., Molendijk, A., and Palme, K.** (2000). Localization of AtROP4 and AtROP6 and interaction with the guanine nucleotide dissociation inhibitor AtRhoGDI1 from Arabidopsis. *Plant Mol Biol* **42**, 515-530.
- Borsani, O., Cuartero, J., Valpuesta, V., and Botella, M.A.** (2002). Tomato *tos1* mutation identifies a gene essential for osmotic tolerance and abscisic acid sensitivity. *Plant J* **32**, 905-914.
- Boutte, Y., and Grebe, M.** (2009). Cellular processes relying on sterol function in plants. *Curr Opin Plant Biol* **12**, 705-713.
- Bouvier-Nave, P., Berna, A., Noiriel, A., Compagnon, V., Carlsson, A.S., Banas, A., Stymne, S., and Schaller, H.** (2010). Involvement of the phospholipid sterol acyltransferase1 in plant sterol homeostasis and leaf senescence. *Plant Physiol* **152**, 107-119.
- Bowler, C., Slooten, L., Vandenbranden, S., De Rycke, R., Botterman, J., Sybesma, C., Van Montagu, M., and Inze, D.** (1991). Manganese superoxide dismutase can reduce cellular damage mediated by oxygen radicals in transgenic plants. *EMBO J* **10**, 1723-1732.
- Boyer, J.S.** (1982). Plant productivity and environment. *Science* **218**, 443-448.
- Buchanan, B.B., Gruissem, W., and Jones, R.L.** (2000). *Biochemistry & molecular biology of plants.* (Rockville, Md.: American Society of Plant Physiologists).
- Bullock, W.O., Fernandez, J.M., and Short, J.M.** (1987). XL1-Blue: A high efficiency plasmid transforming *recA* Escherichia coli strain with beta-galactosidase selection. *Biotechniques* **Vol. 5**, pp. 376-379.
- Campos, N., and Boronat, A.** (1995). Targeting and topology in the membrane of plant 3-hydroxy-3-methylglutaryl coenzyme A reductase. *Plant Cell* **7**, 2163-2174.
- Carland, F.M., Fujioka, S., Takatsuto, S., Yoshida, S., and Nelson, T.** (2002). The identification of CVP1 reveals a role for sterols in vascular patterning. *Plant Cell* **14**, 2045-2058.
- Carol, R.J., and Dolan, L.** (2006). The role of reactive oxygen species in cell growth: lessons from root hairs. *J Exp Bot* **57**, 1829-1834.
- Carol, R.J., Takeda, S., Linstead, P., Durrant, M.C., Kakesova, H., Derbyshire, P., Drea, S., Zarsky, V., and Dolan, L.** (2005). A RhoGDP dissociation inhibitor spatially regulates growth in root hair cells. *Nature* **438**, 1013-1016.
- Carvalho, P., Goder, V., and Rapoport, T.A.** (2006). Distinct ubiquitin-ligase complexes define convergent pathways for the degradation of ER proteins. *Cell* **126**, 361-373.
- Carvalho, P., Stanley, A.M., and Rapoport, T.A.** (2010). Retrotranslocation of a misfolded luminal ER protein by the ubiquitin-ligase Hrd1p. *Cell* **143**, 579-591.
- Chappell, J.** (1995). The Biochemistry and Molecular Biology of Isoprenoid Metabolism. *Plant Physiol* **107**, 1-6.

- Chau, V., Tobias, J.W., Bachmair, A., Marriott, D., Ecker, D.J., Gonda, D.K., and Varshavsky, A.** (1989). A multiubiquitin chain is confined to specific lysine in a targeted short-lived protein. *Science* **243**, 1576-1583.
- Choe, S., Dilkes, B.P., Gregory, B.D., Ross, A.S., Yuan, H., Noguchi, T., Fujioka, S., Takatsuto, S., Tanaka, A., Yoshida, S., Tax, F.E., and Feldmann, K.A.** (1999). The Arabidopsis dwarf1 mutant is defective in the conversion of 24-methylenecholesterol to campesterol in brassinosteroid biosynthesis. *Plant Physiol* **119**, 897-907.
- Clark, R.M., Schweikert, G., Toomajian, C., Ossowski, S., Zeller, G., Shinn, P., Warthmann, N., Hu, T.T., Fu, G., Hinds, D.A., Chen, H., Frazer, K.A., Huson, D.H., Scholkopf, B., Nordborg, M., Ratsch, G., Ecker, J.R., and Weigel, D.** (2007). Common sequence polymorphisms shaping genetic diversity in Arabidopsis thaliana. *Science* **317**, 338-342.
- Clough, S.J., and Bent, A.F.** (1998). Floral dip: a simplified method for Agrobacterium-mediated transformation of Arabidopsis thaliana. *Plant J* **16**, 735-743.
- Clouse, S.D.** (2002). Arabidopsis mutants reveal multiple roles for sterols in plant development. *Plant Cell* **14**, 1995-2000.
- Correll, C.C., Ng, L., and Edwards, P.A.** (1994). Identification of farnesol as the non-sterol derivative of mevalonic acid required for the accelerated degradation of 3-hydroxy-3-methylglutaryl-coenzyme A reductase. *J Biol Chem* **269**, 17390-17393.
- Costa, A., Drago, I., Behera, S., Zottini, M., Pizzo, P., Schroeder, J.I., Pozzan, T., and Lo Schiavo, F.** (2010). H2O2 in plant peroxisomes: an in vivo analysis uncovers a Ca(2+)-dependent scavenging system. *Plant J* **62**, 760-772.
- Cui, F., Liu, L., Zhao, Q., Zhang, Z., Li, Q., Lin, B., Wu, Y., Tang, S., and Xie, Q.** (2012). Arabidopsis Ubiquitin Conjugase UBC32 Is an ERAD Component That Functions in Brassinosteroid-Mediated Salt Stress Tolerance. *Plant Cell*.
- Curtis, M.D., and Grossniklaus, U.** (2003). A gateway cloning vector set for high-throughput functional analysis of genes in planta. *Plant Physiol* **133**, 462-469.
- Dale, S., Arró, M., Becerra, B., Morrice, N.G., Boronat, A., Hardie, D.G., and Ferrer, A.** (1995). Bacterial Expression of the Catalytic Domain of 3-Hydroxy-3-Methylglutaryl-CoA Reductase (Isoform HMGR1) from Arabidopsis thaliana, and Its Inactivation by Phosphorylation at Ser577 by Brassica oleracea 3-Hydroxy-3-Methylglutaryl-CoA Reductase Kinase. *European Journal of Biochemistry* **233**, 506-513.
- DeBose-Boyd, R.A.** (2008). Feedback regulation of cholesterol synthesis: sterol-accelerated ubiquitination and degradation of HMG CoA reductase. *Cell Res* **18**, 609-621.
- del Rio, L.A., Sandalio, L.M., Corpas, F.J., Palma, J.M., and Barroso, J.B.** (2006). Reactive oxygen species and reactive nitrogen species in peroxisomes. Production, scavenging, and role in cell signaling. *Plant Physiol* **141**, 330-335.
- Deng, M., and Hochstrasser, M.** (2006). Spatially regulated ubiquitin ligation by an ER/nuclear membrane ligase. *Nature* **443**, 827-831.
- Deshaies, R.J., and Joazeiro, C.A.** (2009). RING domain E3 ubiquitin ligases. *Annu Rev Biochem* **78**, 399-434.

- Diebold, B.A., and Bokoch, G.M.** (2001). Molecular basis for Rac2 regulation of phagocyte NADPH oxidase. *Nat Immunol* **2**, 211-215.
- Diekmann, D., Abo, A., Johnston, C., Segal, A.W., and Hall, A.** (1994). Interaction of Rac with p67phox and regulation of phagocytic NADPH oxidase activity. *Science* **265**, 531-533.
- Diener, A.C., Li, H., Zhou, W., Whoriskey, W.J., Nes, W.D., and Fink, G.R.** (2000). Sterol methyltransferase 1 controls the level of cholesterol in plants. *Plant Cell* **12**, 853-870.
- Edwards, P.A., and Ericsson, J.** (1999). Sterols and isoprenoids: signaling molecules derived from the cholesterol biosynthetic pathway. *Annu Rev Biochem* **68**, 157-185.
- Enjuto, M., Balcells, L., Campos, N., Caelles, C., Arro, M., and Boronat, A.** (1994). Arabidopsis thaliana contains two differentially expressed 3-hydroxy-3-methylglutaryl-CoA reductase genes, which encode microsomal forms of the enzyme. *Proc Natl Acad Sci U S A* **91**, 927-931.
- Eun, S.O., and Lee, Y.** (1997). Actin filaments of guard cells are reorganized in response to light and abscisic acid. *Plant Physiol* **115**, 1491-1498.
- Farese, R.V., Jr., and Herz, J.** (1998). Cholesterol metabolism and embryogenesis. *Trends Genet* **14**, 115-120.
- Feng, C.-P., and Mundy, J.** (2006). Gene Discovery and Functional Analyses in the Model Plant Arabidopsis. *Journal of Integrative Plant Biology* **48**, 5-14.
- Finger, A., Knop, M., and Wolf, D.H.** (1993). Analysis of two mutated vacuolar proteins reveals a degradation pathway in the endoplasmic reticulum or a related compartment of yeast. *Eur J Biochem* **218**, 565-574.
- Flores-Pérez, Ú., Pérez-Gil, J., Closa, M., Wright, L.P., Botella-Pavía, P., Phillips, M.A., Ferrer, A., Gershenzon, J., and Rodríguez-Concepción, M.** (2010). PLEIOTROPIC REGULATORY LOCUS 1 (PRL1) Integrates the Regulation of Sugar Responses with Isoprenoid Metabolism in Arabidopsis. *Molecular Plant* **3**, 101-112.
- Foreman, J., Demidchik, V., Bothwell, J.H., Mylona, P., Miedema, H., Torres, M.A., Linstead, P., Costa, S., Brownlee, C., Jones, J.D., Davies, J.M., and Dolan, L.** (2003). Reactive oxygen species produced by NADPH oxidase regulate plant cell growth. *Nature* **422**, 442-446.
- Fry, S.C.** (1998). Oxidative scission of plant cell wall polysaccharides by ascorbate-induced hydroxyl radicals. *Biochem J* **332 ( Pt 2)**, 507-515.
- Fryer, M.J., Oxborough, K., Mullineaux, P.M., and Baker, N.R.** (2002). Imaging of photo-oxidative stress responses in leaves. *J Exp Bot* **53**, 1249-1254.
- Gadjev, I., Vanderauwera, S., Gechev, T.S., Laloi, C., Minkov, I.N., Shulaev, V., Apel, K., Inze, D., Mittler, R., and Van Breusegem, F.** (2006). Transcriptomic footprints disclose specificity of reactive oxygen species signaling in Arabidopsis. *Plant Physiol* **141**, 436-445.
- Gao, X., Lu, F., Zhou, L., Dang, S., Sun, L., Li, X., Wang, J., and Shi, Y.** (2009). Structure and mechanism of an amino acid antiporter. *Science* **324**, 1565-1568.
- Gapper, C., and Dolan, L.** (2006). Control of plant development by reactive oxygen species. *Plant Physiol* **141**, 341-345.

- Gardner, R.G., Swarbrick, G.M., Bays, N.W., Cronin, S.R., Wilhovsky, S., Seelig, L., Kim, C., and Hampton, R.Y.** (2000). Endoplasmic reticulum degradation requires lumen to cytosol signaling. Transmembrane control of Hrd1p by Hrd3p. *J Cell Biol* **151**, 69-82.
- Garza, R.M., Tran, P.N., and Hampton, R.Y.** (2009). Geranylgeranyl pyrophosphate is a potent regulator of HRD-dependent 3-Hydroxy-3-methylglutaryl-CoA reductase degradation in yeast. *J Biol Chem* **284**, 35368-35380.
- Gendron, J.M., and Wang, Z.Y.** (2007). Multiple mechanisms modulate brassinosteroid signaling. *Curr Opin Plant Biol* **10**, 436-441.
- Gnann, A., Riordan, J.R., and Wolf, D.H.** (2004). Cystic fibrosis transmembrane conductance regulator degradation depends on the lectins Htm1p/EDEM and the Cdc48 protein complex in yeast. *Mol Biol Cell* **15**, 4125-4135.
- Godar, D.E.** (1999). UVA1 radiation triggers two different final apoptotic pathways. *J Invest Dermatol* **112**, 3-12.
- Goldstein, J.L., and Brown, M.S.** (1990). Regulation of the mevalonate pathway. *Nature* **343**, 425-430.
- Gondet, L., Bronner, R., and Benveniste, P.** (1994). Regulation of Sterol Content in Membranes by Subcellular Compartmentation of Steryl-Esters Accumulating in a Sterol-Overproducing Tobacco Mutant. *Plant Physiol* **105**, 509-518.
- Gonnet, G.H., Cohen, M.A., and Benner, S.A.** (1992). Exhaustive matching of the entire protein sequence database. *Science* **256**, 1443-1445.
- Griffith, M., and Gietz, R.D.** (2003). Escherichia coli endA deletion strain for use in two-hybrid shuttle vector selection. *Biotechniques* **35**, 272-274, 276, 278.
- Guthrie, C., and Fink, G.R.** (1991). Guide to Yeast Genetics and Molecular Biology. (San Diego: Academic Press).
- Haglund, K., Di Fiore, P.P., and Dikic, I.** (2003). Distinct monoubiquitin signals in receptor endocytosis. *Trends Biochem Sci* **28**, 598-603.
- Halliwell, B., and Gutteridge, J.M.C.** (1999). Free radicals in biology and medicine. (Oxford, New York: Clarendon Press; Oxford University Press).
- Hampton, R.Y.** (2002). ER-associated degradation in protein quality control and cellular regulation. *Curr Opin Cell Biol* **14**, 476-482.
- Hampton, R.Y., and Garza, R.M.** (2009). Protein quality control as a strategy for cellular regulation: lessons from ubiquitin-mediated regulation of the sterol pathway. *Chem Rev* **109**, 1561-1574.
- Hampton, R.Y., Gardner, R.G., and Rine, J.** (1996). Role of 26S proteasome and HRD genes in the degradation of 3-hydroxy-3-methylglutaryl-CoA reductase, an integral endoplasmic reticulum membrane protein. *Mol Biol Cell* **7**, 2029-2044.
- Harker, M., Holmberg, N., Clayton, J.C., Gibbard, C.L., Wallace, A.D., Rawlins, S., Hellyer, S.A., Lanot, A., and Safford, R.** (2003). Enhancement of seed phytosterol levels by expression of an N-terminal truncated *Hevea brasiliensis* (rubber tree) 3-hydroxy-3-methylglutaryl-CoA reductase. *Plant Biotechnol J* **1**, 113-121.

- Hartmann, M.-A.** (1998). Plant sterols and the membrane environment. *Trends in plant science* **3**, 170-175.
- Hassink, G., Kikkert, M., van Voorden, S., Lee, S.J., Spaapen, R., van Laar, T., Coleman, C.S., Barteel, E., Fruh, K., Chau, V., and Wiertz, E.** (2005). TEB4 is a C4HC3 RING finger-containing ubiquitin ligase of the endoplasmic reticulum. *Biochem J* **388**, 647-655.
- He, J.X., Fujioka, S., Li, T.C., Kang, S.G., Seto, H., Takatsuto, S., Yoshida, S., and Jang, J.C.** (2003). Sterols regulate development and gene expression in Arabidopsis. *Plant Physiol* **131**, 1258-1269.
- Hegde, R.S., and Ploegh, H.L.** (2010). Quality and quantity control at the endoplasmic reticulum. *Curr Opin Cell Biol* **22**, 437-446.
- Hemmerlin, A., and Bach, T.J.** (2000). Farnesol-induced cell death and stimulation of 3-hydroxy-3-methylglutaryl-coenzyme A reductase activity in tobacco cv bright yellow-2 cells. *Plant Physiol* **123**, 1257-1268.
- Hershko, A., and Ciechanover, A.** (1998). The ubiquitin system. *Annu Rev Biochem* **67**, 425-479.
- Hetherington, A.M., and Woodward, F.I.** (2003). The role of stomata in sensing and driving environmental change. *Nature* **424**, 901-908.
- Hicke, L., Schubert, H.L., and Hill, C.P.** (2005). Ubiquitin-binding domains. *Nat Rev Mol Cell Biol* **6**, 610-621.
- Hirsch, C., Gauss, R., Horn, S.C., Neuber, O., and Sommer, T.** (2009). The ubiquitylation machinery of the endoplasmic reticulum. *Nature* **458**, 453-460.
- Hitchcock, A.L., Auld, K., Gygi, S.P., and Silver, P.A.** (2003). A subset of membrane-associated proteins is ubiquitinated in response to mutations in the endoplasmic reticulum degradation machinery. *Proc Natl Acad Sci U S A* **100**, 12735-12740.
- Horton, R.F.** (1971). Stomatal opening: the role of abscisic acid. *Canadian Journal of Botany* **49**, 583-585.
- Hruz, T., Laule, O., Szabo, G., Wessendorp, F., Bleuler, S., Oertle, L., Widmayer, P., Gruissem, W., and Zimmermann, P.** (2008). Genevestigator v3: a reference expression database for the meta-analysis of transcriptomes. *Adv Bioinformatics* **2008**, 420747.
- Hunter, S., Apweiler, R., Attwood, T.K., Bairoch, A., Bateman, A., Binns, D., Bork, P., Das, U., Daugherty, L., Duquenne, L., Finn, R.D., Gough, J., Haft, D., Hulo, N., Kahn, D., Kelly, E., Laugraud, A., Letunic, I., Lonsdale, D., Lopez, R., Madera, M., Maslen, J., McAnulla, C., McDowall, J., Mistry, J., Mitchell, A., Mulder, N., Natale, D., Orengo, C., Quinn, A.F., Selengut, J.D., Sigrist, C.J., Thimma, M., Thomas, P.D., Valentin, F., Wilson, D., Wu, C.H., and Yeats, C.** (2009). InterPro: the integrative protein signature database. *Nucleic Acids Res* **37**, D211-215.
- Huyer, G., Piluek, W.F., Fansler, Z., Kreft, S.G., Hochstrasser, M., Brodsky, J.L., and Michaelis, S.** (2004). Distinct machinery is required in *Saccharomyces cerevisiae* for the endoplasmic reticulum-associated degradation of a multispanning membrane protein and a soluble luminal protein. *J Biol Chem* **279**, 38369-38378.



- Hwang, J.U., and Lee, Y.** (2001). Abscisic acid-induced actin reorganization in guard cells of dayflower is mediated by cytosolic calcium levels and by protein kinase and protein phosphatase activities. *Plant Physiol* **125**, 2120-2128.
- Ismail, N., and Ng, D.T.W.** (2006). Have you HRD? Understanding ERAD Is DOAble! *Cell* **126**, 237-239.
- Ito, H., Fukuda, Y., Murata, K., and Kimura, A.** (1983). Transformation of intact cells treated with alkali cations. *J. Bacteriol.* **153**, 163-168.
- Jabs, T., Dietrich, R.A., and Dangel, J.L.** (1996). Initiation of runaway cell death in an Arabidopsis mutant by extracellular superoxide. *Science* **273**, 1853-1856.
- Jander, G., Norris, S.R., Rounsley, S.D., Bush, D.F., Levin, I.M., and Last, R.L.** (2002). Arabidopsis map-based cloning in the post-genome era. *Plant Physiol* **129**, 440-450.
- Jang, J.C., Fujioka, S., Tasaka, M., Seto, H., Takatsuto, S., Ishii, A., Aida, M., Yoshida, S., and Sheen, J.** (2000). A critical role of sterols in embryonic patterning and meristem programming revealed by the fackel mutants of Arabidopsis thaliana. *Genes Dev* **14**, 1485-1497.
- Jarosch, E., Taxis, C., Volkwein, C., Bordallo, J., Finley, D., Wolf, D.H., and Sommer, T.** (2002). Protein dislocation from the ER requires polyubiquitination and the AAA-ATPase Cdc48. *Nat Cell Biol* **4**, 134-139.
- Jones, D.T.** (1999). Protein secondary structure prediction based on position-specific scoring matrices. *Journal of Molecular Biology* **292**, 195-202.
- Jones, D.T., Taylor, W.R., and Thornton, J.M.** (1992). The Rapid Generation of Mutation Data Matrices from Protein Sequences. *Comput Appl Biosci* **8**, 275-282.
- Jones, M.A., Shen, J.J., Fu, Y., Li, H., Yang, Z., and Grierson, C.S.** (2002). The Arabidopsis Rop2 GTPase is a positive regulator of both root hair initiation and tip growth. *Plant Cell* **14**, 763-776.
- Kamauchi, S., Nakatani, H., Nakano, C., and Urade, R.** (2005). Gene expression in response to endoplasmic reticulum stress in Arabidopsis thaliana. *FEBS J* **272**, 3461-3476.
- Keller, T., Damude, H.G., Werner, D., Doerner, P., Dixon, R.A., and Lamb, C.** (1998). A plant homolog of the neutrophil NADPH oxidase gp91phox subunit gene encodes a plasma membrane protein with Ca<sup>2+</sup> binding motifs. *Plant Cell* **10**, 255-266.
- Kim, H.B., Schaller, H., Goh, C.H., Kwon, M., Choe, S., An, C.S., Durst, F., Feldmann, K.A., and Feyereisen, R.** (2005). Arabidopsis cyp51 mutant shows postembryonic seedling lethality associated with lack of membrane integrity. *Plant Physiol* **138**, 2033-2047.
- Kirst, M.E., Meyer, D.J., Gibbon, B.C., Jung, R., and Boston, R.S.** (2005). Identification and characterization of endoplasmic reticulum-associated degradation proteins differentially affected by endoplasmic reticulum stress. *Plant Physiol* **138**, 218-231.
- Klahre, U., Noguchi, T., Fujioka, S., Takatsuto, S., Yokota, T., Nomura, T., Yoshida, S., and Chua, N.H.** (1998). The Arabidopsis DIMINUTO/DWARF1 gene encodes a protein involved in steroid synthesis. *Plant Cell* **10**, 1677-1690.
- Klotz, L.O., Kroncke, K.D., and Sies, H.** (2003). Singlet oxygen-induced signaling effects in mammalian cells. *Photochem Photobiol Sci* **2**, 88-94.

- Knop, M., Finger, A., Braun, T., Hellmuth, K., and Wolf, D.H.** (1996). Der1, a novel protein specifically required for endoplasmic reticulum degradation in yeast. *EMBO J* **15**, 753-763.
- Koiwa, H., Bressan, R.A., and Hasegawa, P.M.** (2006). Identification of plant stress-responsive determinants in Arabidopsis by large-scale forward genetic screens. *J Exp Bot* **57**, 1119-1128.
- Koncz, C., and Schell, J.** (1986). The promoter of TL-DNA gene 5 controls the tissue-specific expression of chimaeric genes carried by a novel type of Agrobacterium binary vector *Molecular and General Genetics MGG* **204**, 383-396.
- Koornneef, M., Alonso-Blanco, C., and Stam, P.** (2006). Genetic analysis. *Methods Mol Biol* **323**, 65-77.
- Kostova, Z., Tsai, Y.C., and Weissman, A.M.** (2007). Ubiquitin ligases, critical mediators of endoplasmic reticulum-associated degradation. *Semin Cell Dev Biol* **18**, 770-779.
- Kreft, S.G., and Hochstrasser, M.** (2011). An unusual transmembrane helix in the endoplasmic reticulum ubiquitin ligase Doa10 modulates degradation of its cognate E2 enzyme. *J Biol Chem* **286**, 20163-20174.
- Kreft, S.G., Wang, L., and Hochstrasser, M.** (2006). Membrane topology of the yeast endoplasmic reticulum-localized ubiquitin ligase Doa10 and comparison with its human ortholog TEB4 (MARCH-VI). *J Biol Chem* **281**, 4646-4653.
- Krogh, A., Larsson, B., von Heijne, G., and Sonnhammer, E.L.** (2001). Predicting transmembrane protein topology with a hidden Markov model: application to complete genomes. *J Mol Biol* **305**, 567-580.
- Kwak, J.M., Nguyen, V., and Schroeder, J.I.** (2006). The role of reactive oxygen species in hormonal responses. *Plant Physiol* **141**, 323-329.
- Kwak, J.M., Mori, I.C., Pei, Z.M., Leonhardt, N., Torres, M.A., Dangl, J.L., Bloom, R.E., Bodde, S., Jones, J.D., and Schroeder, J.I.** (2003). NADPH oxidase AtrbohD and AtrbohF genes function in ROS-dependent ABA signaling in Arabidopsis. *EMBO J* **22**, 2623-2633.
- Laloi, C., Apel, K., and Danon, A.** (2004). Reactive oxygen signalling: the latest news. *Curr Opin Plant Biol* **7**, 323-328.
- Laloi, C., Stachowiak, M., Pers-Kamczyc, E., Warzych, E., Murgia, I., and Apel, K.** (2007). Cross-talk between singlet oxygen- and hydrogen peroxide-dependent signaling of stress responses in Arabidopsis thaliana. *Proc Natl Acad Sci U S A* **104**, 672-677.
- Lambert, C.R., Stiel, H., Leupold, D., Lynch, M.C., and Kochevar, I.E.** (1996). Intensity-dependent enzyme photosensitization using 532 nm nanosecond laser pulses. *Photochem Photobiol* **63**, 154-160.
- Laranjeira, S.** (2011). Stress-related genes in *Arabidopsis thaliana*: Investigating the role of squalene epoxidases in sterol biosynthesis and *EGY3* as a putative plastidial heat stress determinant. Ph.D Thesis, Universidade do Minho, Braga, Portugal), pp. 256.
- Lee, J.H., Terzaghi, W., Gusmaroli, G., Charron, J.B., Yoon, H.J., Chen, H., He, Y.J., Xiong, Y., and Deng, X.W.** (2008). Characterization of Arabidopsis and rice DWD proteins and their roles as substrate receptors for CUL4-RING E3 ubiquitin ligases. *Plant Cell* **20**, 152-167.

- Lee, K.P., Kim, C., Landgraf, F., and Apel, K.** (2007). EXECUTER1- and EXECUTER2-dependent transfer of stress-related signals from the plastid to the nucleus of *Arabidopsis thaliana*. *Proc Natl Acad Sci U S A* **104**, 10270-10275.
- Lee, P.C., and Rodgers, M.A.** (1987). Laser flash photokinetic studies of rose bengal sensitized photodynamic interactions of nucleotides and DNA. *Photochem Photobiol* **45**, 79-86.
- Leivar, P., Antolin-Llovera, M., Ferrero, S., Closa, M., Arro, M., Ferrer, A., Boronat, A., and Campos, N.** (2011). Multilevel control of *Arabidopsis* 3-hydroxy-3-methylglutaryl coenzyme A reductase by protein phosphatase 2A. *Plant Cell* **23**, 1494-1511.
- Leivar, P., Gonzalez, V.M., Castel, S., Trelease, R.N., Lopez-Iglesias, C., Arro, M., Boronat, A., Campos, N., Ferrer, A., and Fernandez-Busquets, X.** (2005). Subcellular localization of *Arabidopsis* 3-hydroxy-3-methylglutaryl-coenzyme A reductase. *Plant Physiol* **137**, 57-69.
- Lemaux, P.G.** (2008). Genetically Engineered Plants and Foods: A Scientist's Analysis of the Issues (Part I). *Annu Rev Plant Biol* **59**, 771-812.
- Lemaux, P.G.** (2009). Genetically engineered plants and foods: a scientist's analysis of the issues (part II). *Annu Rev Plant Biol* **60**, 511-559.
- Li, H., and Durbin, R.** (2009). Fast and accurate short read alignment with Burrows–Wheeler transform. *Bioinformatics* **25**, 1754-1760.
- Li, H., Handsaker, B., Wysoker, A., Fennell, T., Ruan, J., Homer, N., Marth, G., Abecasis, G., Durbin, R., and Subgroup, G.P.D.P.** (2009). The Sequence Alignment/Map format and SAMtools. *Bioinformatics* **25**, 2078-2079.
- Li, S., Assmann, S.M., and Albert, R.** (2006). Predicting essential components of signal transduction networks: a dynamic model of guard cell abscisic acid signaling. *PLoS Biol* **4**, e312.
- Liechti, R., and Farmer, E.E.** (2002). The jasmonate pathway. *Science* **296**, 1649-1650.
- Liszskay, A., van der Zalm, E., and Schopfer, P.** (2004). Production of reactive oxygen intermediates (O<sub>2</sub>(-), H<sub>2</sub>O<sub>2</sub>, and (·)OH) by maize roots and their role in wall loosening and elongation growth. *Plant Physiol* **136**, 3114-3123; discussion 3001.
- Liu, L., Cui, F., Li, Q., Yin, B., Zhang, H., Lin, B., Wu, Y., Xia, R., Tang, S., and Xie, Q.** (2011). The endoplasmic reticulum-associated degradation is necessary for plant salt tolerance. *Cell Res* **21**, 957-969.
- Loayza, D., Tam, A., Schmidt, W.K., and Michaelis, S.** (1998). Ste6p mutants defective in exit from the endoplasmic reticulum (ER) reveal aspects of an ER quality control pathway in *Saccharomyces cerevisiae*. *Mol Biol Cell* **9**, 2767-2784.
- Lumbreras, V., Campos, N., and Boronat, A.** (1995). The use of an alternative promoter in the *Arabidopsis thaliana* HMG1 gene generates an mRNA that encodes a novel 3-hydroxy-3-methylglutaryl coenzyme A reductase isoform with an extended N-terminal region. *The Plant Journal* **8**, 541-549.
- Ma, Q.Q., Wang, W., Li, Y.H., Li, D.Q., and Zou, Q.** (2006). Alleviation of photoinhibition in drought-stressed wheat (*Triticum aestivum*) by foliar-applied glycinebetaine. *J Plant Physiol* **163**, 165-175.

- Mandart, E., Dufour, M.E., and Lacroute, F.** (1994). Inactivation of SSM4, a new *Saccharomyces cerevisiae* gene, suppresses mRNA instability due to rna14 mutations. *Mol Gen Genet* **245**, 323-333.
- Manzano, D., Fernandez-Busquets, X., Schaller, H., Gonzalez, V., Boronat, A., Arro, M., and Ferrer, A.** (2004). The metabolic imbalance underlying lesion formation in *Arabidopsis thaliana* overexpressing farnesyl diphosphate synthase (isoform 1S) leads to oxidative stress and is triggered by the developmental decline of endogenous HMGR activity. *Planta* **219**, 982-992.
- Marino, D., Dunand, C., Puppo, A., and Pauly, N.** (2012). A burst of plant NADPH oxidases. *Trends in plant science* **17**, 9-15.
- Martinez, I.M., and Chrispeels, M.J.** (2003). Genomic analysis of the unfolded protein response in *Arabidopsis* shows its connection to important cellular processes. *Plant Cell* **15**, 561-576.
- MASC Report.** (2011). The Multinational Coordinated *Arabidopsis thaliana* Functional Genomics Project. In *Annual Report*.
- McAinsh, B.H.M.R.C.A.M.** (1990). Abscisic acid-induced elevation of guard cell cytosolic Ca<sup>2+</sup> precedes stomatal closure. *Nature* **343**, 186-188.
- Meigs, T.E., Roseman, D.S., and Simoni, R.D.** (1996). Regulation of 3-hydroxy-3-methylglutaryl-coenzyme A reductase degradation by the nonsterol mevalonate metabolite farnesol in vivo. *J Biol Chem* **271**, 7916-7922.
- Melen, K., Krogh, A., and von Heijne, G.** (2003). Reliability measures for membrane protein topology prediction algorithms. *J Mol Biol* **327**, 735-744.
- Men, S., Boutte, Y., Ikeda, Y., Li, X., Palme, K., Stierhof, Y.D., Hartmann, M.A., Moritz, T., and Grebe, M.** (2008). Sterol-dependent endocytosis mediates post-cytokinetic acquisition of PIN2 auxin efflux carrier polarity. *Nat Cell Biol* **10**, 237-244.
- Miller, G., Schlauch, K., Tam, R., Cortes, D., Torres, M.A., Shulaev, V., Dangl, J.L., and Mittler, R.** (2009). The plant NADPH oxidase RBOHD mediates rapid systemic signaling in response to diverse stimuli. *Sci Signal* **2**, ra45.
- Mittler, R.** (2002). Oxidative stress, antioxidants and stress tolerance. *Trends Plant Sci* **7**, 405-410.
- Mittler, R.** (2006). Abiotic stress, the field environment and stress combination. *Trends Plant Sci* **11**, 15-19.
- Mittler, R., and Blumwald, E.** (2010). Genetic engineering for modern agriculture: challenges and perspectives. *Annu Rev Plant Biol* **61**, 443-462.
- Mittler, R., Vanderauwera, S., Gollery, M., and Van Breusegem, F.** (2004). Reactive oxygen gene network of plants. *Trends Plant Sci* **9**, 490-498.
- Mittler, R., Vanderauwera, S., Suzuki, N., Miller, G., Tognetti, V.B., Vandepoele, K., Gollery, M., Shulaev, V., and Van Breusegem, F.** (2011). ROS signaling: the new wave? *Trends Plant Sci* **16**, 300-309.
- Molendijk, A.J., Bischoff, F., Rajendrakumar, C.S., Friml, J., Braun, M., Gilroy, S., and Palme, K.** (2001). *Arabidopsis thaliana* Rop GTPases are localized to tips of root hairs and control polar growth. *EMBO J* **20**, 2779-2788.

- Moller, I.M.** (2001). PLANT MITOCHONDRIA AND OXIDATIVE STRESS: Electron Transport, NADPH Turnover, and Metabolism of Reactive Oxygen Species. *Annu Rev Plant Physiol Plant Mol Biol* **52**, 561-591.
- Moller, I.M., Jensen, P.E., and Hansson, A.** (2007). Oxidative modifications to cellular components in plants. *Annu Rev Plant Biol* **58**, 459-481.
- Moller, S., Croning, M.D., and Apweiler, R.** (2001). Evaluation of methods for the prediction of membrane spanning regions. *Bioinformatics* **17**, 646-653.
- Moon, J., Parry, G., and Estelle, M.** (2004). The ubiquitin-proteasome pathway and plant development. *Plant Cell* **16**, 3181-3195.
- Mori, I.C., and Schroeder, J.I.** (2004). Reactive oxygen species activation of plant Ca<sup>2+</sup> channels. A signaling mechanism in polar growth, hormone transduction, stress signaling, and hypothetically mechanotransduction. *Plant Physiol* **135**, 702-708.
- Mukhopadhyay, D., and Riezman, H.** (2007). Proteasome-independent functions of ubiquitin in endocytosis and signaling. *Science* **315**, 201-205.
- Muller, J., Piffanelli, P., Devoto, A., Miklis, M., Elliott, C., Ortmann, B., Schulze-Lefert, P., and Panstruga, R.** (2005). Conserved ERAD-like quality control of a plant polytopic membrane protein. *Plant Cell* **17**, 149-163.
- Ng, D.T., Spear, E.D., and Walter, P.** (2000). The unfolded protein response regulates multiple aspects of secretory and membrane protein biogenesis and endoplasmic reticulum quality control. *J Cell Biol* **150**, 77-88.
- Niethammer, P., Grabher, C., Look, A.T., and Mitchison, T.J.** (2009). A tissue-scale gradient of hydrogen peroxide mediates rapid wound detection in zebrafish. *Nature* **459**, 996-999.
- Nieto, B., Fores, O., Arro, M., and Ferrer, A.** (2009). Arabidopsis 3-hydroxy-3-methylglutaryl-CoA reductase is regulated at the post-translational level in response to alterations of the sphingolipid and the sterol biosynthetic pathways. *Phytochemistry* **70**, 53-59.
- Noctor, G., and Foyer, C.H.** (1998). ASCORBATE AND GLUTATHIONE: Keeping Active Oxygen Under Control. *Annu Rev Plant Physiol Plant Mol Biol* **49**, 249-279.
- O'Brien, M., Chantha, S.C., Rahier, A., and Matton, D.P.** (2005). Lipid signaling in plants. Cloning and expression analysis of the obtusifoliol 14 $\alpha$ -demethylase from *Solanum chacoense* Bitt., a pollination- and fertilization-induced gene with both obtusifoliol and lanosterol demethylase activity. *Plant Physiol* **139**, 734-749.
- O'Brien, P.J.** (1991). Molecular mechanisms of quinone cytotoxicity. *Chem Biol Interact* **80**, 1-41.
- Ohyama, K., Suzuki, M., Masuda, K., Yoshida, S., and Muranaka, T.** (2007). Chemical phenotypes of the hmg1 and hmg2 mutants of *Arabidopsis* demonstrate the in-planta role of HMG-CoA reductase in triterpene biosynthesis. *Chem Pharm Bull (Tokyo)* **55**, 1518-1521.
- Oliveros, J.C.** (2007). FIESTA Viewer: Gene Expression data handling made easy.

- op den Camp, R.G., Przybyla, D., Ochsenbein, C., Laloi, C., Kim, C., Danon, A., Wagner, D., Hideg, E., Gobel, C., Feussner, I., Nater, M., and Apel, K.** (2003). Rapid induction of distinct stress responses after the release of singlet oxygen in *Arabidopsis*. *Plant Cell* **15**, 2320-2332.
- Orozco-Cardenas, M., and Ryan, C.A.** (1999). Hydrogen peroxide is generated systemically in plant leaves by wounding and systemin via the octadecanoid pathway. *Proc Natl Acad Sci U S A* **96**, 6553-6557.
- Ossowski, S., Schneeberger, K., Clark, R.M., Lanz, C., Warthmann, N., and Weigel, D.** (2008). Sequencing of natural strains of *Arabidopsis thaliana* with short reads. *Genome Res* **18**, 2024-2033.
- Palmer, A.E., and Dittmer, P.J.** (2010). SNAP-shots of hydrogen peroxide in cells. *Chem Biol* **17**, 318-319.
- Pei, Z.M., Murata, Y., Benning, G., Thomine, S., Klusener, B., Allen, G.J., Grill, E., and Schroeder, J.I.** (2000). Calcium channels activated by hydrogen peroxide mediate abscisic acid signalling in guard cells. *Nature* **406**, 731-734.
- Phillips, D.R., Rasbery, J.M., Bartel, B., and Matsuda, S.P.** (2006). Biosynthetic diversity in plant triterpene cyclization. *Curr Opin Plant Biol* **9**, 305-314.
- Pignocchi, C., and Foyer, C.H.** (2003). Apoplastic ascorbate metabolism and its role in the regulation of cell signalling. *Curr Opin Plant Biol* **6**, 379-389.
- Pirovano, W., Feenstra, K.A., and Heringa, J.** (2008). PRALINETM: a strategy for improved multiple alignment of transmembrane proteins. *Bioinformatics* **24**, 492-497.
- Pitzschke, A., and Hirt, H.** (2010). Bioinformatic and systems biology tools to generate testable models of signaling pathways and their targets. *Plant Physiol* **152**, 460-469.
- Plempner, R.K., Bordallo, J., Deak, P.M., Taxis, C., Hitt, R., and Wolf, D.H.** (1999). Genetic interactions of Hrd3p and Der3p/Hrd1p with Sec61p suggest a retro-translocation complex mediating protein transport for ER degradation. *J Cell Sci* **112 ( Pt 22)**, 4123-4134.
- Pose, D.** (2008). La caracterización del mutante de *Arabidopsis thaliana* *dry2/sqe1* revela un papel señalizador de los esteroides en el desarrollo de la planta y en la regulación de las especies reactivas de oxígeno. Ph. D thesis. University of Málaga, Spain, pp. 229.
- Pose, D., and Botella, M.A.** (2009). Analysis of the *Arabidopsis* *dry2/sqe1-5* mutant suggests a role for sterols in signaling. *Plant Signal Behav* **4**, 873-874.
- Pose, D., Castanedo, I., Borsani, O., Nieto, B., Rosado, A., Tacconat, L., Ferrer, A., Dolan, L., Valpuesta, V., and Botella, M.A.** (2009). Identification of the *Arabidopsis* *dry2/sqe1-5* mutant reveals a central role for sterols in drought tolerance and regulation of reactive oxygen species. *Plant J* **59**, 63-76.
- Pospisil, P., Arato, A., Krieger-Liszkay, A., and Rutherford, A.W.** (2004). Hydroxyl radical generation by photosystem II. *Biochemistry* **43**, 6783-6792.

- Proost, S., Van Bel, M., Sterck, L., Billiau, K., Van Parys, T., Van de Peer, Y., and Vandepoele, K.** (2009). PLAZA: a comparative genomics resource to study gene and genome evolution in plants. *Plant Cell* **21**, 3718-3731.
- Raikkonen, J., Monkkonen, H., Auriola, S., and Monkkonen, J.** (2010). Mevalonate pathway intermediates downregulate zoledronic acid-induced isopentenyl pyrophosphate and ATP analog formation in human breast cancer cells. *Biochem Pharmacol* **79**, 777-783.
- Rasbery, J.M., Shan, H., LeClair, R.J., Norman, M., Matsuda, S.P., and Bartel, B.** (2007). *Arabidopsis thaliana* squalene epoxidase 1 is essential for root and seed development. *J Biol Chem* **282**, 17002-17013.
- Ravid, T., Kreft, S.G., and Hochstrasser, M.** (2006). Membrane and soluble substrates of the Doa10 ubiquitin ligase are degraded by distinct pathways. *EMBO J* **25**, 533-543.
- Redman, J.C., Haas, B.J., Tanimoto, G., and Town, C.D.** (2004). Development and evaluation of an *Arabidopsis* whole genome Affymetrix probe array. *Plant J* **38**, 545-561.
- Robson, C.A., and Vanlerberghe, G.C.** (2002). Transgenic plant cells lacking mitochondrial alternative oxidase have increased susceptibility to mitochondria-dependent and -independent pathways of programmed cell death. *Plant Physiol* **129**, 1908-1920.
- Rodríguez-Concepción, M., Campos, N., Ferrer, A., and Boronat, A.** (2011). Biosynthesis of isoprenoid precursors in *Arabidopsis*. In *Isoprenoid Synthesis and Function in Plants and Microorganisms: New Concepts and Experimental Approaches* (T.J. Bach, M. Rohmer, and J. Gerhenson, eds (New York: Springer), in press.).
- Rodriguez, A.A., Grunberg, K.A., and Taleisnik, E.L.** (2002). Reactive oxygen species in the elongation zone of maize leaves are necessary for leaf extension. *Plant Physiol* **129**, 1627-1632.
- Romanos, M.A., Scorer, C.A., and Clare, J.J.** (1992). Foreign gene expression in yeast: a review. *Yeast* **8**, 423-488.
- Rouhier, N., and Jacquot, J.P.** (2002). Plant peroxiredoxins: alternative hydroperoxide scavenging enzymes. *Photosynth Res* **74**, 259-268.
- Sagi, M., and Fluhr, R.** (2001). Superoxide production by plant homologues of the gp91(phox) NADPH oxidase. Modulation of activity by calcium and by tobacco mosaic virus infection. *Plant Physiol* **126**, 1281-1290.
- Sagi, M., and Fluhr, R.** (2006). Production of reactive oxygen species by plant NADPH oxidases. *Plant Physiol* **141**, 336-340.
- Sagi, M., Davydov, O., Orazova, S., Yesbergenova, Z., Ophir, R., Stratmann, J.W., and Fluhr, R.** (2004). Plant respiratory burst oxidase homologs impinge on wound responsiveness and development in *Lycopersicon esculentum*. *Plant Cell* **16**, 616-628.
- Santner, A., and Estelle, M.** (2010). The ubiquitin-proteasome system regulates plant hormone signaling. *Plant J* **61**, 1029-1040.

- Schafer, U.A., Reed, D.W., Hunter, D.G., Yao, K., Weninger, A.M., Tsang, E.W., Reaney, M.J., MacKenzie, S.L., and Covello, P.S.** (1999). An example of intron junctional sliding in the gene families encoding squalene monooxygenase homologues in *Arabidopsis thaliana* and *Brassica napus*. *Plant Mol Biol* **39**, 721-728.
- Schaller, H.** (2003). The role of sterols in plant growth and development. *Prog Lipid Res* **42**, 163-175.
- Schaller, H.** (2004). New aspects of sterol biosynthesis in growth and development of higher plants. *Plant Physiol Biochem* **42**, 465-476.
- Schaller, H.** (2010). Sterol and steroid biosynthesis and metabolism in plants and microorganisms In *Comprehensive Natural Products II Chemistry and Biology*, L.L. Mander, H.-W. (eds), ed (Oxford: Elsevier), pp. 755-787.
- Schaller, H., Gondet, L., Maillot-Vernier, P., and Benveniste, P.** (1994). Sterol overproduction is the biochemical basis of resistance to a triazole in calli from a tobacco mutant. *Planta* **194**, 295-305.
- Schaller, H., Grausem, B., Benveniste, P., Chye, M.L., Tan, C.T., Song, Y.H., and Chua, N.H.** (1995). Expression of the *Hevea brasiliensis* (H.B.K.) Mull. Arg. 3-Hydroxy-3-Methylglutaryl-Coenzyme A Reductase 1 in Tobacco Results in Sterol Overproduction. *Plant Physiol* **109**, 761-770.
- Schnell, J.D., and Hicke, L.** (2003). Non-traditional Functions of Ubiquitin and Ubiquitin-binding Proteins. *Journal of Biological Chemistry* **278**, 35857-35860.
- Schopfer, P., Liskay, A., Bechtold, M., Frahy, G., and Wagner, A.** (2002). Evidence that hydroxyl radicals mediate auxin-induced extension growth. *Planta* **214**, 821-828.
- Schrack, K., Nguyen, D., Karlowski, W.M., and Mayer, K.F.** (2004). START lipid/sterol-binding domains are amplified in plants and are predominantly associated with homeodomain transcription factors. *Genome Biol* **5**, R41.
- Schrack, K., Mayer, U., Martin, G., Bellini, C., Kuhnt, C., Schmidt, J., and Jurgens, G.** (2002). Interactions between sterol biosynthesis genes in embryonic development of *Arabidopsis*. *Plant J* **31**, 61-73.
- Schrack, K., Mayer, U., Horrichs, A., Kuhnt, C., Bellini, C., Dangl, J., Schmidt, J., and Jurgens, G.** (2000). FACKEL is a sterol C-14 reductase required for organized cell division and expansion in *Arabidopsis* embryogenesis. *Genes Dev* **14**, 1471-1484.
- Schroeder, J.I., Kwak, J.M., and Allen, G.J.** (2001). Guard cell abscisic acid signalling and engineering drought hardiness in plants. *Nature* **410**, 327-330.
- Schubert, U., Anton, L.C., Gibbs, J., Norbury, C.C., Yewdell, J.W., and Bennink, J.R.** (2000). Rapid degradation of a large fraction of newly synthesized proteins by proteasomes. *Nature* **404**, 770-774.
- Schulze, S., Koster, S., Geldmacher, U., Terwisscha van Scheltinga, A.C., and Kuhlbrandt, W.** (2010). Structural basis of Na(+)-independent and cooperative substrate/product antiport in CaiT. *Nature* **467**, 233-236.
- Segal, A.W., and Abo, A.** (1993). The biochemical basis of the NADPH oxidase of phagocytes. *Trends Biochem Sci* **18**, 43-47.



- Serino, G., and Deng, X.W.** (2003). The COP9 signalosome: regulating plant development through the control of proteolysis. *Annu Rev Plant Biol* **54**, 165-182.
- Sikorski, R.S., and Hieter, P.** (1989). A system of shuttle vectors and yeast host strains designed for efficient manipulation of DNA in *Saccharomyces cerevisiae*. *Genetics* **122**, 19-27.
- Simossis, V.A., and Heringa, J.** (2005). PRALINE: a multiple sequence alignment toolbox that integrates homology-extended and secondary structure information. *Nucleic Acids Res* **33**, W289-294.
- Simossis, V.A., Kleinjung, J., and Heringa, J.** (2005). Homology-extended sequence alignment. *Nucleic Acids Res* **33**, 816-824.
- Smalle, J., and Vierstra, R.D.** (2004). The ubiquitin 26S proteasome proteolytic pathway. *Annu Rev Plant Biol* **55**, 555-590.
- Smith, M.H., Ploegh, H.L., and Weissman, J.S.** (2011). Road to ruin: targeting proteins for degradation in the endoplasmic reticulum. *Science* **334**, 1086-1090.
- Soares, N.C., Francisco, R., Vielba, J.M., Ricardo, C.P., and Jackson, P.A.** (2009). Associating wound-related changes in the apoplast proteome of *Medicago* with early steps in the ROS signal-transduction pathway. *J Proteome Res* **8**, 2298-2309.
- Sommer, T., and Jentsch, S.** (1993). A protein translocation defect linked to ubiquitin conjugation at the endoplasmic reticulum. *Nature* **365**, 176-179.
- Sonnhammer, E.L., von Heijne, G., and Krogh, A.** (1998). A hidden Markov model for predicting transmembrane helices in protein sequences. *Proc Int Conf Intell Syst Mol Biol* **6**, 175-182.
- Souter, M., Topping, J., Pullen, M., Friml, J., Palme, K., Hackett, R., Grierson, D., and Lindsey, K.** (2002). *hydra* Mutants of *Arabidopsis* are defective in sterol profiles and auxin and ethylene signaling. *Plant Cell* **14**, 1017-1031.
- Stermer, B.A., Bianchini, G.M., and Korth, K.L.** (1994). Regulation of HMG-CoA reductase activity in plants. *J Lipid Res* **35**, 1133-1140.
- Su, W., Liu, Y., Xia, Y., Hong, Z., and Li, J.** (2011). Conserved endoplasmic reticulum-associated degradation system to eliminate mutated receptor-like kinases in *Arabidopsis*. *Proc Natl Acad Sci U S A* **108**, 870-875.
- Sugden, C., Crawford, R.M., Halford, N.G., and Hardie, D.G.** (1999). Regulation of spinach SNF1-related (SnRK1) kinases by protein kinases and phosphatases is associated with phosphorylation of the T loop and is regulated by 5'-AMP. *The Plant Journal* **19**, 433-439.
- Suzuki, H., Achnine, L., Xu, R., Matsuda, S.P., and Dixon, R.A.** (2002). A genomics approach to the early stages of triterpene saponin biosynthesis in *Medicago truncatula*. *Plant J* **32**, 1033-1048.
- Suzuki, M., Nakagawa, S., Kamide, Y., Kobayashi, K., Ohyama, K., Hashinokuchi, H., Kiuchi, R., Saito, K., Muranaka, T., and Nagata, N.** (2009). Complete blockage of the mevalonate pathway results in male gametophyte lethality. *J Exp Bot* **60**, 2055-2064.
- Suzuki, M., Kamide, Y., Nagata, N., Seki, H., Ohyama, K., Kato, H., Masuda, K., Sato, S., Kato, T., Tabata, S., Yoshida, S., and Muranaka, T.** (2004). Loss of function of 3-hydroxy-3-methylglutaryl coenzyme A reductase 1 (HMG1) in *Arabidopsis* leads to dwarfing, early senescence and male sterility, and reduced sterol levels. *Plant J* **37**, 750-761.

- Swanson, R., Locher, M., and Hochstrasser, M.** (2001). A conserved ubiquitin ligase of the nuclear envelope/endoplasmic reticulum that functions in both ER-associated and Matalpha2 repressor degradation. *Genes Dev* **15**, 2660-2674.
- Swanson, S., and Gilroy, S.** (2010). ROS in plant development. *Physiol Plant* **138**, 384-392.
- Takeda, S., Gapper, C., Kaya, H., Bell, E., Kuchitsu, K., and Dolan, L.** (2008). Local positive feedback regulation determines cell shape in root hair cells. *Science* **319**, 1241-1244.
- Tamura, K., Peterson, D., Peterson, N., Stecher, G., Nei, M., and Kumar, S.** (2011). MEGA5: Molecular Evolutionary Genetics Analysis Using Maximum Likelihood, Evolutionary Distance, and Maximum Parsimony Methods. *Mol Biol Evol* **28**, 2731-2739.
- Taylor, J.S., and Raes, J.** (2004). Duplication and divergence: the evolution of new genes and old ideas. *Annu Rev Genet* **38**, 615-643.
- Thrower, J.S., Hoffman, L., Rechsteiner, M., and Pickart, C.M.** (2000). Recognition of the polyubiquitin proteolytic signal. *EMBO J* **19**, 94-102.
- Tomita, M., Irie, M., and Ukita, T.** (1969). Sensitized photooxidation of histidine and its derivatives. Products and mechanism of the reaction. *Biochemistry* **8**, 5149-5160.
- Torres, M.A., and Dangl, J.L.** (2005). Functions of the respiratory burst oxidase in biotic interactions, abiotic stress and development. *Curr Opin Plant Biol* **8**, 397-403.
- Torres, M.A., Onouchi, H., Hamada, S., Machida, C., Hammond-Kosack, K.E., and Jones, J.D.** (1998). Six Arabidopsis thaliana homologues of the human respiratory burst oxidase (gp91phox). *Plant J* **14**, 365-370.
- Travers, K.J., Patil, C.K., Wodicka, L., Lockhart, D.J., Weissman, J.S., and Walter, P.** (2000). Functional and genomic analyses reveal an essential coordination between the unfolded protein response and ER-associated degradation. *Cell* **101**, 249-258.
- Tsang, E.W., Bowler, C., Herouart, D., Van Camp, W., Villarroel, R., Genetello, C., Van Montagu, M., and Inze, D.** (1991). Differential regulation of superoxide dismutases in plants exposed to environmental stress. *Plant Cell* **3**, 783-792.
- Tucker, D.J., and Mansfield, T.A.** (1971). A simple bioassay for detecting "antitranspirant" activity of naturally occurring compounds such as abscisic acid. *Planta* **98**, 157-163.
- Turnbull, C.G.** (2010). Grafting as a Research Tool. In *Plant Developmental Biology - Methods in Molecular Biology*, e. L. Hennig and C. Köhler, ed (New York: Humana Press - Springer Protocols), pp. 11-26.
- Turnbull, C.G., Booker, J.P., and Leyser, H.M.** (2002). Micrografting techniques for testing long-distance signalling in Arabidopsis. *Plant J* **32**, 255-262.
- Vashist, S., and Ng, D.T.** (2004). Misfolded proteins are sorted by a sequential checkpoint mechanism of ER quality control. *J Cell Biol* **165**, 41-52.
- Vembar, S.S., and Brodsky, J.L.** (2008). One step at a time: endoplasmic reticulum-associated degradation. *Nat Rev Mol Cell Biol* **9**, 944-957.

- Vernoud, V., Horton, A.C., Yang, Z., and Nielsen, E.** (2003). Analysis of the small GTPase gene superfamily of Arabidopsis. *Plant Physiol* **131**, 1191-1208.
- Vert, G., Nemhauser, J.L., Geldner, N., Hong, F., and Chory, J.** (2005). Molecular mechanisms of steroid hormone signaling in plants. *Annu Rev Cell Dev Biol* **21**, 177-201.
- Vickers, C.E., Gershenzon, J., Lerdau, M.T., and Loreto, F.** (2009). A unified mechanism of action for volatile isoprenoids in plant abiotic stress. *Nat Chem Biol* **5**, 283-291.
- Vierstra, R.D.** (2003). The ubiquitin/26S proteasome pathway, the complex last chapter in the life of many plant proteins. *Trends Plant Sci* **8**, 135-142.
- Vierstra, R.D.** (2009). The ubiquitin-26S proteasome system at the nexus of plant biology. *Nat Rev Mol Cell Biol* **10**, 385-397.
- Vinocur, B., and Altman, A.** (2005). Recent advances in engineering plant tolerance to abiotic stress: achievements and limitations. *Curr Opin Biotechnol* **16**, 123-132.
- Wagner, D., Przybyla, D., Op den Camp, R., Kim, C., Landgraf, F., Lee, K.P., Wursch, M., Laloi, C., Nater, M., Hideg, E., and Apel, K.** (2004). The genetic basis of singlet oxygen-induced stress responses of Arabidopsis thaliana. *Science* **306**, 1183-1185.
- Walter, J., Urban, J., Volkwein, C., and Sommer, T.** (2001). Sec61p-independent degradation of the tail-anchored ER membrane protein Ubc6p. *EMBO J* **20**, 3124-3131.
- Wasternack, C.** (2007). Jasmonates: an update on biosynthesis, signal transduction and action in plant stress response, growth and development. *Ann Bot* **100**, 681-697.
- Wentzinger, L.F., Bach, T.J., and Hartmann, M.A.** (2002). Inhibition of squalene synthase and squalene epoxidase in tobacco cells triggers an up-regulation of 3-hydroxy-3-methylglutaryl coenzyme a reductase. *Plant Physiol* **130**, 334-346.
- Wilkinson, K.D.** (2005). The discovery of ubiquitin-dependent proteolysis. *Proc Natl Acad Sci U S A* **102**, 15280-15282.
- Willemsen, V., Friml, J., Grebe, M., van den Toorn, A., Palme, K., and Scheres, B.** (2003). Cell polarity and PIN protein positioning in Arabidopsis require STEROL METHYLTRANSFERASE1 function. *Plant Cell* **15**, 612-625.
- Winterbourn, C.C.** (2008). Reconciling the chemistry and biology of reactive oxygen species. *Nat Chem Biol* **4**, 278-286.
- Wong, H.L., Pinontoan, R., Hayashi, K., Tabata, R., Yaeno, T., Hasegawa, K., Kojima, C., Yoshioka, H., Iba, K., Kawasaki, T., and Shimamoto, K.** (2007). Regulation of rice NADPH oxidase by binding of Rac GTPase to its N-terminal extension. *Plant Cell* **19**, 4022-4034.
- Wymer, C.L., Bibikova, T.N., and Gilroy, S.** (1997). Cytoplasmic free calcium distributions during the development of root hairs of Arabidopsis thaliana. *Plant J* **12**, 427-439.
- Xiao, S., Dai, L., Liu, F., Wang, Z., Peng, W., and Xie, D.** (2004). COS1: an Arabidopsis coronatine insensitive1 suppressor essential for regulation of jasmonate-mediated plant defense and senescence. *Plant Cell* **16**, 1132-1142.

- Yamamoto, M., Kawanabe, M., Hayashi, Y., Endo, T., and Nishikawa, S.** (2010). A vacuolar carboxypeptidase mutant of *Arabidopsis thaliana* is degraded by the ERAD pathway independently of its N-glycan. *Biochem Biophys Res Commun* **393**, 384-389.
- Yamashita, A., Singh, S.K., Kawate, T., Jin, Y., and Gouaux, E.** (2005). Crystal structure of a bacterial homologue of Na<sup>+</sup>/Cl<sup>-</sup>-dependent neurotransmitter transporters. *Nature* **437**, 215-223.
- Yang, Z.** (2002). Small GTPases: versatile signaling switches in plants. *Plant Cell* **14 Suppl**, S375-388.
- Zhang, L., and Xing, D.** (2008). Methyl jasmonate induces production of reactive oxygen species and alterations in mitochondrial dynamics that precede photosynthetic dysfunction and subsequent cell death. *Plant Cell Physiol* **49**, 1092-1111.
- Zhang, Z., Lenk, A., Andersson, M.X., Gjetting, T., Pedersen, C., Nielsen, M.E., Newman, M.A., Hou, B.H., Somerville, S.C., and Thordal-Christensen, H.** (2008). A lesion-mimic syntaxin double mutant in *Arabidopsis* reveals novel complexity of pathogen defense signaling. *Mol Plant* **1**, 510-527.
- Zhu, J.K.** (2002). Salt and drought stress signal transduction in plants. *Annu Rev Plant Biol* **53**, 247-273.
- Zhuang, S., Demirs, J.T., and Kochevar, I.E.** (2000). p38 mitogen-activated protein kinase mediates bid cleavage, mitochondrial dysfunction, and caspase-3 activation during apoptosis induced by singlet oxygen but not by hydrogen peroxide. *J Biol Chem* **275**, 25939-25948.

# Appendixes

**APPENDIX I — STANDARD MOLECULAR BIOLOGY METHODS**

**APPENDIX II — OLIGONUCLEOTIDES USED FOR MAP-BASED CLONING**

**APPENDIX III — VECTORS Maps**



# APPENDIX I – STANDARD MOLECULAR BIOLOGY METHODS

## 1. NUCLEIC ACID METHODS

### 1.1. DNA Methods

#### 1.1.1. Oligonucleotide Design and Preparation

Oligonucleotides (primers) were designed with different softwares, namely *OLIGO Primer Analysis Software v6.0* (<http://oligo.net/>) or the *Primer3* online application (<http://frodo.wi.mit.edu/primer3/>) (Rozen and Skaletsky, 2000), with automatic estimation of the GC content, melting temperature, and primer-dimer/hairpin formation. Primer design generally took into consideration the following principles for each pair: optimal Tms, correct primer length, avoidance of primer-dimer and hairpin structures, optimisation of GC content (40-60%), presence of a GC clamp, estimation of optimal annealing temperature (Griffin and Griffin, 1994). Primers stocks were prepared by adding ddH<sub>2</sub>O to a final concentration of 100 µM according to the manufacturer's indication. Working aliquots were subsequently produced at 10 µM, for PCR amplification or sequencing purposes.

#### 1.1.2. Plant Genomic DNA Isolation

Different methods were used to obtain genomic DNA from *A. thaliana* tissues, depending on the nature of the tissue sample and the degree of purity needed: CTAB-based method, Fast DNA extraction method and *ZR Plant/Seed DNA Kit* (Zymo Research).

**CTAB method.** Leaf tissue was harvested from each plant to obtain high integrity and high purity genomic DNA with the CTAB extraction method (Doyle and Doyle, 1987). After having been harvested, the tissue was grinded with liquid nitrogen and subsequently added 700 µL of CTAB buffer, vortexed and incubated for 25 min at 65°C. Samples were centrifuged for 5 min at room temperature and 12000 *g*. The aqueous phase was recovered, precipitated with 1:1 vol of cold (-20°C) isopropanol and centrifuged for 20 min at room temperature and 12000 *g*. The pellet was washed with 300 µL of 70% (v/v) ethanol and centrifuged for 5 min at room temperature and 12000 *g*. The pellet was then dried for 10 min at 37°C, solubilised in 30 µL of 0.1x TE containing RNase A (100 µg mL<sup>-1</sup>), and incubated for 20 min at 37°C. Genomic DNA was kept for 24 h at 4°C to allow complete dissolution of the pellet and stored at -20°C.

---

**CTAB buffer:** 2% (w/v) CTAB; 1.4 M NaCl; 0.1 M Tris-HCl (pH 8.0); 0.02 M EDTA (pH 8.0); add 0.1% (v/v) β-mercaptoethanol before use.

**TE:** 10 mM Tris-HCl (pH 8.0); 1 mM EDTA.

---

**Fast DNA extraction method.** Leaf tissue was harvested from each plant to perform a rapid DNA extraction (Edwards *et al.*, 1991). After having been harvested, the tissue was transferred to a microtube and 400  $\mu$ L of extraction buffer were added prior to grinding the tissue with polypropylene pestles. Microtubes were centrifuged for 5 min at room temperature and 14000 rpm, and the supernatant was transferred to a new microtube containing 300  $\mu$ L of isopropanol. After another centrifugation for 5 min and 14000 rpm, the DNA-containing pellet was rinsed with 500  $\mu$ L of 70% (v/v) ethanol, and spinned down for 2 min. The pellet was air-dried and resuspended in 50-100  $\mu$ L of ultra-pure water.

---

**Extraction buffer:** 200 mM Tris-HCl pH 7.5; 250 mM NaCl; 25 mM EDTA; 0.5% (w/v) SDS.

---

**Root DNA extraction.** Genomic DNA from root tissue was isolated using the *ZR Plant/Seed DNA Kit* (Zymo Research).

### 1.1.3. Plasmid Isolation

Plasmid isolation was performed using the *Wizard Plus SV Minipreps DNA Purification System* (Promega) or *Quiagen Plasmid* (Quiagen) commercial kits, according to the manufacturer's instructions.

### 1.1.4. DNA Fragment Purification

DNA purification from agarose gels, PCR amplifications or endonuclease digestions was performed using the *Wizard SV Gel and PCR Clean-Up System* (Promega) or the *QIAprep Spin Miniprep Kit* (Quiagen) commercial kits, according to the manufacturer's instructions.

### 1.1.5. DNA Precipitation

DNA was added 1/10 volumes of 3 M NaAc pH 5.2 and 2 volumes of ice-cold absolute ethanol, and placed at -20°C for at least 1 hr. Following centrifugation during 5 min at high speeds (~13,000 rpm) at room temperature, the pellet was allowed to air-dry, prior to resuspension in 15  $\mu$ L ultra pure water.

### 1.1.6. DNA Digestion with Endonucleases

DNA digestion with restriction endonucleases was performed according to the procedures described by Sambrook and Russell (2001), and considering the manufacturer's instructions. Reactions were performed in a total volume of 20-50  $\mu$ L for 30 min to ON periods at 37°C. For plasmid linearization, reactions were added 1  $\mu$ L of Shrimp *Alkaline Phosphatase* (SAP) (Fermentas) to promote dephosphorylation of the 5'-phosphorylated ends of DNA, thus preventing re-ligation of the linearized plasmid DNA during cloning experiments. Endonucleases were heat inactivated according to their specification, or the reaction was purified as described in 1.1.6.



### 1.1.7. Amplification of DNA Fragments by Polymerase Chain Reaction (PCR)

Typically, PCR reactions were prepared in a 50  $\mu$ l volume as follows: DNA template (50 ng), Taq polymerase (1 U, 0.5  $\mu$ l), 10x buffer (5  $\mu$ l), 2.5 mM dNTPs (2  $\mu$ l), 2 mM MgCl<sub>2</sub> (4  $\mu$ l from a 25 mM stock), primer (3  $\mu$ l from a 10  $\mu$ M stock) and ddH<sub>2</sub>O (up to 50  $\mu$ l). The PCR reaction was carried out by sequentially performing denaturation (45 sec), annealing (45 sec) and extension (according to the size of the expectable fragments and the polymerase specifications) steps for each cycle of amplification. In a typical reaction, the DNA was denatured at 95°C, primers annealed at 50-70°C (annealing temperature determined experimentally by a PCR annealing gradient), and extension was carried out at 72°C or 68°C (according to manufacturer's specifications). Traditionally, 30-40 amplification cycles were needed. An initial denaturation and final extension steps (10 min each) were also included. For plant diagnostic PCR, DNA was extracted by the Fast DNA extraction method (see section 1.1.2) and 1  $\mu$ L of precipitated genomic DNA was resuspended in 50  $\mu$ L of ultra pure water to be used as template. For *E. coli* colony PCR and yeast colony PCR, one colony was used as template.

### 1.1.8. DNA Sequencing

Plasmid inserts were sequenced by STAB VIDA, Secugen or GATC Biotech services, using universal or purposefully designed primers.

### 1.1.9. Gateway Cloning

LR recombination reaction between *attL* (entry clone) and *attR* (destination vector) recombination sites was carried out to obtain the *attB* expression clones in the pMDC32 vector. The reaction was performed in a total volume of 10  $\mu$ L in 0.2 mL microtubes containing: 50 fmol of a Gateway destination vector (pMDC32), 50 fmol of an *attL*-entry clone (HyPer-As), 2  $\mu$ L of *LR Clonase II* (Invitrogen) and TE buffer (pH 8). Equal molarity was obtained as in the BP reaction. The mix was incubated for 18 h at 25°C. Subsequently, 1  $\mu$ L of Proteinase K (*LR clonase II kit*, Invitrogen) was added and the reaction incubated for 10 min at 37°C. An aliquot of 5  $\mu$ L was used to transform *E. coli* XL1-Blue/DH5 $\alpha$  competent cells. Cells were then plated onto LB agarised medium containing hygromycin (50  $\mu$ g mL<sup>-1</sup>). Colonies were used in a colony PCR with specific primers for the destination vectors, and positives ones were selected in kanamycin (50  $\mu$ g mL<sup>-1</sup>) prior to plasmid isolation and sequencing.

### 1.1.10. Subcloning of PCR Fragments into pGEM-T Easy

DNA fragments were subcloned into the pGEM-T Easy vector (Promega) following the manufacturer's instructions. Ligation of PCR products to pGEM-T Easy was performed by incubating 50 ng of pGEM-T Easy vector with purified PCR product (in a molar ratio of 1:3), 5  $\mu$ L of 2x Rapid Ligation Buffer, 1  $\mu$ L T4 DNA ligase, in a final volume of 10  $\mu$ L, for 1 h at room temperature. Subcloning of PCR fragments obtained with a proofreading polymerase included an adenylation step prior to the ligation reaction, allowing for the generation of the A-tail necessary for ligation to the T-overhangs of the pGEM-T vector. The DNA was adenylated by incubation with 0.25  $\mu$ L of non-proofreading Taq polymerase, 1  $\mu$ L of 10x *Taq Polymerase*

*Reaction Buffer* (Promega) and 0.2 mM of dATP in a total volume of 10  $\mu$ L. Following adenylation, samples were ligated to pGEM-T Easy as described.

An aliquot of the ligation reaction (5  $\mu$ L) was used to transform *E. coli* XL1-Blue/DH5 $\alpha$  cells, as described in section 2.1.2, and plated onto agar-solidified LB Ampicilin supplemented with X-Gal (40  $\mu$ g mL<sup>-1</sup>) and IPTG (50  $\mu$ g mL<sup>-1</sup>) for blue/white screening (cloning products interrupt proLacZ regulation of lacZ, generating white colonies).

#### **1.1.11. Cloning of PCR Fragments into a Vector**

Purified PCR products and isolated plasmids were digested with restriction enzymes that produced compatible DNA overhangs and purified once again to remove the restriction enzymes. Digested PCR fragments were ligated to the respective vector using the *Rapid DNA Dephos & Ligation Kit* (Roche Applied Science) according to the manufacturer's instructions. Briefly, ligation reactions were performed at room temperature for 15 min, using 100 ng of vector and a 3:1 insert-to-vector molar ratio.

## **1.2. RNA Methods**

RNA manipulation was carried out under specific conditions to prevent RNase contamination. Ultra pure water was used in all solutions, previously treated overnight with 0.1% (v/v) DEPC, and autoclaved to destroy DEPC. Ultra pure water and disposable material were autoclaved for 1 hr at 121°C and 1 atm.

### **1.2.1. RNA Extraction**

RNA from plant tissues was isolated using the commercial reagent *TRIZOL* (Invitrogen), following the manufacturer's instructions. Tissue was grinded to a fine powder in liquid nitrogen and 1 mL *TRIZOL* (Invitrogen) was added. Samples were incubated for 5 min at room temperature, and 200  $\mu$ L of chloroform were added, followed by a 3 min incubation at room temperature. The top aqueous phase was recovered after a centrifugation of 15 min at 4°C and 12000 *g*. RNA was precipitated after adding 500  $\mu$ L of isopropanol, and incubated for 10 min at RT. A centrifugation for 10 min at 4°C and 12000 *g* was performed, and the supernatant discarded. The pellet was washed with 1 mL of 75% (v/v) ethanol, vortexed and centrifuged for 5 min at 4°C and 7500 *g*. The pellet was subsequently dried in a flow chamber and then dissolved in 30-50  $\mu$ L of DEPC-treated water. The RNA's concentration and purity was determined spectrophotometrically (Nanodrop *ND-1000 Spectrophotometer*, Alfacene). A 1  $\mu$ g RNA sample was run on a 1% agarose gel to confirm RNA integrity. RNA samples were immediately frozen in liquid nitrogen and stored at -80°C.

### **1.2.2. cDNA Synthesis**

A 2  $\mu$ g RNA sample was treated with DNase I (Sigma) prior to cDNA synthesis. This treatment involved a 15 min incubation period with DNase I at 37°C, followed by inactivation of the enzyme by heat denaturation for 10 min at 70°C. To synthesize the first-strand cDNA, 1  $\mu$ g of RNA was primed with 1  $\mu$ L of Oligo(dT) (0.5  $\mu$ g  $\mu$ L<sup>-1</sup>) (Promega) and DEPC-treated water was added to a final volume of 17.75  $\mu$ L. This

mixture was heated for 5 min at 70°C and cooled quickly on ice for 5 min. Reverse transcription was promoted using the enzyme *M-MLV RT* (Moloney murine leukemia virus reverse transcriptase). A mixture of 1 µL of *M-MLV RT (H-)* (Promega) and its 5x buffer were added to 1.25 µL of *dNTP mix* (10mM) (Promega), and transferred to the first mixture containing the RNA. Reverse transcriptase reaction was carried for 60 min at 50°C, followed by 15 min at 70°C, and the cDNA was stored at -20°C.

### 1.3. Quantification of Nucleic Acids

Nucleic acid quantification was performed spectrophotometrically in a *Nanodrop Spectrophotometer ND-1000* (Alfagene), a micro-volume UV-Vis spectrophotometer for nucleic acid and protein quantitation. A minimum volume of 1.5 µL per sample was used. Nucleic concentration was determined considering that 1  $A_{260} = 50$  ng DNA  $\mu\text{L}^{-1}$  and 1  $A_{260} = 40$  ng RNA  $\mu\text{L}^{-1}$ . To determine the purity of the nucleic acid samples,  $A_{260}/A_{230}$  and  $A_{260}/A_{280}$  ratios were also estimated (Sambrook and Russell, 2001). Relative quantification of DNA nucleic acids for ligation reactions was estimated by the relative fluorescent intensity of the DNA intercalating staining agent, using nucleic acid electrophoretic separation.

### 1.4. Nucleic Acids Electrophoretic Separation

DNA fragments were resolved by electrophoretic separation using a horizontal gel apparatus. Gels were made by melting 0.8-1.2% (w/v) agarose in 0.5x TAE. TAE (0.5x) was also used as running buffer. DNA was stained by adding 1 µL of ethidium bromide (1 mg  $\text{mL}^{-1}$ ) to the melted agarose gel. DNA samples, except those from PCR with *GoTaq Green buffer* were mixed with 0.20 vol. of loading buffer (6x *MassRuler DNA Loading Dye*; Fermentas). *MassRuler DNA Ladder Mix* (an 80-10,000 bp molecular weight standard; Fermentas) and  $\lambda$  DNA digested with *Pst*I were used as molecular weight markers. Alternatively, DNA staining was carried out with the fluorescent intercalating agent *GelRed* (Biotium). *GelRed* was used after the gel run, so the gel was incubated for 25 min in 0.5x TAE solution to a final 0.2x *GelRed* concentration. Gel was visualised under UV light.

---

**50x TAE buffer:** 2 M Tris; 0.95 M acetic acid; 50 mM EDTA<sub>n<sub>2</sub></sub>, pH 8.0

**6X MassRuler DNA Loading Dye:** 10 mM Tris-HCL (pH 7.6); 0.03% bromophenol blue; 60% (v/v) glycerol; 60 mM EDTA.

**Loading buffer:** 30% (w/v) glycerol; 0.1 M EDTA; 0.25% (w/v) bromophenol blue.

---

## 2. TRANSFORMATION OF BACTERIA

### 2.1. Transformation of *E. coli* Cells

The protocol for preparation and transformation of *E. coli* competent cells was based on Inoue *et al.* (1990).

### 2.1.1. *E. coli* Competent Cells Preparation

*E. coli* competent cells were obtained by inoculating 250 mL of SOB medium with a single colony of *E. coli* strains. Cells were grown at 18°C with vigorous shaking (200-250 rpm) until  $A_{600}$  was of 0.6 (2-3 days). The medium was cooled on ice for 10 min and cells were collected by centrifugation for 10 min at 4°C and 2500 *g*. The pellet was resuspended in 80 mL of ice-cold TB buffer, and incubated on ice for 10 min. Cells were centrifuged for 10 min at 4°C and 2500 *g*, and gently resuspended in 20 mL of ice-cold TB buffer with 7% (v/v) DMSO. Cells were subsequently incubated for 10 min on ice and 100  $\mu$ L were aliquoted into microtubes. Competent cells were immediately placed in liquid nitrogen and stored at -80°C.

**TB:** 10 mM Pipes; 15 mM CaCl<sub>2</sub>; 250 mM KCl; 55 mM MnCl<sub>2</sub>. Mix all components except MnCl<sub>2</sub> and adjust pH to 6.7 with KOH. Dissolve MnCl<sub>2</sub> and sterilize the solution using a 0.45  $\mu$ m filter.

---

### 2.1.2. *E. coli* Transformation

*E. coli* cell transformation was initiated by slightly thawing competent cells on ice. The DNA sample (1-20  $\mu$ L) was added to 100  $\mu$ L of cells by gentle mixing, and the mixture was incubated for 30 min at 4°C. Cells were then heat-shocked for 90 sec at 42°C, followed by incubation on ice for 1 min. After addition of 1 mL of SOC (or LB) liquid medium, cells were incubated for 1 hr at 37°C with vigorous shaking (200-250 rpm), spun down for during a few sec ( at 10000 *g* and the pellet resuspended in 100  $\mu$ L of the supernatant. Finally, cells were transferred to agarised LB medium plates containing appropriate antibiotics, and grown overnight at 37°C.

## 2.2. Transformation of *Agrobacterium* Cells

### 2.2.1. Preparation of Electrocompetent Cells

*Agrobacterium* cells (GV3101::pMP90 strain) were inoculated in agarised LB medium, from a -80°C glycerol stock, and grown for 2 days at 28°C. A colony was then resuspended in 5 mL LB liquid medium and grown ON at 28°C and 200 rpm. Cells were harvested by centrifugation for 1 min at 13000 rpm and resuspended in 1 mL of 300 mM sucrose per microtube. The pellet was resuspended in 100  $\mu$ L of 300 mM sucrose. Aliquots of 100  $\mu$ L of competent cells were used for vector electroporation.

### 2.2.2. Electroporation Method

Transformation of *Agrobacterium* by electroporation was performed by mixing 100  $\mu$ L of electrocompetent cells with 100 ng of the vector. After careful mix, an electric pulse was given in an electroporator *Gene Pulser II* (BIO-RAD), which was set to 2.5 kV and 400  $\Omega$ , with a capacitance of 25  $\mu$ F. Subsequently, 1 mL of LB liquid medium was added to cell suspension, shaken, incubated in a microtube for 1 h at 28°C and 200 rpm, and plated onto appropriate selection medium and grown for 48 h at 28°C.

## APPENDIX II – OLIGONUCLEOTIDES USED FOR MAP-BASED CLONING

**Table AII.1 – Detailed Information Regarding the Genetic Markers in Arabidopsis Chromosomes used for Map-based Cloning of *SUD1***

Genetic Marker	Sequence (5'→3')	PCR Annealing temperature (°C)	Polymorphism	Col-0 Amplification product size (bp)	<i>Ler</i> Amplification product size (bp)
<b>Chromosome 1</b>					
T16N11-F	TGCATCTGCTGAAATCGAAC	56	SSLP	1191	508
T16N11-R	CCTCATGTGGAGTTTGCTCA				
F508-F	CATTCCATTCCACTGACCTT	60	SSLP	365	398
F508-R	ATGCAGCAAGTTGATGGCTA				
F14M2-F	GGTTTTAGGGAAAGATATTGATG	55	SSLP	507	303
F14M2-R	CAAAACAATATACGAAGAGACGCA				
T2E6-F	CAAGAATGGAGTCCCGGTTA	60	SSLP	837	597
T2E6-R	TGGAGCATGGTTCAGTCAAG				
ADH1-F	GCGTGACCATCAAGACTAAT	60	CAP (XbaI)	1291	1097+262
ADH1-R	AAAATGGCAACACTTTGAC				
<b>Chromosome 2</b>					
T16F16-F	TCTATACGAATGATAACGGTTTATGG	50	SSLP	500	353
T16F16-R	TGAGCACATTGATTAGAGACTTGA				
T16I21-F	AGATGGTGGACAGCTCTTG TG	55	SSLP	686	381
T16I21-R	GGCAAAACCCTAATGTGGAA				
T20D163-F	CCGAGAAGATCTACAAGAGGC	60	CAP (PstI)	1500	1200+300
T20D163-R	GTCATTGACGGTGCTTTGAGG				
T16B12-F	GTAATCAGTCTAAAGTACACATG	50	SSLP	585	273
T16B12-R	CTAATTTTTGTTTTCGATACT				
F18019-F	AAACATGCGCATCAAACAAA	55	SSLP	1183	634
F18019-R	CCTGGCCTTGCTTTGTAGAC				
<b>Chromosome 3</b>					
F18C1-F	CAAAAATGGGAATTGTGATGG	50	SSLP	1022	439
F18C1-R	GTTTTGCATCGGACGGTTAT				
K5K13-F	GGAAACTGCCGTAGACGAAG	60	SSLP	699	400
K5K13-R	AGTCCTCATTCCCCACAC				
NIT1.2-F	CGGAATTGATGTTTTGGACC	60	SSLP	850	1000
NIT1.2-R	CCCTACATTCTACAACCATGTAGC				
F1I16-F	TGTTGTCGGTTGTTCTTAGCA	50	SSLP	896	625
F1I16-R	TGTTACGTTACGAAGCTC				

Genetic Marker	Sequence (5'→3')	PCR Annealing temperature (°C)	Polymorphism	Col-0 Amplification product size (bp)	Ler Amplification product size (bp)
<b>Chromosome 4</b>					
F6N15-F	GTGTGGTCAGGGCTTCAAAT	56	SSLP	984	830
F6N15-R	TGGTGACTIONCCATTGTCTGC				
T13D4-F	AGAGATGGATTGACGAAAAGCA	55	SSLP	329	235
T13D4-R	AATGGAACTCATGTCTTTGG				
F13C5-F	TTGAATGTTTAGGGTGAAAAG	50	SSLP	692	320
F13C5-R	TCTTTCATCCCACCGTACTTG				
F11C18-F	CATCCCTTCAAGTTCGATTCA	60	SSLP	432	259
F11C18-R	TTCTGGACTTGTTCCAGCTG				
F26P21-F	GCCCTTGAGGACTTGATGAG	55	SSLP	148	138
F26P21-R	TGGTTGTGAGTTTCGCATGT				
F17M5-F	GGCGCTAATGTACTCTTCG	60	SSLP	238	200
F17M5-R	GGGGCTTGCCACAATATTTA				
T16L1-F	AACTTTACATGGGGCAATG	50	SSLP	197	156
T16L1-R	TCCTGATATTCACCAATGCACT				
F1715-F	ATCCAAATCCAAGCTCGATG	55	CAP (PsiI)	670 + 227 + 71	434+237+227+71
F1715-R	TGAACATGACAACCTCCAATCG				
F28A23-F	GGGCTTCCCCTGATATGAAT	60	CAP (BglII)	572 + 279	850
F28A23-R	GAAGCCTCGAGAAGCCATC				
F10M10-F	CCGACATGTAGAAGTTGGGTT	60	SSLP	395	281
F10M10-R	TGCAGTTGTTTGAAACGC				
T4L20-F	CCTCCACCGAGAAACATCAT	50	CAP (HindIII)	855	595+261
T4L20-R	GAAATTGAAAAGAGCCACGA				
F8D20-F	AGTGTATTTCATATGATCTGGTT	55	SSLP	559	376
F8D20-R	GAGATGATTTGCTTGCGAGA				
T9A14-F	CCGCAGCTGCACCTTCTTCAA	55	SSLP	502	258
T9A14-R	TGCATTGATTTCCGTCTTGA				
<b>Chromosome 5</b>					
MJJ3-F	CTTAGGCCTCTTTTGAGGGG	60	SSLP	450	320
MJJ3-R	TTTTACGAAACATTACGCCA				
PAT1.2-F	CATGCTTCATCATTGCC	60	SSLP	706	606
PAT1.2-R	AGCTGAAGCTCTGCCACC				
F14I23-F	GGTGGAGAAATTGCCATTA	55	SSLP	521	165
F14I23-R	TAATAATTTGGAATCACATGTTT				
MIK22-F	ACTTCTCGAGCCATAGG	50	SSLP	646	457
MIK22-R	GACTCTCTACCGTTGATTTA				
MJG14-F	CCGTGAATCCTTGTGCTT	55	SSLP	758	365
MJG14-R	CACGACGAACCCTAGAAACC				
K19E20-F	ATGAGAGCATATGAGAGGAAA	58	SSLP	649	360
K19E20-R	GATGGATTGTGATGTGTTT				
MUB3-F	AAACACGTCTACCATCTAGTCC	60	SSLP	759	443
MUB3-R	TAAACGTGTGGCAAATCCAA				

## APPENDIX III – VECTORS Maps

### Maps of vectors using during cloning procedures

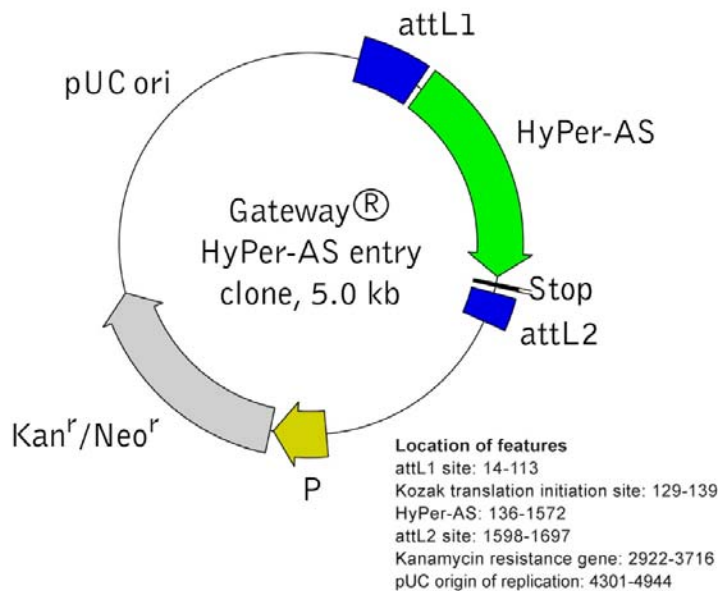


**Figure AIII.1** – HyPer-AS gateway entry clone vector circular map. For vector sequence, please visit the *Evrogen* Web site at <http://www.evrogen.com/support/vector-info.shtml>.

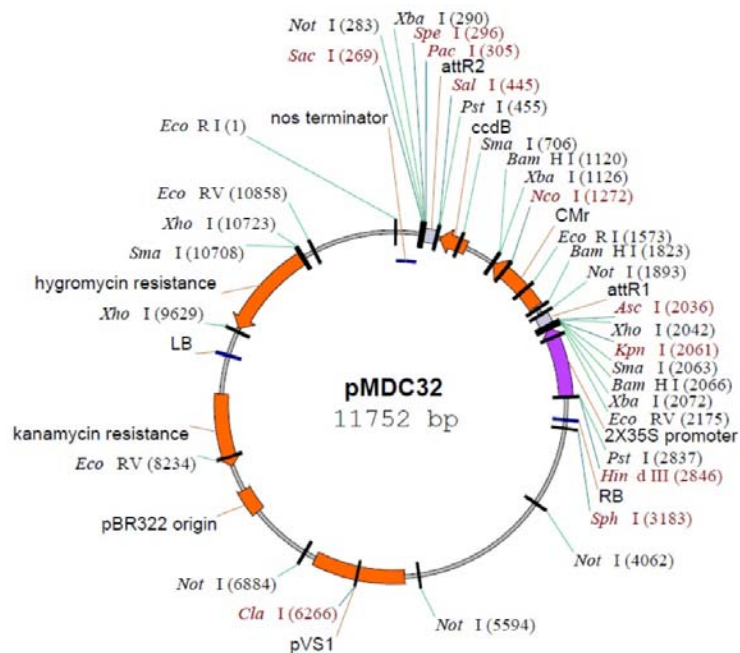


**Figure AIII.2** – pMDC32 destination gateway plant vector circular map (Curtis and Grossniklaus, 2003).

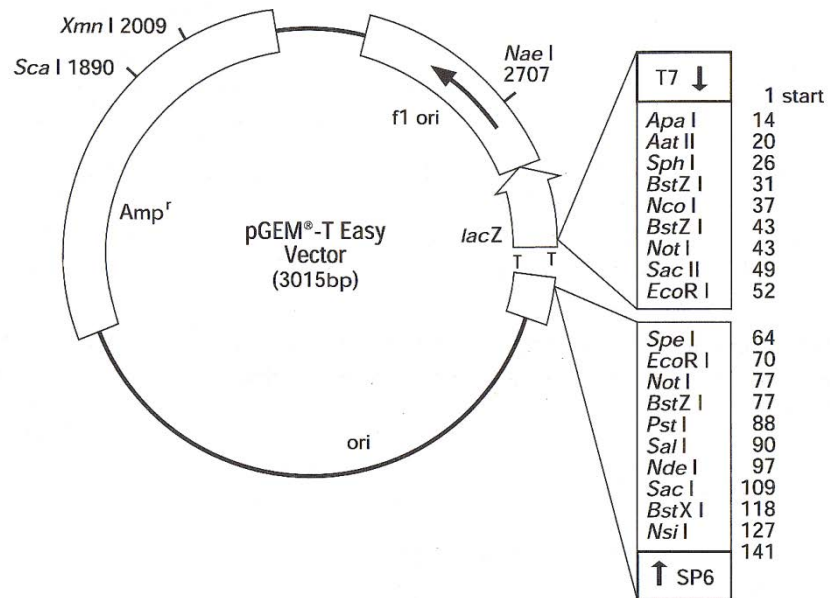


**Figure AIII.3** – pGEM-T subcloning vector circularmap (Marcus *et al.*, 1996).

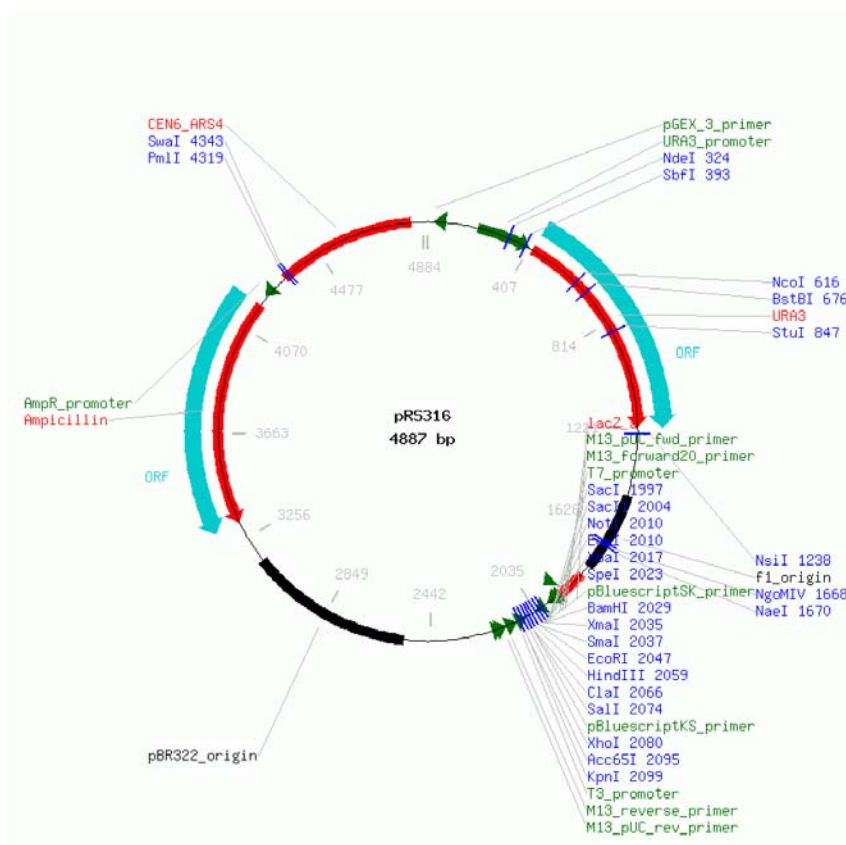


**Figure AIII.4** – pRS316 vector circularmap (Sikorski and Hieter, 1989). For vector sequence, please visit the *addgene plasmid database*, web site at <http://www.lablife.org/vectordb>.



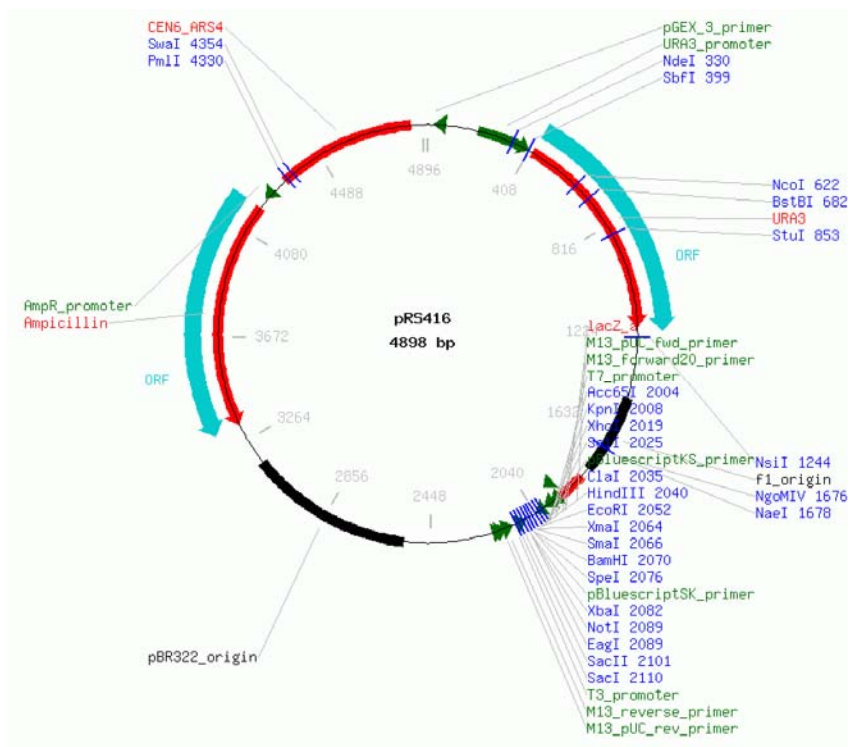


**Figure AIII.5** – pRS416 vector circularmap (Sikorski and Hieter, 1989). For vector sequence, please visit the *addgene plasmid database* web site at <http://www.lablife.org/vectordb>.

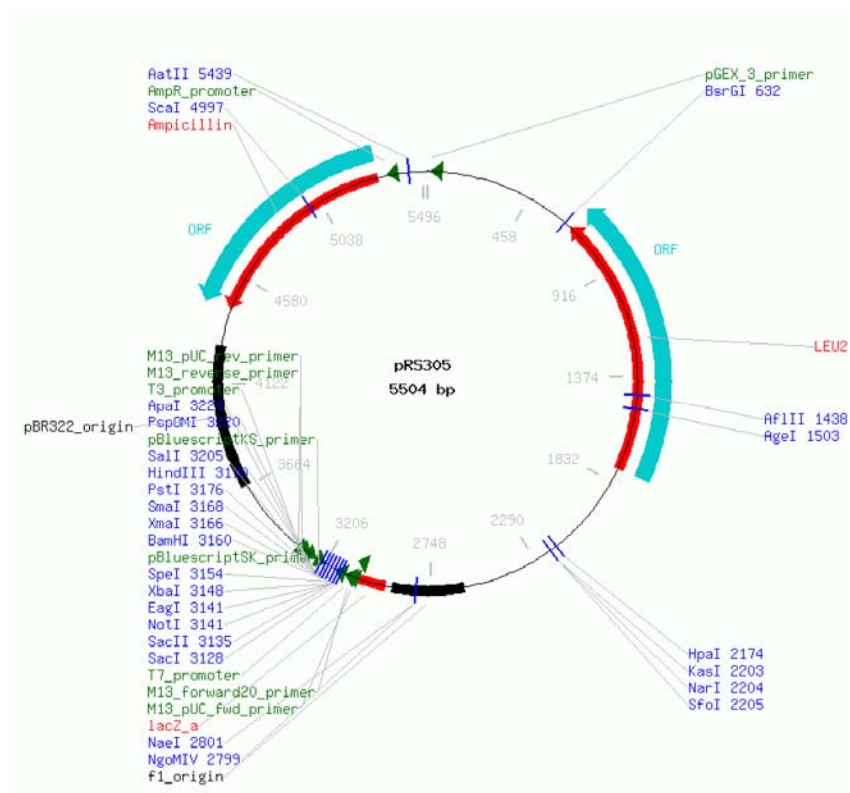


**Figure AIII.6** – pRS305 vector circular map (Sikorski and Hieter, 1989). For vector sequence, please visit the *addgene plasmid database* web site at <http://www.lablife.org/vectordb>.

**APPENDIXES BIBLIOGRAPHIC REFERENCES**

- Curtis, M.D., and Grossniklaus, U.** (2003). A gateway cloning vector set for high-throughput functional analysis of genes in planta. *Plant Physiol* **133**, 462-469.
- Doyle, J.J., and Doyle, J.L.** (1987). A rapid DNA isolation procedure for small quantities of fresh leaf tissue. *Phytochemical Bulletin* **19**, 11-15.
- Edwards, K., Johnstone, C., and Thompson, C.** (1991). A simple and rapid method for the preparation of plant genomic DNA for PCR analysis. *Nucleic Acids Res* **19**, 1349.
- Griffin, H.G., and Griffin, A.M.** (1994). PCR Technology: Current Innovations. (CRC Press).
- Inoue, H., Nojima, H., and Okayama, H.** (1990). High efficiency transformation of Escherichia coli with plasmids. *Gene* **96**, 23-28.
- Marcus, L., Hartnett, J., and Storts, D.R.** (1996). The pGEM®-T and pGEM®-T Easy Vector Systems. In *Promega Notes Magazine*, pp. 36-38.
- Rozen, S., and Skaletsky, H.** (2000). Primer3 on the WWW for general users and for biologist programmers. *Methods Mol Biol* **132**, 365-386.
- Sambrook, J., and Russell, D.W.** (2001). Molecular Cloning: A laboratory manual. (Cold Spring Harbour, New York: Cold Spring Harbour Laboratory Press, ).
- Sikorski, R.S., and Hieter, P.** (1989). A system of shuttle vectors and yeast host strains designed for efficient manipulation of DNA in *Saccharomyces cerevisiae*. *Genetics* **122**, 19-27.



